NOAA Technical Report NWS 24

A Methodology for Point-to-Area Rainfall Frequency Ratios

Washington, D.C.
February 1980

U.S. DEPARTMENT OF COMMERCE
National Oceanic and Atmospheric Administration
National Weather Service

NOAA TECHNICAL REPORTS

National Weather Service Series

The National Weather Service (NWS) observes and measures atmospheric phenomena; develops and distributes forecasts of weather conditions and warnings of adverse weather; collects and disseminates weather information to meet the needs of the public and specialized users. The NWS develops the national meteorological service system and improves procedures, techniques, and dissemination for weather and hydrologic measurements, and forecasts.

NWS series of NOAA Technical Reports is a continuation of the former series, ESSA Technical Report Weather Bureau (WB).

Reports listed below are available from the National Technical Information Service, U.S. Department of Commerce, Sills Bldg., 5285 Port Royal Road, Springfield, Va. 22161. Prices vary. Order by accession number (given in parentheses).

ESSA Technical Reports

WB 1 Monthly Mean 100-, 50-, 30-, and 10-Millibar Charts January 1964 through December 1965 of the IQSY Period. Staff, Upper Air Branch, National Meteorological Center, February 1967, 7 p, 96 charts. (AD 651 101)

WB 2 Weekly Synoptic Analyses, 5-, 2-, and 0.4-Mb Surfaces for 1964 (based on observations of the Meteorological Rocket Network during the IQSY). Staff, Upper Air Branch, National Meteorological Center, April 1967, 16 p, 160 charts. (AD 652 696)

WB 3 Weekly Synoptic Analyses, 5-, 2-, and 0.4-Mb Surfaces for 1965 (based on observations of the Meteorological Rocket Network during the IQSY). Staff, Upper Air Branch, National Meteorological Center, August 1967, 173 p. (AD 662 053)

WB 4 The March-May 1965 Floods in the Upper Mississippi, Missouri, and Red River of the North Basins. J. L. H. Paulhus and E. R. Nelson, Office of Hydrology, August 1967, 100 p.

WB 5 Climatological Probabilities of Precipitation for the Conterminous United States. Donald L. Jorgensen, Techniques Development Laboratory, December 1967, 60 p.

WB 6 Climatology of Atlantic Tropical Storms and Hurricanes. M. A. Alaka, Techniques Development Laboratory, May 1968, 18 p.

WB 7 Frequency and Areal Distributions of Tropical Storm Rainfall in the United States Coastal Region on the Gulf of Mexico. Hugo V. Goodyear, Office of Hydrology, July 1968, 33 p.

WB 8 Critical Fire Weather Patterns in the Conterminous United States. Mark J. Schroeder, Weather Bureau, January 1969, 31 p.

WB 9 Weekly Synoptic Analyses, 5-, 2-, and 0.4-Mb Surfaces for 1966 (based on meteorological rocketsonde and high-level rawinsonde observations). Staff, Upper Air Branch, National Meteorological Center, January 1969, 169 p.

WB 10 Hemispheric Teleconnections of Mean Circulation Anomalies at 700 Millibars. James F. O'Connor, National Meteorological Center, February 1969, 103 p.

WB 11 Monthly Mean 100-, 50-, 30-, and 10-Millibar Charts and Standard Deviation Maps, 1966-1967. Staff, Upper Air Branch, National Meteorological Center, April 1969, 124 p.

WB 12 Weekly Synoptic Analyses, 5-, 2-, and 0.4-Millibar Surfaces for 1967. Staff, Upper Air Branch, National Meteorological Center, January 1970, 169 p.

NOAA Technical Reports

NWS 13 The March-April 1969 Snowmelt Floods in the Red River of the North, Upper Mississippi, and Missouri Basins. Joseph L. H. Paulhus, Office of Hydrology, October 1970, 92 p. (COM-71-50269)

NWS 14 Weekly Synoptic Analyses, 5-, 2-, and 0.4-Millibar Surfaces for 1968. Staff, Upper Air Branch, National Meteorological Center, May 1971, 169 p. (COM-71-50383)

NWS 15 Some Climatological Characteristics of Hurricanes and Tropical Storms, Gulf and East Coasts of the United States. Francis P. Ho, Richard W. Schwerdt, and Hugo V. Goodyear, May 1975, 87 p. (COM-75-11088)

(Continued on inside back cover)

NOAA Technical Report NWS 24

A Methodology for Point-to-Area Rainfall Frequency Ratios

Vance A. Myers and Raymond M. Zehr
Office of Hydrology Silver Spring, Md.

in cooperation with

Engineering Division Soil Conservation Service
U.S. Department of Agriculture

Washington, D.C.
February 1980

U.S. DEPARTMENT OF COMMERCE
Philip M. Klutznick, Secretary

National Oceanic and Atmospheric Administration
Richard A. Frank, Administrator

National Weather Service
Richard E. Hallgren, Director

CONTENTS

CONTENTS (Cont'd)

CONTENTS (Cont'd)

TABLES

ILLUSTRATIONS

NOTATION

A	= area
A,B,Y,Z	= transformed variables. Appendices IV and V
a,b,g,h	= dimensionless scaling and curvature parameters of fitted exponential curves
C_c,C_s,C_x	= dimensionless location coefficient for $cov'(\Delta\Theta)$, s'_L, and $\overline{X}'_L$.
cov	= covariance between simultaneous precipitation quantities indicated by subscripts
cv	= coefficient of variation = $s/\overline{X}$
d	= distance
d_1	= a standard distance; 1 mile in this report
d_s	= d at splice on spliced curves
dR/dt	= precipitation rate
DA	= dimensionless depth-area ratio
DL	= dimensionless depth-length ratio
e	= base of natural logarithms
f	= frequency
$F(r)$	= functional form of a radial profile. Chapter 5
G	= assigned level of a variable y. Appendix I
K	= frequency factor
m	= number of stations. Eq. (2-5)
m	= rank in a series. Appendix I
M	= limit of y, as $\Delta t \to \infty$ or $d \to \infty$; a curve-fitting parameter
n,n_k	= see "normal equations," appendix V
N	= years of record
N'	= standardized length of record. 20 years in this report

P	= precipitation depth accumulated in duration Δt
$\overline{P}_A$	= average P in area A
P_L	= annual maximum $\overline{P}_A$
$\overline{P}_S$	= average P at stations within area A
Pr[ ]	= probability that condition in brackets is true
r	= radius
R	= equivalent radius of area A = $(A/\pi)^{\frac{1}{2}}$
	= radius of a circular area over which an integration is performed
s	= standard deviation
S	= sum of squares of deviations. Eq. (V-5)
Δt	= duration
Δt_1	= a standard duration. One hour in this report
V	= variance
X	= annual maximum precipitation
X_A	= X at a point in general; or at station A of an A,B pair
X_B	= X at station B of an A,B pair
X_b	= precipitation at station B of an A,B pair simultaneous with X_A at station A
X_a	= precipitation at station A of an A,B pair simultaneous with X_B at station B
X_m, X_{5m}, X_L	= annual maximum two-station average, five-station average, and areal average precipitation

$cv_A, s_A, V_A, \overline{X}_A, s_B, \overline{X}_B, cv_b, s_b, V_b, \overline{X}_b, s_a, s_m, V_m, \overline{X}_m, s_{5m}, V_{5m}, \overline{X}_{5m}, s_L, V_L,$

$\overline{X}_L$ = cv,s,V,$\overline{X}$ of series of $X_A, X_B, X_b, X_a, X_m, X_{5m}, X_L$

cov_{Ab}, cov_{aB} = covariance of X_A and X_b; of X_a and X_B

cov_{bb} = covariance of precipitation at two outer stations of five-station set during X_{5m}'s

$V_{\overline{Ab}}$ = variance of quantity $0.5(X_A + X_b)$

$s_N, \overline{X}_N$ = s,$\overline{X}$ for N years

$s_{N'}, \overline{X}_{N'}$ = $s_N, \overline{X}_N$ adjusted to N' years

y = substitute variable for statistic being evaluated

y_m = y of rank m. Appendix I

y_{Pr} = y at probability Pr. Appendix I

y_s = y at d_s

y_o = y at $\Delta t = 0$, a curve fitting parameter

Z_k = variable in "normal equations." Appendix IV

Z_{Pr} = precipitation of probability Pr of not being equaled or exceeded in a year. Appendix I

α = dimensionless coefficient defined in eq. (5-57)

π = 3.14159

ρ = correlation coefficient

σ_N = standard deviation of a sample of N values of the reduced variate. Appendix I; chapter 3

σ_x = standard deviation of X in eq. (3-7)

θ = azimuth in polar coordinates

$a_{in}, b_{in}, M_{in}, a_{out}, b_{out}, M_{out}, y_{out}$ = a,b,M,y for inner and outer segments of a spliced curve. Appendix VI

a_s, b_s = see eq. (III-18)

$r_h\theta_i, r_j\theta_k$ = coordinates of first and second points in polar coordinates. Figure 5-9

$s_{hi}, V_{hi}, s_{jk}, V_{jk}$ = s and V of P at points $r_h\theta_i, r_j\theta_k$ during X_L's

$cov_{hi,jk}$ = covariance of above P values

cov_{min}, cov_{max} = least and greatest values of $cov_{hi,jk}$ per theory and assumptions in chapter 5

$\overline{\quad}$ = average or mean

$[\ ]_U, [\ ]_L$ = upper and lower bounds of a variable

$[\ ]_D$ = value of a variable at an average data point

$\hat{cov}_{Ab}, \hat{V}_b, \hat{y}, \hat{Y}$ = computed or adjusted values of cov_{Ab}, V_b, y, Y

Primes except on N' denote values relative to zero distance, e.g.,

$$\overline{X}'_m(d) = \overline{X}_m(d)/\overline{X}_m(0) = \overline{X}_m(d)/\overline{X}_A$$

$$s'_m(d) = s_m(d)/s_m(0) = s_m(d)/s_A$$

PROLOGUE - METRIC UNITS

At the time of preparation of this report English units were still in use by the National Oceanic and Atmospheric Administration for archiving precipitation measurements and by most engineering organizations in the United States for hydrologic analyses, although change to the metric system was imminent. This report is in English units. Conversion factors are:

1 inch = 25.4 mm

1 mile = 1.609 km

1 mi^2 = 2.590 km^2 = 259 hectares

Air temperature and dewpoint on surface weather maps at the time of preparation of this report are in degrees Fahrenheit and standard upper air charts are denoted by their pressure in millibars. These units are used in chapter 7. Conversion factors are:

$$deg°C = [(deg°F) - 32] \frac{5}{9}$$

1 kilopascal = 10 mb

1 hectopascal = 1 mb

A METHODOLOGY FOR POINT-TO-AREA RAINFALL FREQUENCY RATIOS

Vance A. Myers and Raymond M. Zehr
Office of Hydrology
National Weather Service, NOAA
Silver Spring, Md.

ABSTRACT. A new procedure is developed for calculating geographically fixed depth-area ratios from dense networks of recording precipitation gages. These ratios are needed to reduce published point precipitation frequencies to areal values.

CHAPTER 1. INTRODUCTION

Rainfall Frequency for Engineering Use

A knowledge of the frequency of rainfall of various intensities is basic to the design of structures to carry runoff from rainfall, such as storm sewers and highway culverts; to the modification of natural floodways by dams and levees; and to decisions on flood plain occupancy -- how close to a creek is it prudent to build a home? The Soil Conservation Service, Department of Agriculture (USDA), has underwritten preparation by the National Weather Service of rainfall-frequency atlases for use of that agency in carrying out the watershed protection and flood prevention program authorized by Public Law 566, 83rd Congress. These atlases serve not only the needs of the Soil Conservation Service, but are also used extensively by other Federal agencies, State and local governments, and private engineering firms. The series of atlases accumulated since 1955 now covers the entire United States for precipitation durations up to 10 days and return periods up to 100 years. The atlases are based on detailed analysis of the network of measurements of point rainfall in gages and on much more meager data relating to the areal variation of rainfall in storms. The basic displays in the atlases are sets of isohyets on maps depicting rainfall depths which, over given durations, have stated probabilities of being equalled or exceeded in any one year. The annual probabilities are labeled with the inverse, mean return period.

Areal Reduction of Point Rainfall Frequencies

Each atlas contains an areal reduction nomogram giving ratios of areal average precipitation of a specified return period and duration to the corresponding point value averaged over that area on the maps. These nomograms enable users to adjust the point rainfalls of given frequency to the corresponding areal value needed for a project. We emphasize that this type of areal reduction ratio is an adjustment to convert point rainfall frequency values to areal values of the same duration and return period. This type of

ratio does not describe the morphology of an individual storm, but rather is the ratio of two different expectations. Its character from the theoretical point of view has been discussed by Rodriguez-Iturbe and Mejia (1974). This type of areal reduction ratio of precipitation frequencies is sometimes termed a "geographically fixed depth-area ratio" as distinct from "storm centered" depth-area ratios based on the morphology of individual storms. No information on the latter type of depth-area ratio is developed in this report.

The rainfall frequency analyses are based on annual maximum values. In a particular year the basin average annual maximum for a given duration may occur in a different storm than annual maxima at points within the basin. In fact, for larger areas there is a tendency in many regions for a distinct difference in the seasonal distribution of small maxima for areas and points. The ultimate bases for geographically fixed depth-area ratios are empirical comparisons of appropriate averages of annual maximum point rainfalls with annual maximum areal average rainfalls at the same location. The areal averages are approximated by averaging simultaneous gage catches. This simultaneity requirement limits the precipitation gages that can be used to recorders. The spacing of one recording gage every several counties in the normal climatological network of the United States is not dense enough to provide areal average information on a scale suitable for the water conservation, flood prevention, and other projects of a few hundred square miles or less. Basically, it is necessary to develop the reduction factors from the few existing networks of more densely placed recording gages and extrapolate these results to the remainder of the country. This was first done by the National Weather Service in 1957, as reported in Technical Paper No. 29, Part 1 (U.S. Weather Bureau 1957). Other details of the procedure are found in Technical Paper No. 29, Part 2 (U.S. Weather Bureau 1958) and in NOAA Atlas 2 (Miller et al. 1973). The basic method for deriving geographically fixed depth-area ratios is comprised of the following steps. Steps 2 to 8 are carried out separately for each of a series of durations.

1. Select a group of closely spaced precipitation recording gages.

2. Find the annual maximum of simultaneous rainfall accumulated over the duration and averaged over the gages. The gages are weighted equally or differently depending on the uniformity of their spacing.

3. Fit a frequency curve to this maximum annual series.

4. Carry out the same process for each individual gage in the set.

5. At each of several return periods, average the frequency values abstracted from the frequency curves for the individual selected gages.

6. Abstract the corresponding frequency values from the group average frequency curve from step 3.

7. Take ratio of the step 6 result to the step 5 result.

8. Assign this ratio to the area represented by the group of gages. Selecting this representative area is not an easy question and is discussed in the cited reports. Each depth-area ratio thus determined pertains to a given area, return period, and duration.

9. Amalgamate all calculated ratios into a set that is consistent over duration, area, frequency, and location.

Areal and durational variation of the depth-area ratios is prominent and was depicted in the original Technical Paper No. 29 analysis. Frequency variations and geographical location variation could not be reliably specified from the scattered computed ratios, some of which were derived from very short periods of record, as little as 6 years. It was determined that the best product would be a single nomogram averaged over all dense networks and based on 2-yr return period values, to be used for point-to-area reductions throughout the country and for all return periods up to 100 years. Succeeding reanalyses by the National Weather Service in connection with production of successive atlases and as dense network data became available for a longer span of years did not produce results that were significantly different from the Technical Paper No. 29 nomogram and it was carried forward. This nomogram is reproduced in figure 1-1 from NOAA Atlas 2.

Recently Osborn et al. (1979) developed depth-area ratios by the foregoing methods from 20 years of dense network recording precipitation gage records on two USDA research watersheds, one in New Mexico and one in Arizona. Not unexpectedly, these depth-area ratios differ from the previous values averaged over the whole country.

Objectives of Study

It was decided that it was feasible to reopen the search for geographical variation of depth-area ratios within the conterminous 48 states. The need had been present earlier but the data to respond had not been available. The greatest need is for specification of depth-area ratios different from the national average in the intermountain West. An analysis plan was adopted with depth-area ratios in that region, including variations within the region, as the goal. Major phases include:

1. Develop depth-area ratios from 20 years of data at the USDA Experimental Watersheds at Walnut Gulch, Ariz., and Alamogordo Creek, N.M., as anchor points.

2. Develop a computerized model of the structure of maximum annual rainstorms, and a routine for computing depth-area ratios from these storms, with emphasis on extracting as much information as possible from pairs of recording gages only.

3. Work outward from the anchor points, applying the computerized model to pairs of gages and other data.

The cited paper by Osborn, et al. is from phase 1 of this plan. The present volume is a report on phase 2. This and subsequent phases are facilitated by the recent availability on magnetic tape of NOAA-published precipitation data since 1948 in a format specified by the Office of Hydrology of NWS, for hydrologic analysis (Peck et al. 1977). This included putting the entire record of a station on one magnetic tape, relieving the user of the burden of using a separate tape for each calendar year.

At best, the data for analysis of depth-area ratios for area sizes of a few hundred square miles and less will continue to be sparse. Thus the model necessarily contains large elements of systematic inference.

Other potential applications of the model include search for regional variation of depth-area ratios in the Pacific coast region and in the Eastern United States from gage data, and eventually, with adaptations, analysis of radar data. Digitized radar data is a promising source of observations of areal average rainfall on the scale of a point up to 1 or 2,000 km^2 (Frederick et al. 1977a), but it will be some years before sufficient digitized radar data have accumulated to form reliable annual maximum series.

Properties of Model

The model, derived by experimentation with the station pair emphasis in mind, accomplishes the same objective as the steps on pages 1-2 - 1-3 with differences in major details.

The first and second moments of all annual series are smoothed over area (or interstation distance) and duration rather than at the later stage in old step 9. The smoothing is by fitting a surface in area-duration space (or distance-duration space) defined by exponential formulas containing fitting constants. This is an empirical step, but a good deal of thought was given to how best to accomplish it. The primary fit is to data for pairs of stations representing a range of distances.

Fitted surfaces are derived for five different station pair statistics: first and second moments of the annual maximum 2-station average (chapter 3), first and second moments of rain at the second station simultaneous with the single station annual maximum at the first (chapter 4), and covariance between station annual maxima and the simultaneous rain (chapter 4).

These statistics are then used in various combinations to estimate upper and lower bounds of the first and second moments of annual maximum areal average precipitation. The placement of surfaces between the bounds is by calibration with data from a limited number of quasi-symmetric five-station groups (chapter 5).

Finally, depth-area ratios are derived by processing the first and second areal moments through Chow's generalized frequency equation (chapter 6).

All statistics are carried in relative form throughout the analysis, as the ratio of the statistic at a given area or distance to the corresponding value at zero area or distance.

A schematic diagram of this process is placed in appendix VIII and is intended as a reference. Familiarity with the notation of the report is needed in referring to the diagram.

Chicago Locale

For practicality in computer operations we decided that the development data must be selected from that published routinely by the National Climatic Center and therefore on the magnetic tapes referred to. To secure necessary gage density, the development data would necessarily be drawn from outside the intermountain region. Chicago and vicinity was selected as having the best gage density with nearly complete records over a few hundred square miles.

The main result here is development of an analysis tool for further work. Readers interested in specific results at Chicago are referred to the recent investigations of the Illinois State Water Survey for Chicago and the six surrounding counties (Huff and Vogel 1976; Huff et al. 1978).

A secondary result is that Chicago becomes an anchor point for depth-area regional variation analysis. An important part of the assessment of information for this purpose at anchor points is identification of principal depth-area ratio controlling storm types and documentation of their characteristics. Storm types are known for all parts of the country or can be assessed from weather maps. Storm type can become one transfer function to extrapolate depth-area ratios from measurement sites to ungaged locations. A synoptic storm type analysis is included in this report (chapter 7).

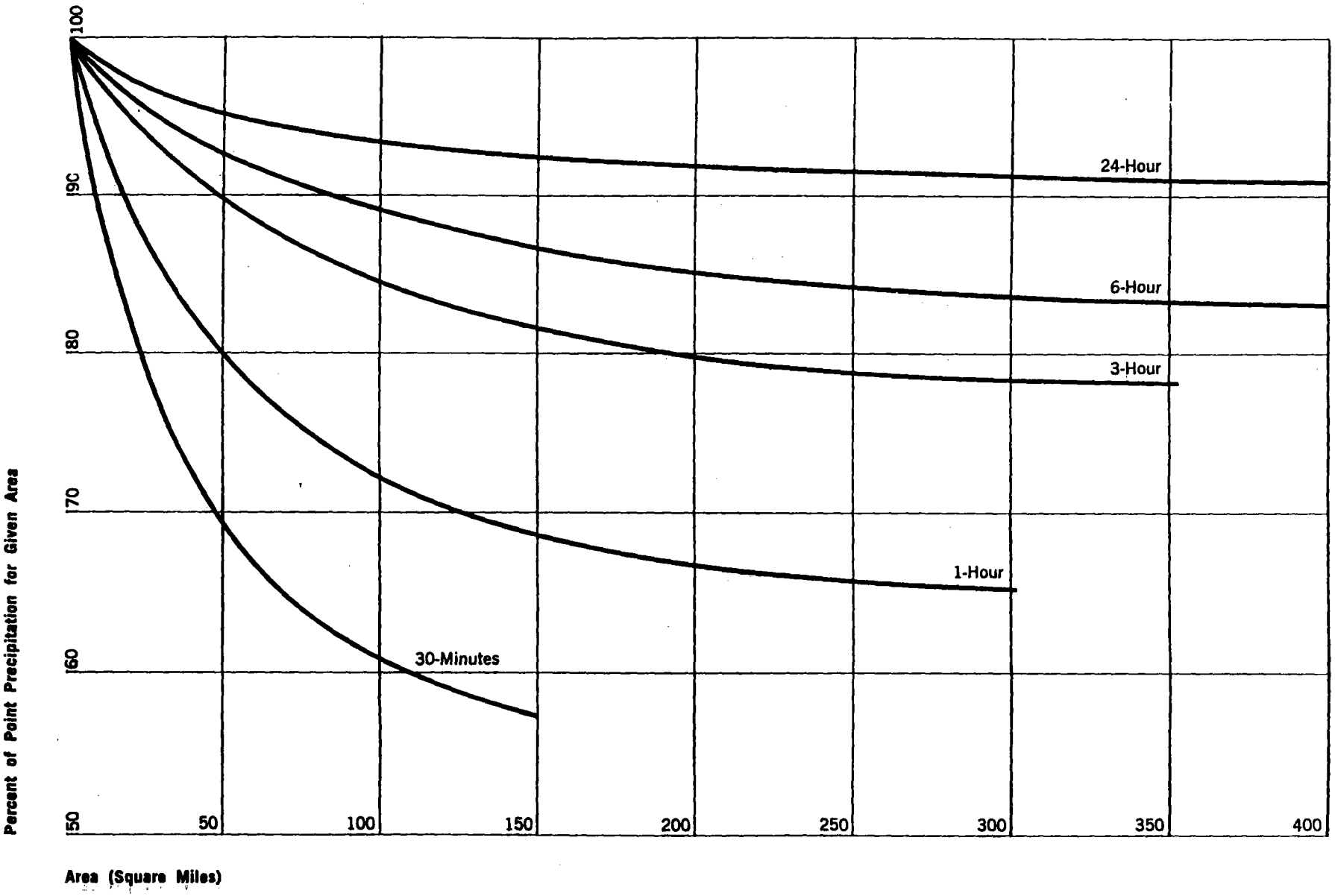

Figure 1-1.--Depth-area ratios, from Miller et al. (1973).

CHAPTER 2. DATA, BASIC PROCESSING, AND TESTING

Data

Network.

A number of recording precipitation gages are maintained by the Metropolitan Sanitary District of Greater Chicago (Huff and Vogel 1976) which, together with Chicago University and National Weather Service stations, form a group of about 15 stations in an area of 200 to 250 mi^2. (The network varies from year to year.) Data from similar networks in other cities are not necessarily collected for publication by the National Weather Service or the National Climatic Center. The stations in the Chicago network are listed in table 2-1 and mapped in figure 2-1. Lockport Power House (near Joliet), Evanston Pumping Station, and Crete, Ill., were added to the Chicago group to extend the distance range. O'Hare International Airport, about 8 mi WNW of station D in figure 2-1, was not established until 1962 and was not used.

Period of record.

The period of record used was 1948-72, beginning in July 1948 at most stations. This entire 25-year record for several stations in a State is contained on a single magnetic tape (Peck et al. 1977). Supplementary tapes incorporating years following 1972, prepared in this format at the National Climatic Center, Asheville, N.C., from time to time, were not available at the initiation of this project in 1976. To introduce data from before 1948, not on magnetic tape, would have been prohibitively expensive.

Season.

In winter the normal freezing weather at Chicago results in substantial periods of accumulated or missing precipitation recorder data. For this reason, the study is restricted to the April-October season. An analysis at four individual stations of seasonal maximum rainfalls for the 1-, 6-, and 24-hr duration with true annual maximum values showed 4 percent of 1- and 6-hr annual maxima in November and March, therefore differing from the seasonal maxima, and 6 percent at the 24-hr duration. The true annual maxima were from the work sheets of previous studies where a considerable hand effort was made to find them. Hereafter throughout this report the term annual maximum value will signify the largest value from April through October. Inferentially, the percentage of winter maxima would be larger for areas than points. The area size at which this becomes significant is not known and could not be determined in any economical manner. It seems unlikely that the effect on depth-area ratios for areas of 2000 km^2 or less, the main interest in this report, would be appreciable. Depth-area ratios derived from comparison of frequencies within the April-October season are accepted as representative of all-year ratios.

Accumulations and missing data.

The decision to eliminate entire years of record at certain stations because

of excessive accumulations and missing periods, made in the course of a previous project (Frederick et al. 1977b), was carried forward to this study. The years of record listed in table 2-2 are those that were retained after this screen.

An accumulated value is a total published in Hourly Precipitation Data with time distribution unknown during preceding hours indicated by asterisks. The same information is recorded on the magnetic tapes. All such accumulated values during the years of record used were linearly interpolated over their period of occurrence and thereafter treated as real hourly data. For a portion of the analysis, accumulations were flagged and hand inspected. They did not appear to have much effect on the principal item abstracted, annual maximum rainfalls for several durations.

All depth-area ratio determinations are made from strictly simultaneous observations. If an hour, day, month, or year is missing at a station, then that hour, day, month, or year is omitted in all processing of station pairs or groups containing that station.

Statistical Processing

Annual maximum series.

The first step in statistical processing is to abstract the annual maximum precipitation for 1, 2, 3, 6, 12, and 24 consecutive hours for each year from the edited data. This was carried out for station-pair averages (chapter 3), group averages (chapter 5), and for each station in each pair or group.

Moments of annual series.

The first moment (mean) and second moment (standard deviation) were found for each annual maximum series from:

$$\overline{X} = \frac{1}{N} \sum_{k=1}^{n} X_k \qquad (2\text{-}1)$$

and

$$s = \left(\frac{1}{N} \sum_{k=1}^{n} (X_k - \overline{X})^2 \right)^{1/2}. \qquad (2\text{-}2)$$

Notation is identified on pages xii - xv. The sums are divided by N, not N-1, as adjustment for bias of sample statistics as estimators of population statistics is inherent in the method used later for fitting a distribution to the sample moments.

Third moments (skew) were also calculated as a trial for a subset of the annual maximum series. The sampling variation was so large that these data had little information content and this step was deleted. In precipitation frequency analysis it is often necessary to impose the skew from considerations external to the immediate data.

The rule in this study is to proceed as far as possible in smoothing the moments over area and duration and delay calculating frequencies or their derivative, depth-area ratios, from the moments until the last possible step. Thus, much of the work is "distribution free" and remains as a valid model regardless of the frequency distribution used.

Adjustment of moments for record length.

Sample moments are biased by sample size. To standardize moments to a single record length for further processing, all are adjusted to a 20-yr record by

$$\overline{X}_{20} = \overline{X}_N + \frac{s_N}{\sigma_N} (\overline{y}_{20} - \overline{y}_N) \ , \tag{2-3}$$

and

$$s_{20} = s_N \frac{\sigma_{20}}{\sigma_N} \ . \tag{2-4}$$

Twenty years is the approximate average sample size after the deletion of years with uncertain data. The above adjustment formulas are derived and the variables defined in appendix II.

Frequency distribution.

The Fisher-Tippett Type I frequency distribution is used in this study. The fitting procedure is essentially that developed by Gumbel (National Bureau of Standards 1953, Gumbel 1958). This distribution has been used by the National Weather Service in all of its rainfall frequency atlases. Studies by Hershfield and Kohler (1960) and Hershfield (1962) have demonstrated the applicability of this distribution to precipitation extremes. In constructing NOAA Atlas 2, Miller et al. tested several distributions (see Frederick et al. 1977b, p. 5) and found the results of all comparable. In view of this comparability, the Gumbel fitting of Fisher-Tippett Type I was continued there for continuity with previous work. The goal of the present study is dimensionless ratios of frequency values. Thus, there is less emphasis on choice of frequency distribution than in studies where absolute magnitude of frequency values is the objective. Depth-area ratios should be insensitive to frequency distribution as long as both numerator and denominator of the ratio are calculated with the same frequency distribution. We continue here the Fisher-Tippett Type I distribution for continuity. A discussion of this fitting procedure is found in appendix I of this report, together with citation of historical papers leading up to it.

The fitting is by the method of moments. Only the first moment (mean) and second (standard deviation) are required for Fisher-Tippett Type I.

Simultaneous rain.

As another indicator of the spatial variation of storms, the rain at each station of a pair simultaneous with each annual maximum at the other station

was abstracted. This was carried out for the pairs in table 2-1 for each of the six standard durations. Some of these simultaneous rains are themselves annual maxima. Simultaneous values can also be zero.

The simultaneous rains are specialized annual series. First and second moments, normalized to 20 years, of these specialized series were calculated in the same manner as for the annual maximum series. Covariance between annual maximum and its associated simultaneous rain was also determined. The use of these statistics is covered in chapter 4.

Representative area.

The objective of Step 8 in the Technical Paper No. 29 depth-area ratio procedure is to define the area over which the moments of the annual series of the true average precipitation are the same as the moments of the station average annual series for the selected group of stations. A representative area, A, for an individual storm would be a portion of the P(x,y) surface, where P is storm precipitation and x and y Cartesian coordinates, such that

$$\overline{P}_A = (1/A) \quad PdA = \overline{P}_S = (1/m)(P_1 + P_2 + \ldots P_m) \tag{2-5}$$

for m stations equally spaced within the area. $\overline{P}_A$ is the true areal average precipitation and P_S station average. If the stations are not evenly spaced and are weighted the concept remains the same. The area so defined would be expected to vary with storms. Thus, the more general conceptual requirement is, for a particular duration and station group,

$$[\overline{X}]_{\overline{P}_A} = [\overline{X}]_{\overline{P}_S} \; ; \quad [s]_{\overline{P}_A} = [s]_{\overline{P}_S} \; , \tag{2-6}$$

where $\overline{X}$ and s are the mean and standard deviation of the maximum annual series. Durational variation of the A that satisfies (2-6) would be expected to be small compared to other uncertainties, and an explicit adjustment for duration has never been attempted. The representative area can be specified only approximately because the form of the P(x,y) surface is known only approximately. Assigning the representative area by certain geometric rules devised on the basis of judgment is treated in the previously cited NWS publications.

That approach to taking into account the composite nonlinearity of precipitation distribution between stations has been fully exploited in the previous studies. In this study we perform the analysis in a different sequence and estimate the form of standardized P(x,y) surfaces. Integration over these continuous surfaces then leads to areal average statistics. Details are given in later chapters.

Testing

Climatic homogeneity.

Whether a significant climatic trend exists across the study area is important in analyzing and interpreting the data. We recommend testing for this in depth-area analysis of any but quite small areas. Huff and Vogel (1976) addressed this question for Chicago. Their findings are summarized in a map of ratio of 24-hr 2-yr rainfall at each station to the value at a station near the midpoint of the rain gage network (their figure 2). This pattern shows a band of values 3 to 5 mi inland from Lake Michigan up to 5 percent higher than the index station but dropping to 95 percent of index farther west. They chose to impose this pattern on a set of local frequency maps in their report. For comparisons from our own data series, the mean and standard deviation of each station's annual maximum series for 1 and 24 hr were plotted on maps. The pattern of the 24-hr mean is very similar to Huff and Vogel's figure 2. This is expected, since the first moment dominates 2-yr frequencies and since the periods of record are about the same, 1948-72 vs. 1949-74. The distribution of 1-hr means is different. We show higher values at some shore stations. The standard deviations exhibit spatial differences which are difficult to interpret on synoptic meteorology grounds. Inspecting this information, we conclude that real climatic variations are likely to exist but are not large and tend to be obscured by sampling variation. We did not investigate nonmeteorologic bias due to rain gage siting. We conclude that it is not possible to separate all these effects at the present time and that for purposes of this report the data should be treated as spatially ergodic.

Time trend.

Huff and Vogel conclude that 24-hr rainfall frequency estimates at Chicago derived from the years late 1940's to mid-1970's are high compared to those from a conceptual stationary climate because of the happenstance of several intense storms during the period. A comparison of station 24-hr rainfall frequencies from the present report with those from U.S. Weather Bureau Technical Paper No. 40 (Hershfield 1961) based on the period of record through the late 1950's, supports this conclusion. The percentage difference between shorter duration rainfall frequencies is less. Time trend testing by Frederick et al. (1977b) implied general stationarity during the 50 years 1923-1972 of 1-hr rainfall frequencies in the Central and Eastern United States. Thus the Chicago results appear to be a local anomaly. We believe it is fortunate rather than the reverse that the period includes these intense storms. The sample appears to include a spectrum of storm types and subtypes that on the average would take longer than 25 years to collect and thus is more representative of the total climatic norm for present purposes than a more typical 25-yr sample.

Squall lines.

The expectation that some annual maximum rainfalls result from squall line activity is confirmed in chapter 7. Radar depictions of precipitation frequently reveal a tendency for heavy rainfall cells to form lines. A station pair oriented along the squall line would be expected to exhibit

higher coherence of simultaneous precipitation than stations aligned perpendicular to the line. If these lines have a preferred orientation, this should be taken into account in the analysis. To test for this feature, the relative mean and standard deviation (defined in chapter 3) of the annual maximum series of average rainfall at two stations were plotted against the distance between the pair of stations and the points identified with the direction of the line connecting the stations. Points are labeled with interstation directions between 90° and 270°. This was repeated for 1, 6, and 24 hr. Figures 2-2 and 2-3 are samples from this analysis. Inspection of figures 2-2, and 2-3 and similar plots for other durations shows no obvious pattern of persisting direction bias. This does not mean that individual storms do not exhibit directionally dependent variation and coherence, but rather that the direction of maximum coherence is not strongly fixed. Huff and Vogel (1976, p. 60) found that 80 percent of a set of heavy one-day storms at Chicago had orientations within an 80° span. From these results, we decided to stratify pairs of stations by distance only.

Table 2-1.--Chicago network precipitation recorders

Name	Index** no.	Letter identifier on fig. 2-1	Number of years used in study	Years station operated
Chicago Calumet Tr Wrks	1522	A	24	1941-73
Chicago Lakeview	1532	B	15	1941-65
Chicago Loyola Univ.	1537	C	17	1941-66
Chicago Mayfair PMP Sta.	1542	D	24	1941-
Chicago N Br. Pump Sta.	1547	E	17	1941-68
Chicago Roseland PMPG	1552	F	24	1941-
Chicago San. Dist. Disp.	1557	G	22*	1941-63
Chicago San. Dist. Off.	1562	H	23	1941-73
Chicago S. Filter Plant	1564	I	23	1948-
Chicago Springfield PMPG	1567	J	21	1941-
Chicago University	1572	K	22	1941-
Chicago Midway WSO AP	1577	L	24	1941-
Chicago WB City	1582	M	16	1941-64
Chicago O'Hare WSO AP	1549	-	0	1962-
Chicago Racine Pump	1557	P	*	1963-
Skokie	7990	R	24	1941-73
Stickney W Side Tr Wks	8278	T	23	1941-73
Crete	2011	U	16	1943-
Evanston Pumping Sta.	2888	V	18	1941-66
Lockport Power House	5136	W	21	1941-74

*G-P treated as one station. Gage relocated 1.6 mi SE March 25, 1963.
**Index numbers from "Climatological Data."

Table 2-2.--Years of record used in study

Station letter identifier	48	49	50	51	52	53	54	55	56	57	58	59	60	61	62	63	64	65	66	67	68	69	70	71	72
A		49	50	51	52	53	54	55	56	57	58	59	60	61	62	63	64	65	66	67	68	69	70	71	72
B		49	50		52	53	54	55	56	57	58	59	60	61	62	63	64								
C		49	50	51	52	53	54	55	56	57	58	59	60	61	62	63	64	65							
D		49	50	51	52	53	54	55	56	57	58	59	60	61	62	63	64	65	66	67	68	69	70	71	72
E		49	50	51	52	53	54	55	56	57	58			61	62	63	64		66	67	68				
F		49	50	51	52	53	54	55	56	57	58	59	60	61	62	63	64	65	66	67	68	69	70	71	72
G/P	48	49	50	51	52	53	54	55	56	57	58	59		61	62	63	64		66	67	68	69	70		72
H		49	50	51	52	53	54	55	56	57	58	59		61	62	63	64	65	66	67	68	69	70	71	72
I		49	50	51	52	53	54	55	56	57	58	59	60	61	62	63	64	65	66	67	68	69	70	71	
J		49	50		52	53	54	55	56		58	59	60	61	62	63	64	65	66	67		69	70	71	72
K		49	50	51	52	53	54	55	56	57	58	59	60	61	62	63	64	65	66	67	68	69		71	
L		49	50	51	52	53	54	55	56	57	58	59	60	61	62	63	64	65	66	67	68	69	70	71	72
M		49	50	61	52	53	54	55	56	57	58	59	60	61	62	63	64								
R		49	50	51	52	53	54	55	56	57	58	59	60	61	62	63	64	65	66	67	68	69	70	71	72
T	48	49	50	51	52		54	55	56	57	58	59		61	62	63	64	65	66	67	68	69	70	71	72
U		49	50	51	52	53	54	55			58	59	60	61		63		65		67			70		72
V		49	50	51	52	53	54	55	56	57	58	59	60	61	62	63	64	65	66						
W		49	50	51	52			55	56	57	58	59	60	61	62		64	65	66	67	68	69	70	71	72

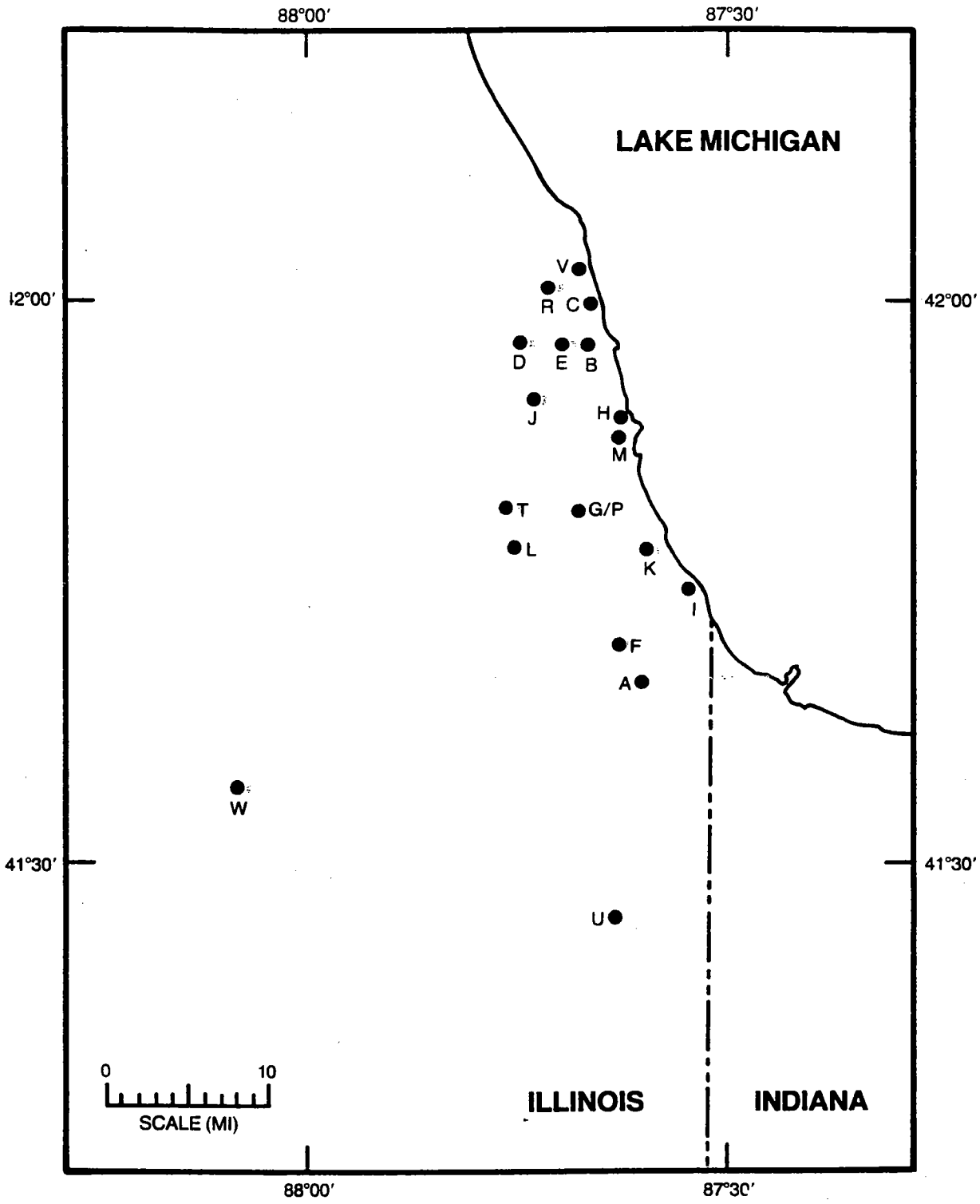

Figure 2-1.--Recording rain gage locations.

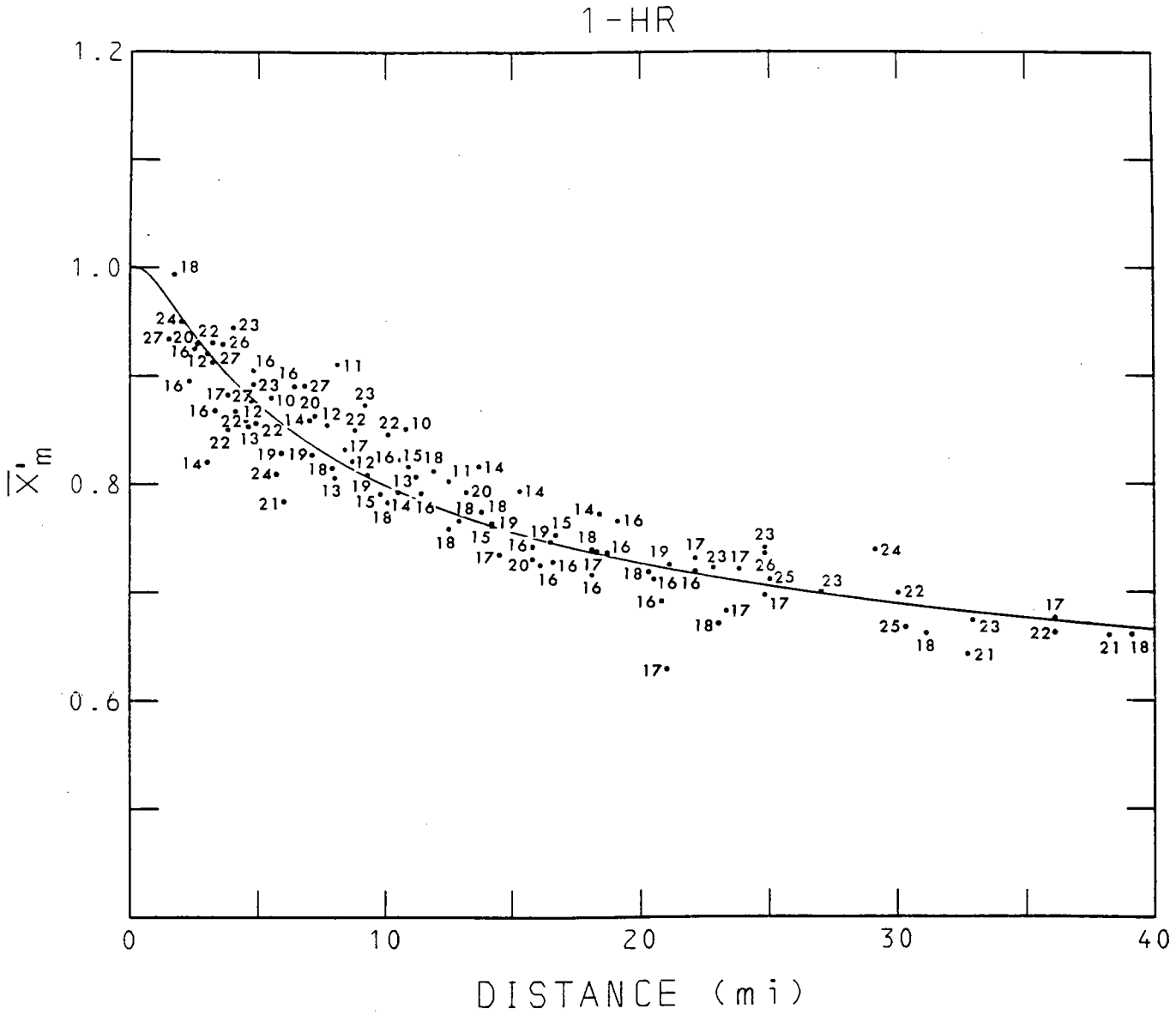

Figure 2-2.--Relative mean of annual series of two-station averages, 1-hr vs. interstation distance. Points identified with direction between stations. Same data as figure 3-1.

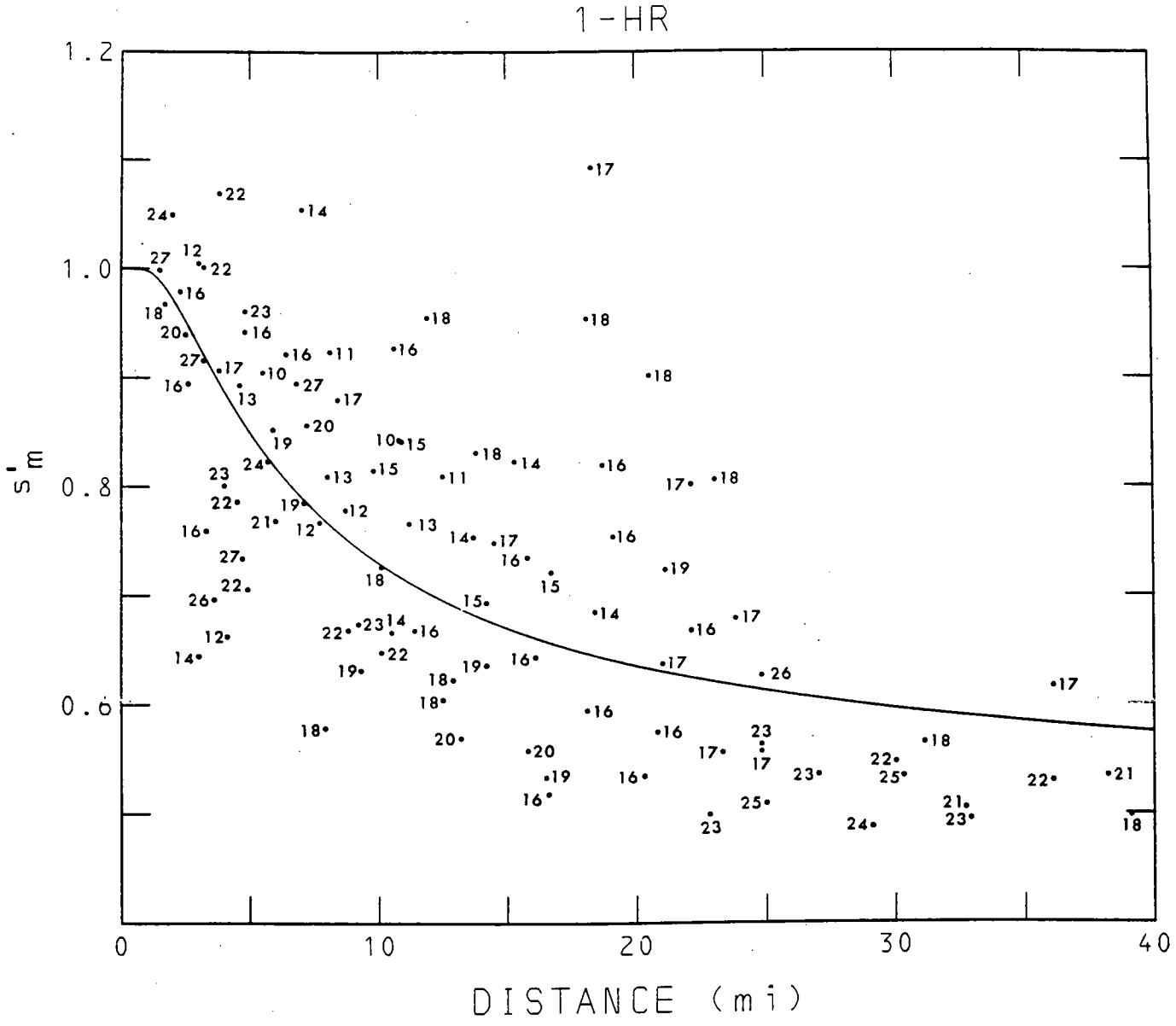

Figure 2-3.--Relative standard deviation of annual series of two-station averages, 1-hr vs. interstation distance. Points identified with direction between stations. Same data as figure 3-4.

CHAPTER 3. STATISTICS OF TWO-STATION AVERAGES

As a convention in this report, "average" refers to an average over points or areas and "mean" to an average over years, e.g., of an annual maximum series.

This chapter develops the first set of fitted surfaces referred to under "properties of the model" in chapter 1. That is, the first and second moments of the annual maximum series of station pair average rainfall are abstracted from the Chicago network data, normalized to a standard record length of 20 years (chapter 2), and smoothed in interstation distance and duration space by fitting surfaces to the data. Depth-length ratios (defined later in the chapter) are calculated from these surfaces. As an aid to later interpretations, the frequency of concurrence and nonconcurrence of the station pair annual maxima with annual maxima at the individual stations is investigated.

Data

The data for this part of the analysis were maximum rainfalls in 1, 2, 3, 6, 12 and 24 consecutive hours averaged over each of the 98 station pairs in table 3-1, abstracted from the edited hourly data for each April-October season (chapter 2). The station-pair list includes all available pairs with interstation distances of less than 4 mi, a selection from 4 to 25 mi to provide approximately uniform coverage with distance, and all pairs available for greater distances without the redundancy of repeating one station and displacing the second only a small fraction of the interstation distance. The April-October maxima are in lieu of the annual maxima which they approximate and hereafter will be referred to as such.

Normalizing

To reduce the order of sampling variation, all station pair moments are placed in relative form by dividing by the zero distance moments (average of the individual station moments). Thus, for a particular station pair,

$$\overline{X}'_m = \overline{X}_m / 0.5(\overline{X}_A + \overline{X}_B), \tag{3-1}$$

$$s'_m = s_m / 0.5(s_A + s_B). \tag{3-2}$$

Subscript m denotes a statistic of pair averages A and B the statistics of the individual stations. Arithmetic averaging was chosen rather than geometric averaging, e.g., $\overline{s} = (s_A\, s_B)^{1/2}$. The latter was found to give undue weight to occasional small values.

It turns out that the record length adjustment (chapter 2, appendix II) is redundant for the relative standard deviation, s'_m. Normalizing all factors in (3-2) for length of record by (II-1) produces no change, i.e.,

$$s'_{mN'} = s_{mN}\frac{\sigma_{N'}}{\bar{\sigma}_N} \Big/ 0.5\left(s_A \frac{\sigma_{N'}}{\bar{\sigma}_N} + s_B \frac{\sigma_{N'}}{\bar{\sigma}_N}\right) \equiv s'_{mN}. \qquad (3\text{-}3)$$

This is not true for the relative mean formula. (II-2) and (3-1) are applied in sequence.

Exponential Fitting Equations

Surfaces were fitted in the distance, d, and duration, Δt, domains to the 6 (durations) x 98 (pairs) = 588 relative means, $\bar{X}'_m$, and relative standard deviations, s'_m. Experimentation lead to fitting both surfaces to the exponential formulas

$$y(d) = 1 - 0.5e^{-[a(d/d_1)^b]^{-1}} \qquad (3\text{-}4)$$

at fixed Δt and

$$y(\Delta t) = y_o + (M - y_o)e^{-[g(\Delta t/\Delta t_1)^h]^{-1}} \qquad (3\text{-}5)$$

at fixed d, where $y = \bar{X}'_m$ or s'_m. These formulas have the desired property of zero derivatives at an abscissa of zero. Constants a and b are scaling and curvature parameters in the distance domain, varying with duration, and g and h in the Δt domain, varying with distance, dictated by the data. Parameters y_o and M have the theoretical form of limiting values of y in the time domain at $\Delta t = 0$ and $\Delta t \to \infty$, respectively, but are dictated by best fit. Limiting values in the distance domain are $y = 1.0$ at $d = 0$, by definition of $\bar{X}'_m$ and s'_m, and $y = 0.5$ as $d \to \infty$, for reasons detailed in appendix III. These limits are inherent in (3-4).

Surfaces of Best Fit

Surfaces of best fit of (3-4) and (3-5) to the 588 $\bar{X}'_m$ or s'_m values are obtained by the series of iterations detailed in appendix V. The definition of "best fit" is approximately the conventional one of minimizing $\Sigma(y - \hat{y})^2$, where $y(d,\Delta t)$ is an original data point and $\hat{y}(d,\Delta t)$ is the corresponding value on the surface. The precise definition of "best fit" is included in appendix V. Briefly, (3-4) is fit to group averages of the original data (appendix V) separately by duration; the durational curve, (3-5), fit to values at fixed distances from the (3-4) curves; (3-4) refit to values at fixed durations from these curves; and repeated to convergence. These fits require log log transformation (appendix IV) of (3-4) and (3-5).

30-Minute Values

A 30-min depth-area curve is published in Weather Bureau Technical Paper No. 40 (Hershfield 1961) and other reports and is desired as an output of the present project. The $\overline{X}'_m(d,\Delta t)$ and $s'_m(d,\Delta t)$ surfaces define the statistics in a mathematical sense at all $\Delta t > 0$, but are fit to data for which the shortest Δt is one hour. Thus, Δt = 30-min profiles on the surfaces lie in the extrapolated zone bounded by $0 < \Delta t < 1$ hour. Inspection of the 30-min profiles indicates they are reasonably reliable, meaning that the range of 30-min values that fit the data well is slight. 30-min values were abstracted from the first fit in the duration domain and included in the second fit in the distance domain, and 30 min is thereafter treated as a standard duration. The $\Delta t = 0$ profiles do not pass the "reasonably reliable" test defined above, and the y_o parameter in (3-5) should be regarded as a curve fitting constant, not a reliable estimate of $\overline{X}'_m(d,0)$ or $s'_m(d,0)$. The lower limit to reliable extrapolation of the surfaces in the duration domain was not determined. Evaluation of the statistics for durations less than 30 min should be based on short duration data from time-matched rain gage records (e.g., Huff 1967, 1-minute values) or single scan radar returns (e.g., Frederick et al. 1977a). See sppendix III for further discussion of limiting values.

Results

The $\overline{X}'_m(d)$ profiles from the fitted $\overline{X}'_m(d,\Delta t)$ surface are shown together with the original data points for durations of 1, 6, and 24 hr in figures 3-1 to 3-3. The data group averages for 5-mi intervals are also depicted by small circles. The corresponding $s'_m(d)$ profiles and data points are depicted in figures 3-4 to 3-6.

The complete sets of profiles of the two statistics in the two domains from the fitted surfaces are depicted, without data, in figures 3-7 and 3-8. The fitting constants are listed in appendix VII.

Depth-Length Ratios

The depth-length ratio is the same as a depth-area ratio (chapter 1), except that the numerator is a frequency value for a 2-station average rather than an areal or a multi-station average. Depth-length ratios are computed from $\overline{X}'_m$ and s'_m and presented here to portray much of the source of the variation of depth-area ratios (chapter 6) in three domains -- spatial, durational, and frequency.

The definition of the depth-length ratio, DL, for a particular frequency, duration, and length is

$$DL(f,\Delta t,d) = \frac{X_m(f,\Delta t,d)}{X_m(f,\Delta t,0)} \qquad (3\text{-}6)$$

We use Chow's (1951, 1964) general equation for frequency analysis,

$$X(f) = \overline{X} + K(f)\sigma_x, \tag{3-7}$$

where $X(f)$ is a magnitude of X at frequency f, $\overline{X}$ and σ_x the first and second moments of the population of X's, and $K(f)$ a frequency factor that depends on the form of the probability distribution and on frequency f. In our case

$$X_m(f,\Delta t,d) = \overline{X}_m(\Delta t,d,N) + K(f,N)s_m(\Delta t,d,N) \tag{3-8}$$

where $X_m(f,\Delta t,d)$ is the annual maximum 2-station average precipitation of frequency f, duration Δt, and interstation distance, d. The K factors for the Gumbel fitting of Fisher-Tippett Type I used in this study are derived and listed in appendix I. There K is sample size dependent and permits substituting $\overline{X}_m(N)$ and $s_m(N)$ from a sample of N years on the right of (3-8), but yields a population estimate of $X_m(f,\Delta t,d)$ on the left.

Substituting (3-8) at d = d and d = 0 in (3-6),

$$DL(f,\Delta t,d) = \frac{\overline{X}_m(\Delta t,d,N) + K(f,N)s_m(\Delta t,d,N)}{\overline{X}_m(\Delta t,0,N) + K(f,N)s_m(\Delta t,0,N)} . \tag{3-9}$$

Place (3-9) in relative form by dividing all the terms on the right by $\overline{X}_A$ and use the definition of coefficient of variation

$$cv_A = s_A/\overline{X}_A \tag{3-10}$$

and the identity

$$(s_m/\overline{X}_A) \equiv (s_m/s_A)(s_A/\overline{X}_A) \equiv s'_m\ cv_A.$$

This gives

$$DL(f,\Delta t,d) = \frac{\overline{X}'_m(\Delta t,d,N) + K(f,N)s'_m(\Delta t,d,N)cv_A(\Delta t)}{1 + K(f,N)cv_A(\Delta t)} . \tag{3-11}$$

The quantity $cv_A(\Delta t)$ is the coefficient of variation of annual maximum point rainfall over duration Δt. Values are listed in table 3-2 and are unweighted averages of the 15 stations within Chicago, A to T in figure 2-1. Each station cv_A at each Δt is evaluated by (3-10) using s_A and X_A normalized to 20 years, per appendix II. The cv_A's in the table are not smoothed. After increasing with duration monotonically to 6 hr, the value drops to a slightly lower magnitude at 12 hr. We suspect that this distribution is characteristic of the population rather than only of the sample, and hypothesize that annual maximum 6-hr storms are comprised of a combination of intense local convective storms and of some of the more intense general

storms, or thunderstorms embedded in general storms, thus the larger coefficient of variation. In any event, tests showed that DL in (3-11) is insensitive to small variations in cv_A. The lack of smoothness of cv_A over duration does not result in DL's that are not smooth.

Depth-length ratios for selected distances, durations, and frequencies are depicted in figures 3-9 to 3-11. These are evaluated from $\overline{X}'_m$ and s'_m surfaces by (3-11) together with cv_A values in table 3-2.

The reversal of the slope of the depth-length ratio vs. frequency apparent in figure 3-10, and also 3-9, is explained by examining the slope of $\overline{X}'_m$ and s'_m surfaces along the durational direction in figures 3-7 and 3-8, recalling that 2-yr values are dominated by the mean in (3-7) and 100-yr values by the standard deviation. The relative means increase rapidly with duration at short durations, then less rapidly. The relative standard deviations increase much less rapidly from 1 to 2 hr than the relative means, but then more rapidly at all other durations out to 24 hr. This combination results in the reversal of the slope of the DL vs. frequency curves between durations of 6 and 24 hr.

Composition of Two-Station Maxima

The make up of two-station average annual maxima is significant in understanding the makeup of areal average annual maxima. Three mutually exclusive composition possibilities for a two-station maximum are:

- both station values themselves annual maxima (**).
- either station value but not the other an annual maximum (*-).
- neither station value an annual maximum (--).

The composition probability in these terms of the X_m values that are the basic data for this chapter is shown in figure 3-12 for durations of 1, 6, and 24 hr. The unsmoothed count of the three compositions is plotted at the interstation distance average for data in 5-mi interstation bands (first band divided into 0-3 and 3-5 mi).

The (*-) category is generally the largest and grows with increasing distance and diminishing duration at the expense of the (**) category. That the (--) category is larger at certain distances at 6 hr than at either 1 hr or 24 hr is unexplained.

Table 3-1.--Station pairs for 2-station statistics

Stations*	Distance (mi)	Years of common record	Stations*	Distance (mi)	Years of common record	Stations*	Distance (mi)	Years of common record
B-E	1.5	13	F-L	8.0	24	B-F	18.1	15
H-M	1.7	15	K-T	8.1	20	C-I	18.1	17
R-V	2.0	18	A-K	8.4	22	E-F	18.3	17
C-V	2.3	17	G/P-I	8.7	20	D-I	18.4	23
B-C	2.5	15	L-M	8.8	16	A-J	18.7	21
L-T	2.6	22	H-T	9.2	22	D-F	19.1	24
A-F	3.0	24	J-L	9.3	21	I-R	20.3	23
C-R	3.0	17	I-M	9.8	16	C-F	20.5	17
C-E	3.2	14	D-T	10.1	22	I-V	20.8	18
D-E	3.2	17	H-L	10.1	23	A-E	21.0	17
D-J	3.3	21	F-T	10.5	22	I-U	21.1	15
G/P-T	3.6	21	M-R	10.6	16	A-D	22.1	24
E-J	3.8	15	I-L	10.8	23	F-R	22.1	24
E-R	3.8	17	J-K	10.9	19	L-W	22.8	21
G/P-L	4.0	21	A-L	11.2	24	F-V	23.0	18
G/P-K	4.1	19	H-I	11.4	22	A-V	23.3	18
D-R	4.5	24	F-M	11.9	16	L-U	23.8	15
I-K	4.6	22	D-L	12.5	24	A-R	24.8	24
B-D	4.7	15	I-T	12.5	21	A-W	24.8	21
B-H	4.8	14	G/P-R	12.9	21	T-W	24.8	20
B-J	4.8	14	B-L	13.2	15	F-W	25.0	21
G/P-M	4.9	15	A-T	13.7	22	G-W	27.0	18
H-J	5.5	20	F-H	13.8	23	K-W	29.1	19
F-I	5.7	23	D-K	14.2	22	J-W	30.0	18
F-K	5.9	22	R-T	14.2	22	I-W	30.3	20
A-I	6.0	23	A-M	14.5	16	H-U	31.1	15
B-M	6.4	15	I-J	15.3	20	D-W	32.7	21
K-L	6.8	22	C-L	15.8	17	H-W	32.9	20
C-J	7.0	15	F-J	15.8	21	D-U	36.1	16
J-R	7.1	21	B-I	16.1	15	R-W	36.1	21
J-T	7.2	19	L-R	16.5	24	V-W	38.2	15
D-H	7.7	23	K-R	16.6	22	R-U	39.1	16
H-K	7.9	21	E-I	16.7	17			

*Letters refer to fig. 2-1.

Table 3-2. Coefficient of variation, cv_A.

Duration (hr)	cv_A [a]
0.5	.3720[b]
1	.3720
2	.3808
3	.3894
6	.4316
12	.4254
24	.4420

a. Average of 15 stations, A to T in fig. 2-1. Computed from 20-year normalized $\overline{X}_A$ and s_A.

b. Extrapolated.

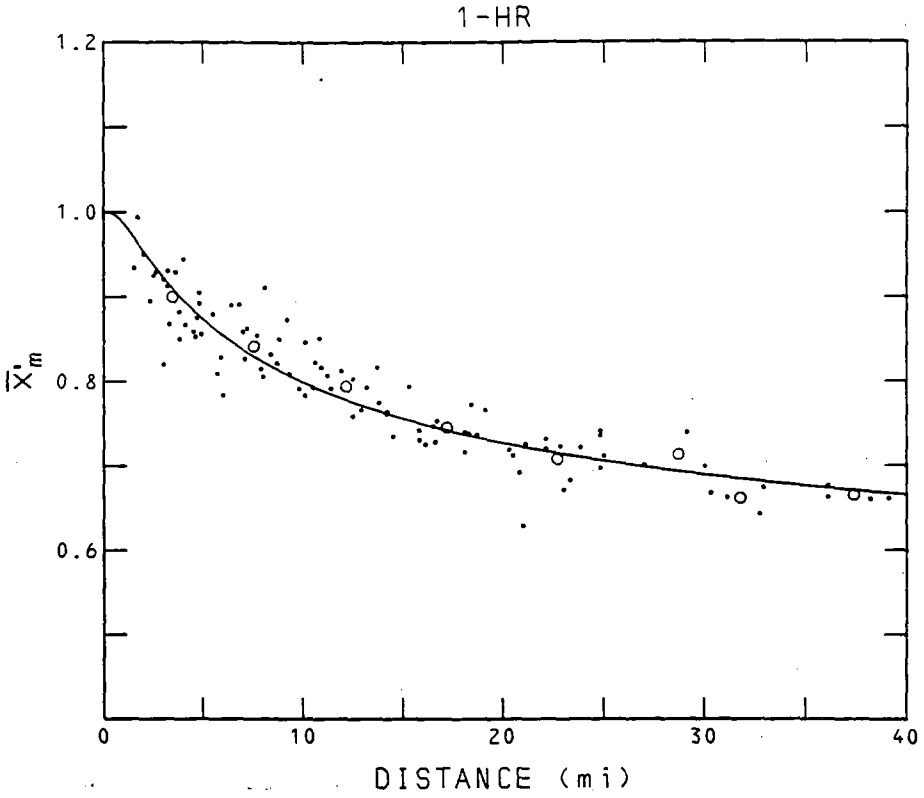

Figure 3-1.--Decay with interstation distance of relative mean of annual series of two-station averages, $\overline{X}'_m$, 1-hr.

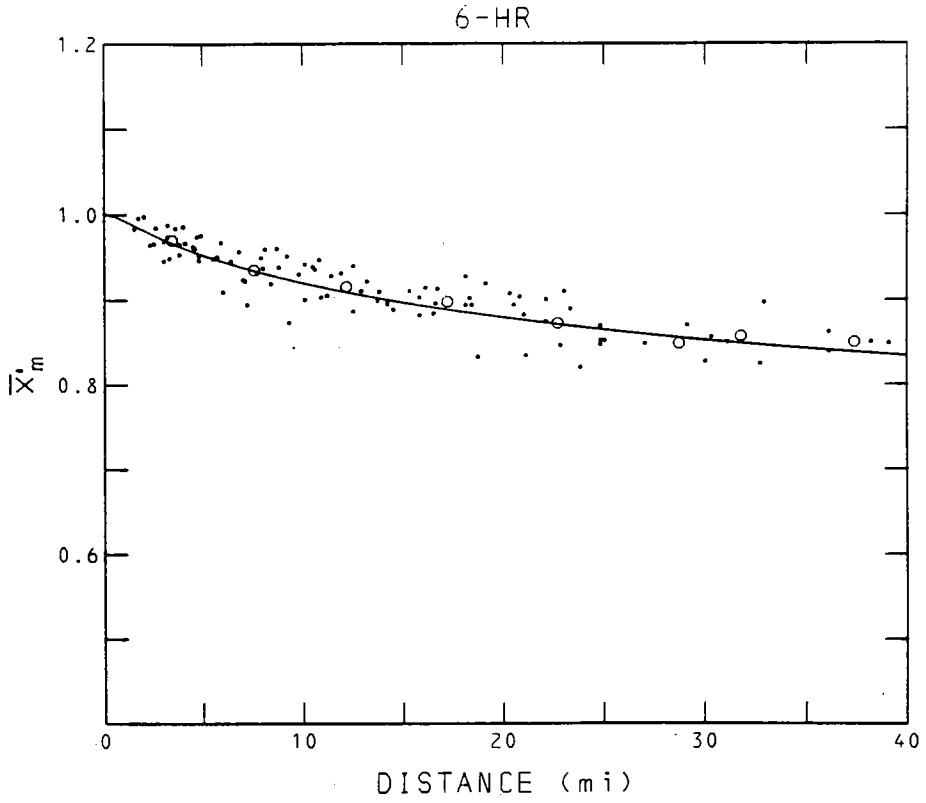

Figure 3-2.--Same as figure 3-1, 6-hr.

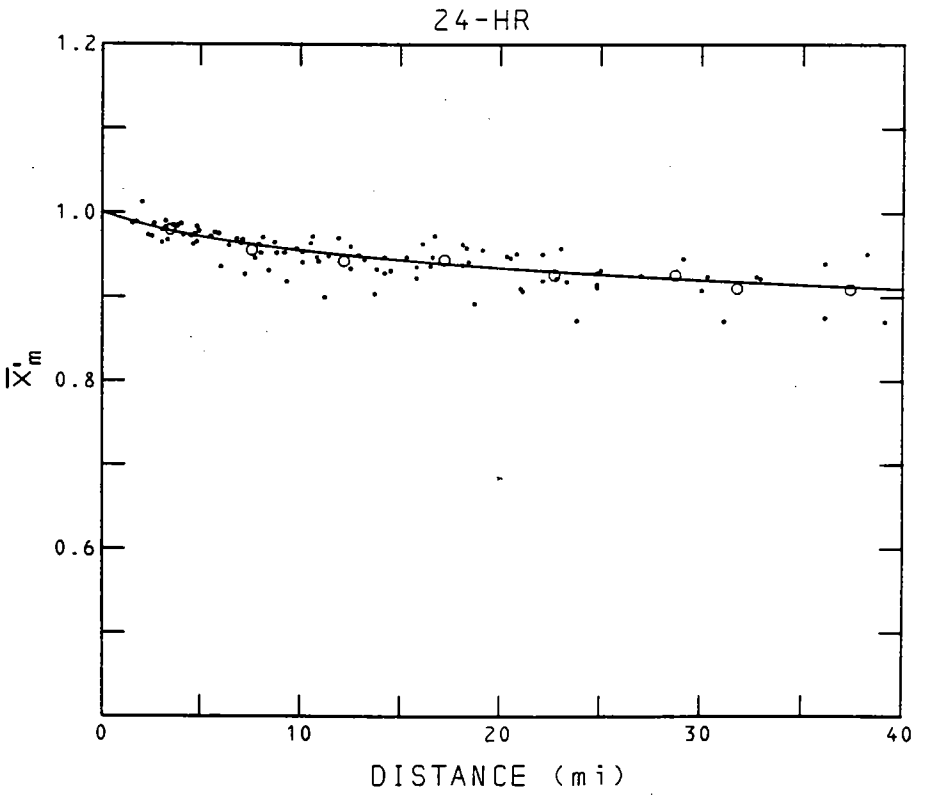

Figure 3-3.--Same as figure 3-1, 24-hr.

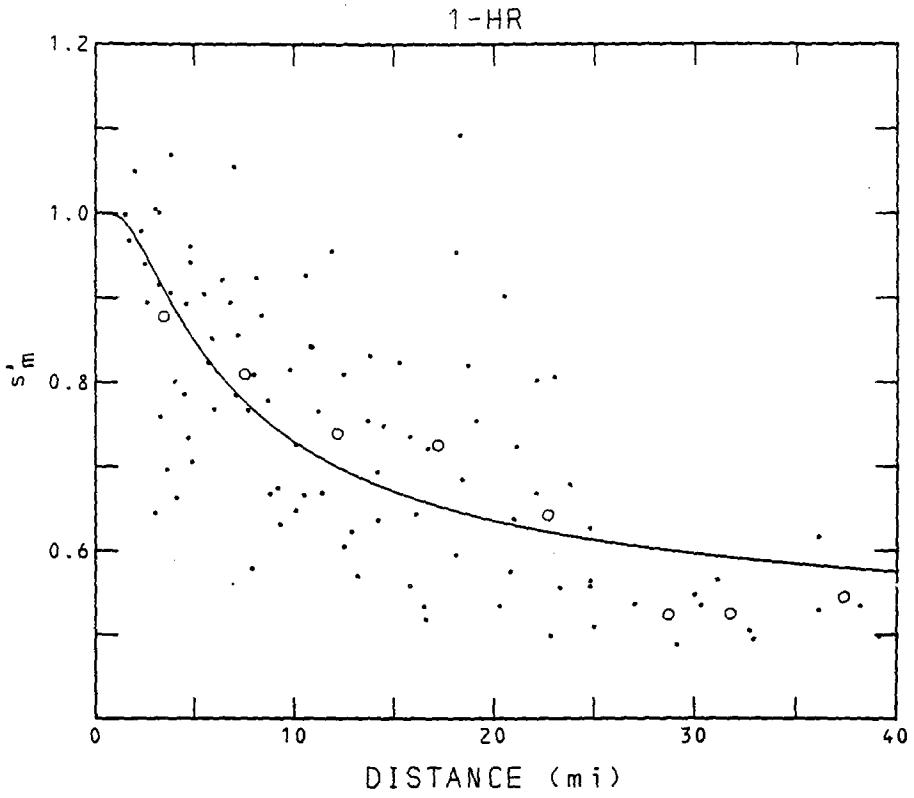

Figure 3-4.--Decay with interstation distance of relative standard deviation of annual series of two-station averages, s'_m, 1-hr.

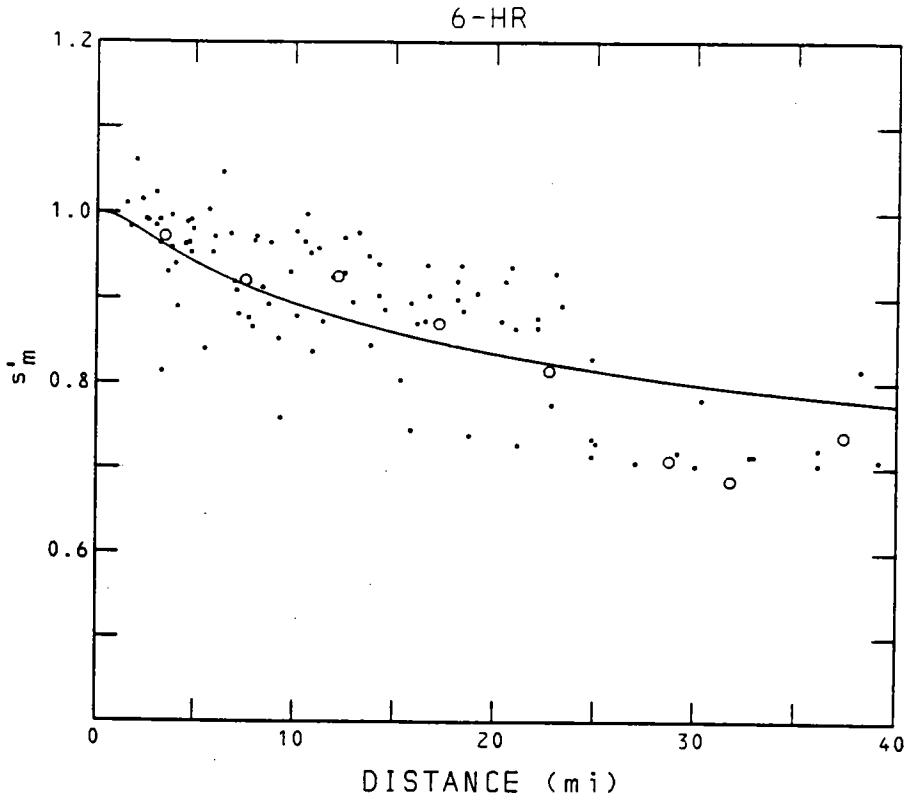

Figure 3-5.--Same as figure 3-4, 6-hr.

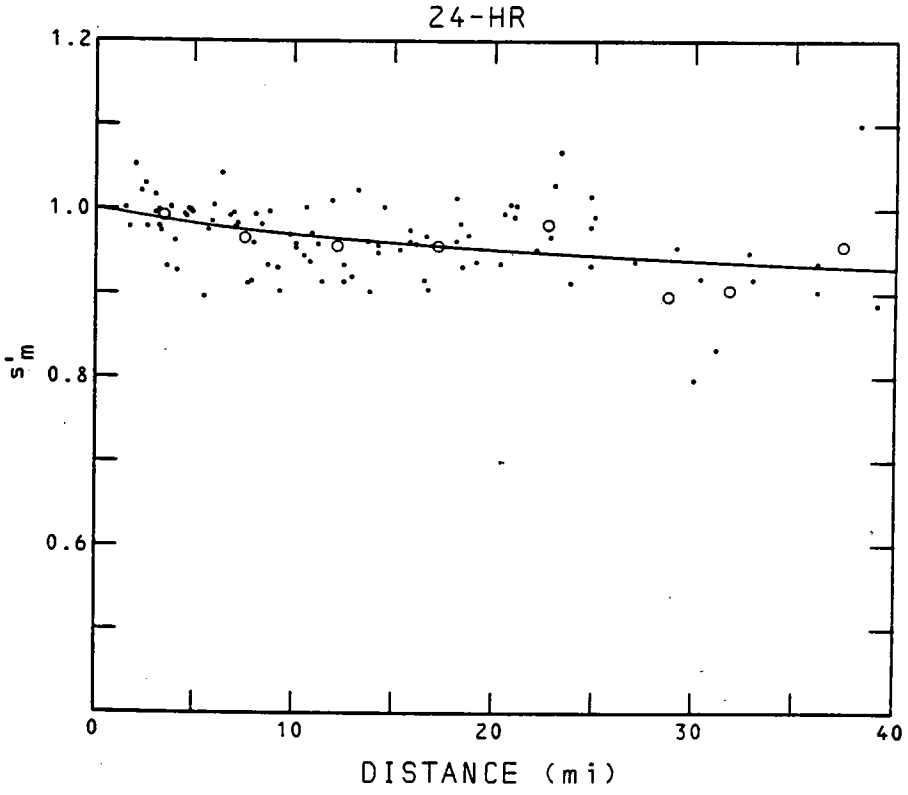

Figure 3-6.--Same as figure 3-4, 24-hr.

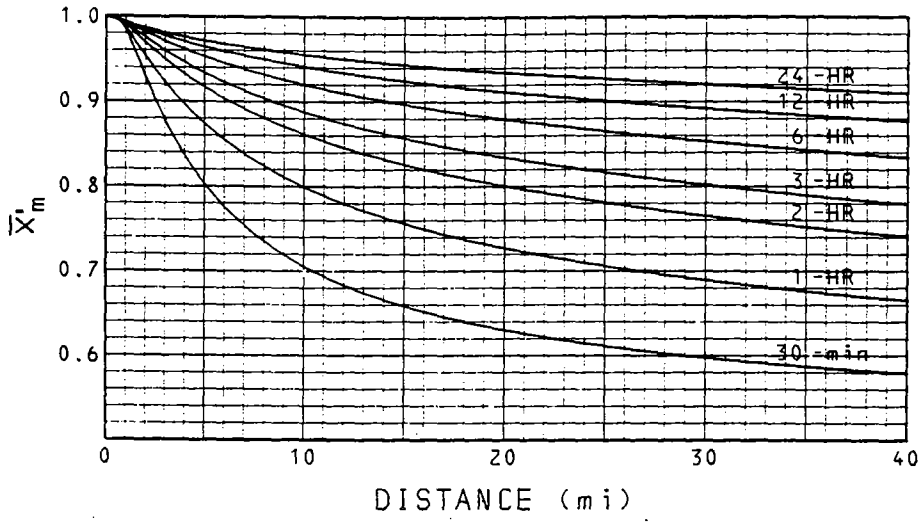

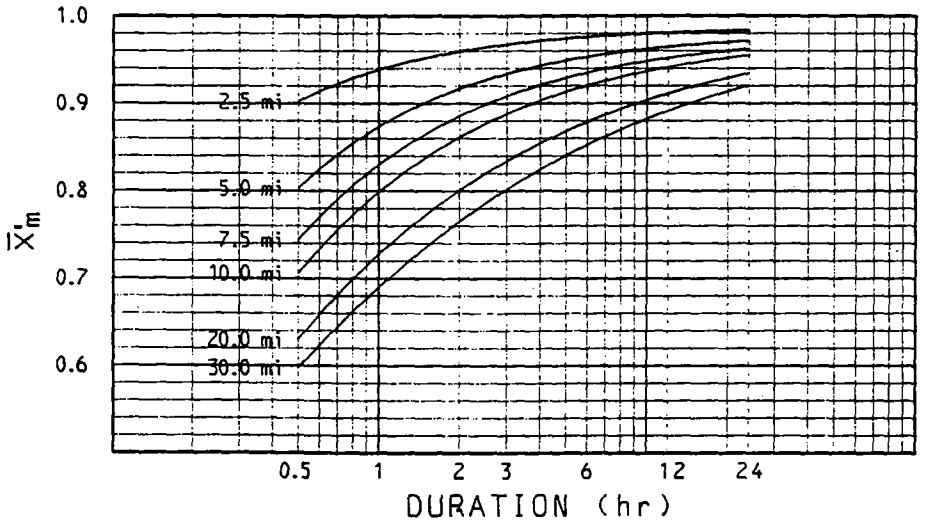

Figure 3-7.--Profiles over distance at constant duration and over duration at constant distance on $\bar{X}'_m$ surface.

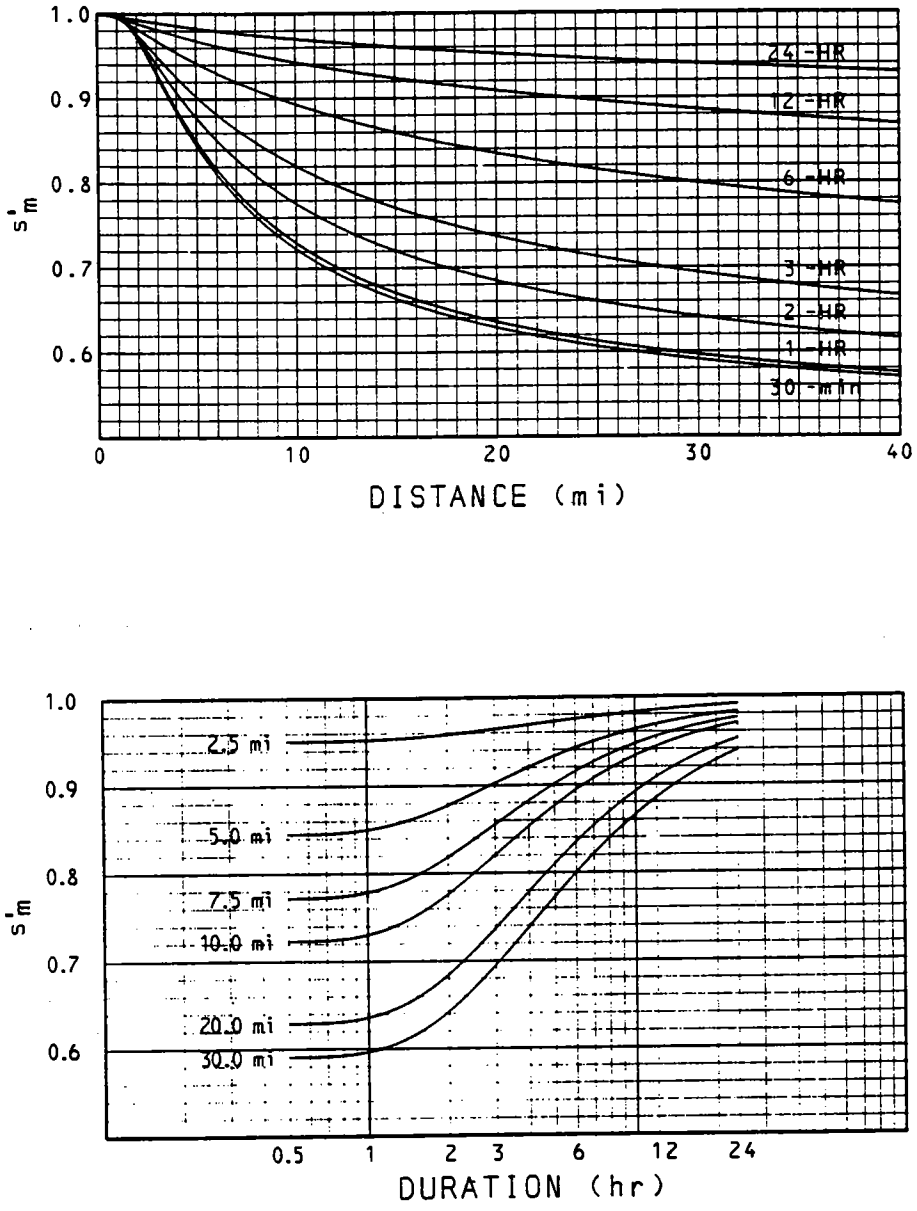

Figure 3-8.--Profiles over distance at constant duration and over duration at constant distance on s'_m surface.

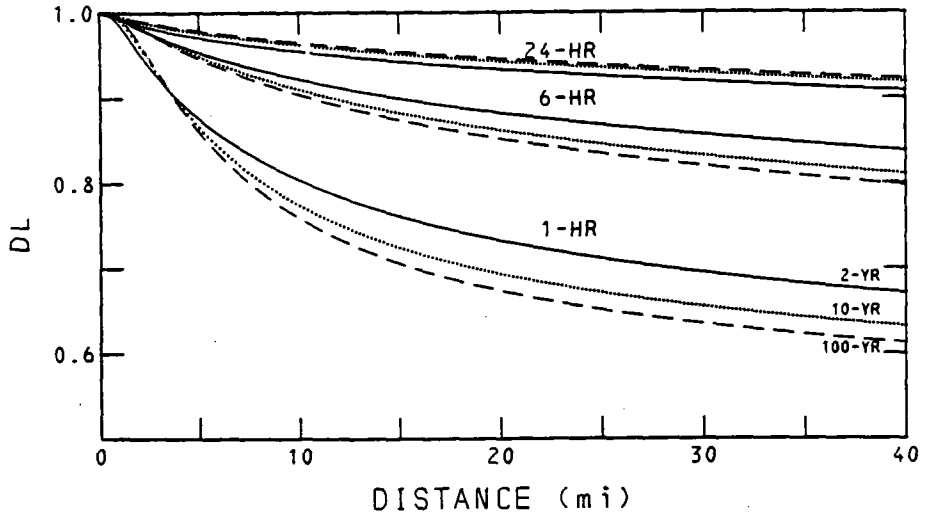

Figure 3-9.--Selected depth-length ratios in the distance domain.

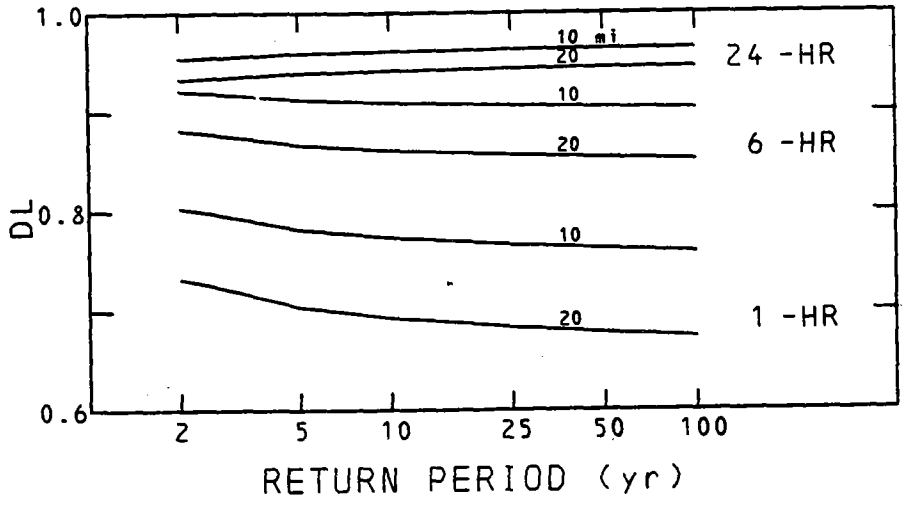

Figure 3-10.--Selected depth-length ratios in the frequency domain.

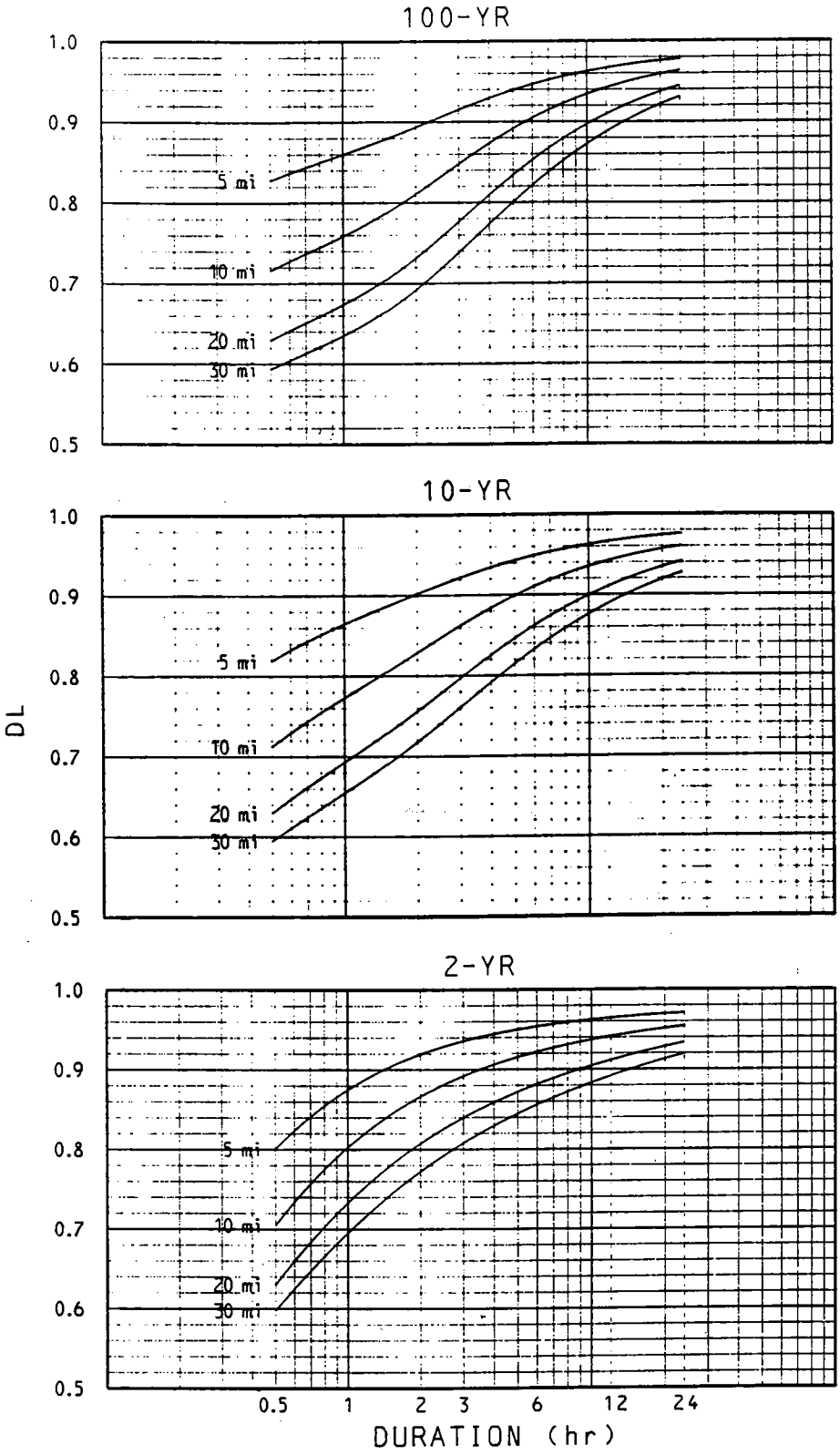

Figure 3-11.--Selected depth-length ratios in the duration domain.

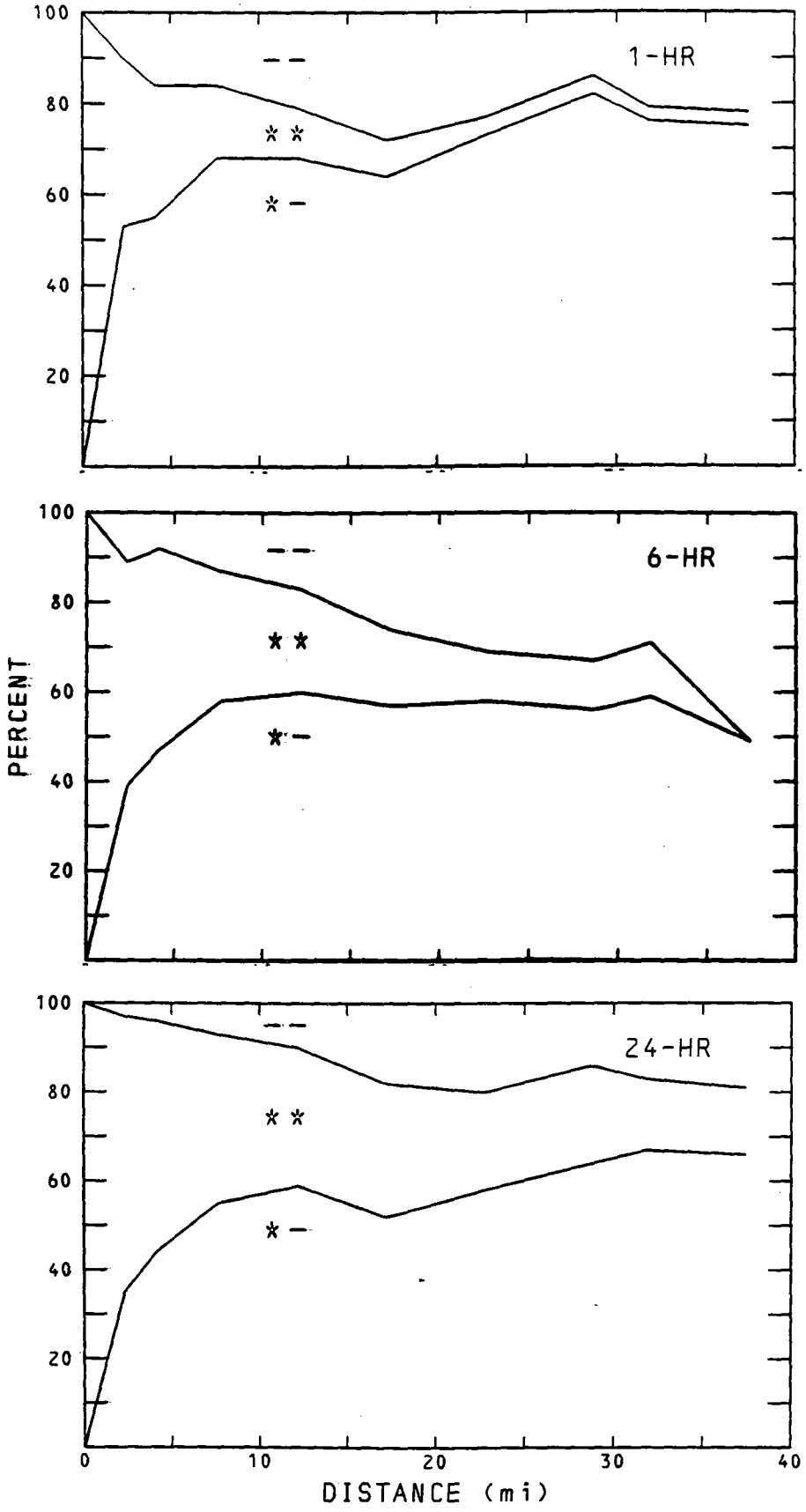

Figure 3-12.--Composition of two-station average annual maxima, X'_m, vs. interstation distance.

CHAPTER 4. STATISTICS OF RAINS SIMULTANEOUS WITH STATION MAXIMA

This chapter develops fitted surfaces for the statistics of the precipitation that falls at the second station simultaneously with annual maximum point rainfall at a first.

Relative Mean, $\overline{X}'_b$

When the annual maximum precipitation for a particular duration falls at a station, the simultaneous rainfall at a second station is a function of the interstation distance, the duration, and, presumably, the magnitude of the annual maximum at the first station. These simultaneous rainfalls form a series of N values in the same manner as the annual maximum series, where N is the number of years of record. The characteristics of the first moment of the series are assessed by fitting an $\overline{X}'_b(d,\Delta t)$ surface to data in a similar manner to $\overline{X}'_m(d,\Delta t)$ in chapter 3. The prime indicates relative to the corresponding zero interstation distance statistic as before, in this case the annual maximum rain with which it is simultaneous, i.e.,

$$\overline{X}'_b(d,\Delta t) \equiv \overline{X}_b(d,\Delta t)\Big/\overline{X}_b(0,\Delta t) \equiv \overline{X}_b(d,\Delta t)\Big/\overline{X}_A(\Delta t). \qquad (4\text{-}1)$$

The foregoing is conceptual. For a station pair, assuming climatic homogeneity, there is no reason to choose one station over the other as "annual maximum" or "simultaneous." Our computational definition of $\overline{X}'_b$ for a station pair is

$$\overline{X}'_b = 0.5 \left[(\overline{X}_b/\overline{X}_A) + (\overline{X}_a/\overline{X}_B)\right] \qquad (4\text{-}2)$$

where the subscript on the left signifies "simultaneous with annual maximum" in general, and the subscripts on the right signify stations A and B explicitly, with upper case subscripts designating annual maximum and lower case subscripts simultaneous with annual maximum. All bars denote mean over available years.

An $\overline{X}'_b(d,\Delta t)$ surface was fitted to the $\overline{X}'_b$ values computed by (4-2) for the 98 station pairs in table 3-1 for six durations in exactly the same manner as for $\overline{X}'_m$ (chapter 3), using the group average procedure, except that the fitting equation in the distance domain is now

$$\overline{X}'_b(d) = 1 - e^{-\left[a(d/d_1)^b\right]^{-1}} \qquad (4\text{-}3)$$

since the limit $\overline{X}'_b(\infty)$ differs from $\overline{X}'_m(\infty)$ (appendix III). Equation (3-5) is the fitting relationship in the duration domain. Details of the fitting routine are outlined in appendix V. The results of the fit are depicted in figures 4-1 to 4-5.

Relative Standard Deviation, s'_b

The relative standard deviation of a series of simultaneous rains for a

station pair for a particular duration is computed from

$$s'_b = \left[(s_b / s_A)(s_a / s_B) \right]^{1/2} \tag{4-4}$$

where the notation is analogous to that in (4-2). The small value problem alluded to in chapter 3 did not show up here.

The s'_b statistic is unique among the statistics evaluated in this study in that it does not vary monotonically with increasing interstation distance from d = 0. Plots of the 98 s'_bs for 1, 6, and 24 hr reveal increases to a maximum value greater than 1.0, followed by decreases, figures 4-6 to 4-8. This unique behavior is explained by considering the coefficient of variation

$$cv_b = s_b / \overline{X}_b. \tag{4-5}$$

Adding terms to (4-5),

$$\frac{s_b}{s_A} = \frac{cv_b}{s_A} \overline{X}_A \frac{\overline{X}_b}{\overline{X}_A} \tag{4-6}$$

and substituting the definitions,

$$s_b \equiv s_b / s_A;\ cv'_b \equiv cv_b / cv_A \equiv cv_b \overline{X}_A / s_A;\ \overline{X}'_b \equiv \overline{X}_b / \overline{X}_A$$

leads to a definition of the relative standard deviation in terms of the relative covariance and relative mean,

$$s'_b = cv'_b\ \overline{X}'_b. \tag{4-7}$$

The rise and fall of s'_b with increasing distance is the net effect of a monotonic decrease of $\overline{X}'_b$, already established, and a monotonic increase of cv'_b. To explain the latter, at small distances the simultaneous rain can range from a value larger than the maximum annual rain at the other station to much smaller; that is, the variance and the coefficient of variation increase with interstation distance initially. At larger distances the behavior of cv'_b is less clear. The limit at $d \to \infty$ is discussed in appendix III. In any event, as an empirical fact cv'_b increases monotonically from 1.0 with increasing interstation distance within the range analyzed in this study. Group average points are shown in figure 4-9 for three durations. We can take advantage of this monotonic variation of cv'_b to fit s'_b to data indirectly, as outlined in the next paragraph.

Relative coefficient of variation, cv'_b.

Group average values of cv'_b were computed from group average values of $\overline{X}'_b$ and s'_b by (4-7) and a $cv'_b(d, \Delta t)$ surface fitted by the iteration procedure used for other statistics (appendix V).

The fitting equation in the distance domain is

$$cv'_b(d) = 1 + M\left[1 - e^{-a(d/d_1)^b}\right] \qquad (4\text{-}8)$$

where a and b are the data-dictated curvature and scaling parameters and M a limit parameter without physical significance (limiting values of statistics are discussed in appendix III. The fitting equation in the duration domain is the same as for the other statistics, (3-5). The profiles resulting from this fit are depicted in figures 4-10 to 4-11. The reversal of the slope of the curves from the other statistics is taken care of in using (3-5) by the fact that the value of the zero duration intercept, y_o, is now larger instead of smaller than the value of the effective large duration asymptote, M. Profiles of s'_b in the distance and duration domains are computed by (4-7) from the respective $\overline{X}'_b$ and cv'_b profiles in figures 4-4 and 4-5, and 4-10 and 4-11. These are depicted in figures 4-12 and 4-13.

Relative Covariance, cov'_{Ab}

The relative covariance of simultaneous rain with annual maximum rain, cov'_{Ab}, is the final two-station statistic required for later use. This statistic measures the tendency of the larger (or smaller) simultaneous rains to be associated with the larger (or smaller) annual maxima. The definition of this covariance in a general sense is

$$cov_{Ab} = (1/N)\Sigma(X_A - \overline{X}_A)(X_b - \overline{X}_b) \qquad (4\text{-}9)$$

and of relative covariance

$$cov'_{Ab} = cov_{Ab}/s_A^2. \qquad (4\text{-}10)$$

The average relative covariance for a station pair is computed from

$$cov'_{Ab} = 0.5\left[(cov_{Ab}/s_A^2) + (cov_{aB}/s_B^2)\right] \qquad (4\text{-}11)$$

where, as before, subscripts on the left are general and on the right refer to specific stations.

Another method of averaging based on another definition of covariance,

$$cov_{Ab} = \rho_{Ab} s_A s_b \qquad (4\text{-}12)$$

where ρ_{Ab} is the correlation coefficient, was tested and found to give averages that in general are essentially equivalent to those from (4-11). Eq. (4-11) was used.

This covariance is expected to become essentially zero at some interstation distance (appendix III). Plotted data indicate the cov'_{Ab}, in common with many covariances and autocorrelations, (e.g., Townsend 1976) can cross to

negative values with increasing d before returning towards zero. This crossover is illustrated in figure 4-14 for the 1-hr duration. The data do not extend to large enough distances to define the expected return to zero. The fitting equation in the distance domain is

$$cov'_{Ab} = 1 - Me^{-[a(d/d_1)^b]^{-1}}, \qquad (4\text{-}13)$$

where M is a fitting parameter of convenience. The fitting equation in the durational domain is the same as for the other statistics, (3-5).

Fits to cov'_{Ab} data by the group average procedure are illustrated for 1, 6, and 24 hr in figures 4-14, 4-15, and 4-16 (solid curves). Profiles of covariances and autocorrelations in a spatial domain generally have the shape of the 24-hr curve in figure 4-16, bell-shaped around zero distance and an inflection point in the profile at an appreciable distance. On the 1-hr curve (fig. 4-14) the inflection point is so close to the origin that the bell shape is imperceptible to the eye, and values of cov'_{Ab} from the curve in the distance range of about 1 to 2 miles are significantly lower than they would be on a fitted curve of more traditional shape. Tests showed that these low values have a noticeable effect on depth-area ratios for small areas computed by the methods to be presented in chapters 5 and 6. We concluded that a more traditional bell shape should be imposed in compensation for the lack of data at distances of less than 3 miles. One method of doing this would be to modify the fitting formula to include another constant. In lieu of this, a new profile defined by (4-13), with b fixed at 1.0, is spliced from d = 0 to $d = d_s$, a selected short distance. The new segment has the same ordinate and the same slope as the original curve at d_s. These two degrees of freedom lead to a calculation of a and M for the spliced segment. This was done for durations of 0.5 to 3 hr, with d_s equal to 3.45 mi, the abscissa of the first group average. The spliced segment for 1 hr is shown by the dashed curve in figure 4-14. For details of the splicing procedure, see appendix VI.

Profiles of cov'_{Ab} in the distance and duration domains are depicted in figures 4-17 and 4-18, respectively. Both were obtained by the standard procedure of fitting to (4-13), then splices substituted on the distance domain profiles inside of 3.45 mi for the indicated durations. The duration profiles were adjusted by hand to agree.

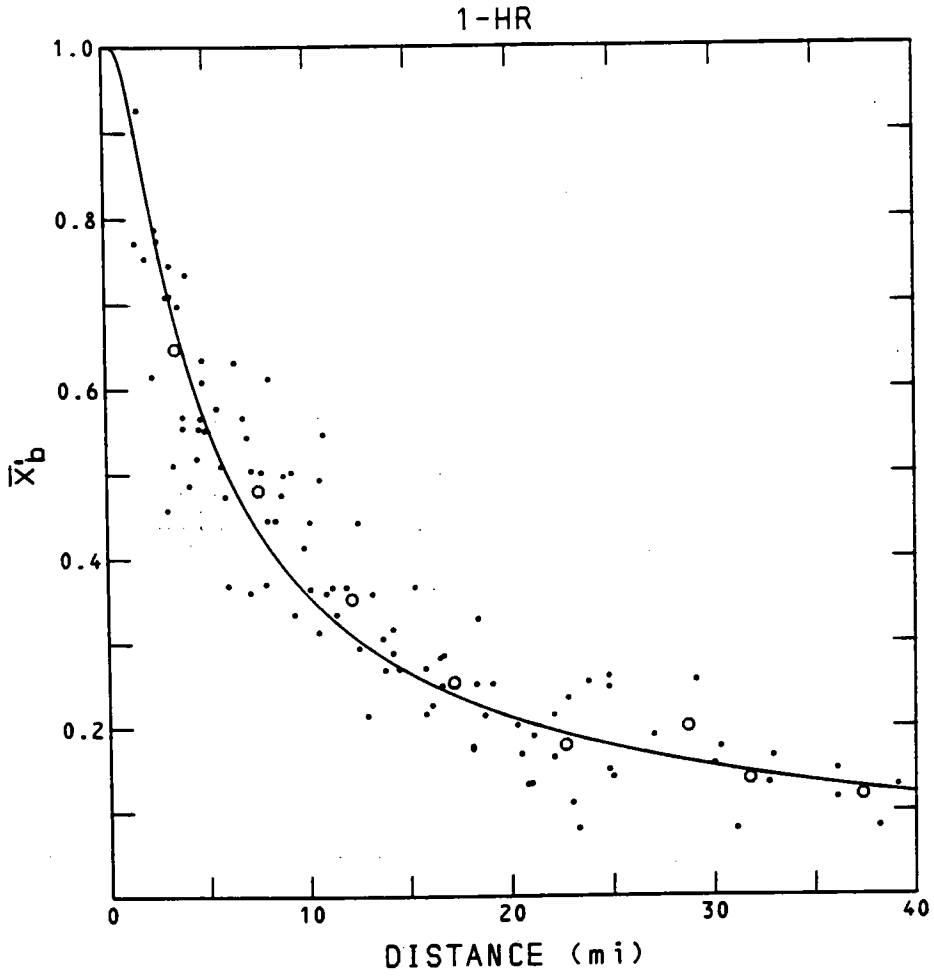

Figure 4-1.--Decay with interstation distance of relative mean of simultaneous rains, $\bar{X}'_b$, 1-hr.

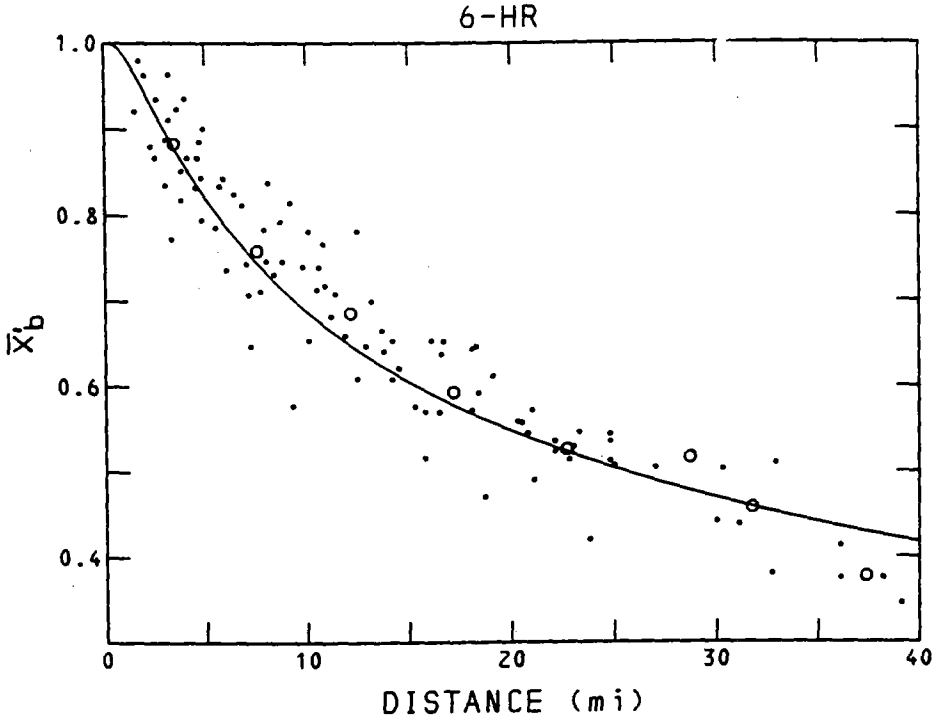

Figure 4-2.--Same as figure 4-1, 6-hr.

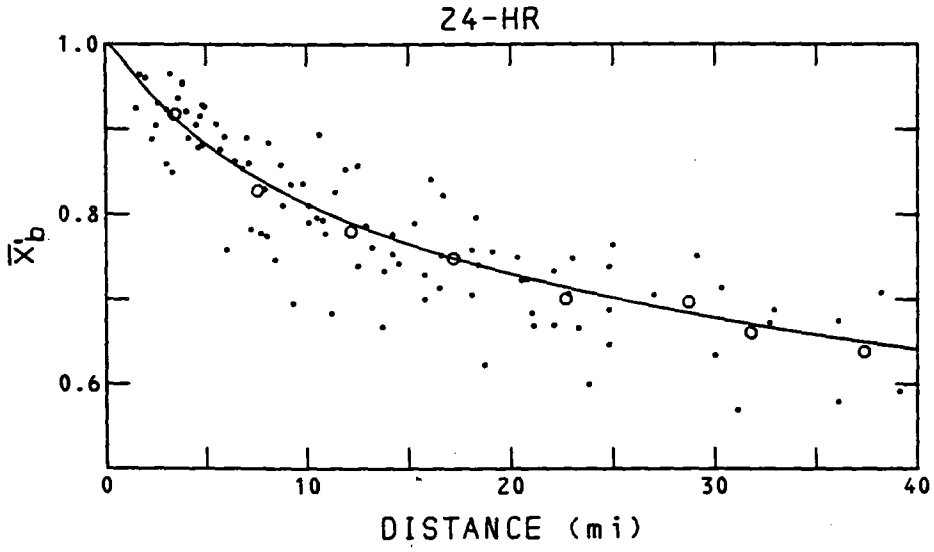

Figure 4-3.--Same as figure 4-1, 24-hr.

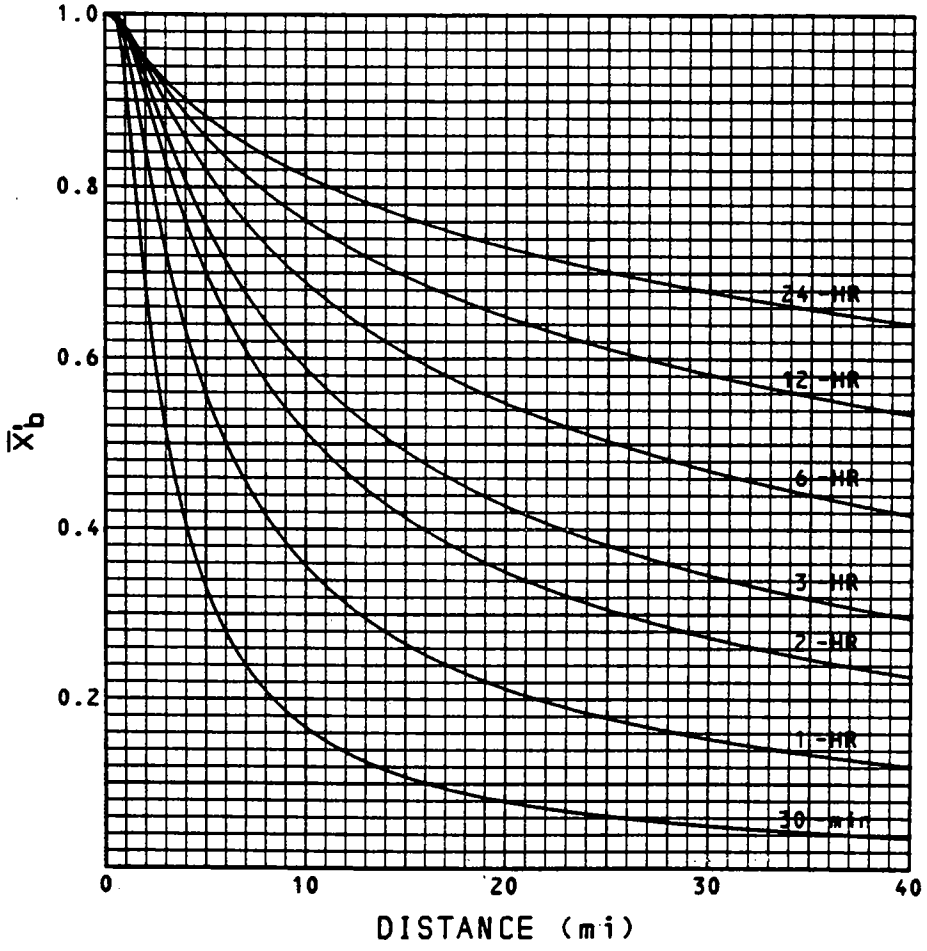

Figure 4-4.--Profiles over distance at constant duration on $\bar{X}'_b$ surface.

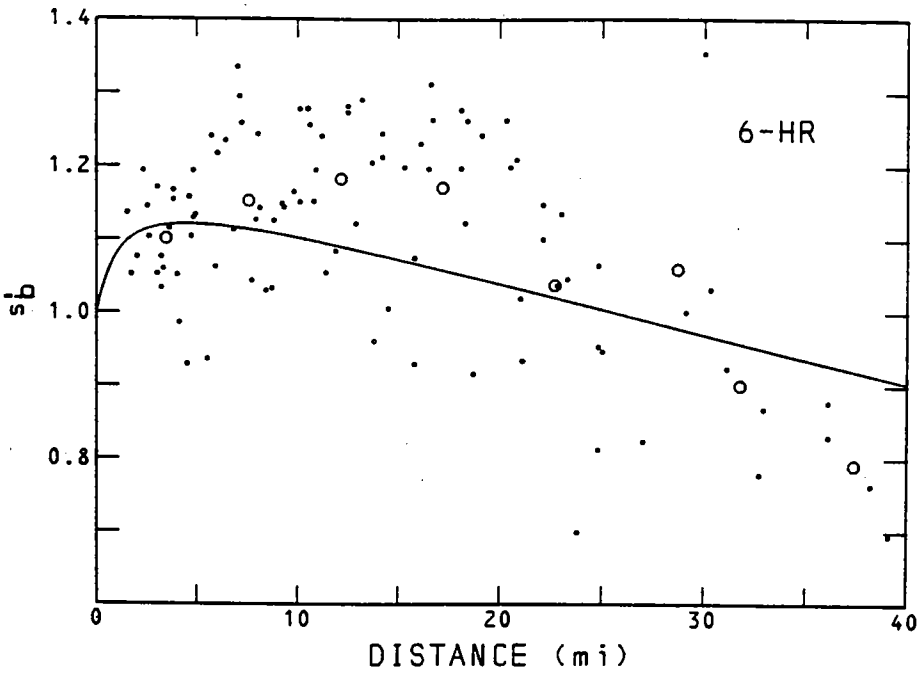

Figure 4-7.--Same as figure 4-6, 6-hr.

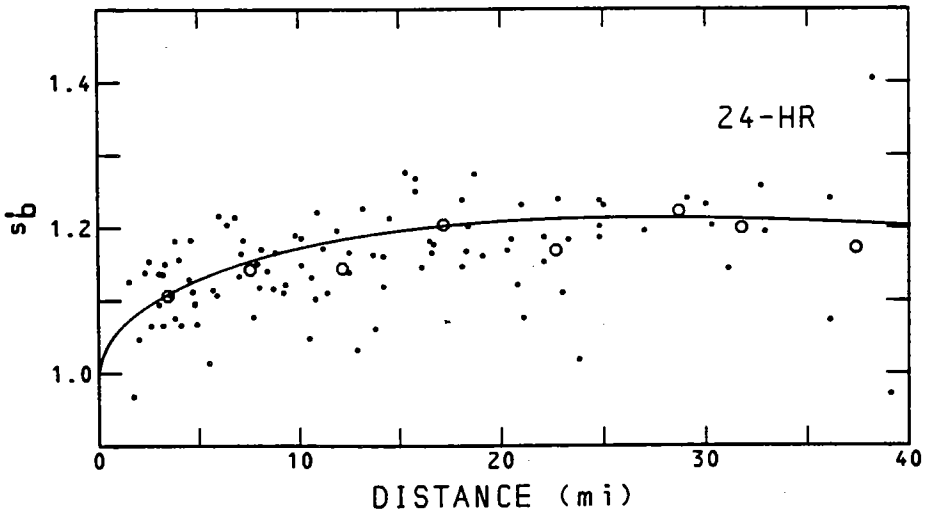

Figure 4-8.--Same as figure 4-6, 24-hr.

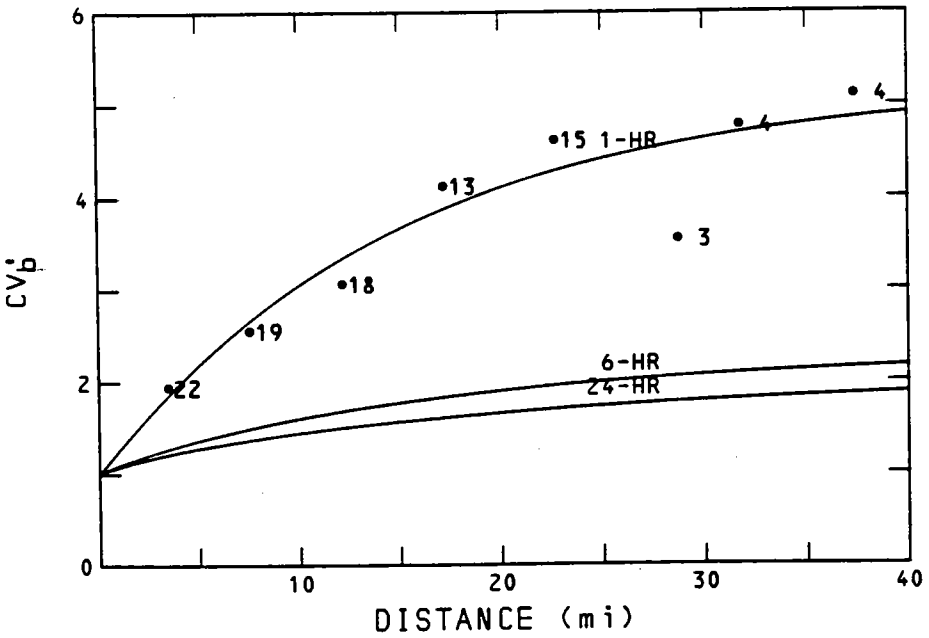

Figure 4-9.--Variation with interstation distance of relative coefficient of variation of simultaneous rains, cv_b', 1-, 6-, and 24-hr.

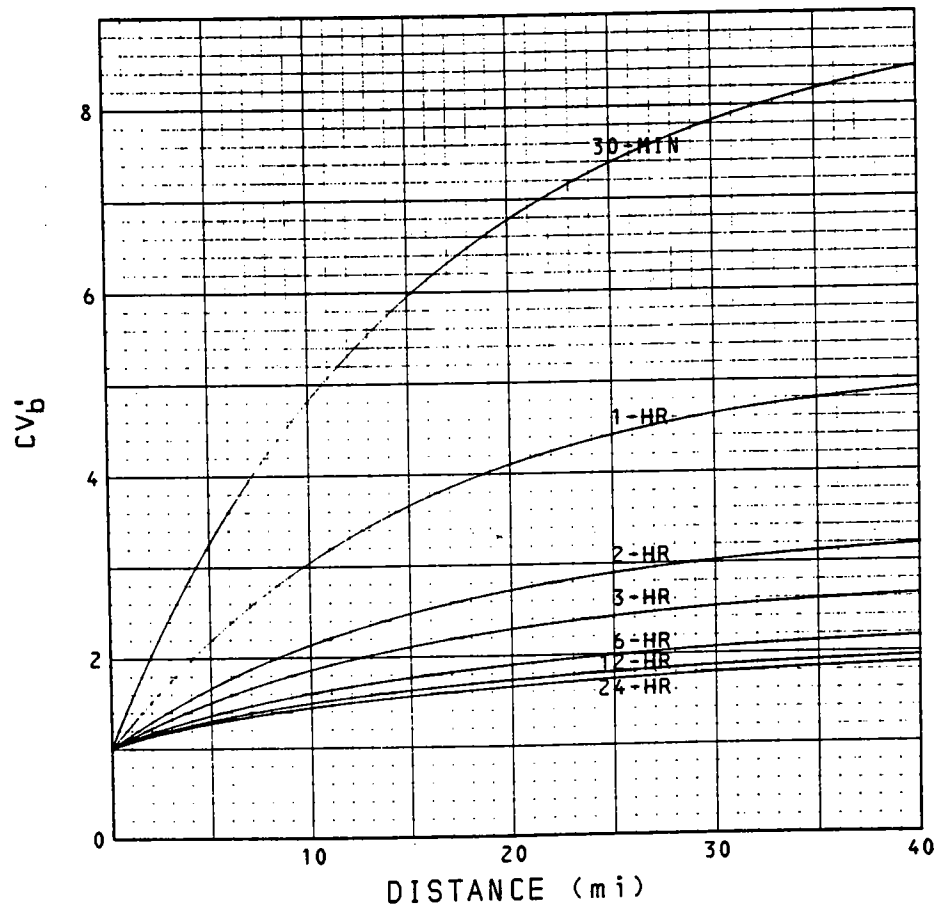

Figure 4-10.--Profiles over distance at constant duration on cv_b' surface.

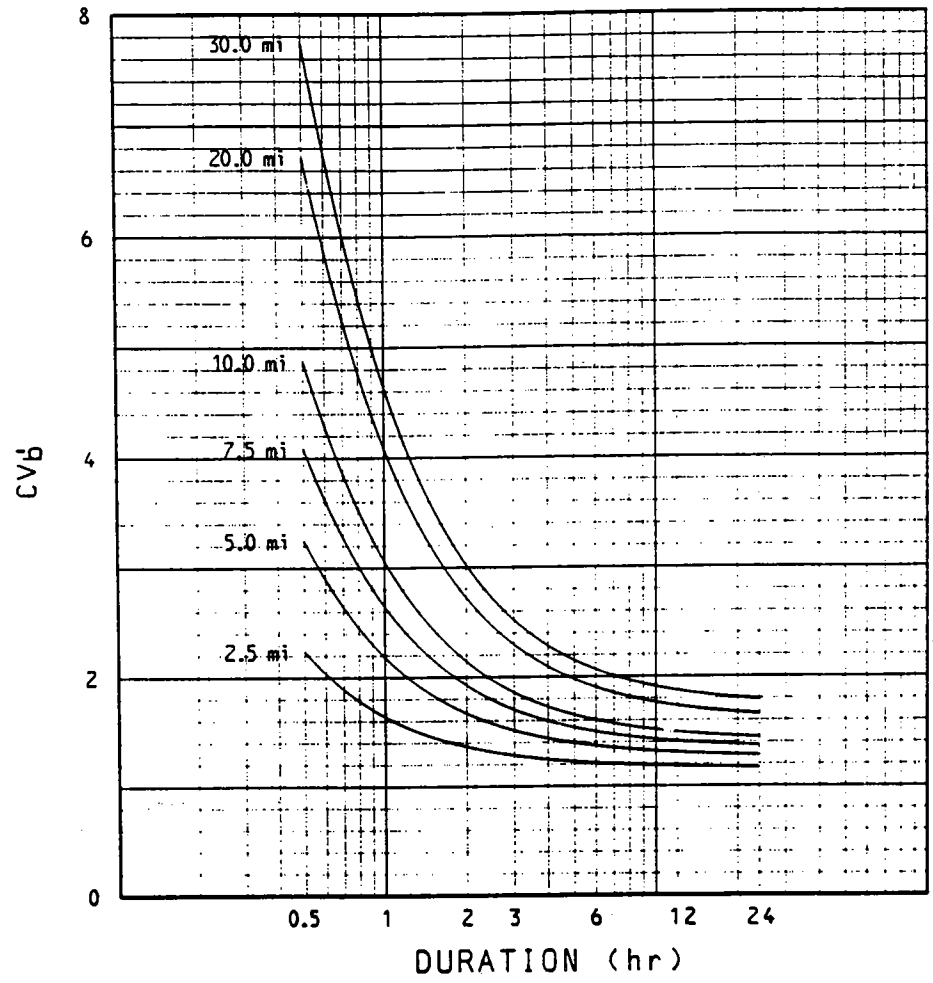

Figure 4-11.--Profiles over duration at constant distance on cv_b' surface.

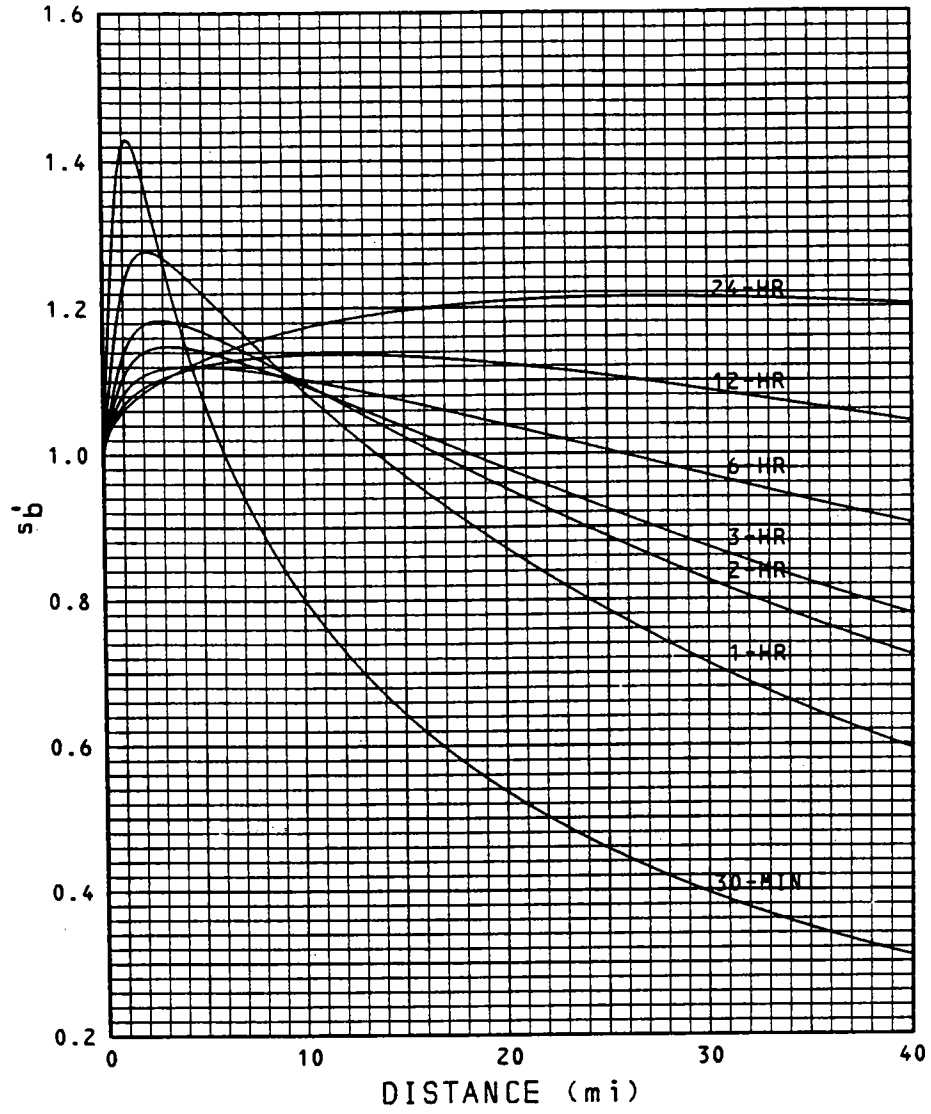

Figure 4-12.--Profiles over distance at constant duration on s'_b surface.

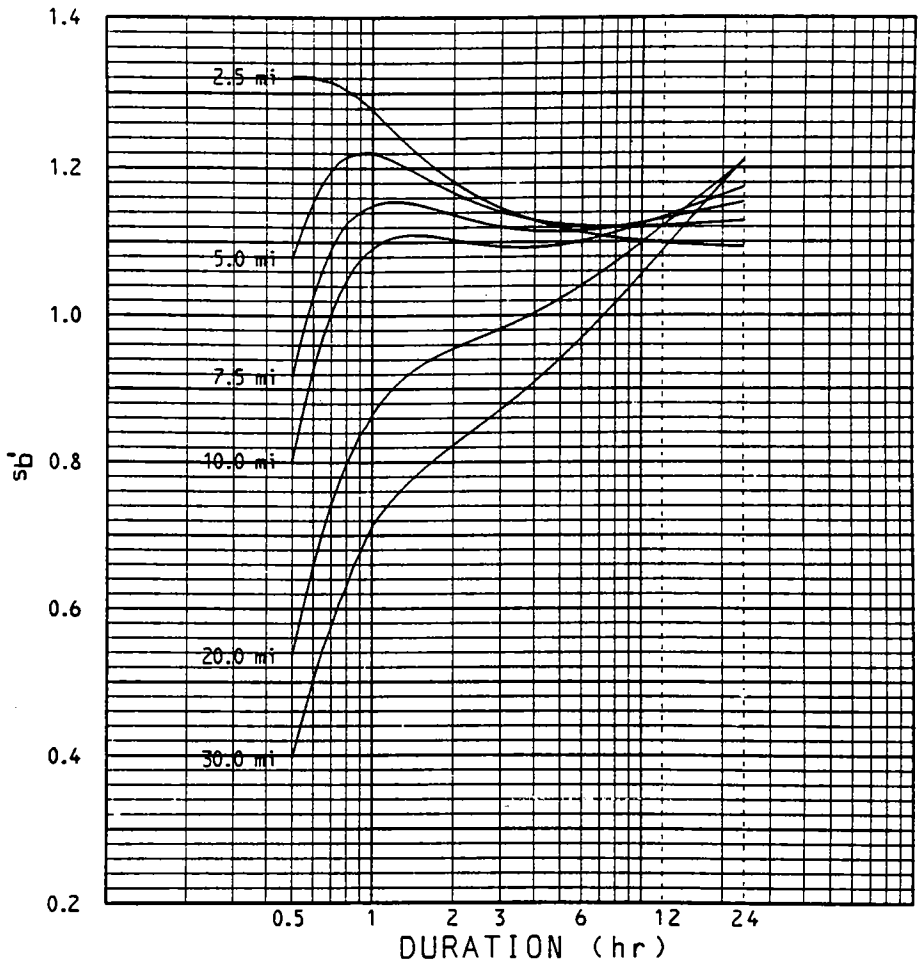

Figure 4-13.--Profiles over duration at constant distance on s_b' surface.

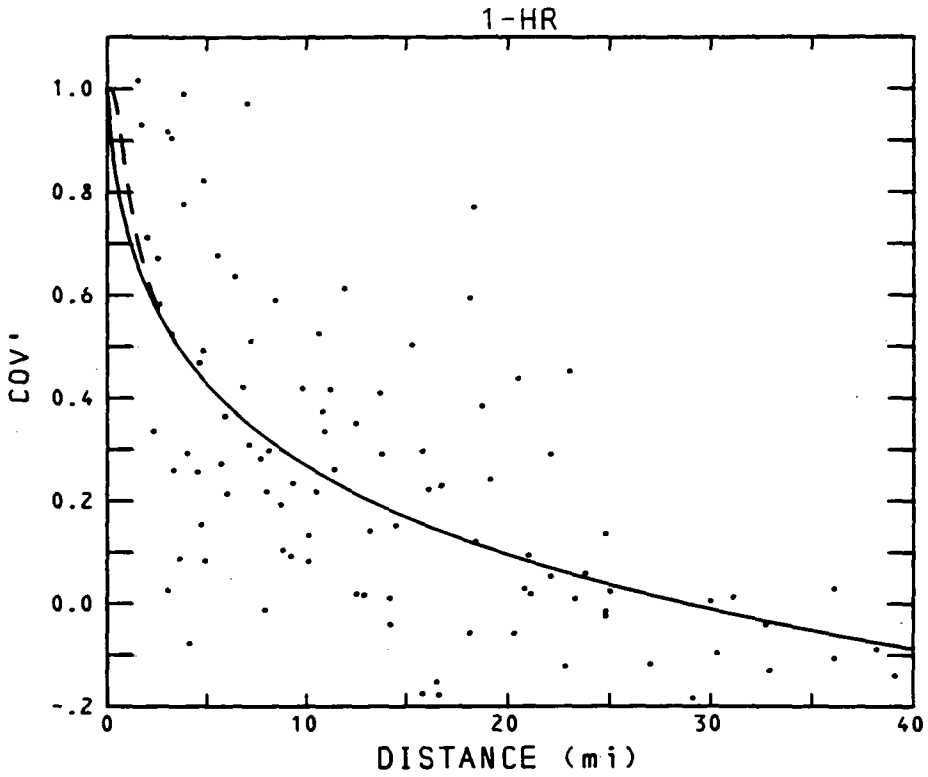

Figure 4-14.--Variation with interstation distance of relative covariance of maximum annual point rainfall and simultaneous rain at a second point, cov'_{Ab}, 1-hr.

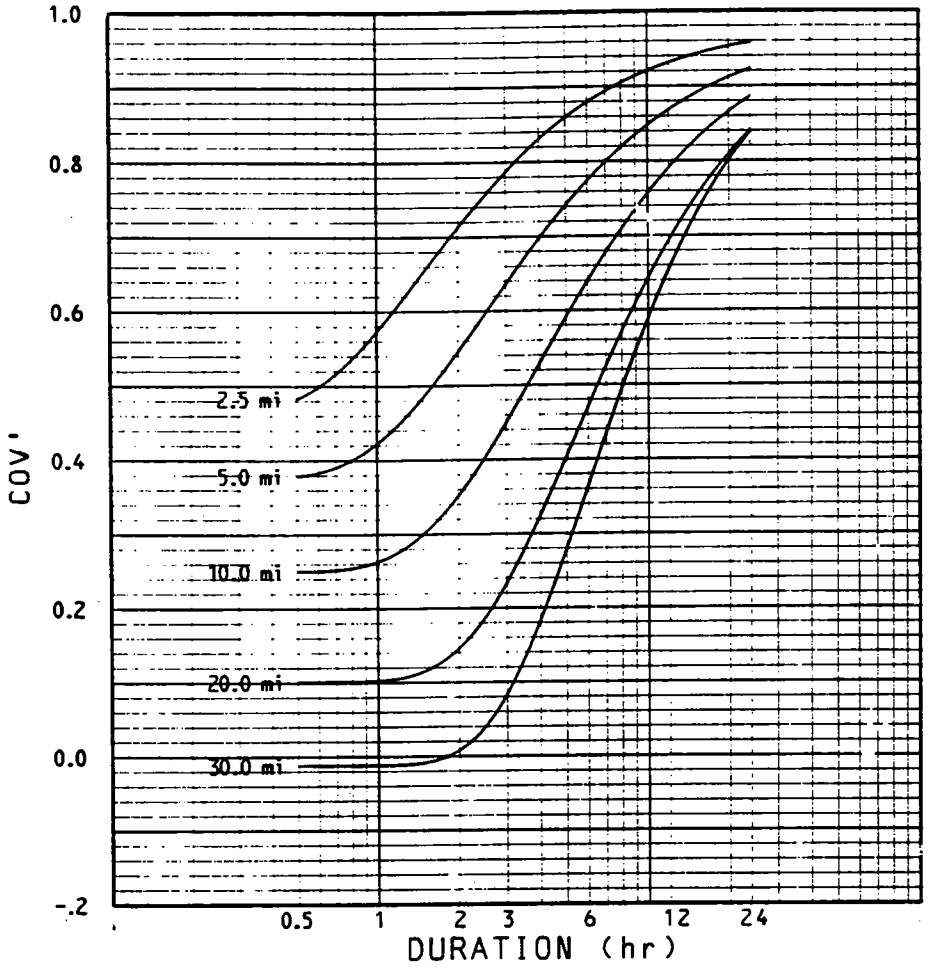

Figure 4-18.--Profiles over duration at constant distance on cov'_{Ab} surface.

CHAPTER 5. STATISTICS OF AREAL AVERAGES

This chapter estimates first and second moments of annual maximum areal average rainfall. First, the areal moments are estimated from the simultaneous rain statistics of chapter 4 and the two-station average statistics of chapter 3, respectively. These estimates are bounds about the true values. Then, the final estimates are established between the bounds by calibration with moments of annual maximum rainfall averaged over selected five-station sets. In doing this last, differences between five-station averages and true areal averages are taken into account from geometric considerations. These moments will be applied in the next chapter to derive depth-area ratios.

The areal moments are developed for circular areas. A basin of more or less regular shape of area A has an equivalent radius R

$$R = (A/\pi)^{1/2} \tag{5-1}$$

Its depth-area ratios and other statistics are considered equivalent to those for the circular area. Elongated basins are special cases not covered.

Relative Mean, $\overline{X}'_L$

For a circular area of radius R, over some time increment, Δt, the areal average precipitation, $P_L(R,\Delta t)$ is

$$P_L(R,\Delta t) = \frac{1}{\pi R^2} \int_0^{2\pi} \int_0^R P(r,\theta,\Delta t) r dr d\theta \tag{5-2}$$

where $P(r,\theta,\Delta t)$ is point precipitation over the same time increment. The series of the largest $P_L(R,\Delta t)$ each year form an annual maximum series. The average of this series, $\overline{X}_L$, for N years is

$$\overline{X}_L = \frac{1}{N\pi R^2} \sum_{k=1}^{N} \left[\int_0^{2\pi} \int_0^R X_\beta(r,\theta) r dr d\theta \right]_k \tag{5-3}$$

where X_β is point rainfall during the areal annual maximum. $\overline{X}_L$ is understood to be $\overline{X}_L(R,\Delta t)$. Hereafter in this chapter R and Δt are generally omitted in this context and the relations are understood to apply to any R and Δt within

the range of the investigation. The storms, like the basin, have a circularly symmetric counterpart. $F_L(r)$ is defined as a monotonically decreasing function that satisfies

$$\bar{X}_L = \frac{2}{R^2}\int_0^R F_L(r)\,r\,dr \qquad (5\text{-}4)$$

where the value of $\bar{X}_L$ is from (5-3).

Substituting the definitions

$$\bar{X}'_L \equiv \bar{X}_L \,/\, F_L(0);\; F'_L(r) \equiv F_L(r) \,/\, F_L(0) \qquad (5\text{-}5)$$

in (5-4) results in the normalized form

$$\bar{X}'_L = \frac{2}{R^2}\int_0^R F'_L(r)\,r\,dr\ . \qquad (5\text{-}6)$$

$\bar{X}'_L$ in this expression depends on the correlation structure of the storms from which it is derived and $F'_L(r)$ should have the traditional shape of an autocorrelation function, bell-shaped around $r \to 0$, with an exponential or similar decay beyond an inflection point. Estimating $F'_L(r)$ and integrating (5-6) are the subject of the remainder of this section.

Bounds.

Consider the following subsets of the population of rainfalls in duration Δt over the circular basin:

The events producing the annual maximum

1. basin average rainfall
2. point rainfall at the basin center
3. average of center point rainfall and concurrent rainfall at a preselected point on the basin perimeter.

Each of these rainfalls forms an annual series. The first and second moments of the series for subset 1 are the quantities sought in this chapter. $F'_L(r)$ is the average radial profile of the circular equivalents of the storms of this subset.

The radial profile obtained by averaging the relative rainfall $P'(r,\theta) = P(r,\theta)/P(r = 0)$ over the members of subset 2 and over azimuth obviously is a trace of $\bar{X}'_b$ as defined in chapter 4. $\bar{X}'_b$ is a random statistic depending on d (or r) only. Each year's member of subset 2 is a real storm and is one

candidate for selection for subset 1. Thus, comparing the basin average rainfalls in any particular year, the subset 1 value can never be less than the subset 2 value, and often will be larger. It follows that

$$F'_L(r) \simeq \overline{X}'_b(d) \tag{5-7}$$

is a lower bound to $F'_L(r)$. Here r = d.

Averaging the annual maxima that identify the members of subset 3 for a particular R yields a magnitude. Obviously, a plot of these magnitudes vs. R for all such subsets is a trace of $\overline{X}'_m(d)$ as defined in chapter 3. This profile is the basis for another estimate of $F'_L(r)$,

$$F'_L(r) \simeq 2\overline{X}'_m(d) - 1 \ . \tag{5-8}$$

Here the average in $\overline{X}'_m$ has been decoupled by reference to the definition of X'_m. The quantity on the right is the ratio of the lesser of the pair to the greater.

The rain at the perimeter point in subset 3 is not a random quantity. Its magnitude is part of the criterion for admission to the subset. Approximation (5-8) has the character of substituting single point maxima (on the right) for azimuthal average maxima (on the left), and thus is biased high. (5-8) is an upper bound to $F'_L(r)$.

These bounds to $F'_L(r)$ lead to bounds for $\overline{X}'_L(R)$ through (5-6). This expression is integrated numerically for each bound by

$$X'_L(R) = \frac{\sum_{j=1}^{m} [F'_L(r_j)]\ r_j}{\sum_{j=1}^{m} r_j} \tag{5-9}$$

where R is divided into m equal segments and

$$r_j = (R/m)(j - 0.5) \tag{5-10}$$

as illustrated in figure 5-1. Substituting eqs. (5-7) and (5-8) in (5-9) and integrating with m = 10 gives lower and upper bounds to $\overline{X}'_L$, the solid curves in figures 5-2 and 5-3 for 1, 6, and 24 hr. The bounds were computed for all standard durations. The $\overline{X}'_b$ and $\overline{X}'_m$ data for this were calculated with the formulas and constants listed in appendix VII, and are the data in figures

4-4 and 3-7. Placing values between these bounds is the subject of the next paragraph.

Calibration with five-station data.

An empirical calibration of the position of the $\overline{X}'_L$ surface between the bounds was made with data from sets of five stations selected from the Chicago network corresponding as closely as possible to the idealized pattern of figure 5-4a. The 23 selected are listed in table 5-1. A typical member of this set is shown in figure 5-4b. A theoretical weighting to approximate the average over a circular area from center and perimeter points is 0.25 for the center and 0.75 for the perimeter points, collectively. These are the respective fractions of a circular area lying closest to the center and to the perimeter. The five-station average rainfall, P_5, was computed for each hour of each April - October season for each of the five-station patterns by

$$P_5 = 0.248P_A + 0.188(P_{bb_1} + P_{bb_2} + P_{bb_3} + P_{bb_4}), \qquad (5\text{-}11)$$

where the theoretical weights have been rounded to three decimal places. The subscripts are identified in figure 5-4a. The four outer stations were given equal weights irrespective of their exact distances.

Annual maximum values of P_5 for each of the standard durations were found in the usual manner for each year for each five-station set. The mean $\overline{X}_{5m}$ of each of the resulting annual series was converted to relative form, $\overline{X}'_{5m}$, by dividing by the mean of the annual series for the center station. These $\overline{X}'_{5m}$ values are plotted in figures 5-2 and 5-3 for 1-, 6-, and 24-hr at abscissa $A = \pi\overline{d}^2$, where $\overline{d}$ is defined on figure 5-4.

To eliminate the effect of numerical differences between bounds computed by small-step numerical integration by (5-9) and bounds derived from center and perimeter values only, bounds were also computed from the $\overline{X}'_b$ and $\overline{X}'_m$ by

$$X'_L(R) = 0.25 + 0.75X'_b(R) \qquad (5\text{-}12)$$

and

$$\overline{X}'_L(R) = 1.5X'_m(R) - 0.5 , \qquad (5\text{-}13)$$

respectively. The latter is derived by combining (5-8) with the weights.

These "five-station" bounds are plotted as dashed lines in figures 5-2 and 5-3. The five-station estimates, based on curve end points only, drop below the integrated bounds where the original $\overline{X}'_b$ or $\overline{X}'_m$ curve (fig. 4-4 or 3-7) averages convex upward, and are higher where the original curve averages convex downward.

There is no definite trend with distance of the location of the plotted points between the bounds. The average position of the 23 points is plotted on the figures as an average point at 7.9 miles. Its relative position between the bounds is considered representative for all distances and the best estimate that can be obtained from this set of data. A position factor, C_x, is computed between the "five-station" bounds by

$$C_x = \frac{[\overline{X}'_L]_D - [\overline{X}'_L]_L}{[\overline{X}'_L]_U - [\overline{X}'_L]_L} \tag{5-14}$$

where D denotes an average data point and U and L denote upper and lower bounds, all at the average distance or radius for the station groups. The bounds and C_x factors at this R are depicted as a function of Δt in figure 5-5.

Fitted surface.

There is no positive trend of C_x with Δt, lower curve of figure 5-5. The average value, weighting by equal log Δt intervals,

$$\overline{C}_x = 0.2\ [(C_x)_{24} + (C_x)_{12} + (C_x)_6 + (C_x)_3 + (C_x)_{1.5}]$$

$$(C_x)_{1.5} = 0.5\ [(C_x)_2 + (C_x)_1] \tag{5-15}$$

is $\overline{C}_x = 0.77$. Applying this factor between the integrated bounds at all R and all Δt yields the final $\overline{X}'_L$ surface. The profiles on this surface in the areal and durational domains are portrayed in figures 5-6 and 5-7.

Relative Standard Deviation, s'_L

For compactness of notation and simplicity, the development of the second moment will be in terms of the variance,

$$V_L \equiv s_L^2 \qquad V_L' \equiv s_L^2 / V_A \equiv s_L'^2 \ . \tag{5-16}$$

The variance of the average of a quantity over an area is the average of the covariance between all combinations of two points in the area:

$$V_L = \frac{1}{A^2} \int_A \int_A \mathrm{cov}_{x_1y_1, x_2y_2} \, dA\,dA \ , \tag{5-17}$$

where $\mathrm{cov}_{x_1y_1, x_2y_2}$ denotes covariance between the series of quantities at position x_1y_1 and the simultaneous quantities at position x_2y_2.

Numerical integration.

Numerical forms of (5-17) for N equally spaced points are,

combination form:

$$V_L = \frac{1}{N^2} \sum_{j=1}^{N} \sum_{k=1}^{N} \mathrm{cov}_{jk} \tag{5-18}$$

and,

permutation form:

$$V_L = \frac{1}{N^2} \sum_{j=1}^{N} \sum_{k=j}^{N} \mathrm{cov}_{jk}\alpha \qquad \begin{matrix} \alpha = 1, j = k \\ \alpha = 2, j \neq k \end{matrix} \tag{5-19}$$

An equivalent permutation form is (Gilbra 1973, p. 112),

$$V_L = \frac{1}{N^2} \left[\sum_{j=1}^{N} V_j + 2 \sum_{j=1}^{N} \sum_{k=j+1}^{N} \mathrm{cov}_{jk} \right] \tag{5-20}$$

based on the identity,

$$\mathrm{cov}_{jk} \equiv V_j \qquad j = k \ . \tag{5-21}$$

Where the points are not equally spaced and each is characterized by its own increment of area, ΔA, the permutation form is

$$V_L = \frac{\sum_{j=1}^{N} \sum_{k=j}^{N} \mathrm{cov}_{jk} \Delta A_j \Delta A_k \alpha \qquad \alpha = \frac{1}{2}, k = j}{\sum_{j=1}^{N} \sum_{k=j}^{N} \Delta A_j \Delta A_k \, \alpha \qquad \alpha = 1, k \neq j} \tag{5-22}$$

We evaluate V_L' for a circular area in the circularly symmetrical case by (5-22). Defining appropriate estimates of the relative covariance for use in this expression is a subject of much of the rest of this section. The numerical integration is based on the grid in figure 5-8, where points are placed at the midpoint of Δr intervals but at the bounds of $\Delta\theta$ intervals. Because of symmetry, integration is required over only half the circle to obtain an areal average statistic, and one of each pair of points can remain on a selected azimuth. With the radius, R, of the circle divided into m equal elements and 180° of azimuth into n equal elements

$$\begin{aligned} \Delta r &= R/m \\ \Delta\theta &= \pi/n \end{aligned} \tag{5-23}$$

(5-22) becomes in this application, using the relative form,

$$V_L'(R) = \frac{\sum_{h=1}^{m} \sum_{j=h}^{m} \sum_{k=1}^{n+1} \text{cov}'_{hi,jk} r_h r_j \alpha\beta}{\sum_{h=1}^{m} \sum_{j=h}^{m} \sum_{k=1}^{n+1} r_h r_j \alpha\beta} . \tag{5-24}$$

$$\alpha = \tfrac{1}{2}, j=h \qquad \beta = \tfrac{1}{2}, k=1, n+1$$
$$\alpha = 1, j\neq h \qquad \beta = 1, k=2,\ldots n$$
$$i = 1$$

Here $\text{cov}_{hi,jk}$ is the covariance of rainfalls during areal average annual maxima at points $r = r_h$, $\theta = \theta_i$ and $r = r_j$, $\theta = \theta_k$, and

$$\begin{aligned} r_h &= (R/m)(h - 0.5) \\ r_j &= (R/m)(j - 0.5) \\ \theta_i &= 0 \\ \theta_k &= (\pi/n)(k-1) \end{aligned} \tag{5-25}$$

The primes denote division by the center variance, V_A.

Partial correlation.

The covariance structure for use in (5-24) can be inferred in one dimension from two-station statistics, especially along the radial direction. We must deal also with the general case, illustrated schematically by points hi and

jk in figure 5-9. The covariance structure along the two radii places limits on the covariance between quantities at the two general points. To define these limits we resort to conventional partial correlation theory.

The partial correlation coefficient between magnitudes at any points 1 and 3 while values are held fixed at a third point 2, $\rho_{13.2}$, is

$$\rho_{13.2} = \frac{\rho_{13} - \rho_{12}\rho_{23}}{[(1 - \rho_{12}^2)(1 - \rho_{23}^2)]^{\frac{1}{2}}} , \tag{5-26}$$

where all the ρ's on the right are common (zero order) correlation coefficients between magnitudes at the points indicated by subscripts. Substituting the notation of the present application in (5-26)

$$\begin{aligned} \rho_{hijk.A} &= \rho_{13.2} \\ \rho_{hi,A} &= \rho_{12} \\ \rho_{jk,A} &= \rho_{23} \\ \rho_{hi,jk} &= \rho_{13} \end{aligned} \tag{5-27}$$

and rearranging leads to the relation of the correlation coefficient to the partial correlation and the other coefficients,

$$\rho_{hi,jk} = \rho_{hi,A}\rho_{jk,A} + \rho_{hijk.A}[(1 - \rho_{hi,A}^2)(1 - \rho_{jk,A}^2)]^{\frac{1}{2}} . \tag{5-28}$$

For the subset of point pairs where $r_j = r_h$, by circular symmetry $\rho_{jk,A} = \rho_{hi,A}$. For this subset (5-28) simplifies to

$$\rho_{hi,jk} = \rho_{hi,A}^2 + \rho_{hijk.A}(1 - \rho_{hi,A}^2). \tag{5-29}$$

The theoretically possible range of the partial correlation is -1 to 1. A more realistic range in the present application is from approximately zero to 1. Using this latter range for the next step and substituting these limits in (5-28) and (5-29):

In the general case,

$$(\rho_{hi,jk})_{min} = \rho_{hi,A}\rho_{jk,A} \tag{5-30}$$

$$(\rho_{hi,jk})_{max} = (\rho_{hi,jk})_{min} + \left[(1 - \rho^2_{hi,A})(1 - \rho^2_{jk,A})\right]^{\frac{1}{2}} . \qquad (5\text{-}31)$$

For the $r_j = r_h$ subset,

$$(\rho_{hi,hk})_{min} = \rho^2_{hi,A} \qquad (5\text{-}32)$$

$$(\rho_{hi,hk})_{max} = 1.0. \qquad (5\text{-}33)$$

Covariance range.

The correlation coefficient range and the covariance range are closely related and are connected by the definition of the correlation coefficient, (4-12). This may be written

$$\rho_{m,n} = cov_{m,n}/(s_m s_n) \qquad (4\text{-}12)$$

where m and n are dummy subscripts denoting any variables.

Using this, the covariance limit statements corresponding to (5-30) to (5-33) are:

In the general case,

$$(cov_{hi,jk})_{min} = (cov_{hi,A} cov_{jk,A})/V_A \qquad (5\text{-}34)$$

$$(cov_{hi,jk})_{max} = (cov_{hi,jk})_{min} + s_{hi} s_{jk} \left[\left(1 - \frac{cov^2_{hi,A}}{V_{hi} V_A}\right)\left(1 - \frac{cov^2_{jk,A}}{V_{jk} V_A}\right)\right]^{\frac{1}{2}} \qquad (5\text{-}35)$$

In the $r_j = r_h$ subset,

$$(cov_{hi,hk})_{min} = (cov_{hi,A})^2/V_A \qquad (5\text{-}36)$$

$$(cov_{hi,hk})_{max} = V_{hi} \qquad (5\text{-}37)$$

In the relative form these limit statements are:

In the general case,

$$(\mathrm{cov}'_{hi,jk})_{min} = \mathrm{cov}'_{hi,A}\mathrm{cov}'_{jk,A} \tag{5-38}$$

$$(\mathrm{cov}'_{hi,jk})_{max} = (\mathrm{cov}'_{hi,jk})_{min} + s'_{hi}s'_{jk}\left[\left(1 - \frac{\mathrm{cov}'^{2}_{hi,A}}{V'^{2}_{hi}}\right)\left(1 - \frac{\mathrm{cov}'^{2}_{jk,A}}{V'^{2}_{jk}}\right)\right]^{\frac{1}{2}} \tag{5-39}$$

and in the $r_j = r_h$ subset,

$$(\mathrm{cov}'_{hi,hk})_{min} = \mathrm{cov}'^{2}_{hi,A} \tag{5-40}$$

$$(\mathrm{cov}'_{hi,hk})_{max} = V'_{hi} \tag{5-41}$$

The covariance inherently converges to the local variance as the interpoint distance approaches zero. In relative form,

$$\lim_{d_{hi,jk} \to 0} (\mathrm{cov}'_{hi,jk}) = V'_{hi} \tag{5-42}$$

This is a general property required of an algorithm for estimating covariance and is a statement that the covariance in general converges to the subset maximum, (5-41), as $d_{hi,jk} \to 0$. Formally, for terms in (5-39),

$$\lim_{d_{hi,jk} \to 0} \begin{bmatrix} \mathrm{cov}'_{jk,A} = \mathrm{cov}'_{hi,A} \\ s'_{jk} = s'_{hi} \end{bmatrix} \tag{5-43}$$

provided cov and s are spatially continuous. Taking the limit of (5-39) and using (5-43) leads to (5-42).

The decay of the relative covariance from the relative variance at d = 0 to the minimum specified by (5-38) or (5-40) is investigated empirically later.

Framework for estimating from two-station statistics.

Inspection of the covariances of rainfalls at outer stations of the five-station sets in table 5-1 shows that these covariances during five-station

weighted average annual maxima (maximum P_5 in (5-11)) in general are smaller than covariances between an outer station and the center station at the same interstation distance. This suggests for a circular storm model a different variation of the covariance in the radial and azimuthal directions. The following procedure is adopted for estimating covariances for the numerical integration over a circular area by (5-24) from chapter 4 data. It is adapted to estimating from chapter 3 data in a later paragraph. These are empirically derived methods for taking into account the major inferences from the data in a systematic manner. There are doubtless others and further investigation of covariance structure would be an appropriate subject for later investigations.

Estimate from chapter 4 data.

RADIAL VARIATION OF COVARIANCE. For the point pairs on the same radius, $\theta_k = \theta_i$, approximate the covariance relative to the variance at the inner of the two points, by cov_{Ab} from two-station data, over the same interpoint distance and relative to its center variation. That is,

$$cov_{hi,ji}/V_{hi} \simeq cov_{Ab}(\Delta r)/V_A \qquad \Delta r = r_j - r_h \tag{5-44}$$

$$V_{hi} \simeq V_b(r_h) \quad .$$

Whence, identically,

$$cov'_{hi,ji} \simeq cov'_{Ab}(\Delta r)\ V'_b(r_h) \quad . \tag{5-45}$$

This estimate is made from figures 4-17 and 4-12 data, with $V'_b \equiv (s'_b)^2$ for the latter.

AZIMUTHAL VARIATION OF COVARIANCE. For point pairs of equal radii, $r_j = r_h$, assume that $cov'_{hi,hk}$ decays monotonically with increasing $\Delta\theta = \theta_k - \theta_i$. At $\Delta\theta = 0$,

$$(cov'_{hi,hk})_{max} = V'_{hi} \simeq V'_b(r_h) \tag{5-46}$$

(in agreement with (5-41)) to the minimum specified by (5-40) at some $\Delta\theta$ to be determined empirically for each Δt. This minimum is

$$(cov'_{hi,hk})_{min} \simeq [cov'_{Ab}(r_h)]^2 \quad . \tag{5-47}$$

Establish a position coefficient, C_c, at each duration

$$C_c(\Delta\theta) = \frac{\text{cov}(\Delta\theta) - \text{cov}_{min}}{\text{cov}_{max} - \text{cov}_{min}} \tag{5-48}$$

where the maximum and minimum are defined by (5-37) and (5-36), and are independent of the assumptions (5-46) and (5-48). We turn to the same five-station sets used to evaluate C_x to evaluate C_c also.

These calibration covariances are between each possible pair of outer stations during the five-station annual maxima, per (5-11) ff. The angle $\Delta\theta$ is defined in figure 5-4b. For each duration C_c was averaged over $\Delta\theta$ bands

$$C_c(\overline{\Delta\theta}) \simeq \frac{\overline{\text{cov}}(\overline{\Delta\theta}) - \overline{\text{cov}_{min}}}{\overline{\text{cov}_{max}} - \overline{\text{cov}_{min}}} \; . \tag{5-49}$$

Here $\overline{\text{cov}}(\overline{\Delta\theta})$ is the average covariance for all outer station pairs in the data set having $\Delta\theta$ within the band. The $\overline{\text{cov}_{min}}$ term is evaluated by (5-34) for these same point pairs, and averaged over the pairs. The $\overline{\text{cov}_{max}}$ term is the outer station variance averaged over all outer stations for all 23 five-station data sets, and thus is the same for all $\Delta\theta$ bands. The $\Delta\theta$ values are also themselves averaged within each band.

Figure 5-10, upper panel, is a plot of the $C_c(\overline{\Delta\theta},\Delta t)$ values determined as above. The covariance decays to a minimum ($C_c = 0$) within the data range at all durations except 24 hours. The angle at which the minimum is attained appears to increase with duration, as expected.

A smooth $C_c(\Delta\theta,\Delta t)$ surface is fit to these curves, details and fitting constants in appendix IV. The profiles on the surface at constant Δt are depicted on the lower panel of figure 5-10. These smoothed values are applied to evaluating each relative covariance in the $r_j = r_h$ subset in integrations by (5-24). Negative C_c's are set to zero.

The formula for the relative covariance is, from rearranging (5-48) and dividing by V_A:

$$\text{cov}'_{hi,hk}(\Delta t) = \text{cov}'_{min}(r_h,\Delta t) + C_c(\Delta\theta,\Delta t)[\text{cov}'_{max}(r_h,\Delta t) - \text{cov}'_{min}(r_h,\Delta t)] \tag{5-50}$$

where,

$$\Delta\theta = \theta_k - \theta_i .$$

$C_c(\Delta\theta,\Delta t)$ = from figure 5-10, lower.

$\text{cov}'_{max}(r_h,\Delta t) \simeq V'_b(r_h,\Delta t) \equiv s'^2_b(r_h,\Delta t)$, from figure 4-12.

$\text{cov}'_{min}(r_h,\Delta t) \simeq [\text{cov}'_{Ab}(r_h,\Delta t)]^2$ from figure 4-17.

GENERAL VARIATION OF COVARIANCE. In the general case $\theta_k \neq \theta_i$, $r_j \neq r_h$, the relative covariance $\text{cov}'_{hi,jk}$, is computed similar to the above but with cov'_{min} and cov'_{max} generalized. The algorithm is (5-50) with

$$\text{cov}'_{min} = \text{cov}'_{Ab}(r_h)\ \text{cov}'_{Ab}(r_j) \tag{5-51}$$

$$\text{cov}'_{max} = \text{cov}'_{Ab}(\Delta r)\ V'_b(r_h) \tag{5-52}$$

$$\Delta r = r_j - r_h .$$

This is a generalization that includes the algorithms for the $r_j = r_h$ and $\theta_k = \theta_i$ subsets. The latter were presented first for tutorial reasons.

Integration.

Estimating $\text{cov}'_{hi,jk}$ from cov'_{Ab} and s'_b by the above algorithm and integrating numerically for selected circle sizes by (5-24) with m = 10, n = 18 in (5-23), yields an estimated $V'_L(A,\Delta t)$ surface. The corresponding s'_L profiles were computed for each standard Δt. This is illustrated for 1-hr by the upper solid curve of figure 5-11.

Analogous to the procedure with the mean (fig. 5-5), the bound was also computed from a five-point grid instead of continuous data and is illustrated in figure 5-11 by the upper dashed line.

A weighting formula for the five points is derived as follows: For any four-item average with three items randomly drawn from population 2 and the fourth from population 1, the variance is, from (5-20),

$$V_{avg} = \frac{1}{16}\left(\overline{V_1} + \overline{3V_2} + \overline{6\ \text{cov}_{12}} + \overline{6\ \text{cov}_{22}}\right) . \tag{5-53}$$

Averages of five points weighted by (5-11) have the statistical characteristics of a four-point unweighted average. (5-53) applies here in the following form:

$$V'_L(A) = \frac{1}{16}\left[1.0 + 3V'_b(R) + 6\text{cov}'_{Ab}(R) + 4\text{cov}'_{bb}(r=R,\Delta\theta=90°) + 2\text{cov}'_{bb}(r=R,\Delta\theta=180°)\right] . \tag{5-54}$$

In this formula cov'_{bb} is the covariance between two outer stations in the pattern of figure 5-4a. A permutation review will show that the covariance between adjacent stations ($\Delta\theta = 90°$) in a symmetrical model appears twice as often as the covariance at opposite stations ($\Delta\theta = 180°$). Thus "6 cov_{22}" in (5-53) is divided 4 and 2 between these in (5-54). These cov'_{bb} terms are evaluated by (5-50) with the indicated r and $\Delta\theta$.

Estimate from chapter 3 data.

Chapter 3 determines the moments for annual maximum values of the average of rainfall at two stations. The statistics of chapter 4 are for events in which the annual maximum is at one station. Many of these events, but not all, are the same; see figure 3-12. Here we place the variances in equivalent form and determine an adjustment factor to convert chapter 3 data to the chapter 4 format. We can then determine a bound for s'_L from chapter 3 data by the same algorithm as before.

The variance of the quantity, average of rainfall at a station experiencing its annual maximum and the simultaneous rainfall at another station, $V'_{\overline{Ab}}$, is, by (5-20),

$$V'_{\overline{Ab}} = 0.25(1.0 = V'_b + 2cov'_{Ab}) \quad . \tag{5-55}$$

Rearranging,

$$4V'_{\overline{Ab}} - 1.0 = V'_b + 2cov'_{Ab} \quad . \tag{5-56}$$

The intent here is to start with V'_m as the estimator of the variance of a two-point average rather than V'_b. The approximate comparative magnitudes are introduced into the system by defining $\alpha(\Delta t,r)$ as the factor satisfying

$$4V'_m(\Delta t,r) - 1.0 = \alpha(\Delta t,r).[V'_b(\Delta t,r) + 2cov'_{Ab}(\Delta t,r)] \tag{5-57}$$

where the V'_m is the square of s'_m in figure 3-8, and V'_b and cov'_{Ab} are from figures 4-12 and 4-17. The procedure for computing the chapter 3 bound is then to repeat the entire routine for computing the chapter 4 bound, except that wherever a V'_b or cov'_{Ab} is called for, $\hat{V}'_b$ or $\hat{cov}'_{Ab}$ from

$$\hat{V}'_b = \alpha V'_b \tag{5-58}$$

$$\hat{cov}'_{Ab} = \alpha cov'_{Ab}$$

is substituted, with the α determined in each instance by (5-57). Values of s'_L determined by this process are plotted in figures 5-11 and 5-12, both with the complete grid and the five-point grid, and turn out to be the lower bound.

The 1-hr five-point bound lies considerably above the complete grid bound in figure 5-11 at R values greater than 2 or 3 miles. This is due to the concave upward curvature of the cov'_{Ab} surface, figure 4-17. It is apparent that estimates based on only the two points r = 0, r = R will be high compared to estimates from the cov'_{Ab} profile at more frequent intervals of r.

Calibration.

The relative standard deviation s'_{5m} was computed for the same maximum annual five-station average rainfall series that was the basis for $\overline{X}'_{5m}$. The values are plotted in figure 5-11 for 1 hr. There is no distinct dependence on distance of the position of the plotted points with respect to the five-point (dashed curve) bounds. Similar results (not shown) were obtained for other durations.

All four bounds and the mean ordinate for the plotted points, all at R = 7.9 mi and for all durations, are depicted in figure 5-12. The lower bound for five points from chapter 3 data appears to approximate the observed five-point data when all durations are considered. That is, if we were to define a C_s placement factor between the dashed bounds analogous to C_x in (5-14),

$$C_s(\overline{\Delta t}) \simeq 0 \ . \tag{5-59}$$

The lower bound by small-step integration from chapter 3 data (lower solid curve of figures 5-11 and 5-12) is adopted as the best estimate of $s'_L(A)$ for all Δt in the study. It is not known to what extent (5-59) is a general characteristic. For the present we regard it only as the result of a particular calibration and assume that $C_s(\overline{\Delta t})$ will be small but not necessarily zero in other geographical regions.

Fitted surface.

To recapitulate, the steps to estimate any $s'_L(A,\Delta t)$ are,

(a) R from A by (5-1).

(b) $r = r_h$, $r = r_j$, from R and m by (5-25).

(c) $\alpha(\Delta t,r)$ from $V'_m(\Delta t,r)$, $V'_b(\Delta t,r)$, and $cov'_{Ab}(\Delta t,r)$ by (5-57).

(d) $\hat{V}'_b(\Delta t,r)$, $\hat{cov}'_{Ab}(\Delta t,r)$ from $V'_b(\Delta t,r)$ and $cov'_{Ab}(\Delta t,r)$ by (5-58).

(e) $\text{cov}'_{hi,jk}(\Delta t)$ by (5-50) from $\hat{V}'(\Delta t,r)$ and $\hat{\text{cov}}'_{Ab}(\Delta t,r)$ in required formulas.

(f) Integrate $V'_L(R,\Delta t)$ by (5-24) from step (e) $\text{cov}'_{hi,jk}(\Delta t)$ values.

(g) $s'_L(R,\Delta t) \equiv [V'_L(R, t)]^{\frac{1}{2}}$

Profiles on the $s'_L(A,\Delta t)$ surface computed in this way are presented in figures 5-13 and 5-14.

Table 5-1.--Five-station groups

Stations*		Distance¢				
Center	Outer	Min	Max	Avg	N#	YEARS
G/P	HJKL	4.0	6.3	5.4	16	1949-50, 52-56, 58-59, 61-64, 66-67, 69
K	FHIL	4.6	7.9	6.3	21	1949-59, 61-69, 71
G/P	DFHT	3.6	9.6	7.2	20	1949-52, 54-59, 61-64, 66-70, 72
G/P	HJKT	3.6	6.3	5.3	15	1949-50, 52, 54-56, 58-59, 61-64, 66-67, 69
E	CHJR	3.2	5.5	4.1	12	1949-50, 52-56, 58, 61-64
G/P	DHIL	4.0	9.9	7.4	20	1949-59, 61-64, 66-70
K	AHIL	4.6	8.4	6.9	21	1949-59, 61-69, 71
E	BDJR	1.5	3.8	3.1	12	1949-50, 52-56, 58, 61-64
E	CDHR	3.2	5.5	3.9	14	1949-58, 61-64
F	GIUW	5.7	25.0	14.1	10	1949-52, 55, 58-59, 61, 67, 70
L	IRUW	10.8	23.8	18.5	12	1949-52, 55, 58-61, 65, 67, 70
K	AHIT	4.6	8.4	7.3	20	1949-52, 54-59, 61-69, 71
G/P	DFHL	4.0	9.6	7.3	21	1949-59, 61-64, 66-70, 72
K	FHIT	4.6	8.4	7.3	20	1949-52, 54-59, 61-69, 71
K	FGHI	5.3	9.9	7.3	19	1949-59, 61-64, 66-69
E	BCDJ	1.5	3.8	2.9	12	1949-50, 52-56, 58, 61-64
J	CDMT	3.3	7.2	5.9	12	1949-50, 52, 54-56, 58-59, 61-64
G/P	DFMT	3.6	9.6	6.9	14	1949-52, 54-59, 61-64
G/P	ALMR	4.0	12.9	8.6	15	1949-59, 61-64
K	AILM	4.6	8.4	6.5	16	1949-64
L	DHUW	10.1	23.8	17.3	12	1949-52, 55, 58-59, 61, 65, 67, 70, 72
G/P	IUVW	9.9	27.0	19.2	9	1949-52, 55, 58-59, 61, 70
E	BDJV	1.5	4.7	3.3	12	1949-50, 52-56, 58, 61-64

* Letters refer to figure 1-1

¢ Miles from outer station to center station

\# Years of simultaneous record

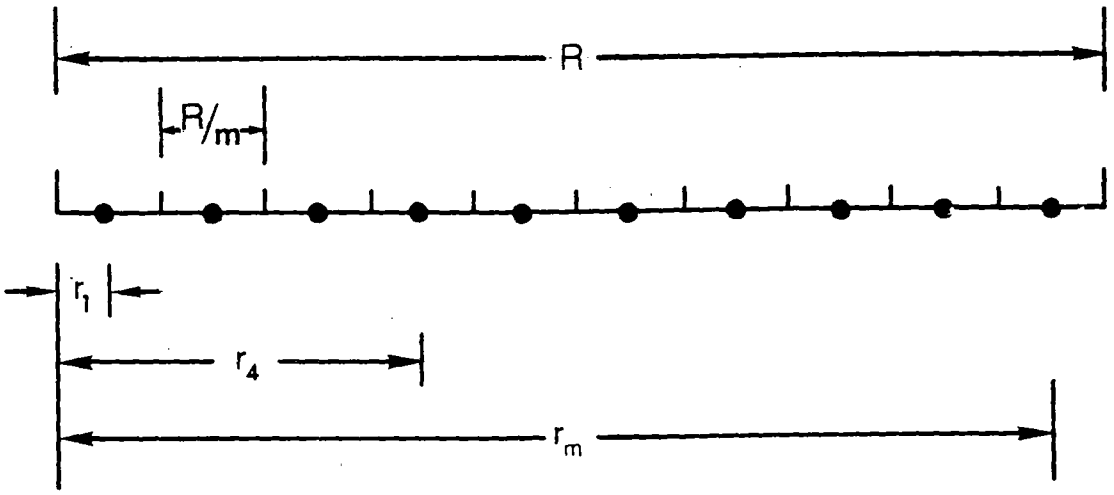

Figure 5-1.--Grid system along a radius.

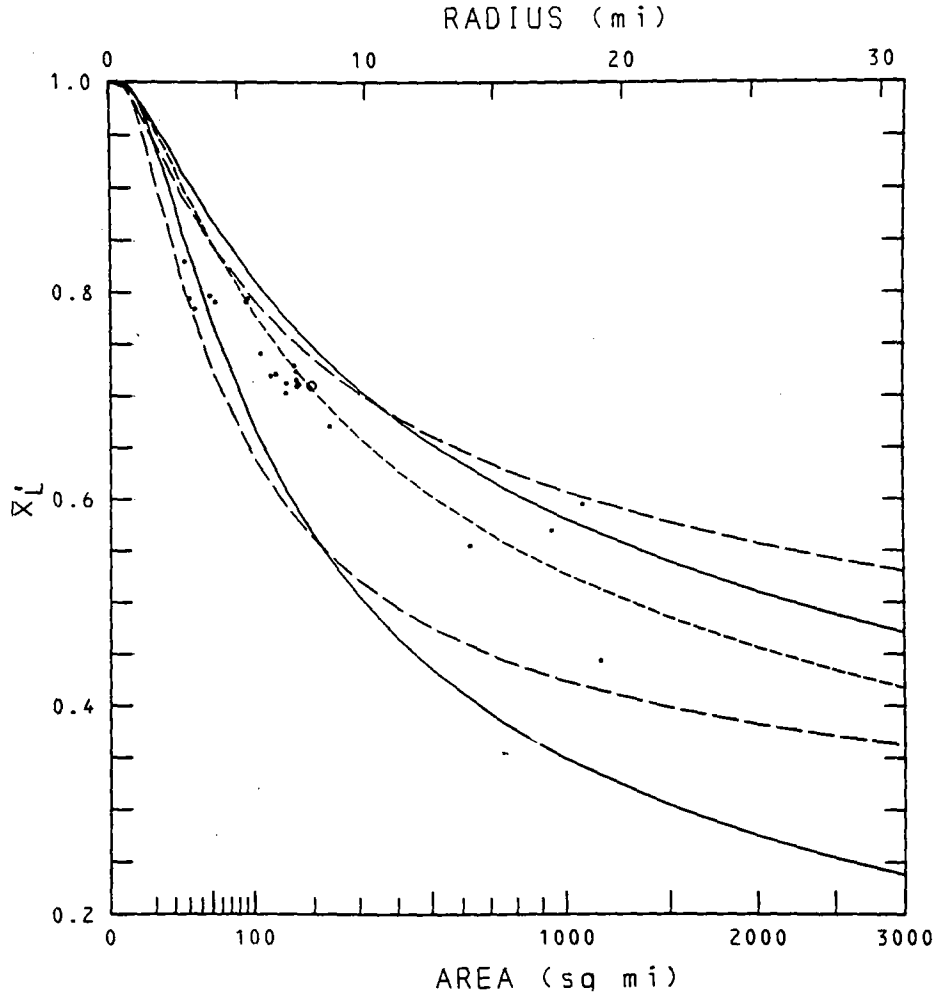

Figure 5-2.--Relative means, $\bar{X}'_L$, 1-hr.

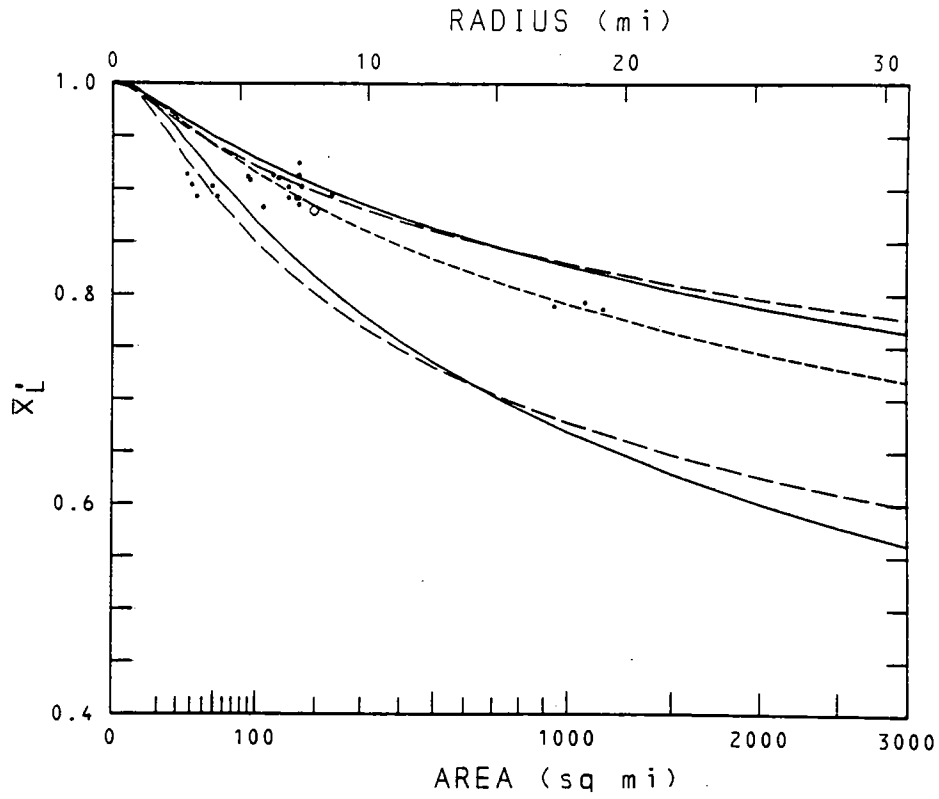

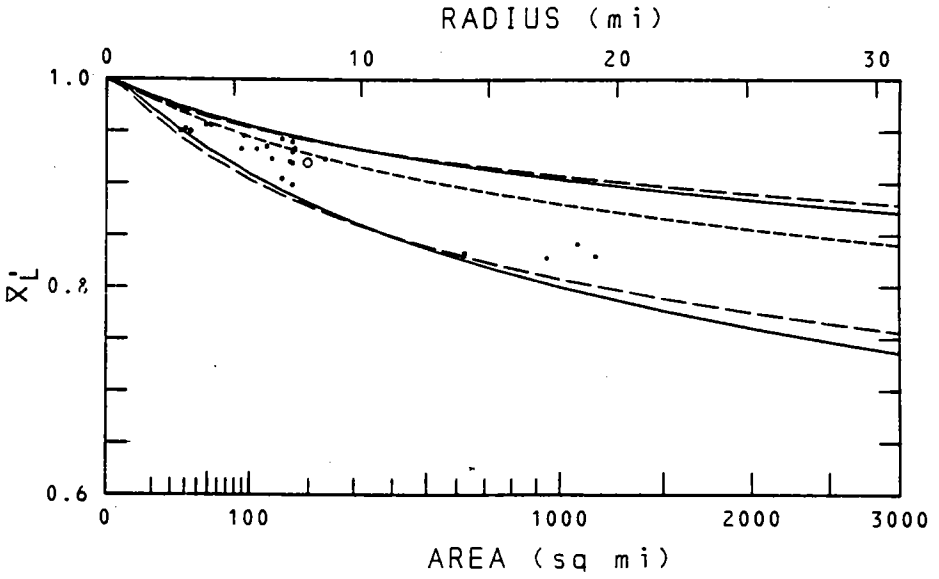

Figure 5-3.--Same as figure 5-1, 6- and 24-hr.

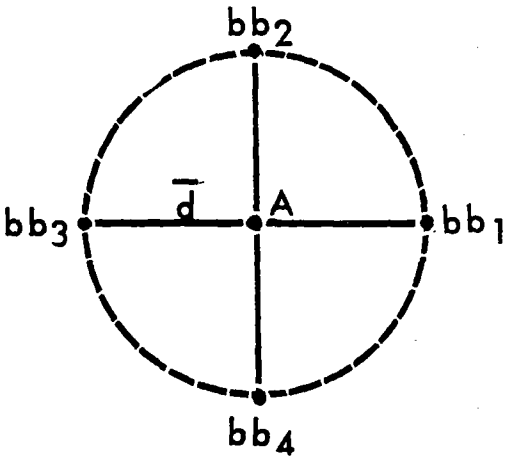

(a) Idealized

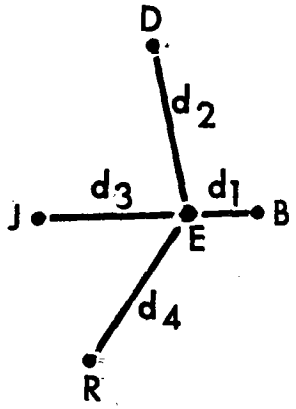

$$\bar{d} = 0.25(d_1 + d_2 + d_3 + d_4)$$

(b) Actual

Figure 5-4.--5-station pattern (a) Idealized; (b) Sample of pattern from Chicago network.

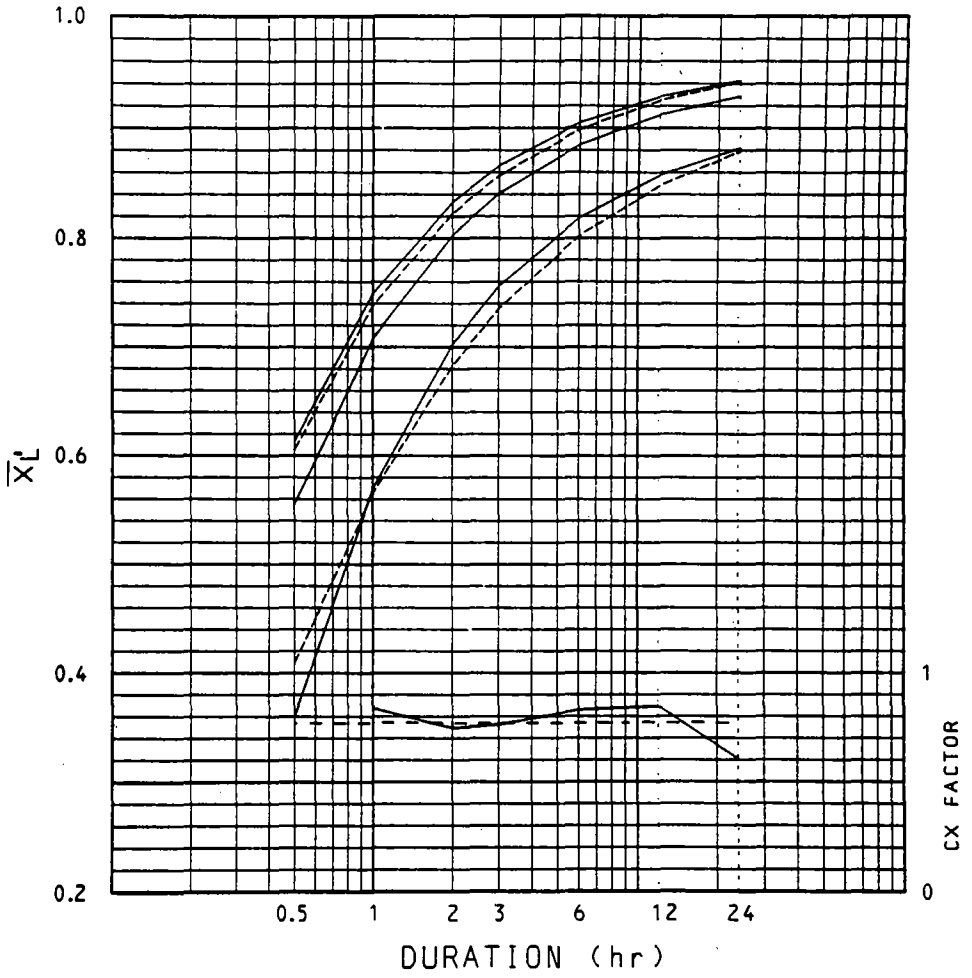

Figure 5-5.--Durational variational of X'_L bounds and data R = 7.9 mi, upper; C_x factor, observed and smoothed, lower.

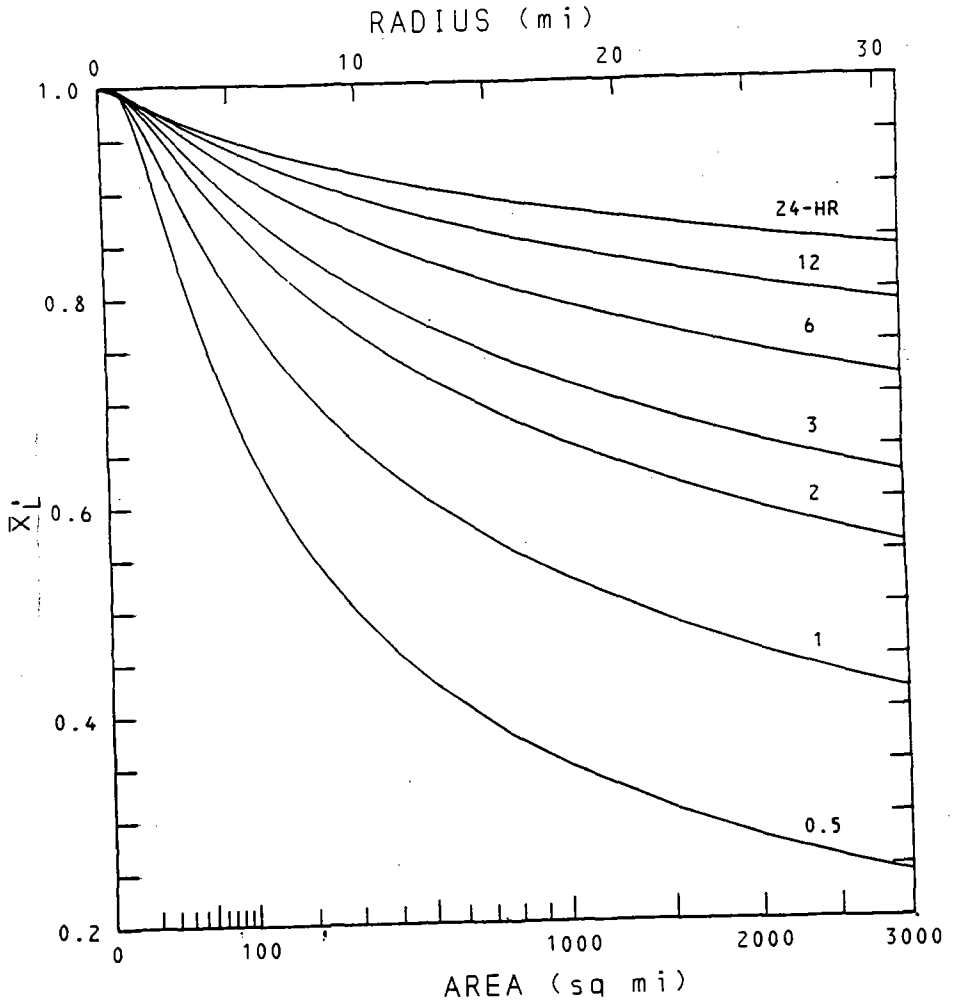

Figure 5-6.--Profiles over area at constant duration on $\bar{X}'_L$ surface.

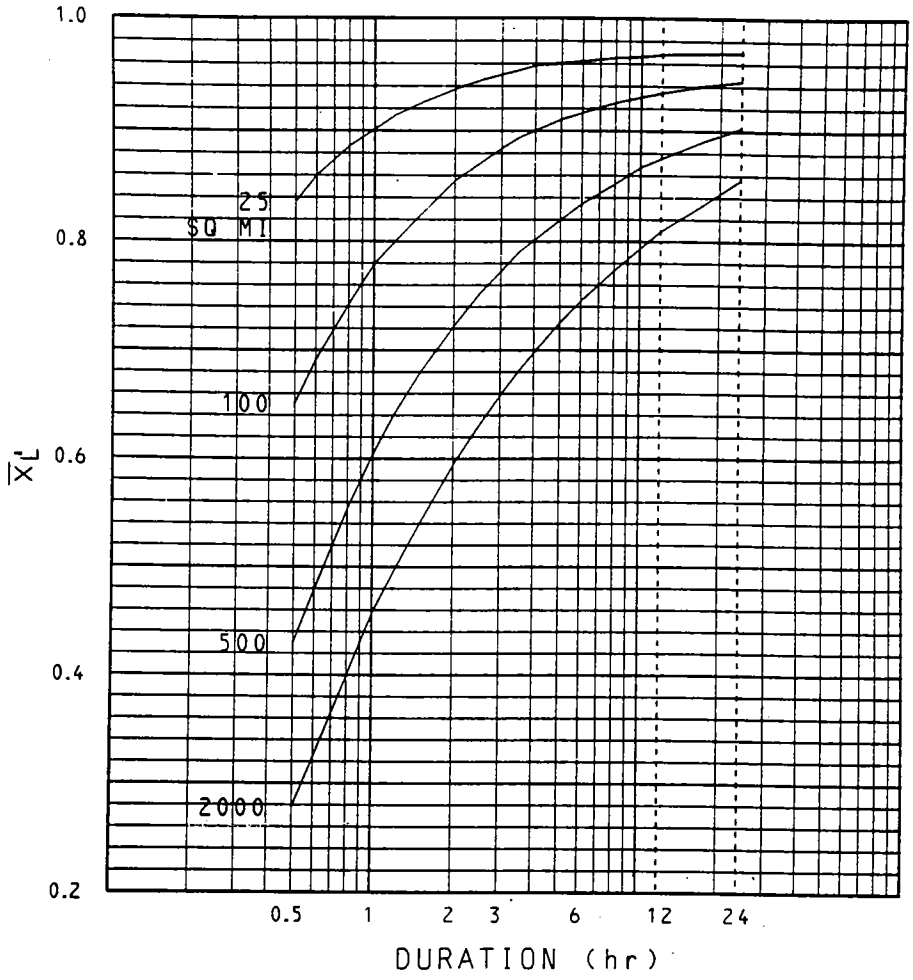

Figure 5-7.--Profiles over duration at constant area on $\overline{X}_L'$ surface.

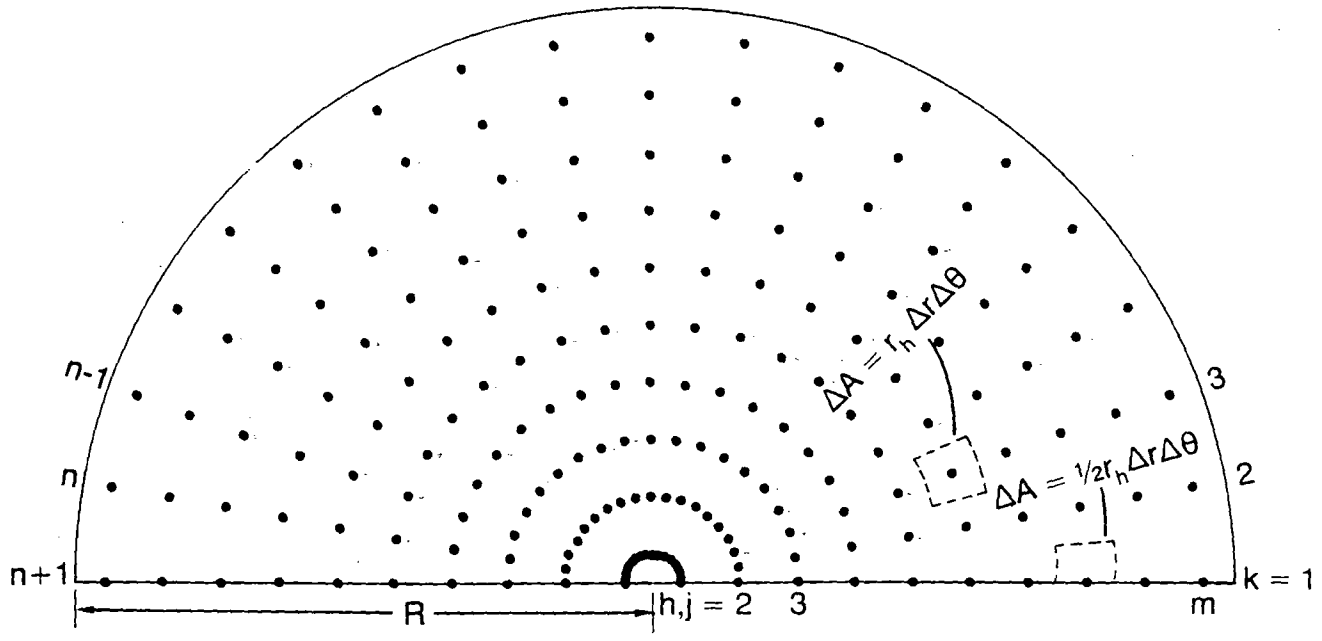

Figure 5-8.--Grid for numerical integration over a circular area by eq. (5-24).

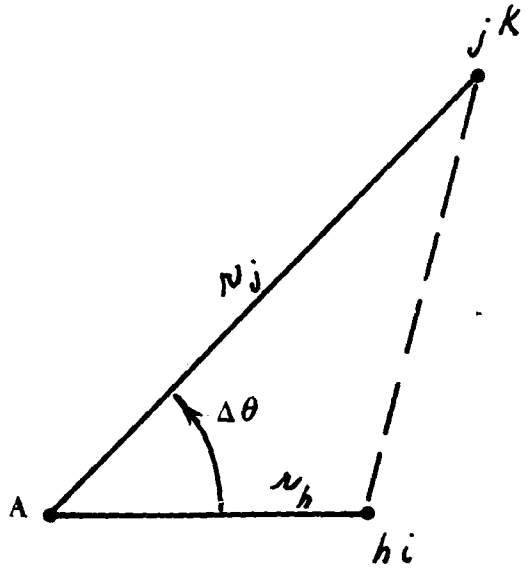

$$\Delta\theta = \theta_\kappa - \theta_i$$

Figure 5-9.--Definition of points for application of partial correlation theory.

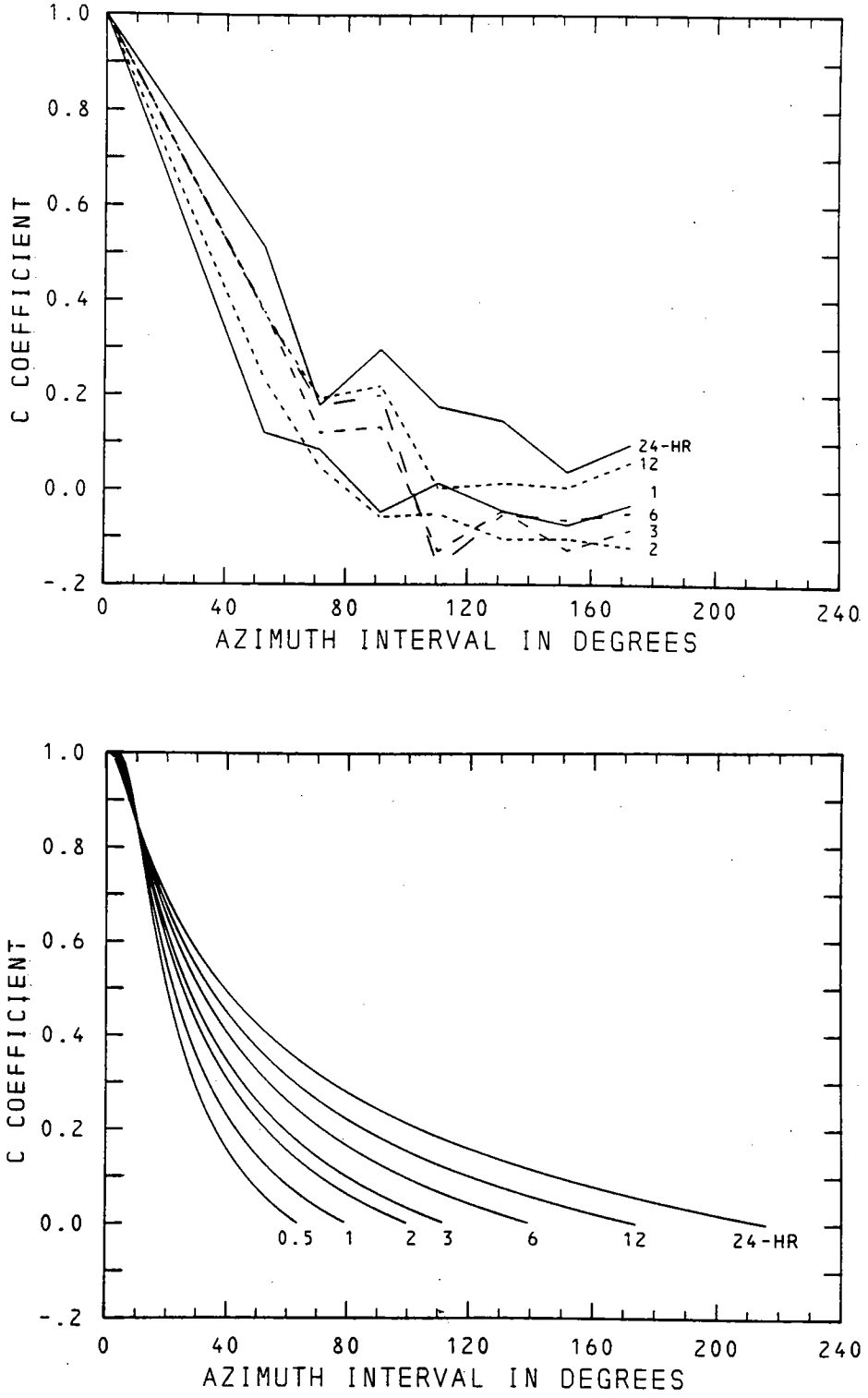

Figure 5-10.--Covariance position coefficient, C_c, vs. $\Delta\theta$.

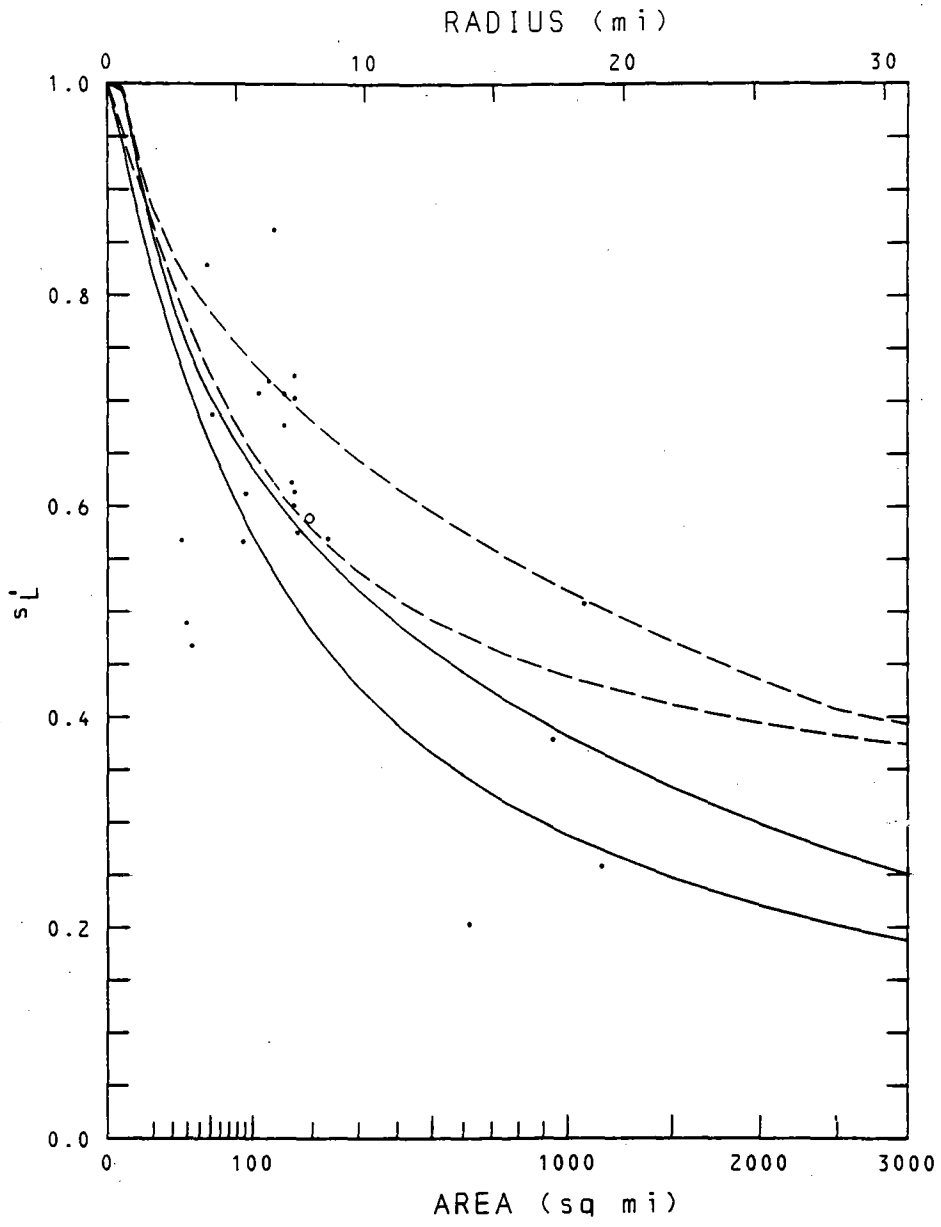

Figure 5-11.--Relative standard deviation, s'_L, 1-hr.

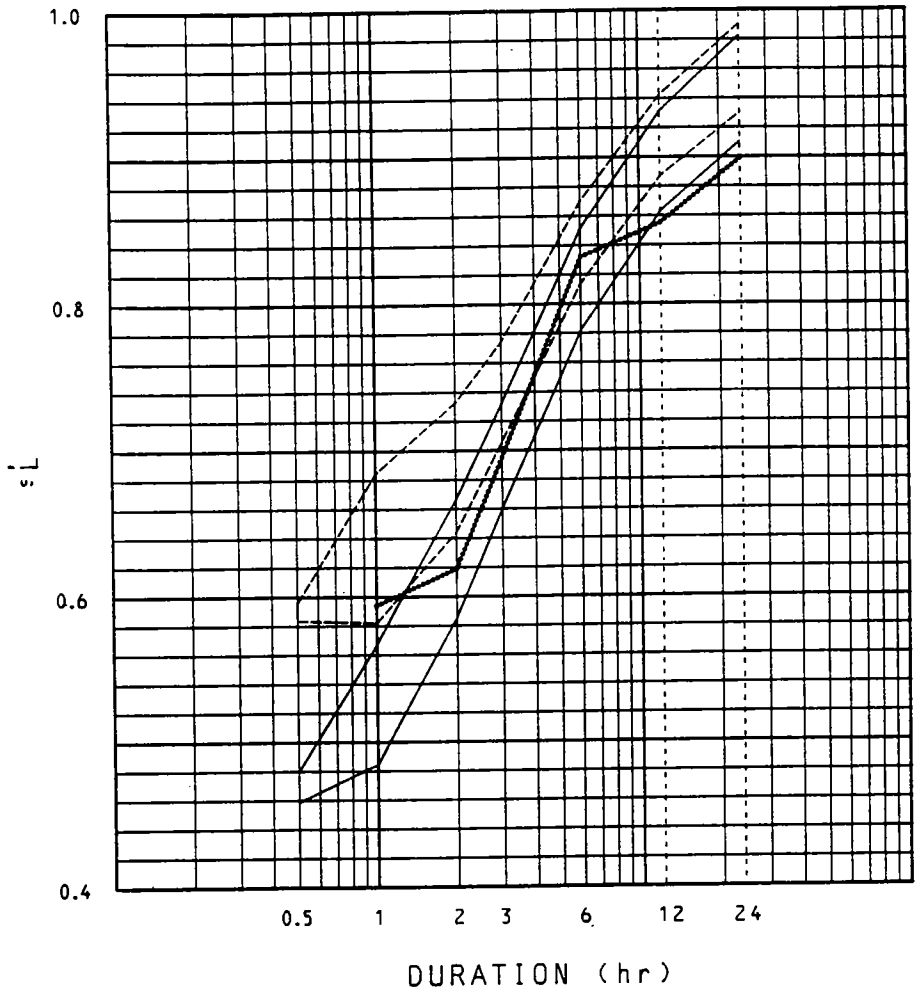

Figure 5-12.--Durational variation of s'_L bounds and data R = 7.9 mi.

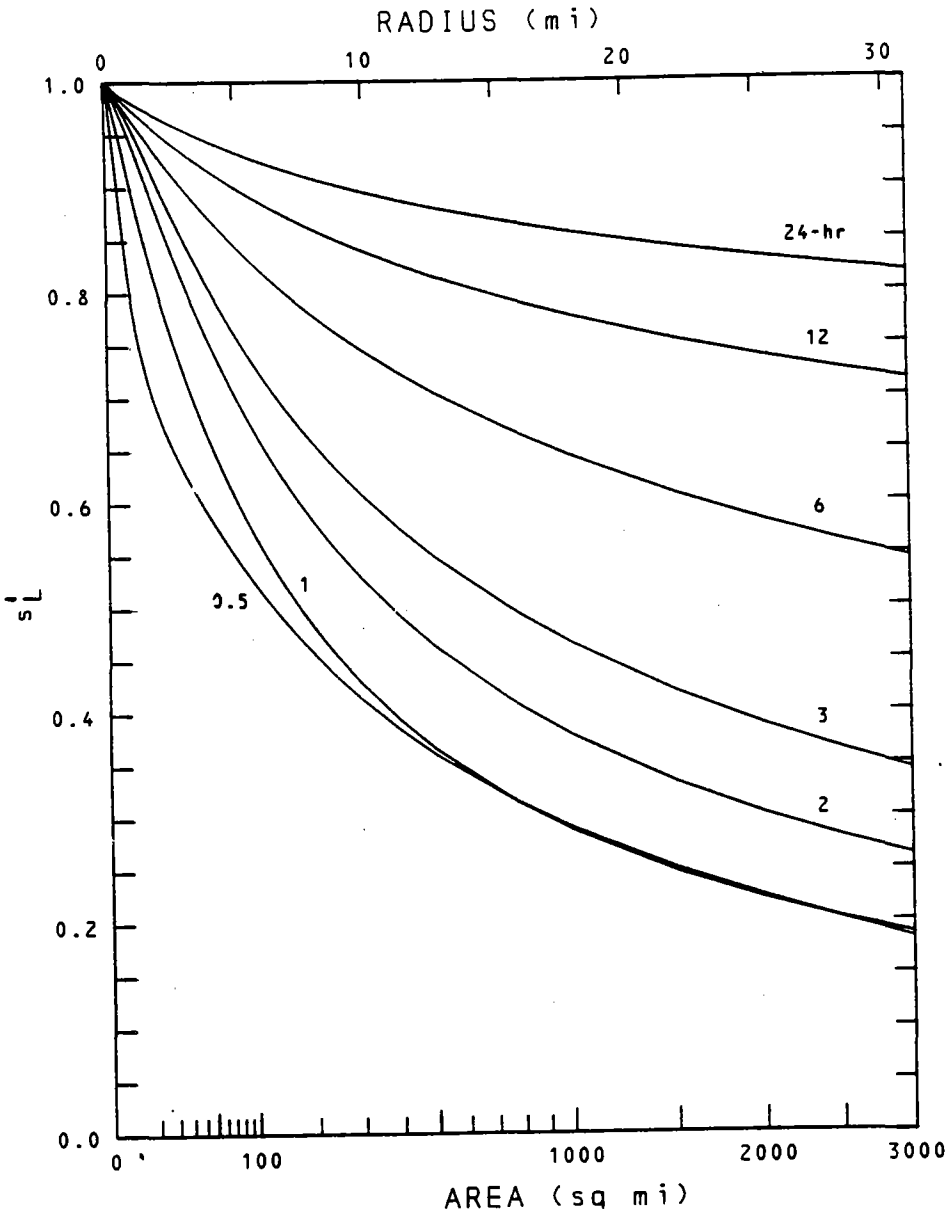

Figure 5-13.--Profiles over area at constant duration on s'_L surface.

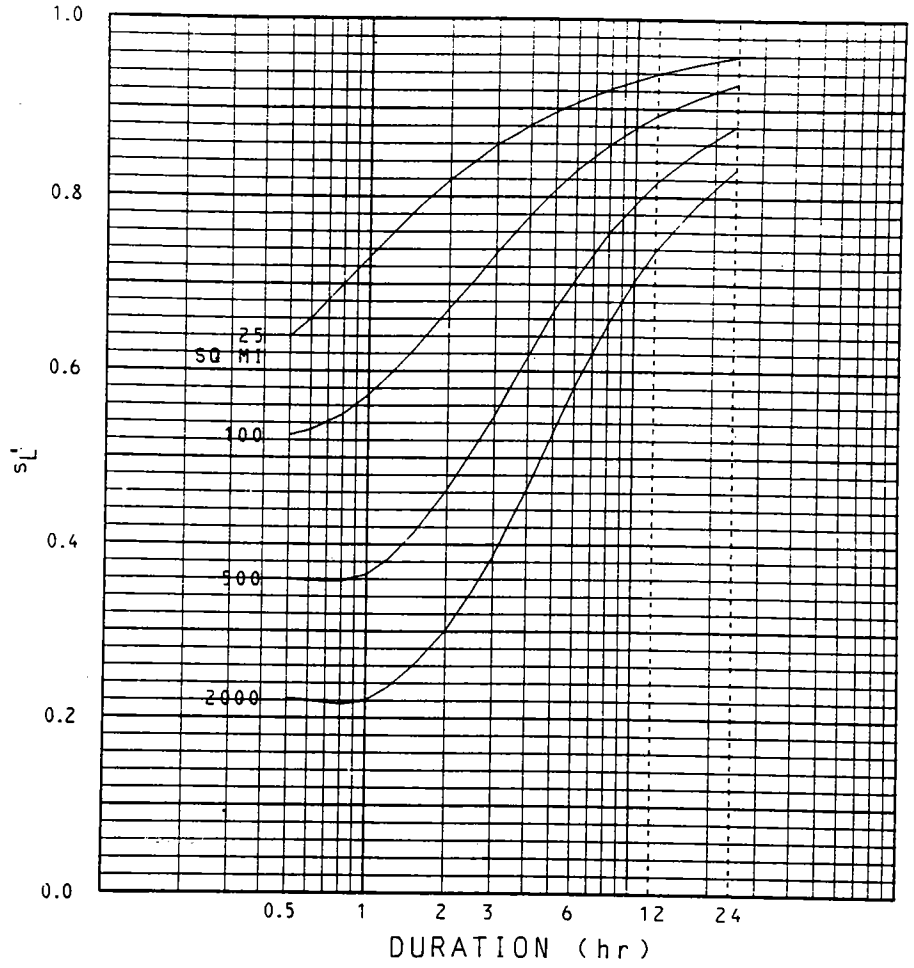

Figure 5-14.--Profiles over duration at constant area on s'_L surface.

CHAPTER 6. DEPTH AREA RATIOS

This chapter brings us to the end result of this investigation, geographically fixed depth-area ratios. The necessity for these in hydrologic applications of precipitation frequencies was covered in the introductory chapter. The depth-area ratios are computed from the means and standard deviations of the annual series of averages over circular areas developed in chapter 5. Comparisons are given with previous results.

Depth-Area Ratio Computation

The geographically fixed depth-area ratio, DA, for a particular frequency, duration, and area size is by definition

$$DA(f,\Delta t,A) = \frac{X_L(f,\Delta t,A)}{X_L(f,\Delta t,0)} . \qquad (6\text{-}1)$$

This is analogous to (3-6) defining the depth-length ratio. Here A is area and subscript L applies to area (subscript A having been reserved for a different meaning). Introducing the definitions of relative statistics and of station coefficient of variation into (6-1) leads to the following formula for the depth-area ratio:

$$DA(f,\Delta t,A) = \frac{\overline{X}'_L(\Delta t,A,N) + K(f,N)s'_L(\Delta t,A,N)cv_A(\Delta t)}{1 + K(f,N)cv_A(\Delta t)} . \qquad (6\text{-}2)$$

The development of this formula is strictly analogous to that for the depth-length ratio formula, (3-11). All terms on the right must apply to the same record length, N. All statistics in this study are normalized to 20 years (chapter 2 and appendix II). X_L and s_L are from the results of chapter 5, cv_A from table 3-2, and K from table I-1 in appendix I.

Depth-Area Ratio Results

Depth-area ratios computed by (6-2) are shown in different depictions in figures 6-1 to 6-5. Depth-area ratios decrease with increasing area. This is almost by definition since the ratio is a comparison to a point (zero area) frequency. Depth-area ratios increase with increasing duration, in agreement with all previous results. Differences from the point value diminish with increasing duration. Depth-area ratios decrease somewhat with decreasing frequency (longer return period). This is a new result not clearly brought out in previous results though not unexpected.

Comparison with Previous Results

The depth-area ratios of figure 6-1 are compared with the ratios previously published by the National Weather Service (fig. 1-1) in figure 6-5. The present study is for Chicago, the previous results for all of the United

States, though Chicago is prominent in the development data. Thus exact correspondence should not be expected. The previous 30-minute curve, as the present one, is essentially an extrapolation. The comparison speaks for itself and is considered satisfactory.

Geographically fixed depth-area ratios have been developed also by Huff and Vogel (1976), their table 1, from several sets of data in central Illinois, assuming a logarithmic variation of the ratio with area. Their results are also compared with the results of this study in figure 6-5. For short durations, the integration over an area of a few hundred square miles with a closely spaced grid gives lower values of depth-area ratios than those derived directly from statistics of averages over a few stations. This is illustrated by the bounds in figure 5-14. It is not known if this is a factor in the differences at a few hundred square miles between the results of Huff and Vogel and the present analysis.

Depth-area Ratios for Larger Areas

The depth-area ratios are extended to 5,000 mi^2 in figure 6-6 to provide convenient tentative information. This area size corresponds approximately to the largest interstation distance of 39 mi (table 3-1) in the development data, through (5-1). Ratios at this area size are strongly influenced by implicit extrapolation from smaller interstation distances through the fit to all data.

Records from the standard climatological network of recording precipitation gages while contributing little to specification of areal average rainfall over a few hundred square miles, do have information content on areal average rainfall over several thousand square miles. These records should be applied to any definitive determination of areal average rainfall frequencies for this area size.

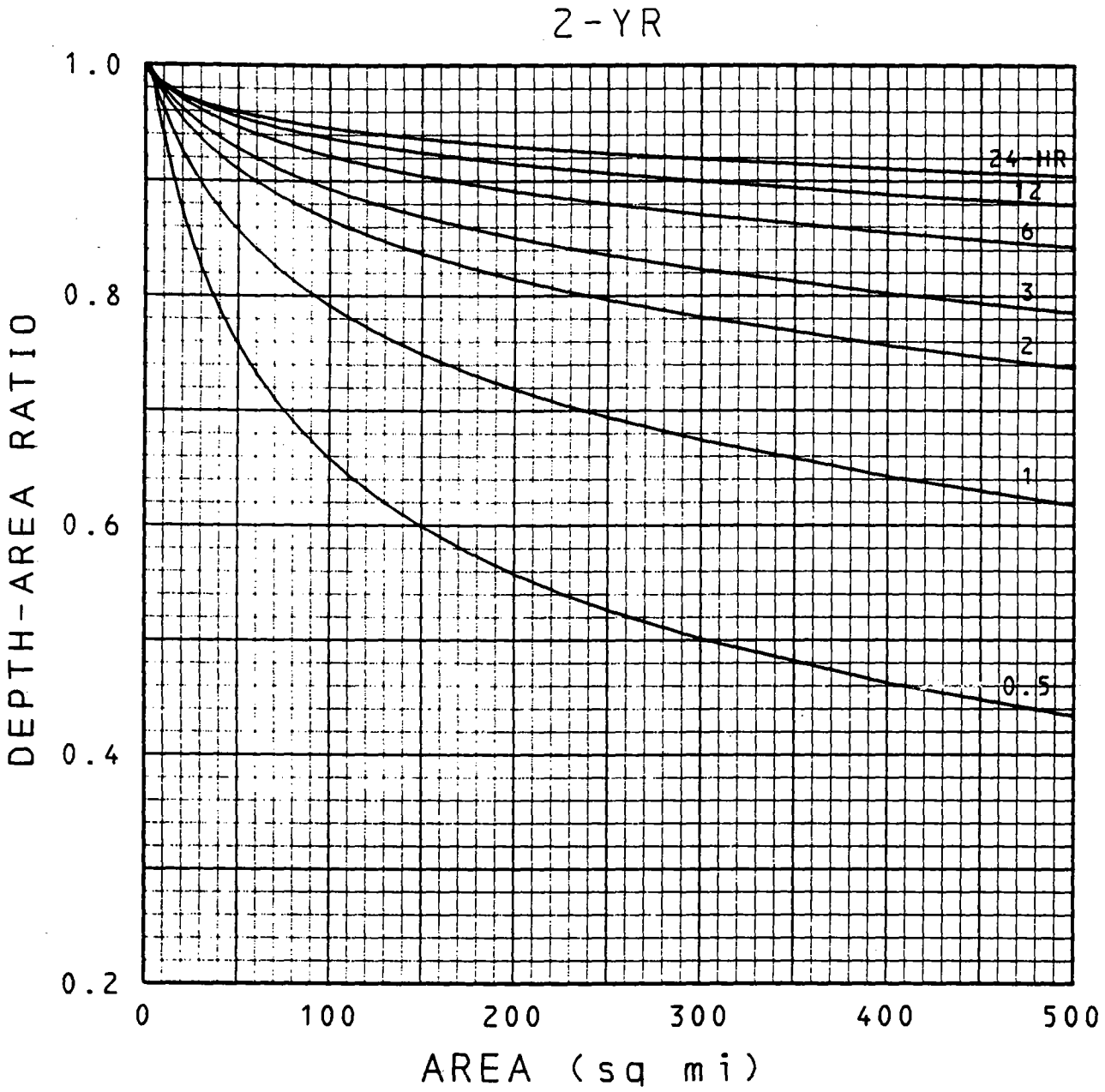

Figure 6-1.--Depth-area ratios. Chicago, Ill. Areal profiles to 500 mi^2, by duration, 2-yr.

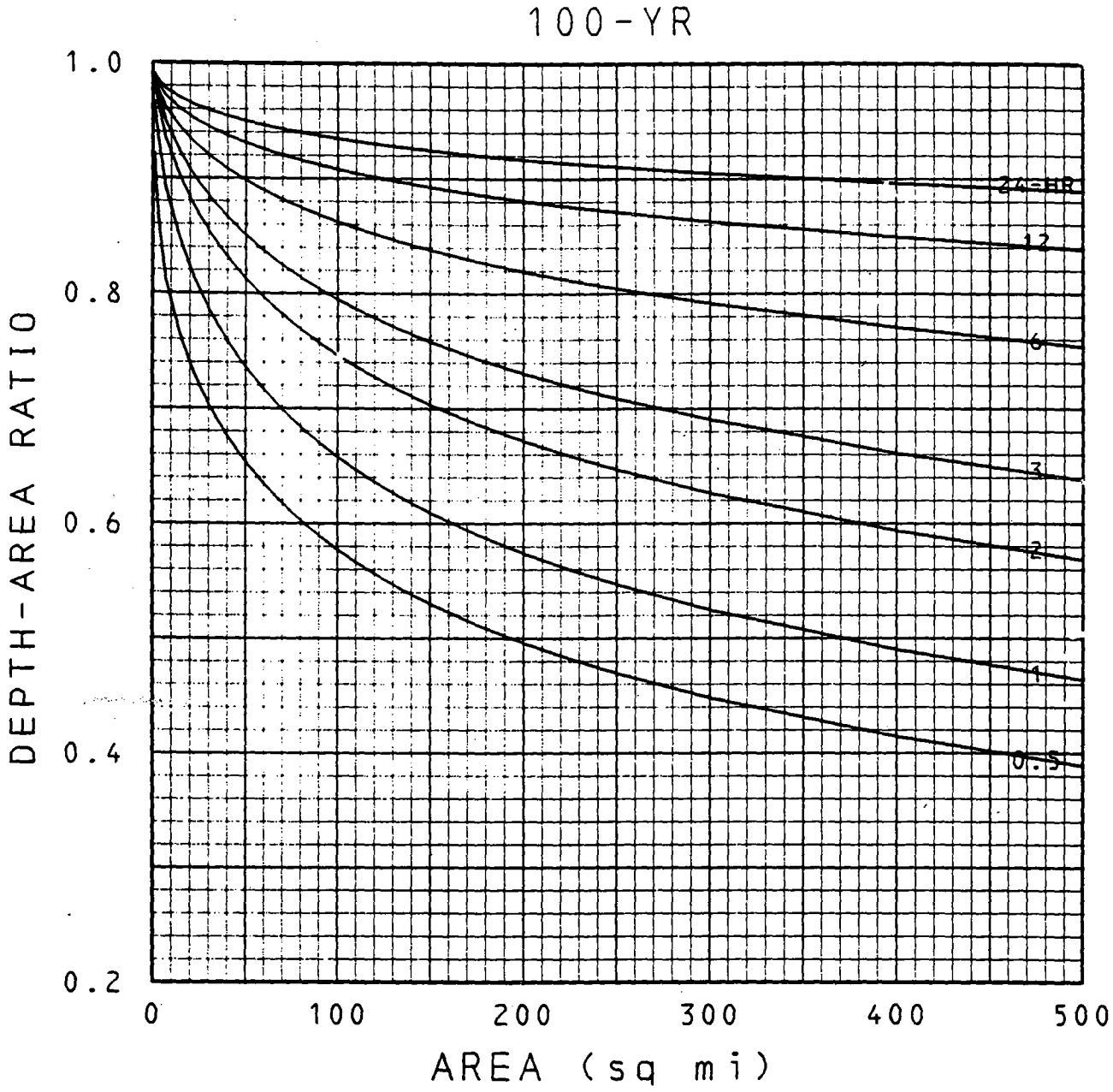

Figure 6-2.--Same as figure 6-1, 100-yr.

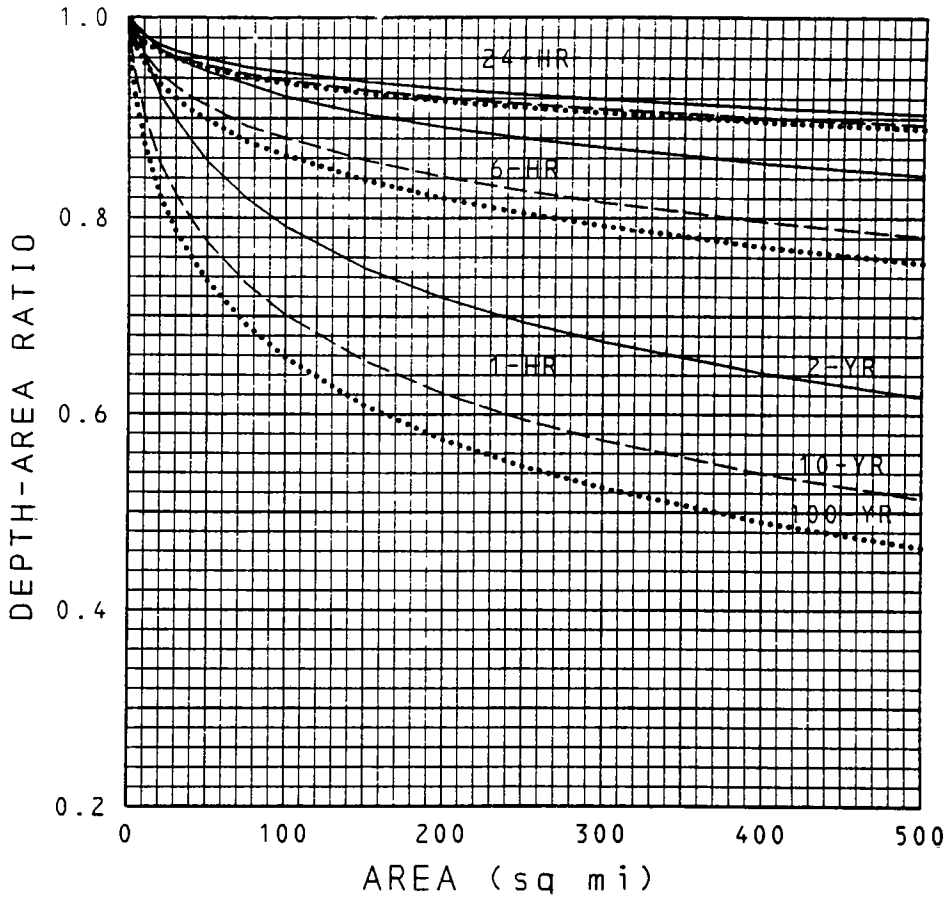

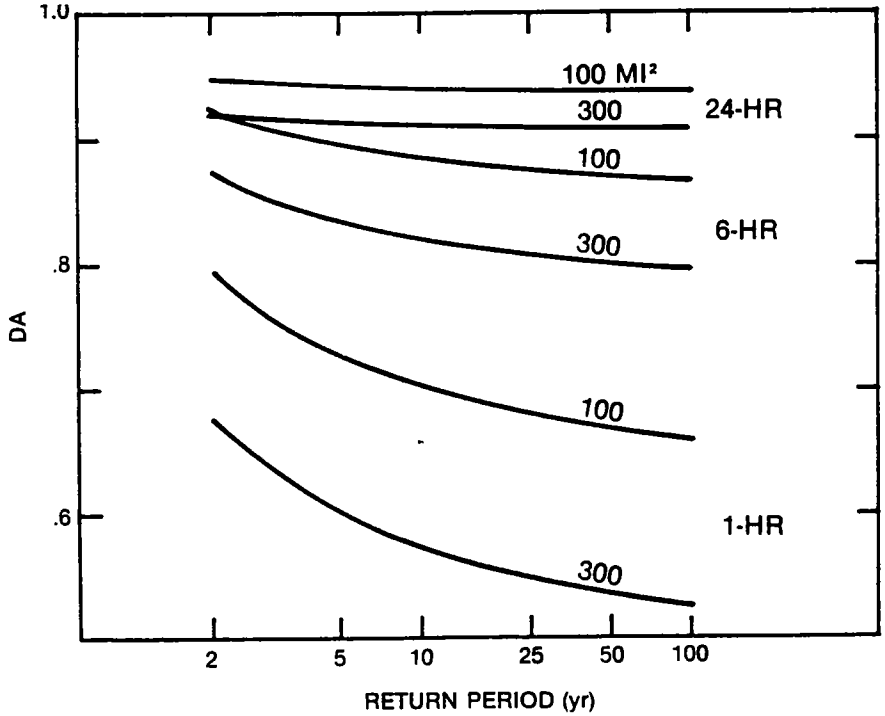

Figure 6-3.--Depth-area ratios. Chicago, Ill. Areal and frequency profiles for selected durations and return periods.

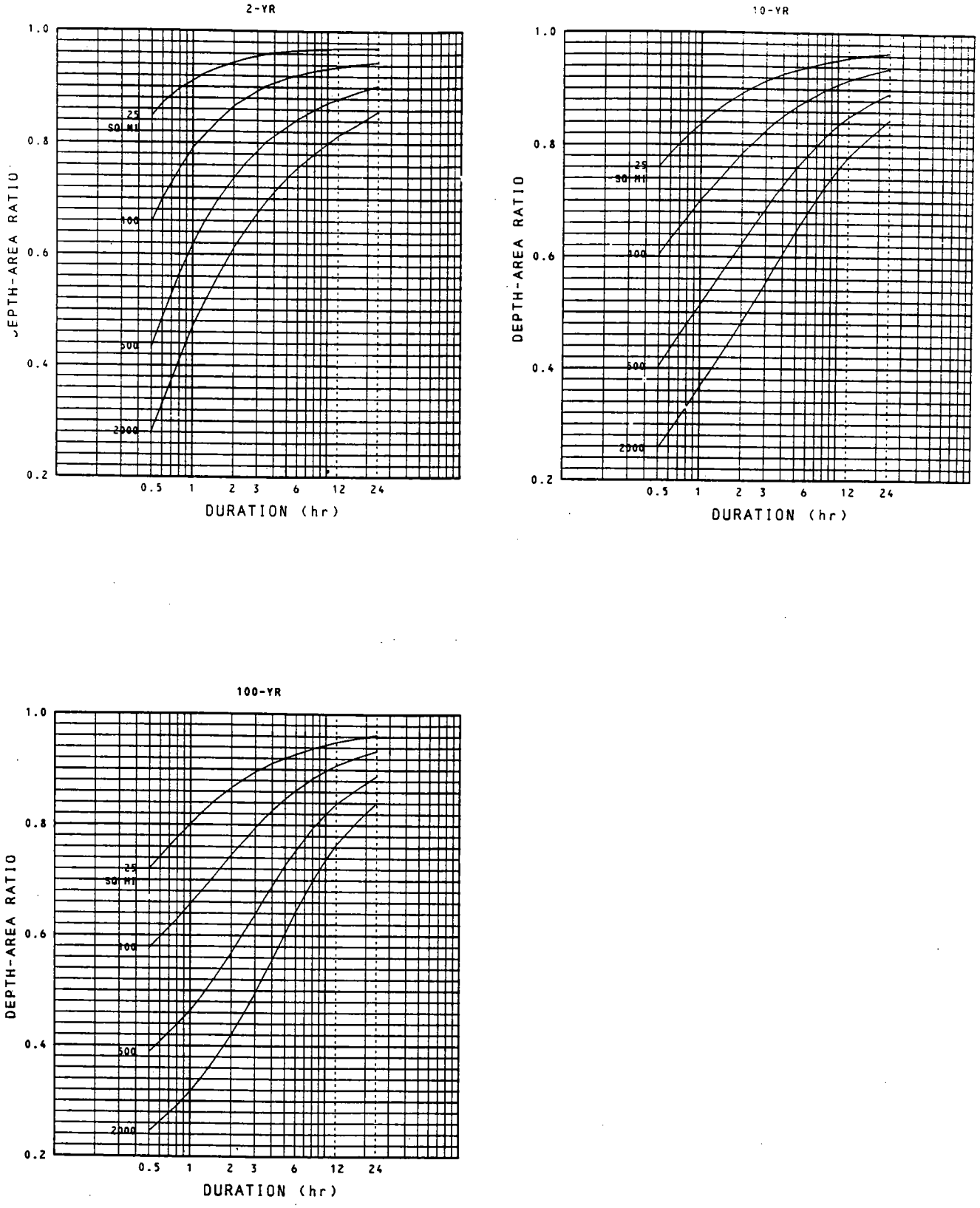

Figure 6-4.--Depth-area ratios. Chicago, Ill. Durational profiles at selected area sizes and return periods.

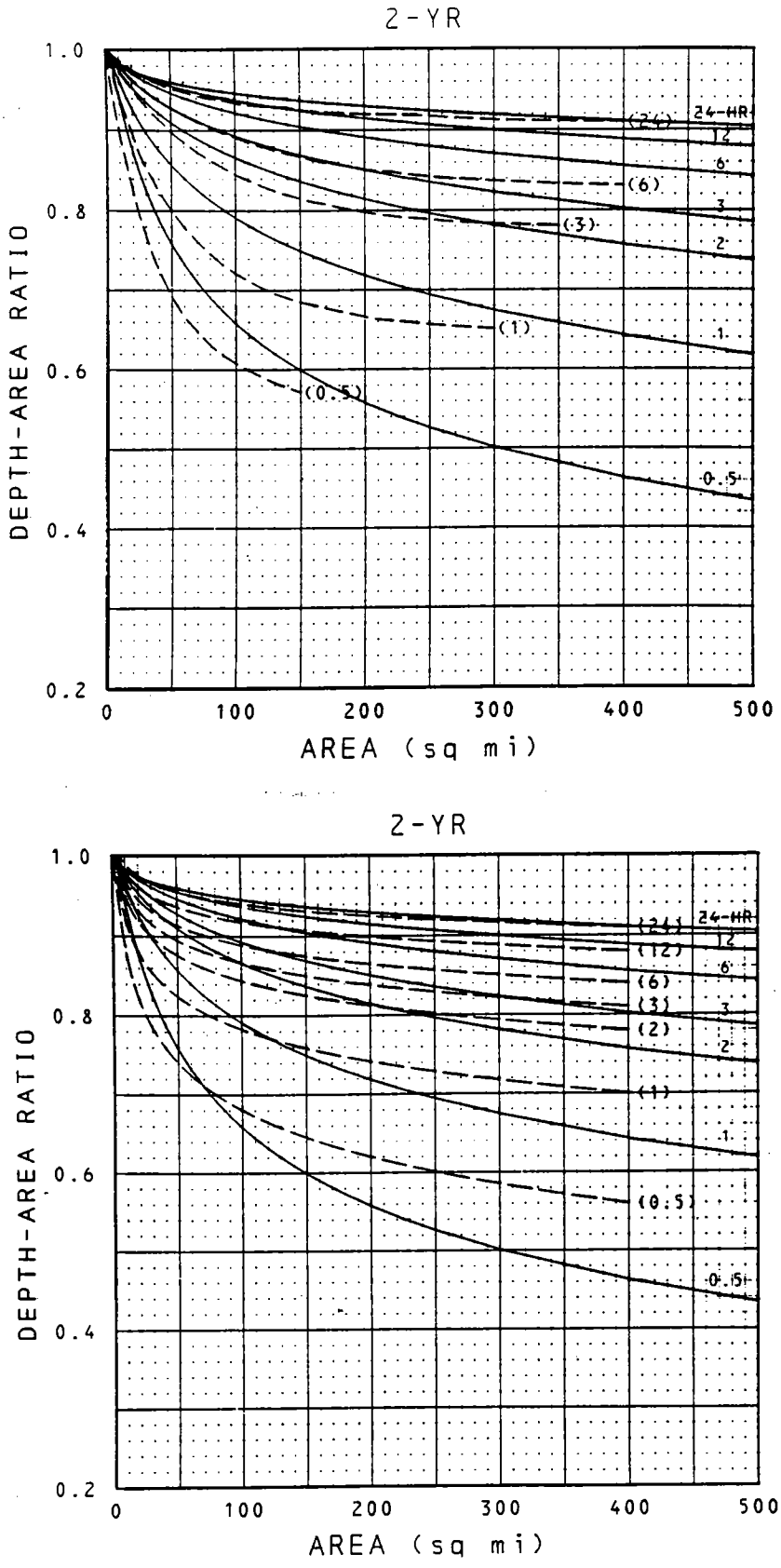

Figure 6-5.--Comparison of depth-area ratios of this study for Chicago with figure 1-1 (upper) and Huff and Vogel's (1976) for Illinois (lower).

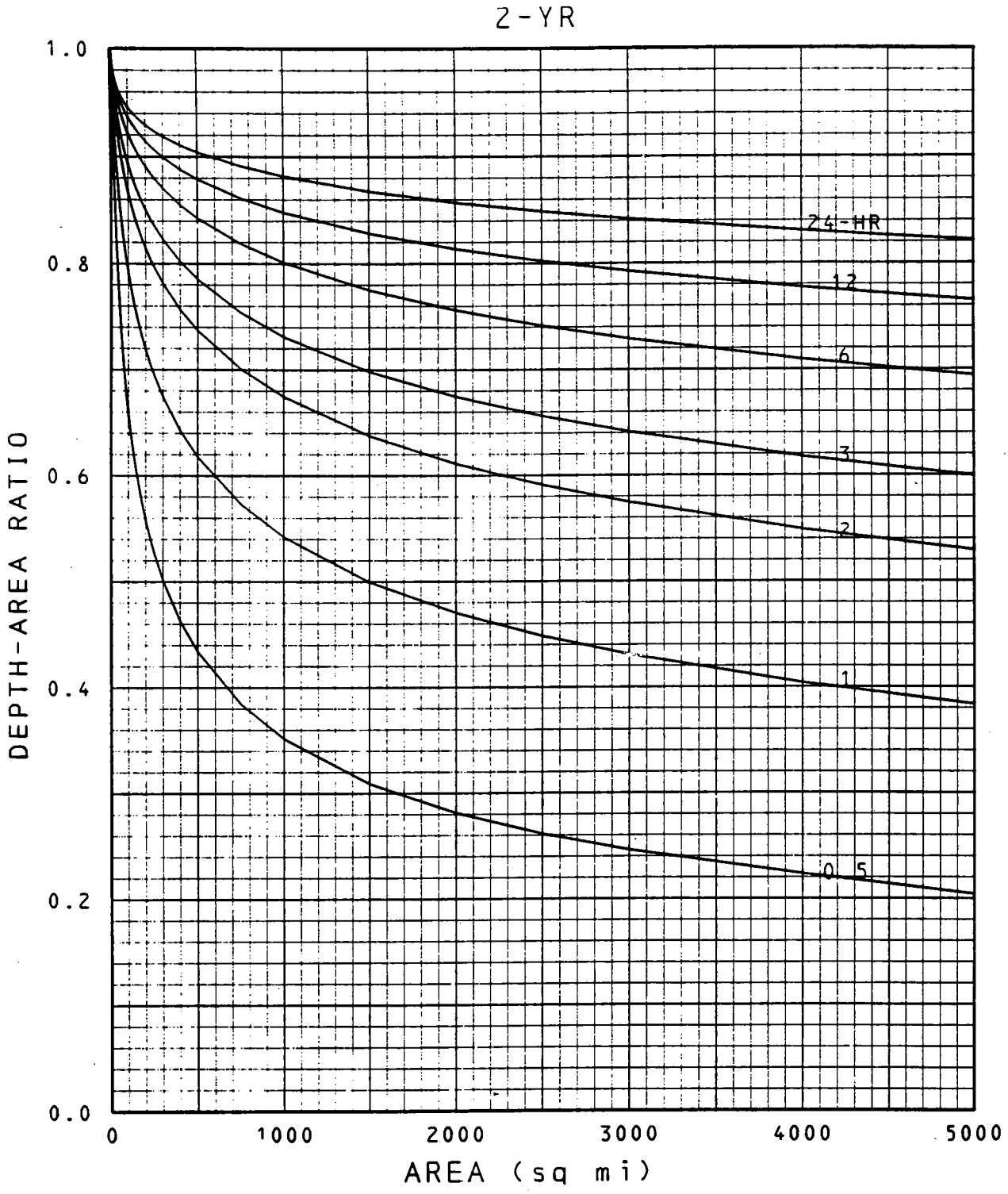

Figure 6-6.--Same as figure 6-1, to 5000 mi^2.

CHAPTER 7. SYNOPTIC ANALYSIS OF INDIVIDUAL HEAVY RAIN EVENTS

Synoptic Types

The annual maximum rainfalls that comprise the primary data set for this study were produced by a large number of storms. The synoptic meteorological data fields were evaluated for 20 of the more extreme heavy rain events that were selected from the annual maximum rainfalls with durations of 1, 2, 3, 6, 12, and 24 hours. Table 7-1 lists the dates, times, and rainfall amounts. As expected, these storms occurred with a variety of weather patterns. These were grouped into four synoptic weather types.

Nearly all precipitation in midlatitudes occurs as a result of the upward vertical motion induced either directly or indirectly by moving waves in the westerlies. These have dimensions of horizontal wavelengths in the 2000-3500 km range and a vertical depth from the surface to 25-30 km. These are generally termed short waves as distinct from the longer, nearly stationary, more stable and persistent waves. With this in mind, three synoptic types were defined according to a subjective evaluation of the vertical motion associated with the short wave. These were designated "weak," "strong," and "intense." A fourth synoptic weather type was assigned to an easily identified case where the rain occurred with the remnants of a tropical cyclone (hurricane). This type is uncommon at Chicago, but is responsible for many annual maximum rains in much of the Southern and Eastern regions of the United States (Cry 1967).

The familiar surface patterns of fronts, cyclones, and anticyclones are single level depictions of the migrating short waves. At all levels, the magnitudes of temperature and pressure gradients are well related to the size and strength of the short wave vertical motion field. However, many annual maximum rainfalls occur in thunderstorms which generate very intense vertical motions on a smaller scale. Therefore, the "weak," "strong," and "intense" designations used here are not well related to the intensity of precipitation but indicate the character of the synoptic scale weather system responsible for initiating and organizing the heavy rain event.

The distribution of the selected storms according to synoptic type and month of occurrence is shown in table 7-2. As explained in chapter 2, only storms occurring in the April through October period are included in this study. Detailed descriptions of the four synoptic weather types are given below.

I. Weak. The heavy rain is the immediate result of intense thunderstorms. The thunderstorm complex as a whole moves slowly and influences a smaller area than the other weather types defined here. Surface dew point temperatures are generally greater than 70°F. A weak stationary or slow-moving surface front is often present in the vicinity of the heavy rain area. Upper-level winds are light with anticyclonic horizontal shear. The short wave is weak and often barely noticeable. The typical season of occurrence for the "weak" weather type is midsummer.

II. Strong. Precipitation is predominantly convective with thunderstorms widespread over a large area. The heavy rain occurs with a warm front, squall line in the warm sector, a cold front, or a combination of these features. Surface dew point temperatures are generally in the 60^{o}-70^{o}F range. A well-defined, fast-moving short wave moves in an easterly direction. Associated with this disturbance is a surface low pressure center which passes 300-800 km to the north of the heavy rain area. The "strong" weather type occurs most often in late spring or early autumn.

III. Intense. Steady rain falling from stratiform clouds is predominant but embedded showers and thunderstorms may also occur. Annual maximum rains resulting from the "intense" weather type are usually for durations of 12 hours or longer. Surface temperatures and dew points are generally 40^{o}-50^{o}F. The polar jet stream in the upper troposphere is located near the heavy rain area. An upper-level pressure trough or closed low pressure circulation is well defined. A deep surface low tracks south of the heavy rain area so that no surface fronts pass through the area. Early spring and late autumn are the typical seasons of occurrence.

IV. Tropical. A hurricane or tropical storm moves inland and northward from the Gulf of Mexico. The heavy rain falls as the tropical disturbance weakens over land and interacts with the midlatitude circulation. Typically, occurrence coincides with the late summer and autumn hurricane season.

It should be noted that these descriptions apply to the 20 heavy rain events selected for the Chicago area. A similar classification of synoptic weather types at other locations would likely result in different specific features.

A more objective delineation between types might be based on a numerical evaluation of the size and strength of the synoptic-scale vertical velocity field. Other more easily measured quantities strongly correlated with the vertical velocity field might be used, such as 500-mb vorticity advection, 500-mb temperature gradients, and 200-300 mb wind speeds.

Individual storms of the Type III designation are most extreme at the 24-hr duration, while Type I storms are most extreme at 1 and 2-hr durations. This suggests that the largest rainfall rates occur with Type I storms. Type II annual maximum storms are more evenly distributed among durations.

The major feature differentiating Type II from Type I is that with Type II the synoptic-scale features dominate in initiating and organizing the thunderstorms. It was previously mentioned that a stationary or slow moving front is often present with Type I storms. We may presume that smaller scale frontal boundaries not shown on synoptic-scale maps may be important features with many of the heavy rain events. The frontal boundary resulting from the production of a meso-high by previous thunderstorms has been associated with many thunderstorms that cause flash floods (Maddox et al. 1979).

Examples of Synoptic Types

Type I (weak) event.

During the afternoon and evening of July 12, 1957, intense rains fell throughout the metropolitan Chicago area. Based on hourly rainfalls averaged over the network (in this case 14 individual stations equally weighted), this storm was the most extreme of the 1948-72 analysis period at durations from 2 to 24 hr. The 12-hr duration yielded rainfall amounts with the smallest probability of occurrence. At some stations 2-hr amounts of about 3 inches were the heaviest of the 25-yr record. Nearly all the rain, over 7.5 inches at some stations, fell between noon and midnight (CST). Precipitation mass curves for two stations are shown in figure 7-1.

Detailed isohyetal analyses for this storm indicate rainfalls were heaviest in northwest portions of the metropolitan Chicago area, and lightest near the shore of Lake Michigan. A field survey indicated total storm rainfalls of 9 inches in some parts of Chicago, and an additional rainfall maximum of 11.1 inches at Kankakee, Ill., 50 miles south of Chicago (Huff et al. 1958; Huff and Vogel 1976).

The surface weather analysis for 0000 CST, July 13, 1957, is depicted in figure 7-2, and figure 7-3 shows the 500-mb analysis for 1800 CST, July 12, 1957. This storm is classified as Type I (weak) occurrence because of the light 500-mb winds, small temperature gradients, and the lack of a well defined short wave. No large differences are noted in the large scale flow patterns before and after the storm.

Note the stationary front on the surface analysis (figure 7-2) which was located just south of Chicago during the 12-hr period of heavy rain. This was likely an important feature in providing the lift necessary to initiate convection as the very moist air near the surface flowed northward. As thunderstorms moved eastward with the upper level winds which were approximately parallel to this surface front, new thunderstorm cells were generated along the boundary. Maddox et al. (1979) have identified 38 flash floods during the period 1973-77 associated with this type of weather pattern. Their terminology classifies this as a "frontal" type. Maddox et al. also identify a "meso-high" type of flash flood event that would also be classified as a Type I (weak), and a "synoptic" type that coincides with Type II (strong).

Type II (strong) event.

A flood of major proportions occurred October 9-11, 1954, in the Chicago area. Property damage was widespread and severe (Nash and Chamberlain 1954). Precipitation mass curves at two selected stations are shown in figure 7-4. Most of the rainfall with this storm occurred between 1900 CST on the 9th and 0600 CST on the 10th. During this period, a frontal boundary was located in the Chicago area. This front drifted southward

slowly and then moved back to the north as a surface low pressure center moved northeast from central Kansas midday on the 9th, to near Green Bay, Wis., on the evening of the 10th. A second period of heavy rain fell between 1600 CST and 2000 CST on the 10th. During this latter period a line of thunderstorms, generated within the warm sector, passed through the Chicago area. Lesser amounts of rain fell at midday on the 11th, associated with a cold front passage (fig. 7-5). Winds at 500 mb were west-southwesterly during the entire storm period (fig. 7-6).

The 500-mb flow pattern over North America changed dramatically during the period October 7-13, 1954, with complete reversal in the long wave positions. A long wave ridge with small amplitude was located at about 95°W longitude on the 7th (fig. 7-7). Over the following several days a deep long wave trough developed at the same longitude (fig. 7-8). During this period a series of short waves moved rapidly through the Central U.S. as the long wave trough became more well defined. This resulted in complex and rapidly changing surface pressure and frontal patterns with intense cyclogenesis on the 12th and 13th in the Central Plains. The new surface low tracked to the north of Chicago and had much stronger circulation than the October 9-10 system, but did not produce as much rain in the Chicago area.

Additional information and insights pertaining to the typical scale and areal coverage of thunderstorm systems can be obtained from radar data. National Weather Service radar data were available for only a few of the 20 storms examined. One of these was a Type II storm which occurred in the Chicago area on August 16, 1968. Most of the rain fell between 0800 CST and 2300 CST. Amounts were most extreme at 3- and 6-hr durations. Intense thunderstorms moved through Chicago just ahead of a vigorous cold front which passed through the area around 0200 CST, August 17. The surface weather map for 0600 CST, August 16, 1968, is shown in figure 7-9.

Figures 7-10 and 7-11 show a series of photographs of the PPI scope of a WSR-57 radar depicting the areal configuration of the thunderstorms. The radar was located in south central Chicago. The echo near the center of the scope is the characteristic ground clutter pattern, which is present on all photographs and obliterates the precipitation echoes near the center. At 1500 CST (first in series of fig. 7-10), no rain was falling in the immediate Chicago area and thunderstorms were limited to extreme northwestern Illinois and small areas of southern Wisconsin and Michigan. In the next several hours, numerous new thunderstorms developed and the group of thunderstorm cells moved through the Chicago area. By 0200 CST (last in the series of fig. 7-10), the precipitation area was well to the south and east of Chicago. Individual thunderstorm cells moved generally to the east-northeast, while the large area of precipitation moved to the east-southeast.

Figure 7-11 depicts the intensity characteristics of the thunderstorms which later moved through Chicago. All photographs in the series are at approximately the same time, but at various attenuation levels. In the last of the series only the strongest precipitation echoes remain on the scope. In this case, the -42 dB level indicates estimated instantaneous rainfall rate of about 5.0 inches/hour (Weather Bureau et al. 1973).

Type III (intense) event.

During the 24-hr period of 0300 CST, May 11 to 0300 CST, May 12, 1966, the Chicago network averaged 3.19 inches of rain. The precipitation was predominantly steady rain falling from stratiform clouds. Surface temperatures were quite cool -- 40° to 50°F. A deep surface low tracked from eastern Colorado to about 50 km south of Chicago and continued to the east-northeast (fig. 7-12). The strong polar front jet stream associated with this storm system has 500-mb wind speeds as high as 75 knots (fig. 7-13). Precipitation events of this type are typical of the winter season, and occur less frequently in other seasons.

Type IV (tropical) event.

During the afternoon of September 11, 1961, Hurricane Carla moved inland at Port O'Connor, Texas. Wind gusts to 175 mph occurred in some areas with gusts to 75 mph along nearly all of the Texas Gulf coast (Dunn 1962). This was one of the most intense and destructive hurricanes ever to strike the United States Gulf coast. At 1800 CST, September 13, 1961, the dissipating circulation of the storm was located near St. Louis, Mo., and moved to Lake Huron in the next 12 hours, passing south of Chicago (fig. 7-14).

The surface analysis for 0000 CST, September 13, 1961, shows the tropical cyclone in its dissipating stage, centered in Oklahoma, and interacting with a midlatitude frontal system (fig. 7-15). The areal distribution of the rainfall was fairly uniform. The stations in Chicago received about 3 inches with most of it falling in the 6-hr period 2200-0200 CST, September 13-14, 1961. This was the third largest 6-hr amount during the 25-yr analysis period for the Chicago network average.

Table 7-1.--Twenty heavy rain events with synoptic types and representative rainfall amounts.

Date	Beginning hour[1] (CST)	Synoptic Type	Annual maxima (inches) Network average[2] 1-hr	6-hr	24-hr	Greatest at Individual Station 1-hr stn.		6-hr stn.		24-hr stn.	
June 14, 1949	03	II	0.78	2.10	3.27	1.17	E	3.16	E	4.64	D
June 2, 1950	03	II	*	*	3.42	1.39	D	3.30	J	4.88	J
May 10, 1951	03	III	*	1.20	3.04	*		1.74	F	3.63	F
Aug. 18, 1954	04	II	1.39	*	*	2.11	I	2.89	J	*	
Oct. 3, 1954	05	II	*	2.55	*	1.88	A	5.18	A	*	
Oct. 9, 1954	18	II	*	*	5.89	1.70	K	3.07	K	6.88	A
Aug. 29, 1955	17	II	*	1.97	2.47	0.88	J	3.36	I	3.22	A
July 12, 1957	12	I	1.33	5.01	5.96	2.50	H	6.47	D	7.69	D
June 25, 1959	20	I	0.78	2.47	2.48	2.06	L	4.58	L	4.58	L
July 2, 1960	19	II	1.09	1.97	1.98	1.84	A	2.29	B	4.88	J
Aug. 4, 1961	15	II	*	*	*	1.64	J	*		3.45	C
Sept.13, 1961	03	IV	0.75	2.72	2.88	0.88	A	3.31	D	3.58	D
July 1, 1962	20	I	0.58	2.26	2.41	1.50	J	3.63	D	3.79	D,J
Apr. 29, 1963	06	III	*	*	2.50	*		1.58	C,J	3.17	C
May 11, 1966	02	III	*	*	3.19	*		1.63	J	3.77	A
June 10, 1967	12	I	0.70	2.47	2.50	3.89	G/P	5.32	H	5.98	G/P
Aug. 16, 1968	17	II	1.19	2.84	2.95	1.69	D	3.73	L	3.83	L
July 17, 1969	02	I	0.74	1.64	2.12	1.55	L	3.25	T	4.78	T
Aug. 24, 1971	18	II	0.87[3]	*	*	1.95	J	2.22	A	2.22	A
Sept.28, 1972	19	II	*	*	2.05[3]	2.32	L	3.65	L	3.68	L

*Indicates annual maximum did not occur on this date.

[1]Beginning hour applies to the largest duration for individual station annual maxima.

[2]From 15-station average including all stations except U, V, and W (fig. 2-1).

[3]From 6-station average including stations A, G/P, H, I, L, and R (fig. 2-1).

Table 7-2.--Summary of synoptic type classification.

Synoptic Type	Number of Cases	Month of Occurrence
I Weak	5	6, 6, 7, 7, 7
II Strong	11	6, 6, 7, 8, 8, 8, 8, 8, 9, 10, 10
III Intense	3	4, 5, 5
IV Tropical	1	9

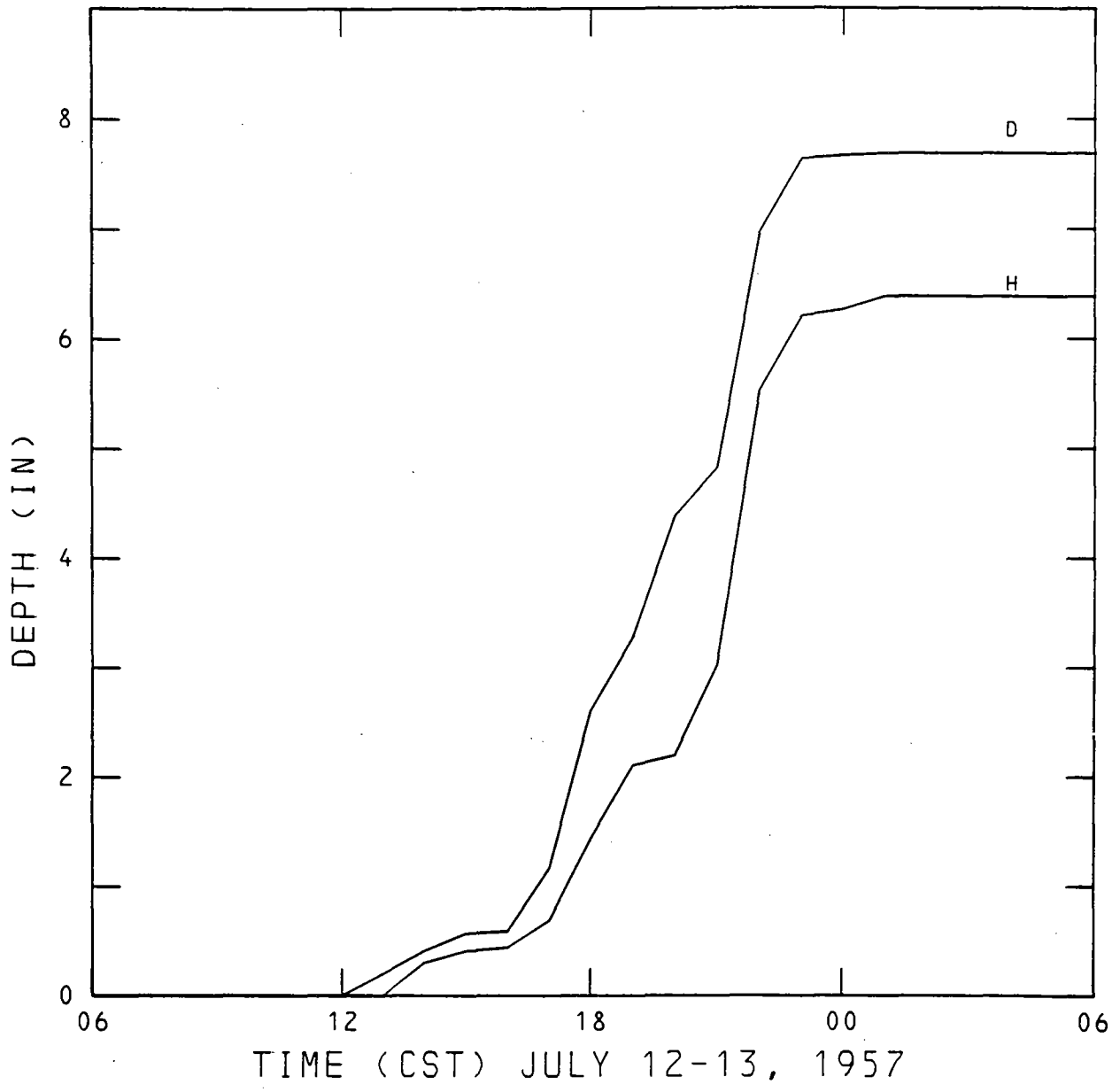

Figure 7-1.--Precipitation mass curves for Chicago Mayfair (Station D) and Chicago Sanitation District Office (Station H), July 12-13, 1957.

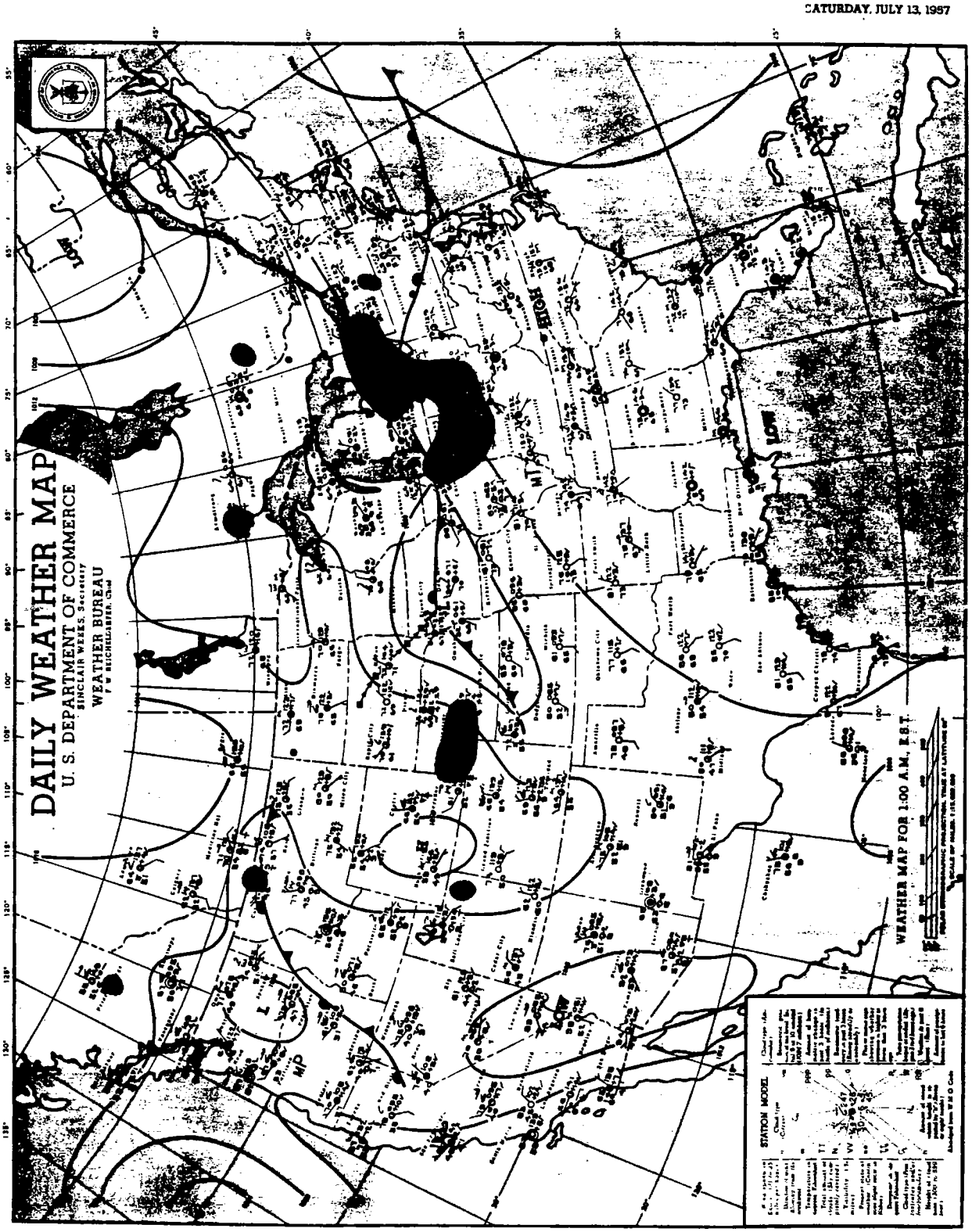

Figure 7-2.--Surface weather analysis at 0000 CST, July 13, 1957.

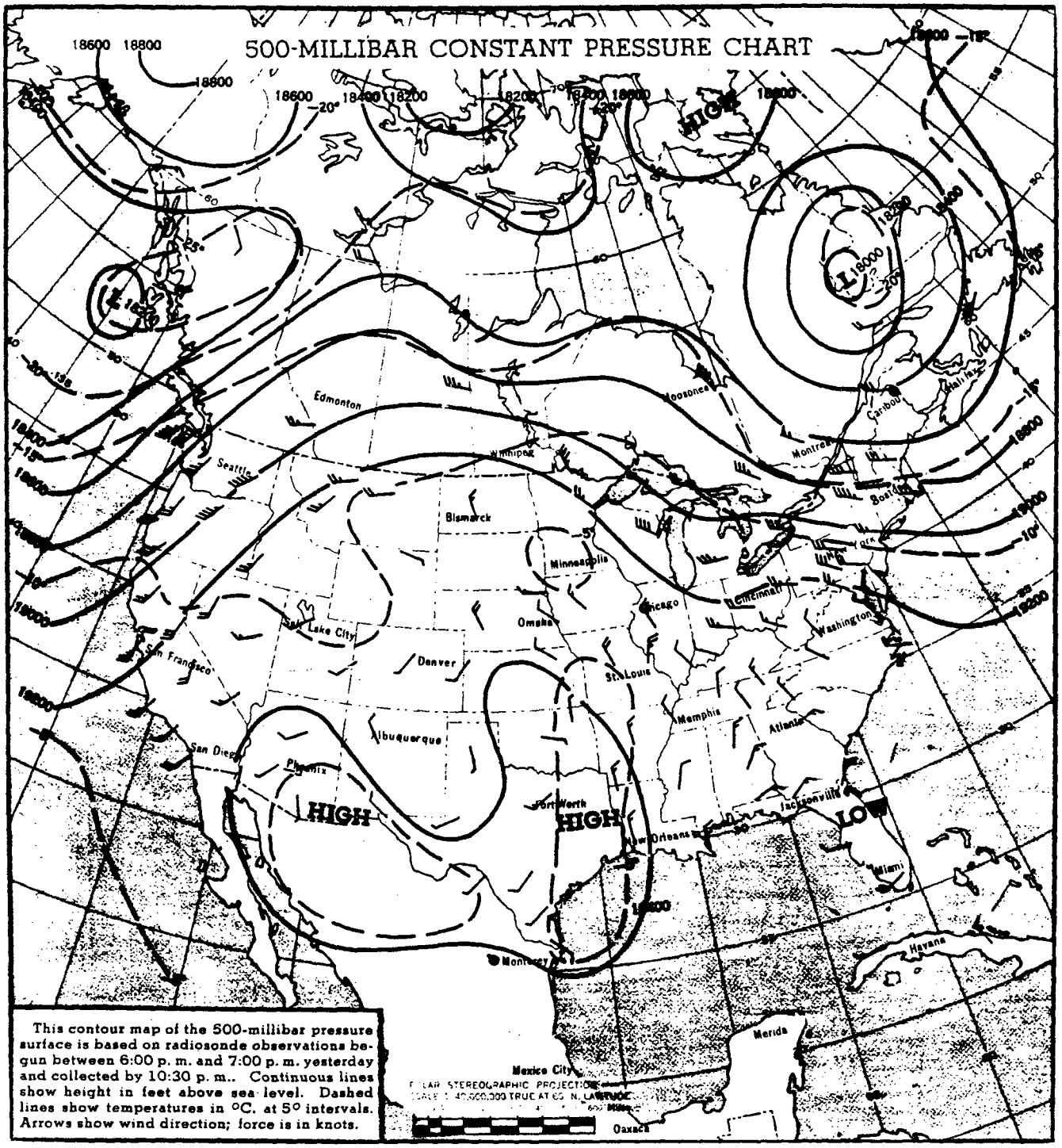

Figure 7-3.--500-mb analysis at 1800 CST, July 12, 1957.

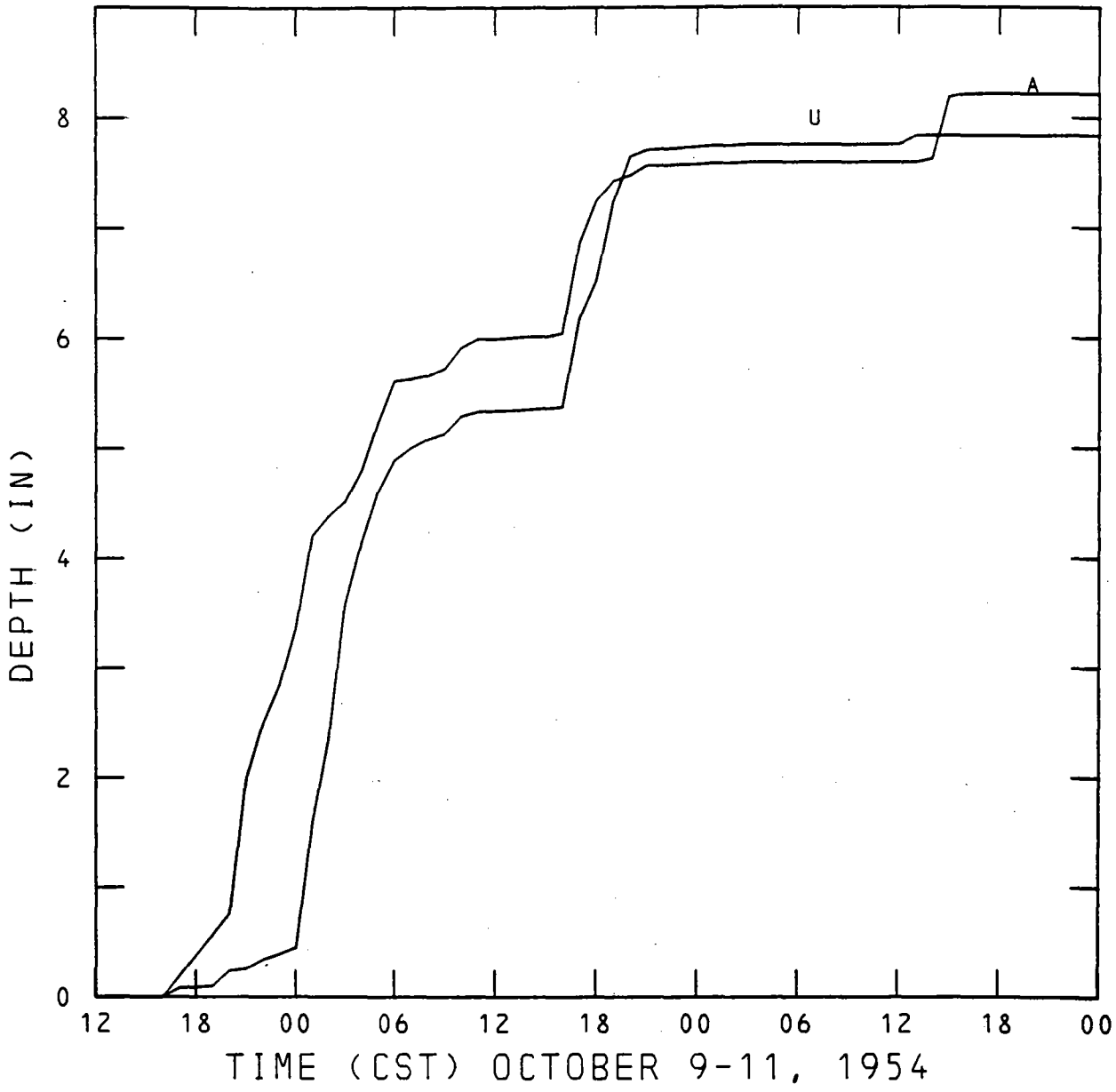

Figure 7-4.--Precipitation mass curves for Chicago Calumet Treatment Works (Station A) and Crete (Station U), October 9-11, 1954.

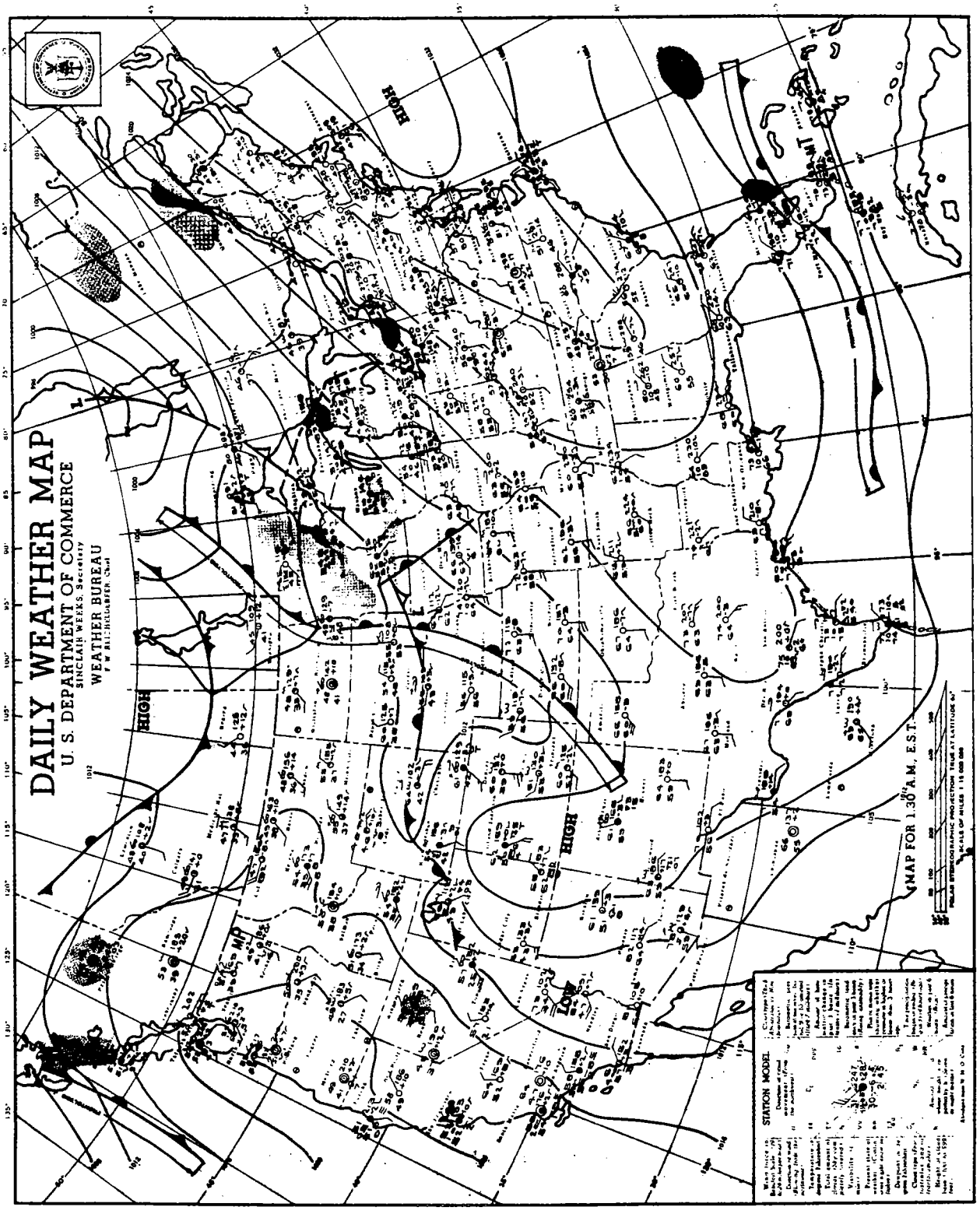

Figure 7-5a.--Surface weather analysis 0030 CST, October 9, 1954.

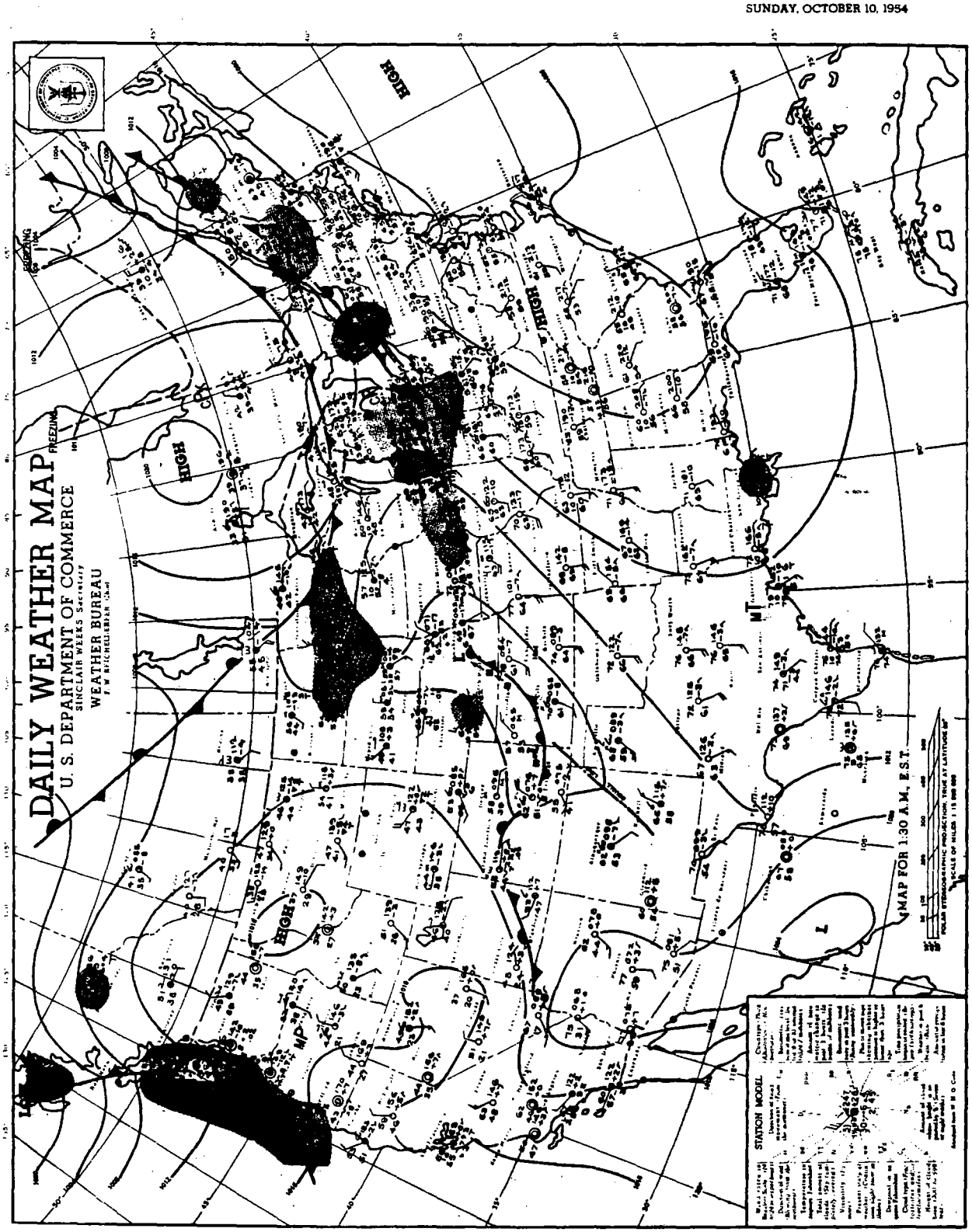

Figure 7-5b.--Surface weather analysis 0030, October 10, 1954.

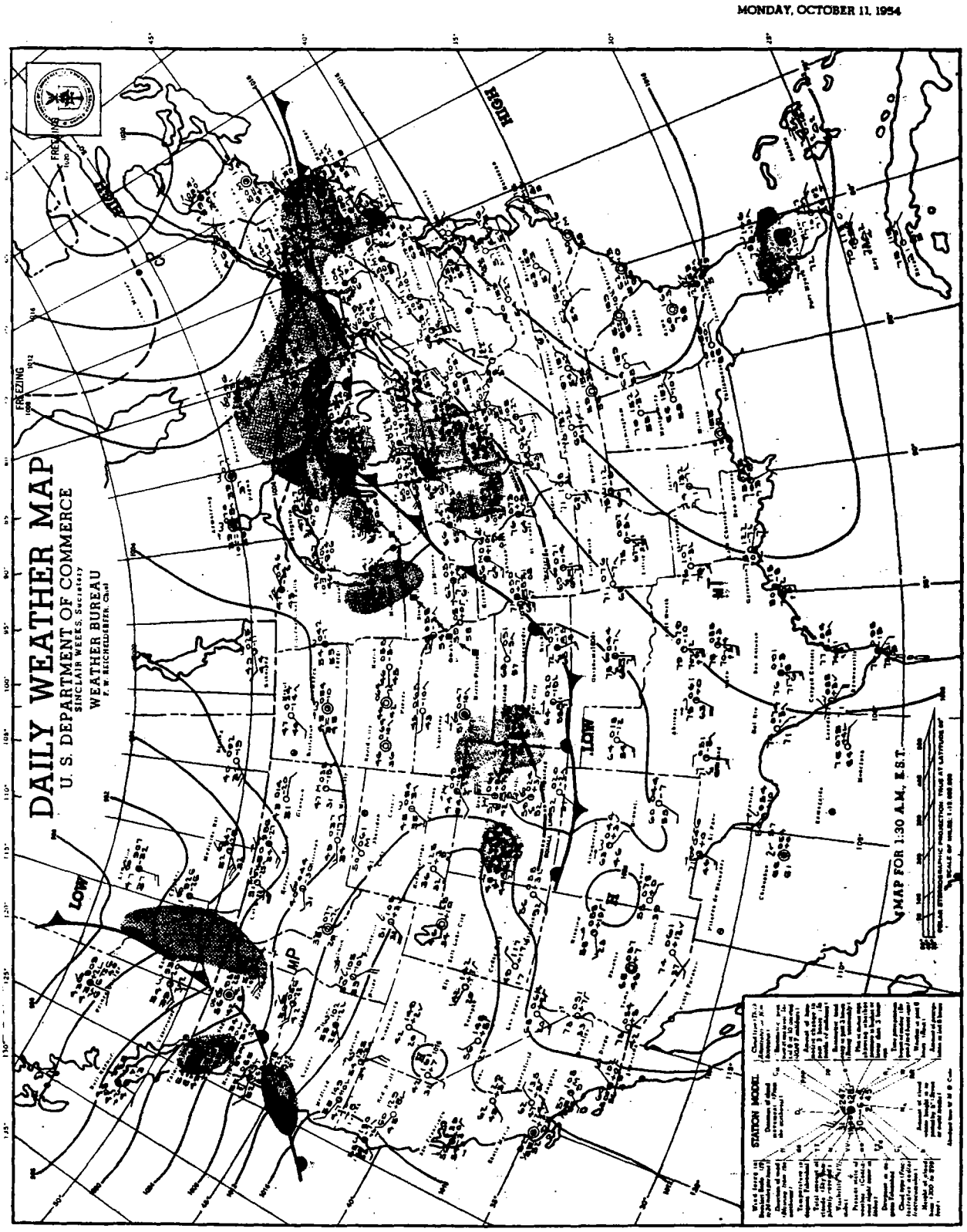

Figure 7-5c.--Surface weather analysis 0030 CST, October 11, 1954.

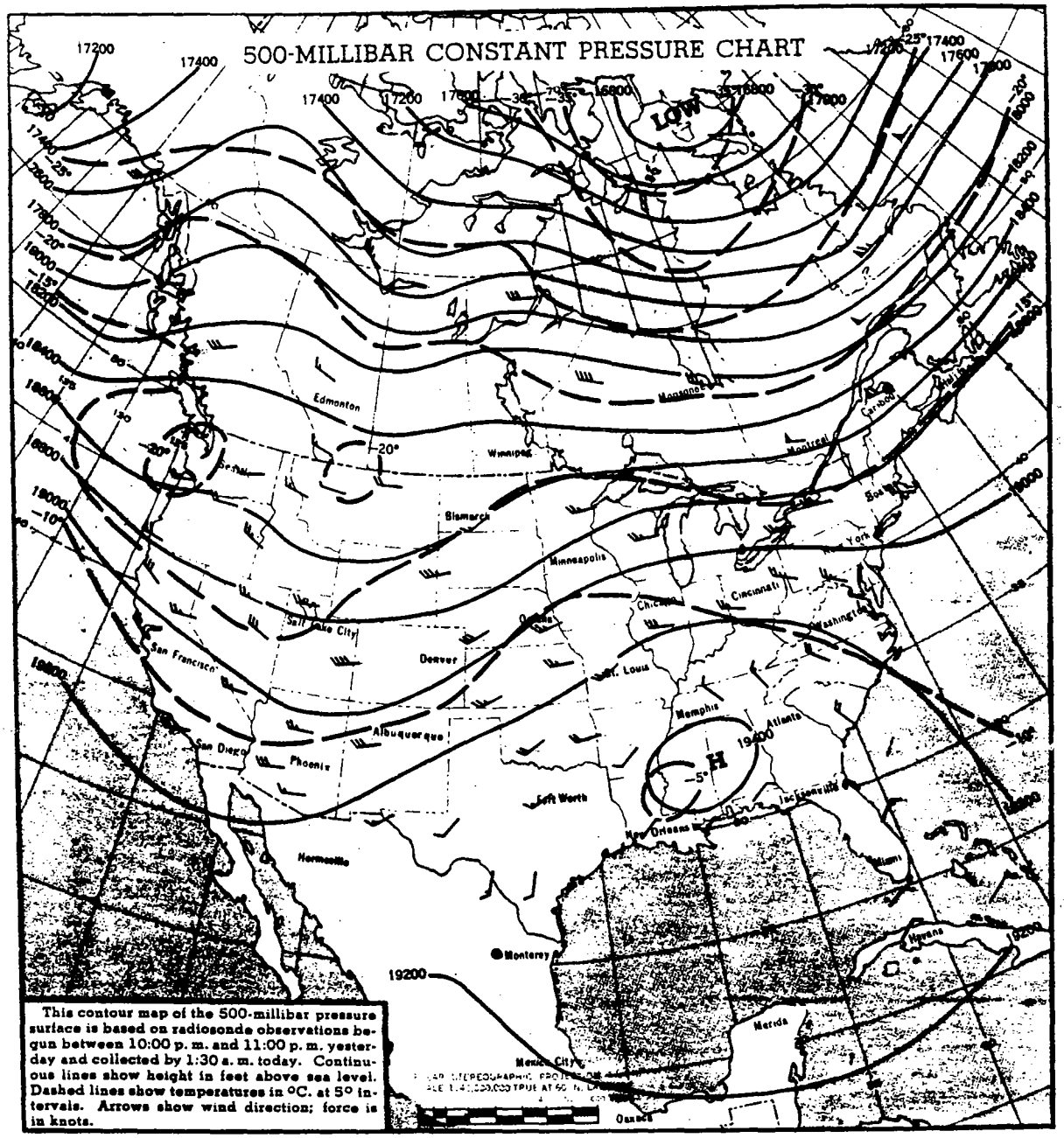

Figure 7-6.--500-mb analysis at 2200 CST, October 9, 1954.

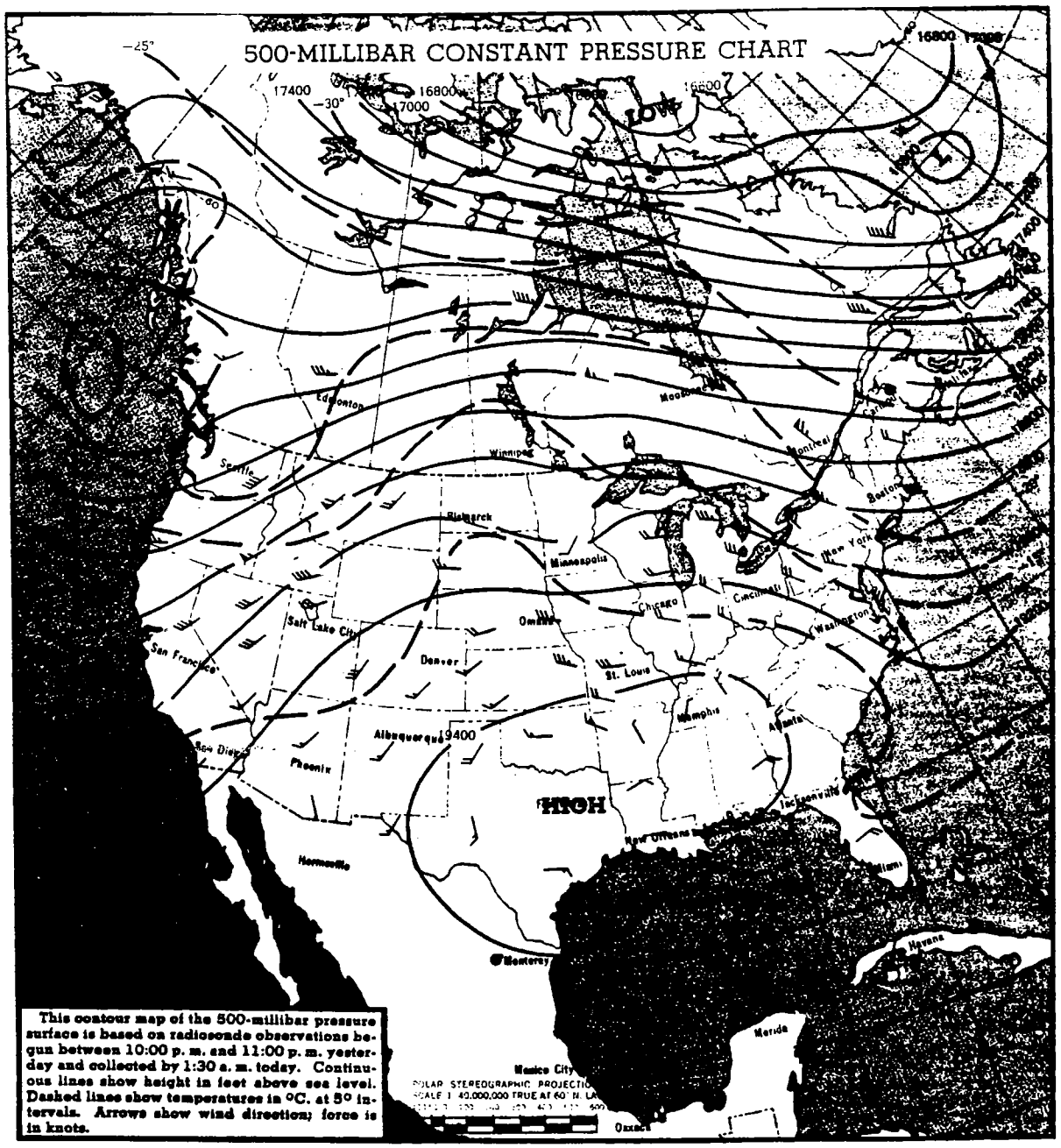

Figure 7-7.--500-mb analysis at 2200 CST, October 7, 1954.

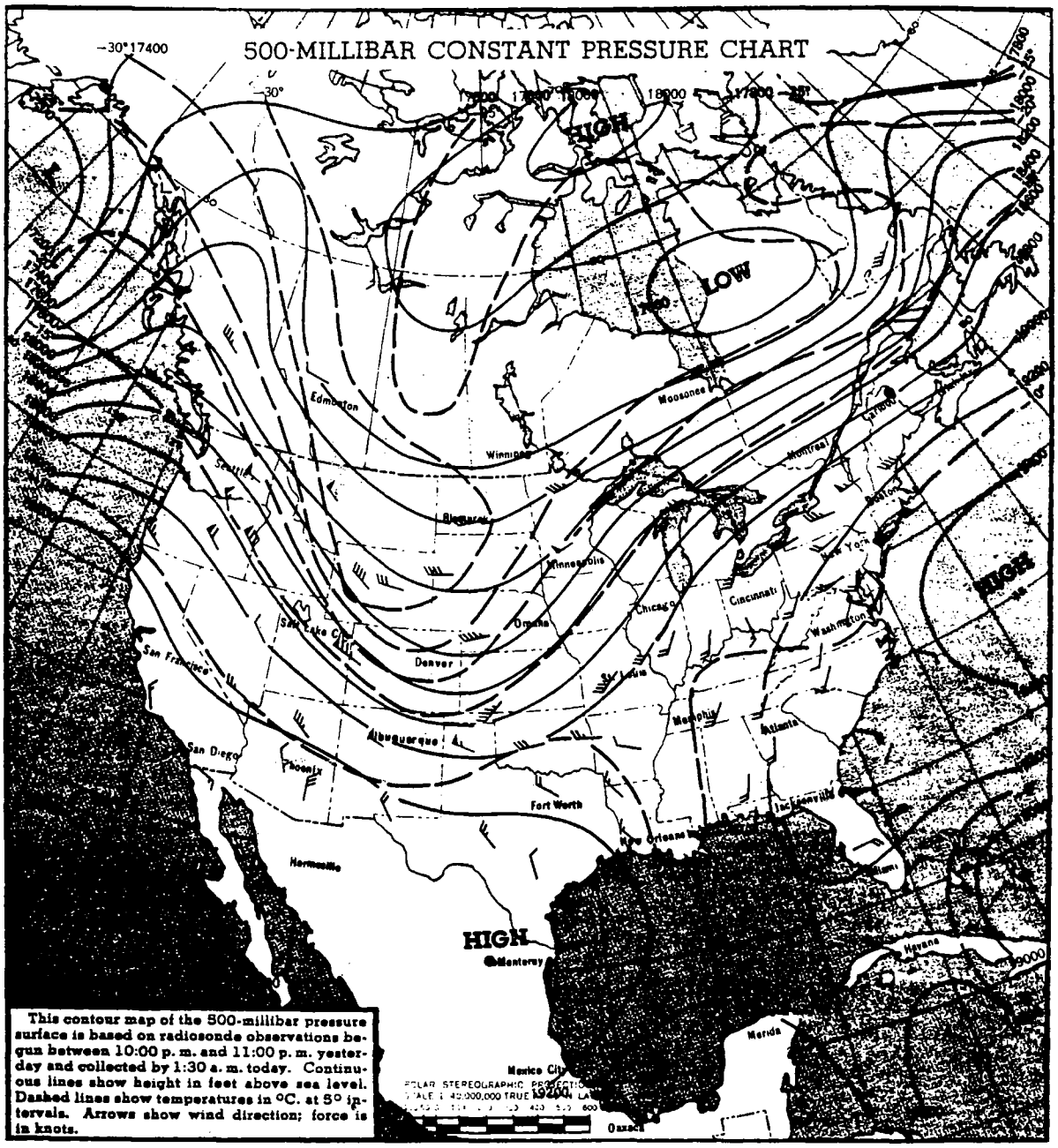

Figure 7-8.--500-mb analysis at 2200 CST, October 13, 1954.

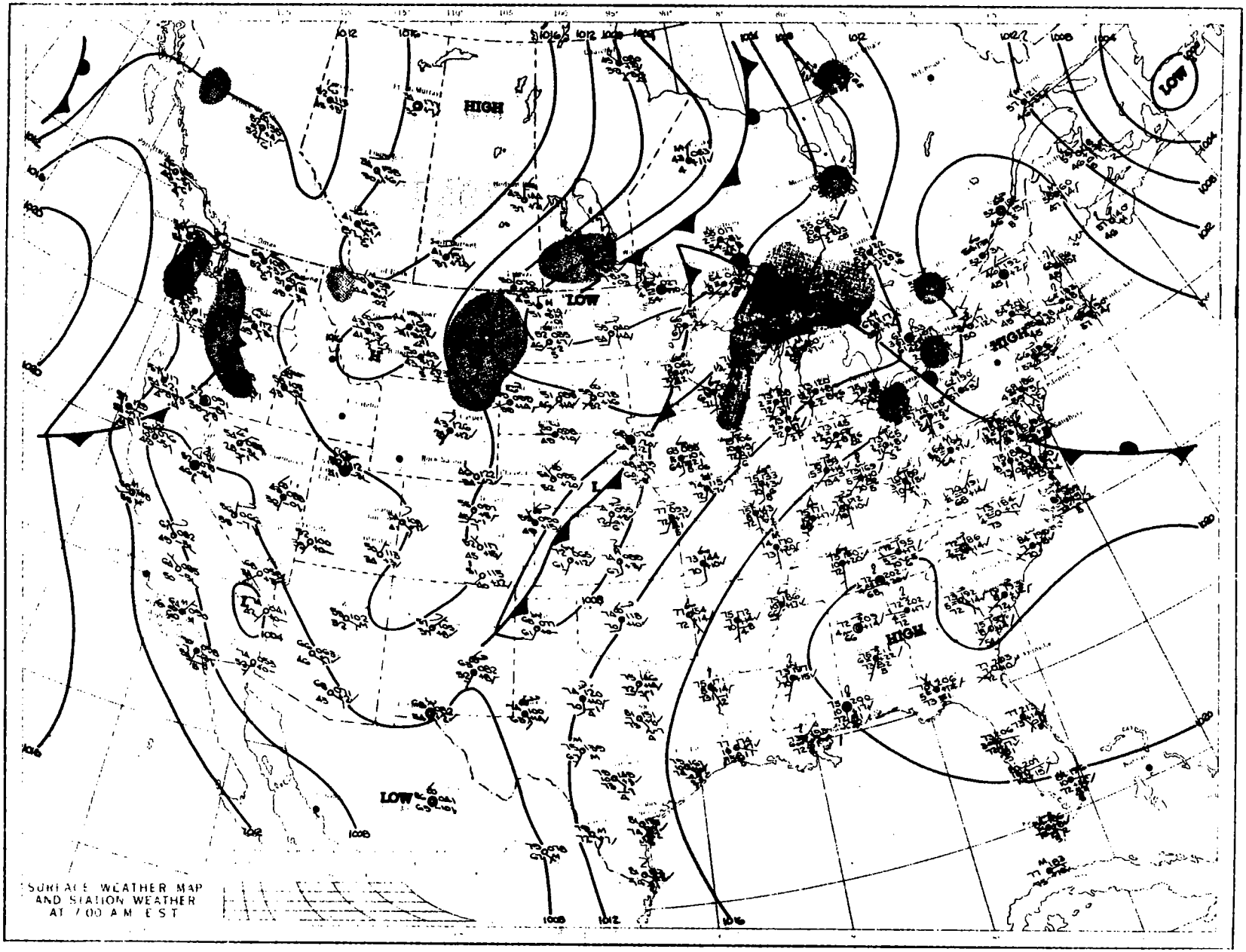

Figure 7-9.--Surface weather analysis at 0600 CST, August 16, 1968.

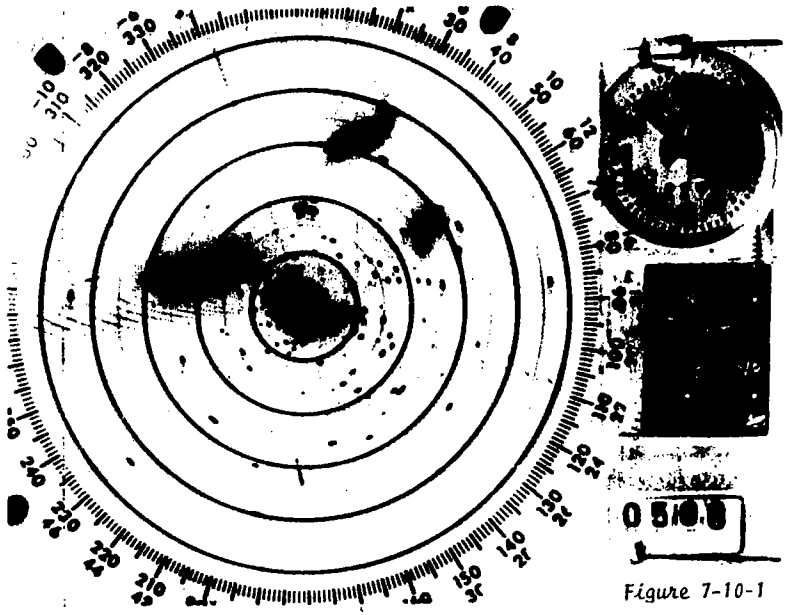

Figure 7-10-1

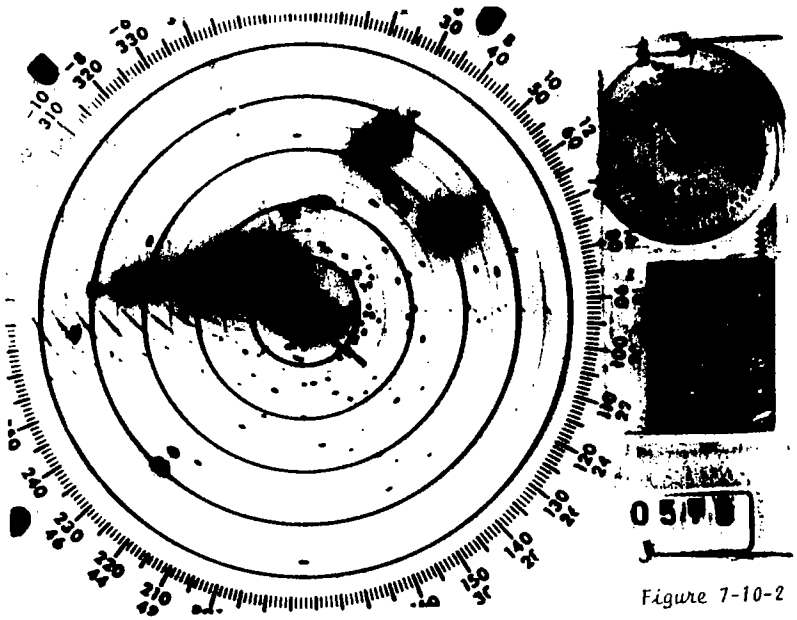

Figure 7-10-2

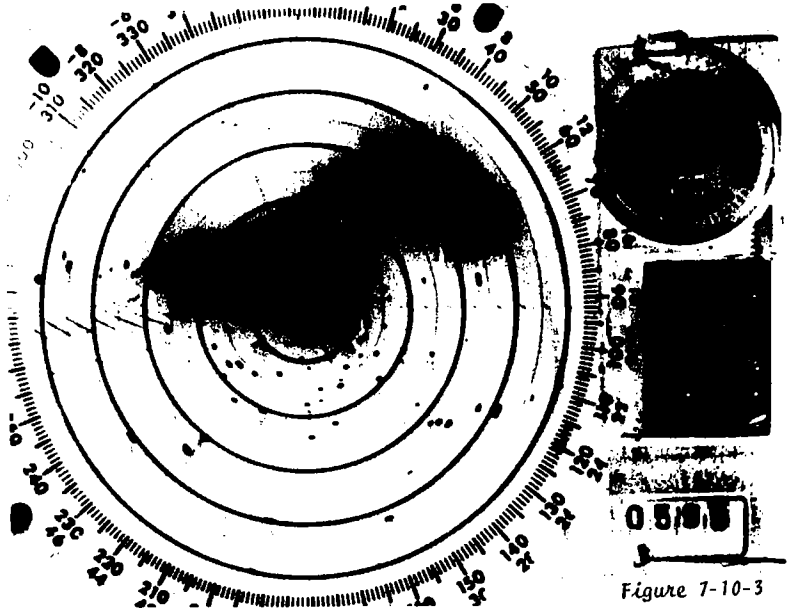

Figure 7-10-3

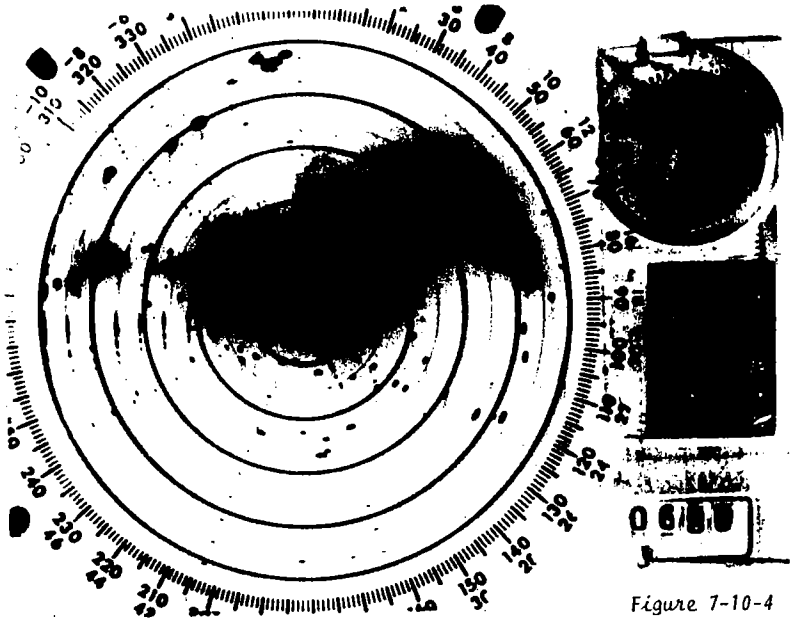

Figure 7-10-4

Figure 7-10.--Photographs of PPI scope of WSR-57 radar located at Chicago, Ill. Hourly sequence for period 2100 GMT, August 16, 1968 to 0800 GMT, August 27, 1968. Range is 250 n.mi. with marks at 50 n.mi. intervals. Attenuation is 0 dB.

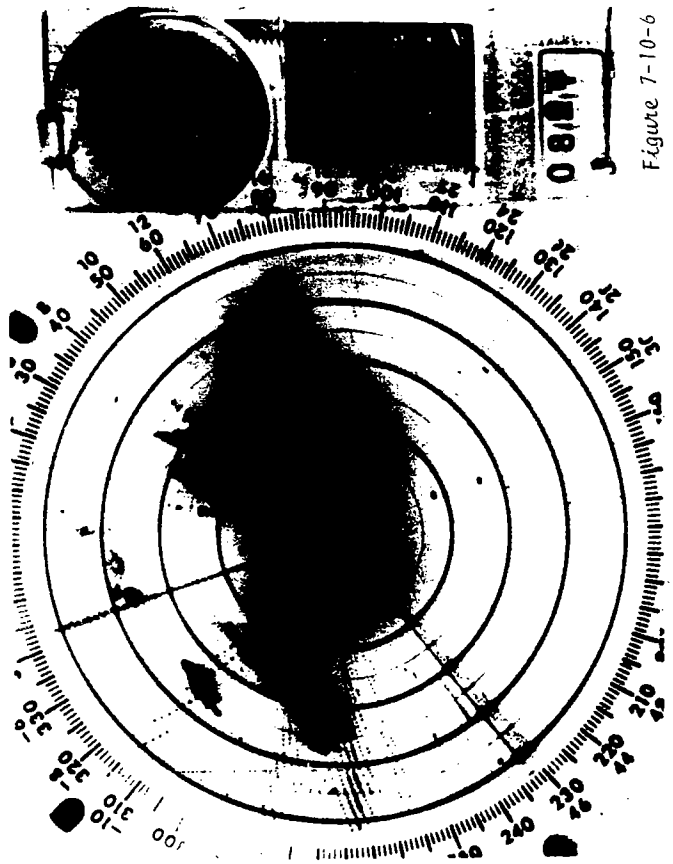

Figure 7-10-6

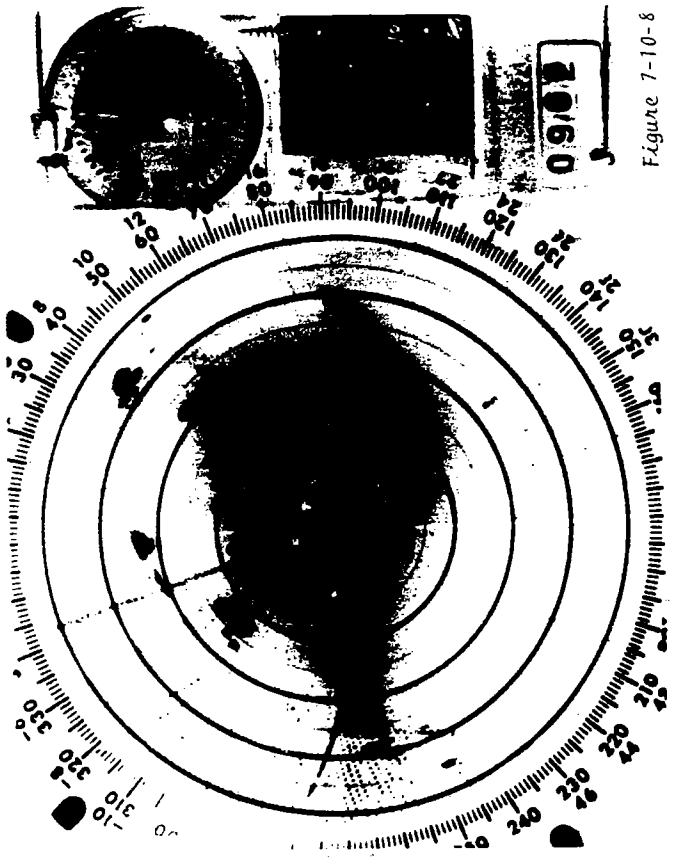

Figure 7-10-8

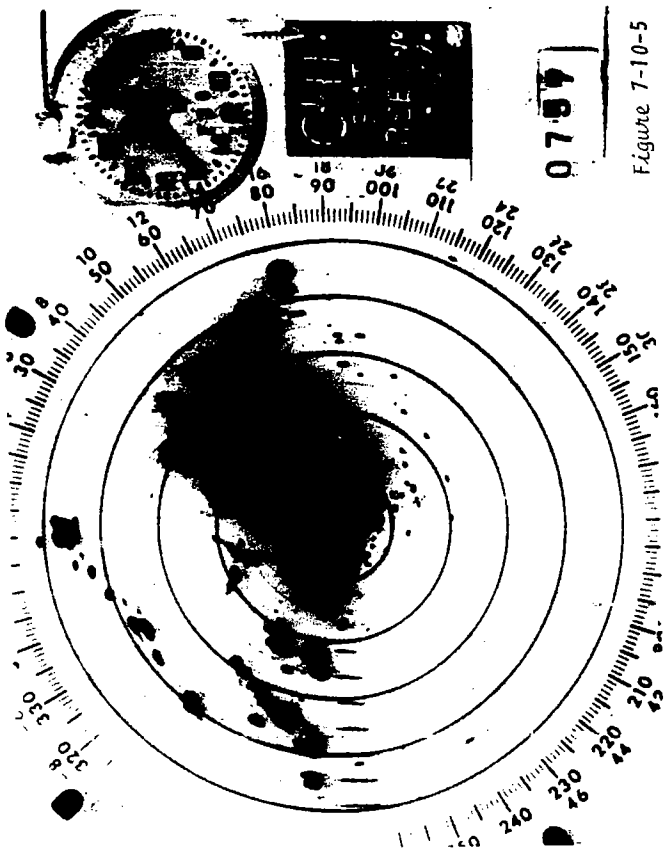

Figure 7-10-5

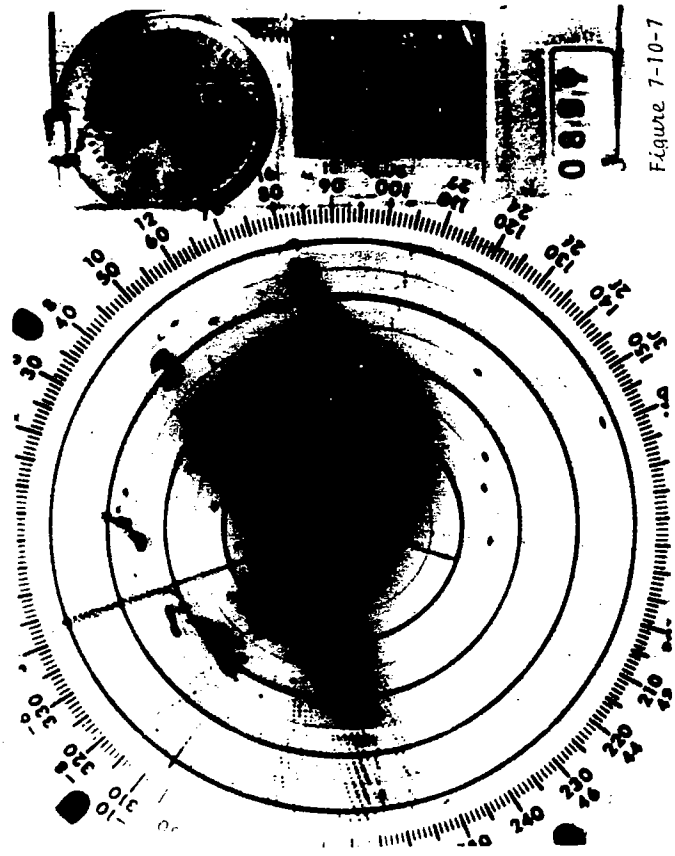

Figure 7-10-7

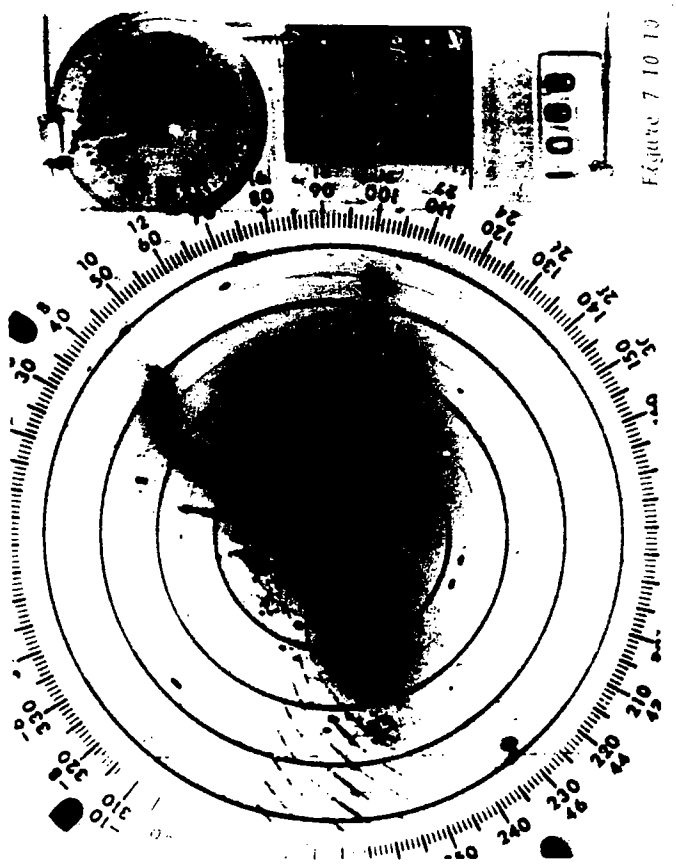

Figure 7-10-10

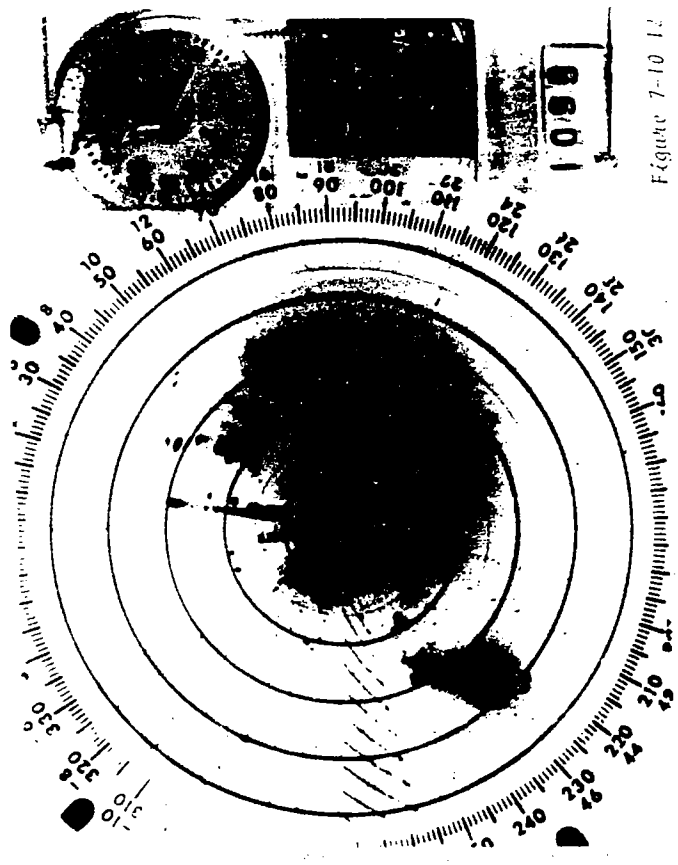

Figure 7-10-12

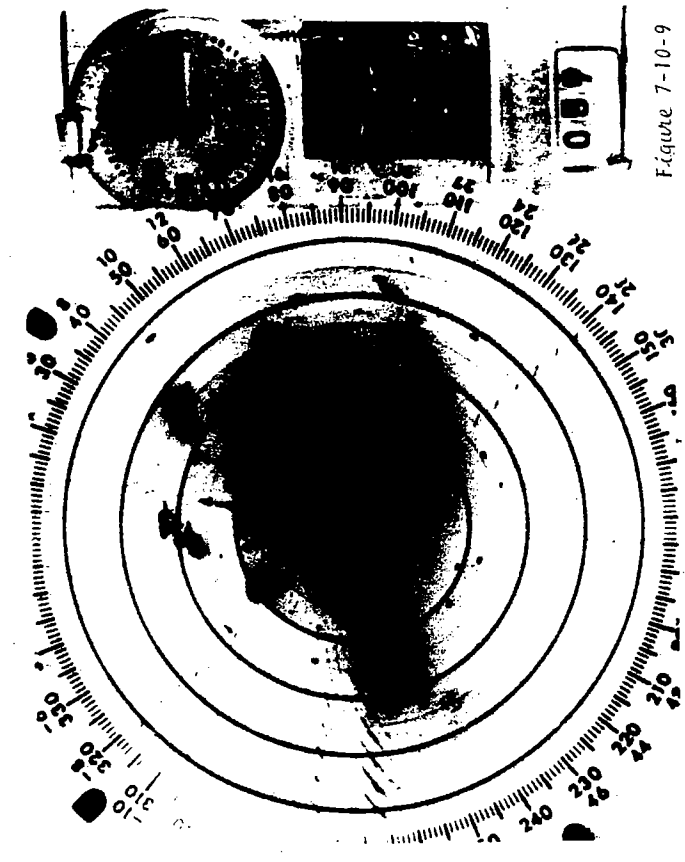

Figure 7-10-9

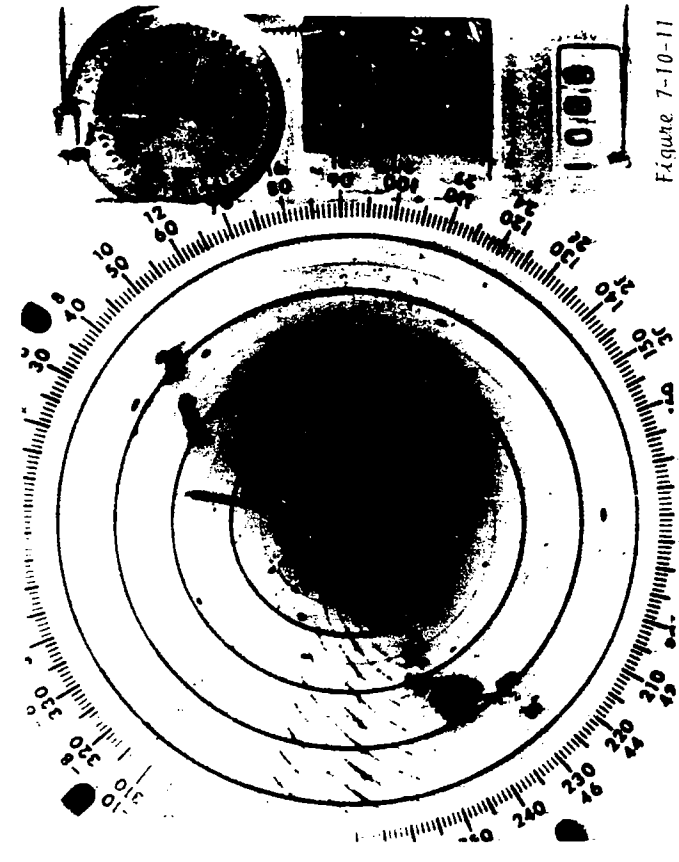

Figure 7-10-11

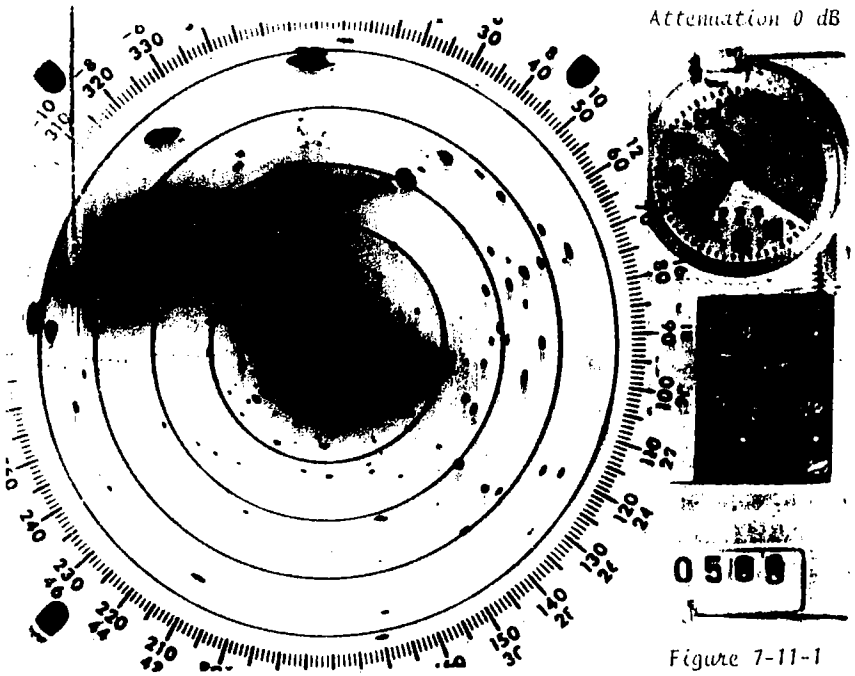

Figure 7-11-1

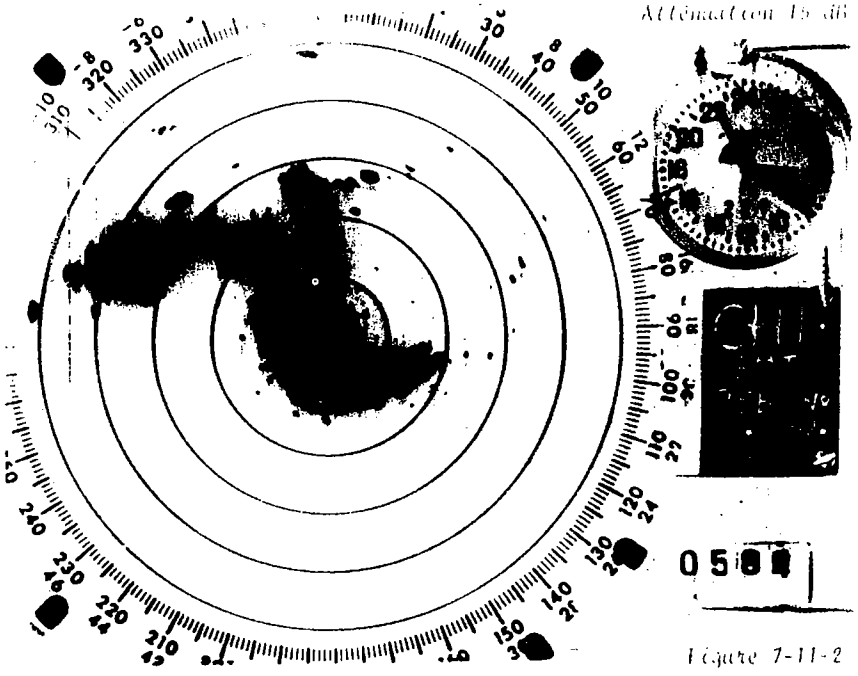

Figure 7-11-2

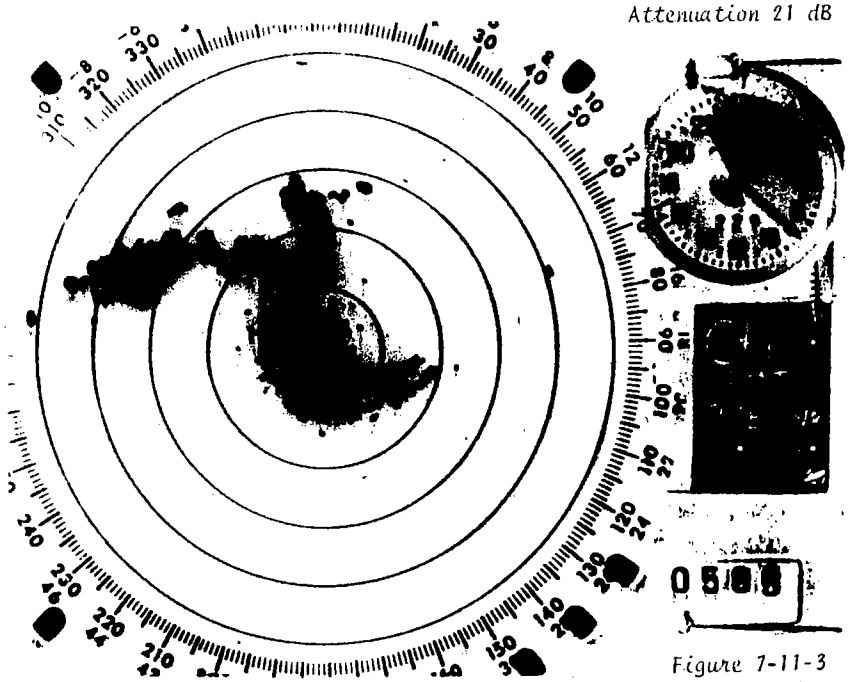

Figure 7-11-3

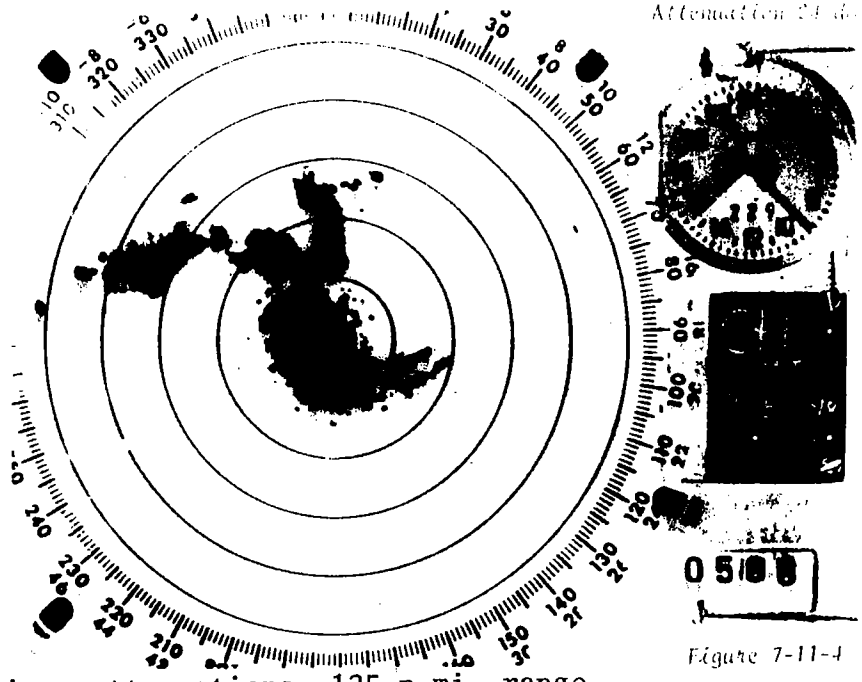

Figure 7-11-4

Figure 7-11.--Same as figure 7-10 with varicus attenuations, 125 n.mi. range.

Attenuation 30 dB

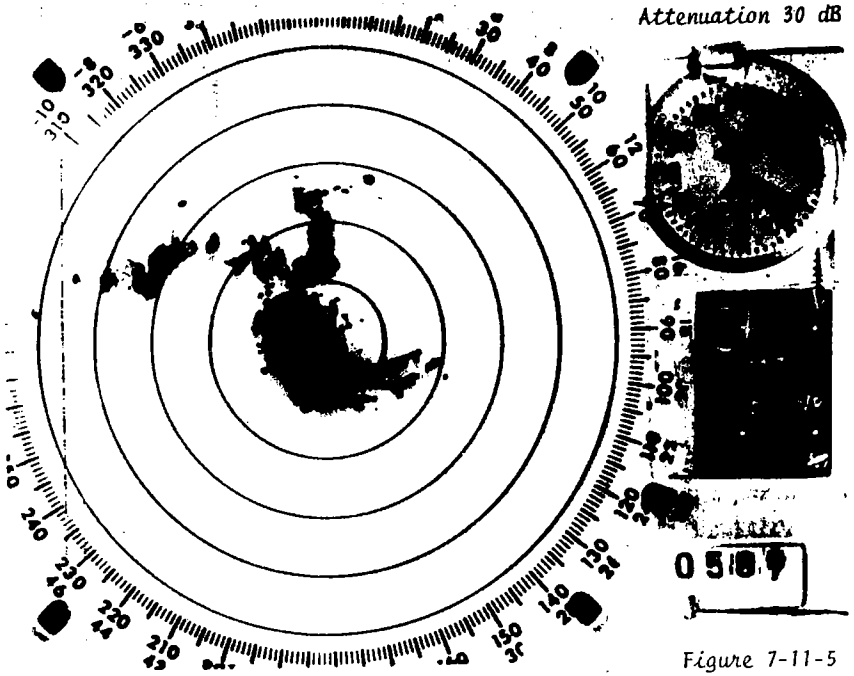

Figure 7-11-5

Attenuation 33 dB

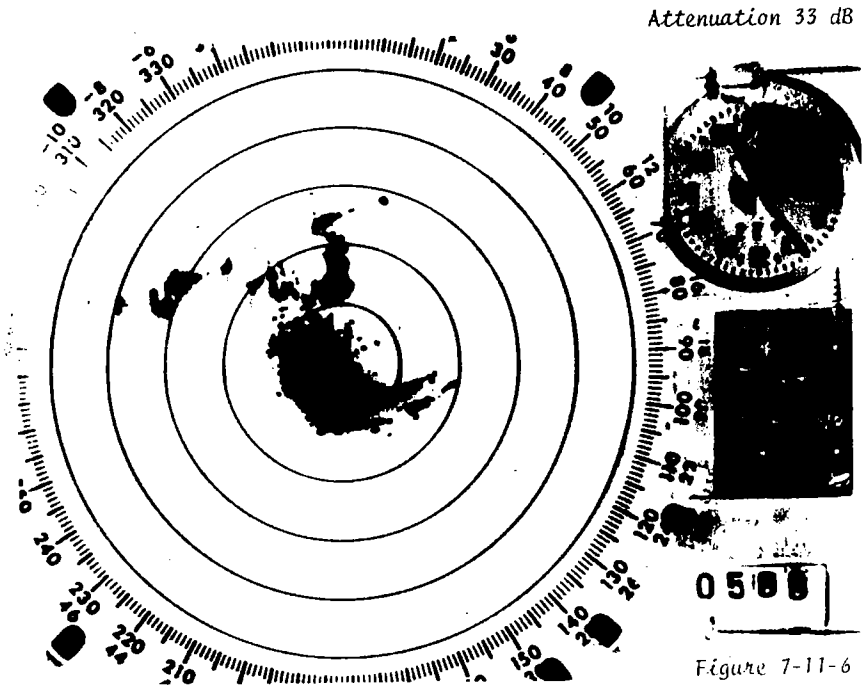

Figure 7-11-6

Attenuation 39 dB

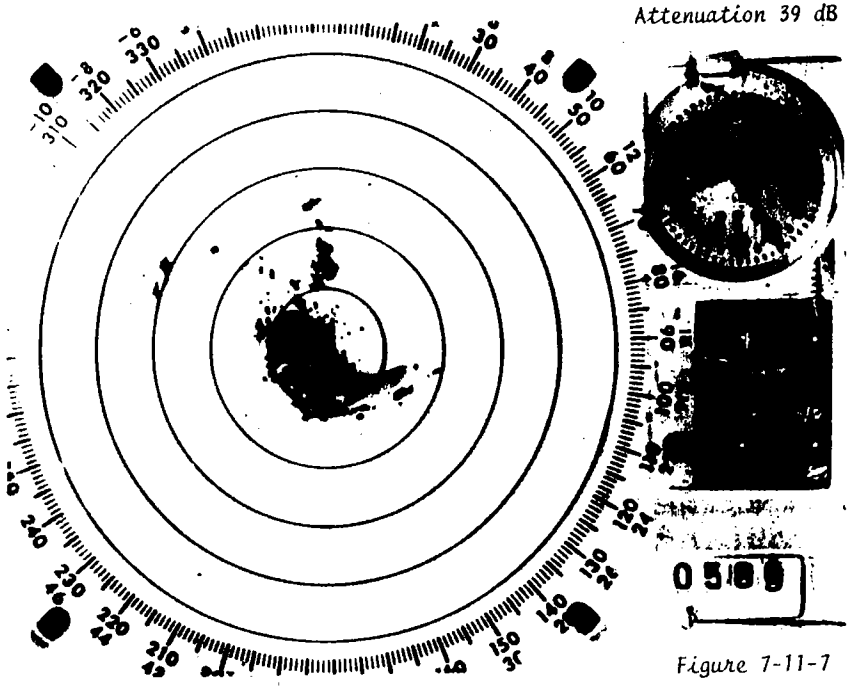

Figure 7-11-7

Attenuation 45 dB

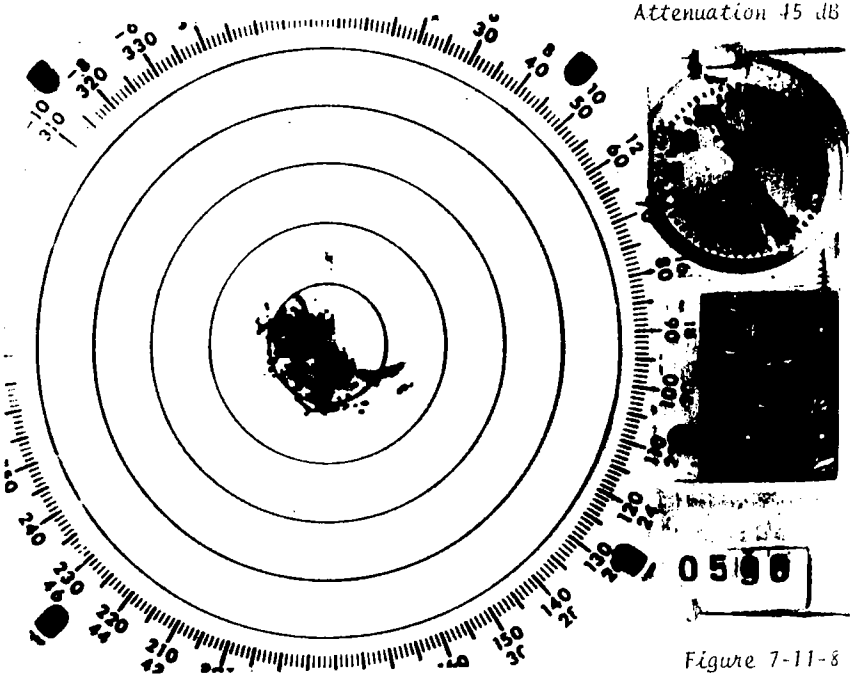

Figure 7-11-8

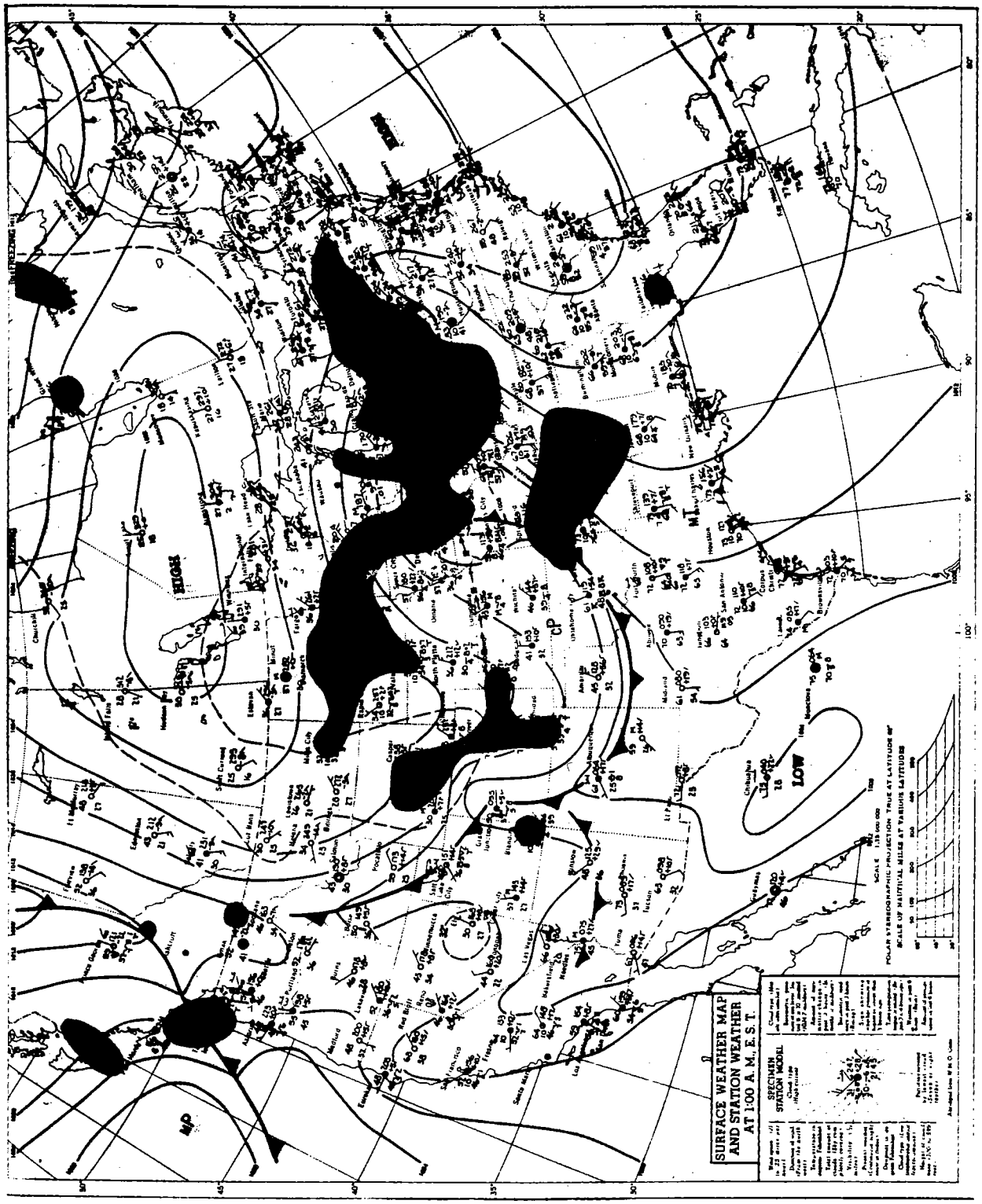

Figure 7-12.--Surface weather analysis at 0000 CST, May 12, 1966.

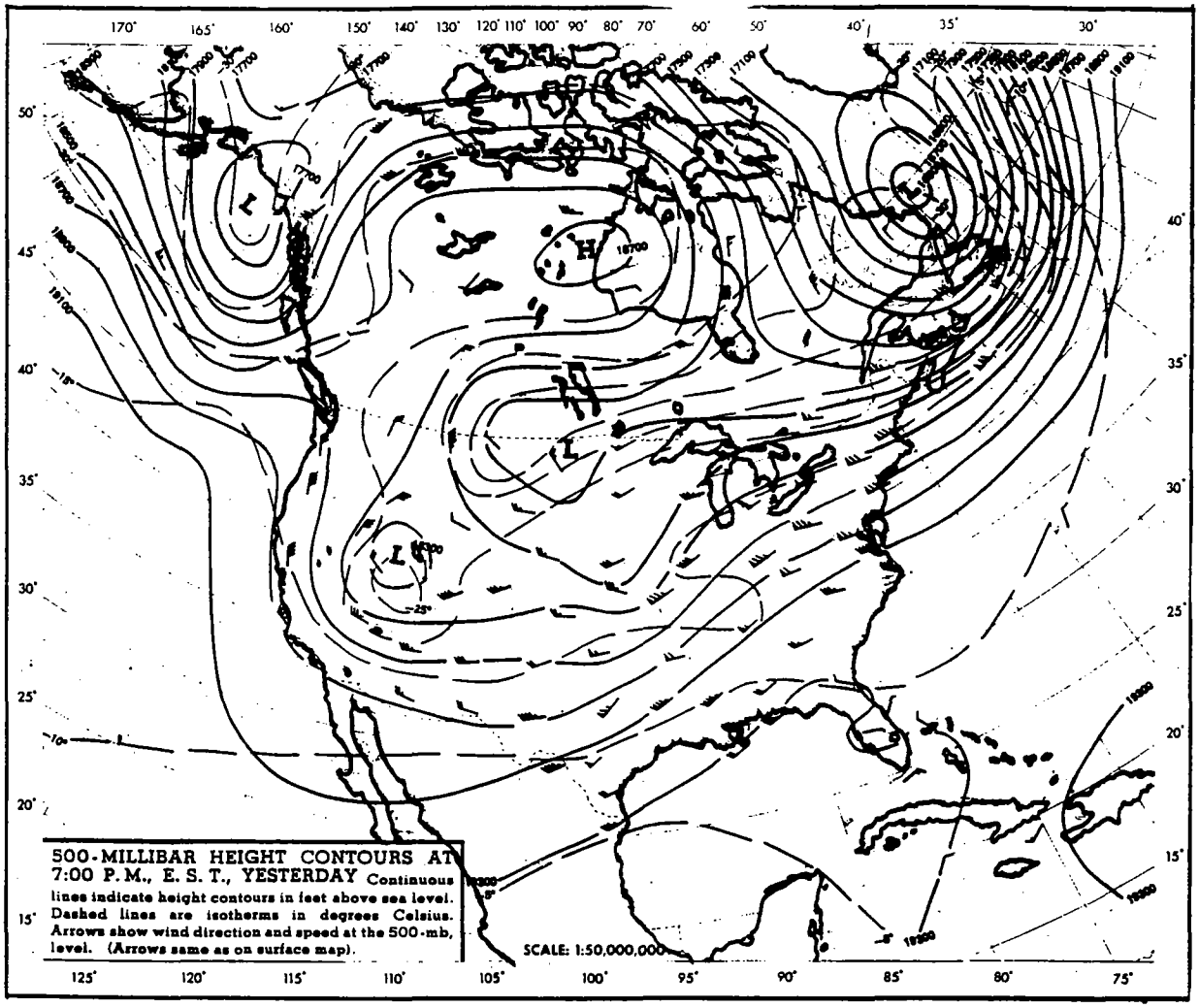

Figure 7-13.--500-mb analysis at 1800 CST, May 11, 1966.

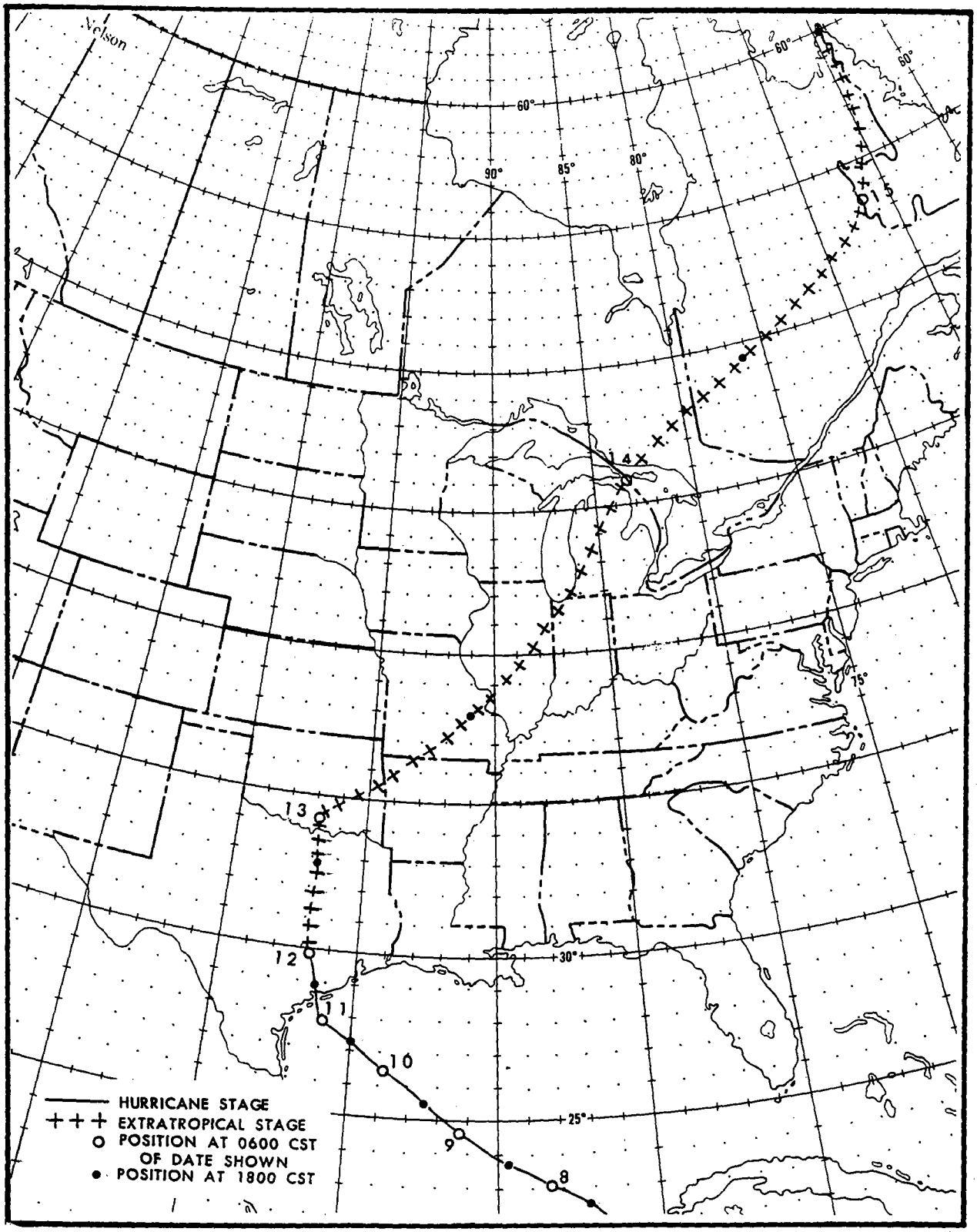

Figure 7-14.--Path of Hurricane Carla, September 3-15, 1961.

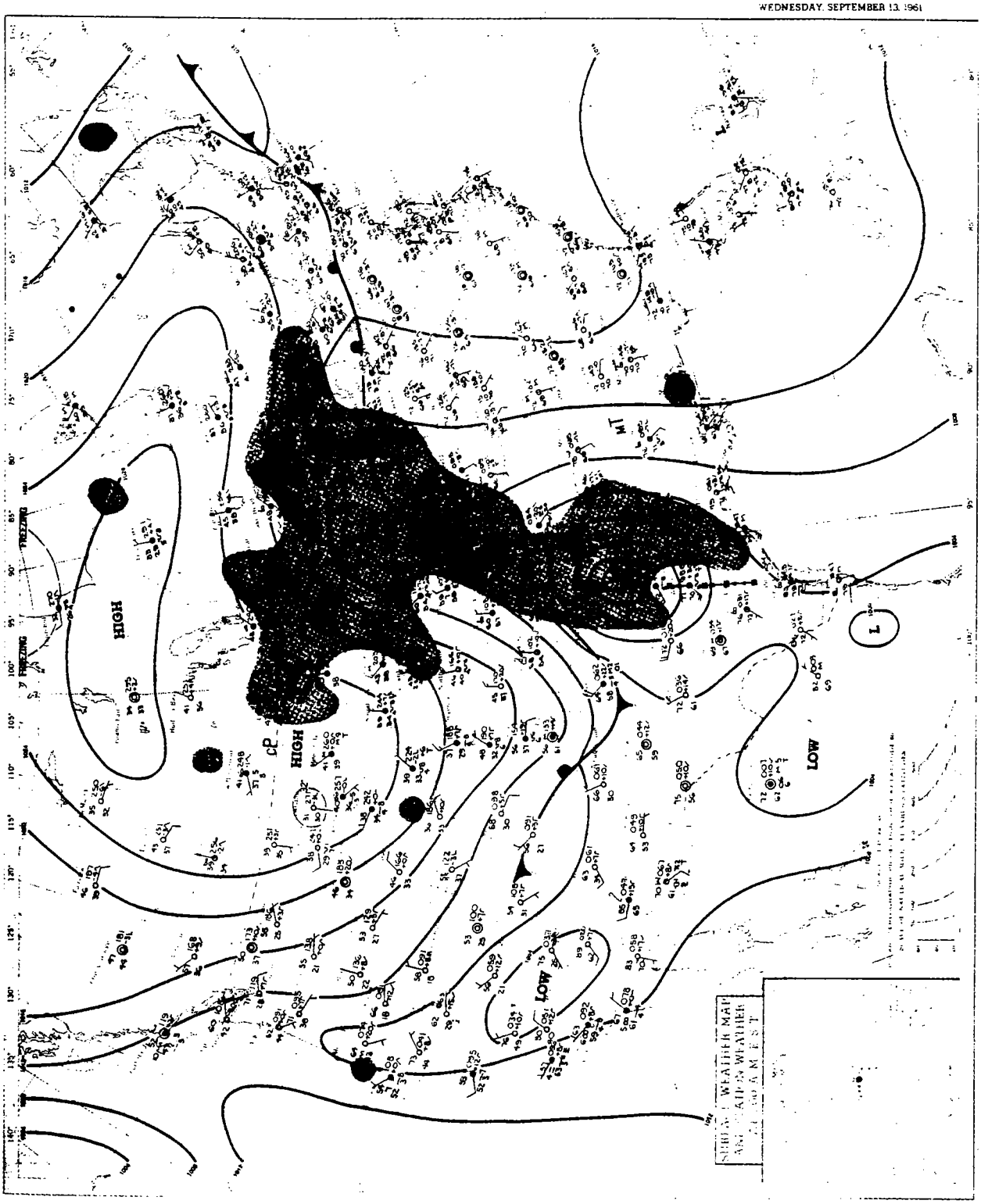

Figure 7-15.--Surface weather analysis at 0000 CST, September 13, 1961.

CHAPTER 8. SUMMARY

This study develops a new procedure for calculating the geographically fixed depth-area ratios needed to reduce published point precipitation frequencies to areal values for the same duration and return period.

The approach is to fit surfaces in interstation distance-precipitation duration space to the first and second moments (mean and standard deviation) of annual maximum two-station average precipitation, and to certain other statistics of two-station precipitation. From these statistics, upper and lower bounds of the first and second moments of annual maximum true areal average precipitation are estimated by theory developed for the purpose. The positions of the areal moments between these bounds are then set by a calibration with the moments of a limited number of annual maximum multistation averages. The moments of the areal average annual maxima thus synthesized are compared with the moments of single station annual series in a formula derived from Chow's generalized frequency equation to yield depth-area ratios. The frequency factor K corresponding to the Gumbel fitting of the Fisher-Tippett Type I distribution is used at this step.

The emphasis on extracting maximum information from pairs of recorders lays the groundwork for searching for regional variation of depth-area ratios from station pair data only, where dense network data are not available, and provides a theory for doing this. The theory cannot overcome the uncertainty in storm correlation structure in a region where not even pairs of recorders are reasonably closely spaced.

The method of treating all variables as spatially continuous functions and fitting surfaces in distance-duration space avoids the problem of earlier methods of assigning a representative area to a group of precipitation gages. The surfaces are defined by exponential formulas containing empirical fitting constants. Limiting values of variables in the formulas are assigned in some instances by theoretical deduction, in others by fit to the data.

The fitted surfaces provide a convenient rational basis for extrapolating depth-area ratios to areas and durations a reasonable distance beyond the range of data explicitly analyzed. They also provide a rational basis for defining depth-area variation with return period (frequency), not clearly evident by previous methods.

The method is illustrated by application to 25 years of precipitation recorder data in and near Chicago, all published in Hourly Precipitation Data and available to this project on magnetic tape. The "annual maxima" are drawn from the April-October season to avoid the considerable labor in quality control of the data during freezing winter weather. Depth-area ratio results are comparable to those from previous studies.

An essential part of a complete depth-area ratio evaluation from a dense network is a synoptic meteorology appraisal of predominant storm types controlling depth-area ratios, as a guide to interpolating or extrapolating the ratios to areas lacking closely spaced data. One chapter of the present report is devoted to this.

Much of the computer programming of this method is adaptable to deriving probabilistic statements of another quantity needed by hydrologist designers -- areal distribution of design storm rainfall within a basin. Work is planned in that direction.

ACKNOWLEDGMENT

This investigation was funded by the Soil Conservation Service, USDA, through the Hydrology Branch, Engineering Division.

REFERENCES

Bruce, J.P., and R.H. Clark, 1966: Introduction to Hydrometeorology. Pergamon Press, New York, 319 pp.

Cry, G.W., 1967: Effects of tropical cyclone rainfall on the distribution of precipitation over the eastern and southern United States. ESSA Professional Paper No. 1, Environmental Science Services Administration, U.S. Department of Commerce, Washington, D.C., 67 pp.

Chow, V.T., 1951: A general formula for hydrologic frequency analysis. Trans. Am. Geophys. Union, 32:231-237.

Chow, V.T., 1964: Statistical and probability analysis of hydrologic data. In V.T. Chow (ed.), Handbook of Hydrology, McGraw-Hill, New York, pp. 8-1 to 8-42.

Dunn, G.E., 1962: The hurricane season of 1961. Mon. Wea. Rev., 90:107-119.

Environmental Data Service, 1951-72: Hourly Precipitation Data, National Oceanic and Atmospheric Administration, U.S. Department of Commerce, Asheville, N.C.

Fisher, R.A., and L.H.C. Tippett, 1928: Limiting forms of the frequency distribution of the largest or smallest member of a sample. Proc. Cambridge Phil. Soc., 24:180-190.

Fréchet, M., 1927: Sur la loi de probabilité de l'écart maximum. Ann. de la Soc. polonaise de Math., Kracow, 6:93-116.

Frederick, R.H., V.A. Myers, and E.P. Auciello, 1977a: Storm depth-area curves derived from digitized radar data. Water Resources Research, 13: 675-679.

Frederick, R.H., V.A. Myers, and E.P. Auciello, 1977b: Five- to 60-minute precipitation frequency for the eastern and central United States. NOAA Tech. Mem. NWS HYDRO-35, National Weather Service, National Oceanic and Atmospheric Administration, Silver Spring, Md., 36 pp.

Galambos, J., 1978: The Asymptotic Theory of Extreme Order Statistics. John Wiley & Sons, New York, 352 pp.

Gilbra, I.N., 1973: Probability and Statistical Inference for Scientists and Engineers, Prentice-Hall, Englewood Cliffs, N.J., 596 pp.

Gringorton, I.I., 1963: A simplified method of estimating extreme values from data samples. J. App. Meteorol., 2:82-89.

Gumbel, E.J., 1941: The return period of flood flows. Annal. Math. Statist., 12:153-190.

1958: Statistics of Extremes, Columbia University Press, New

...eld, D.M., 1961: Rainfall frequency atlas of the United States for ...rations from 30 minutes to 24 hours and return periods from 1 to 100 years. U.S. Weather Bureau Tech. Paper No. 40, Washington, D.C., 115 pp.

Hershfield, D.M., 1962: An empirical comparison of the predictive value of three extreme-value procedures. J. Geophys. Res., 67:1535-1542.

Hershfield, D.M., and M.A. Kohler, 1960: An empirical appraisal of the Gumbel extreme-value procedure. J. Geophys. Res., 65:1737-1746.

Huff, F.A., 1967: Time distribution of rainfall in heavy storms. Water Resources Research, 3:1007-1019.

Huff, F.A., S. A. Changnon, N.G. Towery, and J.L. Vogel, 1978: Chicago hydrometeorological area project: a comprehensive new study of urban hydrometeorology. Final Report, National Science Foundation Grant ENY76-01447, Illinois State Water Survey, Urbana, 51 pp.

Huff, F.A., R.G. Semonin, S.A. Changnon, and D.M.A. Jones, 1958: Hydrometeorological analysis of severe rainstorms in Illinois, 1958. Report of Investigation 35, Illinois State Water Survey, 79 pp.

Huff, F.A., and J.L. Vogel, 1976: Hydrometeorology of heavy rainstorms in Chicago and northeastern Illinois, Phase I, historical studies. Report of Investigation 82, Illinois State Water Survey, 63 pp.

Jenkinson, A.F., 1955: The frequency distribution of the annual maximum (or minimum) value of meteorological elements. Quar. J. Royal Meteorol. Soc., 81:158-171.

Jenkinson, A.F., 1969: Statistics of extremes. In Estimation of Maximum Floods, WMO Tech. Note No. 98, Geneva, pp. 183-227.

Maddox, R.A., C.F. Chappell, and L.R. Hoxit, 1979: Synoptic and mesoscale aspects of flash flood events. Bull. Amer. Meteorol. Soc., 60:114-123.

Miller, J.F., R.H. Frederick, and R.J. Tracey, 1973: Precipitation-frequency atlas of the western United States. NOAA Atlas 2, National Weather Service, National Oceanic and Atmospheric Administration, Silver Spring, Md., eleven volumes.

Nash, W.P., and L.W. Chamberlain, 1954: Some aspects of the heavy rains in the Chicago area, October 9-11, 1954. Mon. Wea. Rev., 82:305-316.

National Bureau of Standards, 1953: Probability tables for the analysis of extreme value data. NBS Applied Math Series 22, U.S. Gov. Printing Office, Washington, D.C., 32 pp. Introduction by E.J. Gumbel.

Osborn, H.B., L.V. Lane, and V.A. Myers, 1979: Rainfall/watershed relationships for southwestern thunderstorms. Submitted to Transactions, American Society Agricultural Engineers.

Peck, E.L., J.C. Monro, and M.L. Snelson, 1977: Hydrometeorological data base for the United States. Preprints, Second Conference on Hydrometeorology, 25-27 October 1977, Toronto, American Meteorological Society, Boston, pp. 75-78.

Rodríguez-Iturbe, I., and J.M. Mejía, 1974: On the transformation of point rainfall to areal rainfall. Water Resources Research, 10:729-735.

Townsend, A.A., 1976: The Structure of Turbulent Shear Flow, 2d ed., Cambridge University Press, 429 pp.

U.S. Weather Bureau, Air Weather Service, and Naval Weather Service, 1973: Operations procedures for radar and radar remoting. Weather Radar Manual, Part C, Section III, U.S. Department of Commerce, U.S. Department of the Air Force, and U.S. Department of the Navy, Washington, D.C.

U.S. Weather Bureau, 1957-60: Rainfall intensity--frequency regime, Part 1--the Ohio Valley; Part 2--southeastern United States," Tech. Paper No. 29, U.S. Department of Commerce, Washington, D.C.

World Meteorological Organization, 1974: Guide to hydrological practices. 3d Ed., WMO No. 168, Geneva, pp. 5.20-5.30.

APPENDIX I. GUMBEL FITTING OF FISHER-TIPPETT TYPE I EXTREME VALUE DISTRIBUTION

The Extreme Value Distribution

Fisher-Tippett Type I (Fisher and Tippett 1928) is based on the distribution of a dimensionless variable G called the reduced variate, with a probability distribution

$$\Pr[G \leq y] = e^{-e^{-y}} \tag{I-1}$$

Pr[ ] is the probability that the statement in brackets is true, y any assigned level of G for which the probability of not being exceeded is to be evaluated, and e the base of natural logarithms. There are theoretical reasons (Gumbel 1958) for expecting a series of values all of which are maximums from independent samples of equal and sufficient size drawn from the same population, to have a probability distribution like (I-1), if the variable is essentially unbounded and is suitably scaled. Properties of (I-1) include that $\Pr[G \leq y]$ ranges from 0 to 1 as y goes from $-\infty$ to $+\infty$ and that the probability density function is skewed to the right. The mode (highest value of the density function) is at $y = 0$ at a probability of $e^{-1} = 0.368$.

The inverse of (I-1) is

$$y = -\log\,(-\log \Pr[G \leq y]). \tag{I-2}$$

Fitting Procedure

Choice of fitting procedure is an independent step from choice of theoretical distribution. Choice of fitting procedure subdivides into choice of "plotting position" and definition of "best fit."

Gumbel (1958) proposes a fitting procedure that can be applied either graphically or computationally. He illustrated this method earlier, for flood extremes on a river, in a bulletin of the National Bureau of Standards (1953). Gumbel cites theoretical and practical reasons for preferring an $m/(N + 1)$ plotting position to other positions that had been advocated up to that time. Here m is the rank from lowest to highest of an individual extreme observation in a sample of N such extreme observations, annual maxima in our case. The plotting position applies to the reduced variate as well as the extreme observations. Assigning a plotting position is equivalent to assigning a probability, and combining these two facts, N y's are evaluated by substituting $m/(N + 1)$ for Pr in (I-2) to evaluate each y:

$$y_m = -\log\,(-\log \frac{m}{N+1}) \ . \tag{I-3}$$

The Gumbel procedure is then to make a linear regression fit of the ranked extreme observations to the corresponding rank y_m as defined in (I-3). The linear regression fit implicitly defines "best fit." The two linear regression coefficients are then location and scaling parameters to apply (I-2) to the annual series.

In practice rainfall frequencies are obtained directly by the equivalent procedure (Hershfield 1962) of solving

$$Z_{Pr} = \overline{X}_N + (y_{Pr} - \overline{y}_N) \frac{s_N}{\sigma_N} \qquad \text{(I-4)}$$

where Z_{Pr} is the estimated rainfall depth of probability Pr of not being equalled or exceeded in any one year, $\overline{X}_N$ is the mean of the N sample X's and s_N their standard deviation, y_{Pr} is y from (I-2) at probability Pr,

$$y_{Pr} = -\log (-\log Pr) \qquad \text{(I-5)}$$

$\overline{y}_N$ is the mean of the y_m's from (I-3),

$$\overline{y}_N = \frac{1}{N}\left[\sum_{m=1}^{N} - \log \left(-\log \frac{m}{N+1}\right)\right] \qquad \text{(I-6)}$$

and σ_N their standard deviation,

$$\sigma_N = \left(\frac{1}{N}\left[\sum_{m=1}^{N} -\log \left(-\log \frac{m}{N+1}\right)\right]^2 - \overline{y}_N^{\,2}\right)^{1/2}. \qquad \text{(I-7)}$$

The quantity

$$K(Pr,N) = (y_{Pr} - \overline{y}_N)/\sigma_N \qquad \text{(I-8)}$$

can be precomputed from (I-5) to (I-7) and tabulated for desired Pr's and N's. K(Pr,N = 20 yr) values are listed in table I-1, and $\overline{y}_N$ and σ_N values in table I-2. A more extensive table of K's is given by the World Meteorological Organization (1974, table 5.3). Desired rainfall frequency values can then be calculated directly from sample mean and standard deviation together with a tabular K(Pr,N) value, according to the linear form

$$Z_{Pr} = \overline{X}_N + K(Pr,N)s_N \qquad \text{(I-9)}$$

obtained by substituting (I-8) in (I-4).

Table I-1.--Coefficient K for Gumbel fitting of Fisher-Tippett Type I

N = 20

Return period (years)	Probability, Pr, of not being exceeded (per year)	K(Pr,N)
2	0.5	-0.1478
5	0.8	0.9187
10	0.9	1.6247
25	0.96	2.5169
50	0.98	3.1787
100	0.99	3.8356

Table I-2.--Reduced variate statistics for Gumbel fitting of Fisher-Tippett Type I

N	$\bar{y}_N$	σ_N
15	.51284	1.02057
16	.51537	1.03060
17	.51768	1.03973
18	.51980	1.04807
19	.52175	1.05574
20	.52355	1.06282
21	.52522	1.06938
22	.52678	1.07547
23	.52823	1.08115
24	.52959	1.08646
25	.53086	1.09144

References

The Gumbel fitting of Fisher-Tippett Type I has not been widely discussed in standard statistics textbooks. Sources in English that trace the development of this procedure include Fisher and Tippett (1928), Gumbel (1941, 1958), Jenkinson (1955, 1969), Hershfield and Kohler (1960), National Bureau of Standards (1953), Chow (1964), Bruce and Clark (1966), and the World Meteorological Organization (1974). A recent comprehensive textbook by Galambos (1978) brings these threads together and includes an extensive bibliography.

Fisher and Tippett's work is based on a stability postulate that the extremes of extremes of samples must have the same distribution form as the extremes, as set forth in a paper in French by Fréchet (1927) cited by Jenkinson, Chow, and Gumbel.

APPENDIX II. RECORD LENGTH ADJUSTMENTS

In evaluating depth-area ratios by (6-2) record length N must be common to relative moments $\overline{X}'$ and s' and to frequency factor K. Further, $\overline{X}'$ and s' are from surfaces fitted to data of unequal record length in original form. To make the fitted surfaces pertain to an unambiguous record length, and lead to an unambiguous choice of K, individual $\overline{X}'$ and s' values are normalized to a common record length before fitting the surface.

The expected standard deviations, s, of samples of different sizes from a common population with a Fisher-Tippett Type I distribution are proportional to the corresponding standard deviations, σ, of the reduced variate,

$$s_{N'} = s_N(\sigma_{N'}/\sigma_N) \qquad \text{(II-1)}$$

where N and N' are original and standard sample size, respectively. Values of σ are found in table I-2.

Sample means are likewise scaled on the reduced variate. Writing (I-4) for N and N' for an arbitrary probability, Pr,

$$Z_{Pr} = \overline{X}_N + (y_{Pr} - \overline{y}_N)\frac{s_N}{\sigma_N} \qquad \text{(I-4)}$$

$$Z_{Pr} = \overline{X}_{N'} + (y_{Pr} - \overline{y}_{N'})\frac{s_{N'}}{\sigma_{N'}} \cdot \qquad \text{(I-4a)}$$

Eliminating Z_{Pr} and y_{Pr} between the two and using (II-1) results in

$$\overline{X}_{N'} = \overline{X}_N + (s_N/\sigma_N)(\overline{y}_{N'} - \overline{y}_N) \cdot \qquad \text{(II-2)}$$

In this study all sample moments are adjusted to an N' of 20 years by (II-2) and (II-1) before further processing. These formulas are similar to, but not identical with, a more generalized sample size debiasing method proposed by Gringorten (1963).

APPENDIX III. LIMITING VALUES OF STATISTICS

Theoretical limits are deduced for each of the several two-station statistics at zero and infinite interstation distance and precipitation duration as guides to fitting surfaces to data over a restricted range. A fixed approximation to the theoretical limit is adopted for certain limits. For others, the theoretical value of the limit is a guide to the functional form of the surface, with the specific value of the limit selected by regression analysis of the data. These considerations are summarized in this appendix.

Zero distance limit

Relative statistics $\overline{X}'_m$, s'_m, $\overline{X}'_b$, s'_b, cov'_{Ab}, and cv'_b are equal to 1.0 at d = 0 by definition.

Large distance limit

$\overline{X}'_b$. The correlation of X_b and X_A values decays to zero at some distance much less than d = ∞. Beyond the distance of zero correlation, X_b is climatological rather than dependent on X_A.

Expected (most probable) values are: of a single X_b, zero; of $\overline{X}_b$, the climatological mean rate (mean seasonal precipitation, e.g., April-October total, divided by number of Δt's in a season); and of $\overline{X}'_b$, the $\overline{X}_b$ expectation divided by $\overline{X}_A$ for the duration. Climatological $\overline{X}'_b$s in the Chicago climate on this basis are approximately 0.004, 0.012, and 0.037 for Δt = 1, 6, and 24 hr, respectively. The $\overline{X}'_b$ data out to 40 miles (e.g., figs. 4-1 to 4-3) cannot sense the difference of these values from zero, and we set

$$\lim_{d\to\infty} \overline{X}'_b = 0 \qquad \text{(III-1)}$$

as a good approximation for fitting curves to 40 mi. This limit of the mean also requires, since no X'_b can be negative

$$\lim_{d\to\infty} X'_b = 0 \ . \qquad \text{(III-2)}$$

Condition (III-1) is a property of eq. (4-3).

$\overline{X}'_m$: For X'_ms with composition (*-) (chapter 3),

$$X'_m = 0.5\ (X'_A + X'_b) = 0.5 + 0.5\ X'_b \qquad \text{(III-3)}$$

and, by substitution of (III-2),

$$\lim_{d\to\infty} X'_m = 0.5 + \lim_{d\to\infty} X'_b = 0.5 \ . \qquad \text{(III-4)}$$

For X'_ms with composition (--),

$$\lim_{d\to\infty} X'_m = \text{some positive value} > 0.5. \qquad \text{(III-5)}$$

The (*-) composition dominates, e.g., figure 3-12. The (**) class is negligible at large d. An average of (III-4) and (III-5) weighted by composition probability would yield a limit at $d \to \infty$ slightly greater than 0.5. The data to d = 40 mi cannot sense this difference, e.g., figures 3-1 to 3-3, and we set

$$\lim_{d\to\infty} \bar{X}'_m = 0.5 \ . \qquad \text{(III-6)}$$

Eq. (3-4) has this property.

s'_b: Taking the definition of s'_b,

$$s'_b = \frac{1}{s_A}\left[\frac{1}{N}\sum (X_b - \bar{X}_b)^2\right]^{1/2}$$

$$= \frac{1}{s_A}\left[\frac{1}{N}\sum X_A\,(X'_b - \bar{X}'_b)^2\right]^{1/2} \qquad \text{(III-7)}$$

to the limit and substituting (III-1) and (III-2) results in

$$\lim_{d\to\infty} s'_b = 0 \ . \qquad \text{(III-8)}$$

This is not applied explicitly in fitting an s'_b surface. Rather, the surface is derived from $\bar{X}'_b$ and cv'_b surfaces (chapter 4) by

$$s'_b = \bar{X}'_b cv'_b \ . \qquad \text{(4-7)}$$

s'_m: Multiplying (III-6) by X_A, gives, for X_ms with composition (*-),

$$\lim_{d\to\infty} X_m = 0.5X_A \ . \qquad \text{(III-9)}$$

If all X_ms were of this category, it would follow that (s_m is the standard deviation of X_m and s_A of X_A),

$$\lim_{d\to\infty} s_m = 0.5s_A \qquad \text{(III-10)}$$

and,

$$\lim_{d\to\infty} s'_m = \lim_{d\to\infty} (s_m/s_A) = 0.5 \ . \qquad \text{(III-11)}$$

The admixture of the (--) category raises the limit slightly above 0.5, but the data to 40 mi cannot perceive this difference, e.g., figures 3-4 to 3-6. We adopt (III-11) as applying to the full data set, and fit the s'_m surface with eq. (3-4).

cov'_{Ab}: Combining (III-1) and (III-2) with the definition of covariance,

$$cov_{Ab} = \frac{1}{N}\sum (X_A - \bar{X}_A)\ (X_b - \bar{X}_b) \qquad \text{(III-12)}$$

indicates that

$$\lim_{d\to\infty} cov'_{Ab} = 0 \ . \qquad \text{(III-13)}$$

Covariance in many natural systems crosses to negative before returning to near zero at large displacements, as discussed in chapter 4. Data for Δt = 1 hr (fig. 4-14) suggest that cov'_{Ab} has this property. Data of this study do not extend to sufficiently large distance to define accurately the crossover and return toward zero. A cov'_{Ab} surface is fit asymptotically at $d\to\infty$ to M, a fitting parameter of convenience without physical significance intended to give a good fit at $d \leq 40$ mi, by (4-13).

cv'_b: In the main analysis, s'_b is computed from other statistics by (4-7). The reverse is applied here and we infer the cv'_b limit from $\bar{X}_b$ and s'_b limits:

$$\lim_{d\to\infty} cv'_b = \lim_{d\to\infty} s'_b \Big/ \lim_{d\to\infty} \bar{X}'_b \ . \qquad \text{(III-14)}$$

Substituting (III-8) and (III-1),

$$\lim_{d\to\infty} cv'_b = 0/0 \ . \qquad \text{(III-15)}$$

Applying l'Hopital's rule,

$$\lim_{d\to\infty} cv'_b = \lim_{d\to\infty} \left[\frac{\partial s'_b}{\partial d} \Big/ \frac{\partial \bar{X}'_b}{\partial d} \right] . \qquad \text{(III-16)}$$

Differentiating (4-3),

$$\frac{\partial \overline{X}'_b}{\partial d} = \frac{b}{a(d/d_1)^{b+1}} (\overline{X}'_b - 1) \quad . \tag{III-17}$$

An explicit formulation has not been written for $s'_b(d)$. It is reasonable to assume that the decay of s'_b with d is exponential and similar to $\overline{X}'_b$, with derivative by analogy to (III-17),

$$\frac{\partial s'_b}{\partial d} = \frac{b_s}{a_s(d/d_1)^{b_s+1}} (s'_b - 1) \tag{III-18}$$

where subscript s distinguishes the constants from their $\overline{X}'_b$ counterparts. Whether cv'_b approaches 0 or ∞ as $d \to \infty$ depends on relative decay rates. Formally, substituting (III-17) and (III-18) in (III-16),

$$\lim_{d\to\infty} cv'_b = \lim_{d\to\infty} \left[\frac{b_s}{a_s(d/d_1)^{b_s+1}} (s'_b - 1) \Big/ \frac{b}{a(d/d_1)^{b+1}} (\overline{X}'_b - 1) \right]$$

$$= \lim_{d\to\infty} \left[\frac{a}{a_s} \frac{b_s}{b} (d/d_1)^{b-b_s} \frac{s'_b - 1}{\overline{X}'_b - 1} \right] = \frac{a}{a_s} \frac{b_s}{b} \lim_{d\to\infty} (d/d_1)^{b-b_s}$$

$$\left.\begin{aligned} &= \infty \quad b > b_s \\ &= 0 \quad b < b_s \end{aligned}\right\} , \tag{III-19}$$

If $b < b_s$, as seems likely from comparing the corresponding constants in tables VII-1 and VII-3 for $\overline{X}'_m$ and s'_m, the $cv'_b(d)$ profile approaches zero as $d \to \infty$.

In any event, this is not detectable from data within the range $0 < d < 40$ mi (figs. 4-9 to 4-11). A curve-fitting constant of convenience, M, where $0 < M < \infty$ and dictated by the data, is used as the value of the effective asymptote. It has no physical significance.

Zero duration limit

The six relative statistics all have finite values at $\Delta t = 0$, and are the quotients of rainfall rates. For example, the definition of X'_m,

$$X'_m(d,\Delta t) = X_m(d,\Delta t) \Big/ X_A(d,\Delta t) \qquad \text{(III-20)}$$

with limit

$$\lim_{\Delta t\to 0} X'_m(d,\Delta t) = \lim_{\Delta t\to 0} X_m(d,\Delta t) \Big/ \lim_{\Delta t\to 0} X_A(\Delta t) = 0/0$$

can be evaluated at the limit by 1'Hopital's rule:

$$\lim_{\Delta t\to 0} X'_m(d,\Delta t) = \lim_{\Delta t\to 0} \frac{\partial X_m(d,\Delta t)}{\partial \Delta t} \Big/ \lim_{\Delta t\to 0} \frac{\partial X_A(\Delta t)}{\partial \Delta t} . \qquad \text{(III-21)}$$

The numerator on the right is to be interpreted for a particular year as the maximum annual value of the simultaneous rainfall rates averaged over two stations distance d apart, and the denominator the average of the maximum annual rates at the two stations individually, not necessarily simultaneous. Both of these are finite measurable quantitites, and their quotient is finite and positive. This is clarified by writing (III-21) in the form

$$\lim_{\Delta t\to 0} X'_m(d,\Delta t) = \left[\frac{dR}{dt}\right]_{mx}(d) \Big/ \left[\frac{dR}{dt}\right]_{xA} \qquad \text{(III-22)}$$

where dR/dt denotes rainfall rate, subscript m as usual the average of simultaneous values over two stations, subscript x the annual maximum, and A the average of the individual station annual maximum rates. Taking a mean of (III-22) over years,

$$\lim_{\Delta t\to 0} \overline{X}'_m(d,\Delta t) = \overline{\left[\frac{dR}{dt}\right]_{mx}(d)} \Big/ \overline{\left[\frac{dR}{dt}\right]_{xA}} . \qquad \text{(III-23)}$$

Similar formulations in terms of rates apply to the other statistics, leading to finite limits as $\Delta t \to 0$.

The principle time domain equation, (3-5), has the required property of a finite value of the fitting statistic at $\Delta t = 0$, namely y_o. The value of this constant at a particular d is dictated by the fit to the available data (appendix V). If the data include $\Delta t = 0$ values, the departure of the computed y_o from the corresponding data point is minimized along with all other departures. This study does not use any data values at $\Delta t = 0$, and the y_o on each time domain profile is an extrapolation from $\Delta t \geq 1$ hr. Negative values of y_o are permitted in this type of fit and are obtained; the constant is treated as a fitting parameter only. Using extrapolated values on the resulting fitted surface at $\Delta t = 0.5$ hr but not at $\Delta t = 0$ is discussed in chapter 3.

Large duration limit

$\overline{X}'_m$: It is a well-known characteristic of long duration storms not dominated by orographic processes that the large gradients on the isohyetal map for a maximum intensity period of the storm, say for the maximum 6 hr, are not generally maintained in subsequent or prior increments of the storm in the same areal pattern or in the same location. The storm moves. The areal pattern of rain summed over these additional time increments is flat compared to the pattern during the maximum period. Without going into a formal proof, it is evident that *if* storm depth grows without limit as $\Delta t \to \infty$, the "flat" part of the storm will progressively dominate and that X_b and X_A will converge:

$$\lim_{\Delta t \to \infty} X_b(\Delta t) = X_A(\Delta t) \ . \qquad \text{(III-24)}$$

Whence, from the definition of X_m,

$$\lim_{\Delta t \to \infty} X_m(\Delta t) = 0.5\left(\lim_{\Delta t \to \infty} X_A + \lim_{\Delta t \to \infty} X_b\right) = \lim_{\Delta t \to \infty} X_A \qquad \text{(III-25)}$$

which may be written

$$\lim_{\Delta t \to \infty} X'_m(\Delta t) = \lim_{\Delta t \to \infty} X_m(\Delta t) \Big/ \lim_{\Delta t \to \infty} X_A(\Delta t) = 1.0 \ . \qquad \text{(III-26)}$$

The corresponding mean is,

$$\lim_{\Delta t \to \infty} \overline{X}'_m(\Delta t) = 1.0 \ . \qquad \text{(III-27)}$$

As a matter of fact, trial fits to data show that the closest fit is obtained with

$$\lim_{\Delta t \to \infty} \overline{X}'_m = M = 1.0 - \text{small value} \qquad \text{(III-28)}$$

rather than (III-27). This implies that effectively storms do not grow without limit with increased Δt and that data for $\Delta t \leq 24$ hr can "feel" a storm limit. The data are allowed to select M in (III-28) by minimizing squares of deviations from the surface specified by (3-5).

s'_m, $\overline{X}'_m$, s'_b, cov'_{Ab}, cv'_b: In a system in which (III-24) is true in all cases, it can be shown that

$$\left.\begin{array}{l} \lim\limits_{\Delta t\to\infty} s'_m \\ \lim\limits_{\Delta t\to\infty} \bar{X}'_b \\ \lim\limits_{\Delta t\to\infty} s'_b \\ \lim\limits_{\Delta t\to\infty} cov'_{Ab} \\ \lim\limits_{\Delta t\to\infty} cv'_b \end{array}\right\} = 1.0 \; . \qquad \text{(III-29)}$$

For the present data set, surfaces with limits slightly less than 1.0 at $\Delta t \to \infty$ fit best for all statistics. All are fit by (3-5) with M dictated by the data.

APPENDIX IV. TRANSFORMATION OF EQUATIONS FOR SURFACE FITTING

This appendix lists the log-log transformation of the equations that define surfaces fitted to data. The log-log transformations are linear and permit a fit by least squares linear regression. All logarithms are to the base e.

The several equations for fitting in distance-duration space are:

$$y(d) = 1 - 0.5e^{-[a(d/d_1)^b]^{-1}}, \tag{3-4}$$

$$y(d) = 1 - e^{-\left[a(d/d_1)^b\right]^{-1}}, \tag{4-3}$$

$$y(d) = 1 - Me^{-\left[a(d/d_1)^b\right]^{-1}}, \tag{4-13}$$

$$y(d) = 1 + M\left[1 - e^{-a(d/d_1)^b}\right], \tag{4-8}$$

$$y(\Delta t) = y_o + (M - y_o)e^{-[g(\Delta t/\Delta t_1)^h]^{-1}} \tag{3-5}$$

Eqs. (3-4) and (4-3) are particular cases of the general form, (4-13). Taking the log of (4-13),

$$\log[1 - y(d)] = \log M - [a(d/d_1)^b]^{-1} \tag{IV-1}$$

or

$$-\log \frac{1-y(d)}{M} = \frac{1}{a(d/d_1)^b} .$$

Inverting and taking the log again,

$$\log\left[-\log \frac{1-y(d)}{M}\right]^{-1} = \log a + b \log(d/d_1) . \tag{IV-2}$$

Substituting the transformations,

$$\left.\begin{aligned} Y &= \log\left[-\log \frac{1-y(d)}{M}\right]^{-1} \\ A &= \log a \\ B &= b \\ Z &= \log(d/d_1) \end{aligned}\right\} \tag{IV-3}$$

leads to the standard linear form,

$$Y = A + BZ \ . \qquad \text{(IV-4)}$$

To fit (3-4), M is set equal to 0.5 in (IV-3); to fit (4-3), M = 1.0; to fit (4-13), M is set at a succession of values and (IV-4) is fit to the data at each M (appendix V).

Eq. (4-8) is transformed similarly. Taking the log,

$$\log\left[1 - \frac{y(d)-1}{M}\right] = -a(d/d_1)^b$$

Taking the log again

$$\log\left(-\log\left[1 - \frac{y(d)-1}{M}\right]\right) = \log a + b \log(d/d_1) \ . \qquad \text{(IV-5)}$$

Substituting the transformation,

$$\left.\begin{aligned} Y &= \log\left(-\log\left[1 - \frac{y(d)-1}{M}\right]\right) \\ A &= \log a \\ B &= b \\ Z &= \log (d/d_1) \end{aligned}\right\} \qquad \text{(IV-6)}$$

leads to the standard form, (IV-4). This is fit, as before, at a succession of assigned values of M.

Taking the log of the time domain equation, (3-5),

$$\log\left(\frac{y(\Delta t)-y_o}{M - y_o}\right) = -\frac{1}{g(\Delta t/\Delta t_1)^h} \ .$$

Change sign, invert, and take log again

$$\log\left[-\log\left(\frac{y(\Delta t)-y_o}{M - y_o}\right)\right]^{-1} = \log g + h \log(\Delta t/\Delta t_1) . \qquad \text{(IV-7)}$$

Substitute the transformations,

$$\left.\begin{aligned} Y &= \log\left[-\log\left(\frac{y(\Delta t)-y_o}{M-y_o}\right)\right]^{-1} \\ A &= \log g \\ B &= h \\ Z &= \log\,(\Delta t/\Delta t_1) \end{aligned}\right\} \qquad \text{(IV-8)}$$

leading once more to (IV-4) for an assigned M.

The $C_c(\Delta\Theta,\Delta t)$ surface, figure 5-10, is defined by,

at fixed Δt:

$$C_c(\Delta\theta) = 1 - Me^{-[a\Delta\theta^b]^{-1}} \qquad \text{(IV-9)}$$

and at fixed C_c:

$$\Delta\theta(\Delta t) = g(\Delta t/\Delta t_1)^h \qquad \text{(IV-10)}$$

Eq. (IV-9) is (4-13) written for the present variables, and is transformed and fitted in the same way. Taking the log of (IV-10)

$$\log[\Delta\theta(\Delta t)] = \log g + h \log(\Delta t/\Delta t_1) \qquad \text{(IV-11)}$$

and using the transforms,

$$\left.\begin{aligned} A &= \log g \\ B &= h \\ Z &= \log(\Delta t/\Delta t_1) \end{aligned}\right\} \qquad \text{(IV-12)}$$

gives the standard linear form, (IV-4).

APPENDIX V. FITTING ROUTINE FOR CURVES AND SURFACES

Steps followed in iterative fitting of surfaces to data are listed in this appendix. These are carried out separately for $\overline{X}'_m$, s'_m, $\overline{X}'_b$, cov'_{Ab}, cv'_b, and C_c. The equations that specify the surfaces for 2-station statistics are (3-4), (4-3), (4-8), and (4-13) in the distance domain and (3-5) in the duration domain. Steps to solve these are given first. The equations for C_c are (IV-9) and (IV-10). Solution of these is covered in a separate parallel list of steps.

A. GROUP AVERAGES (Step 1)

A few $\overline{X}'_m$, s'_m, and cov'_{Ab} values are larger than the nominal maximum of 1.0 as a result of normal scatter of the data, e.g., figures 3-3 and 4-14. The log-log transforms used in fitting surfaces cannot recognize these legitimate data values. To permit all points to influence the fitted surfaces, they are fitted to group averages of the data, with the requirement that groups be large enough that no group average y equal or exceed 1.0. For the two-station statistics, the 98 data points (table 3-1) are grouped into 0-5 mi, 5-10 mi, ---- distance bands. The linear average is taken within each group of both y and distance. The surface is then fitted to these y,d average points. Testing with distance bands of 3 to 8 miles showed the resulting surface is not sensitive to the choice made. Group averages are plotted in figure 3-1 and a few other selected figures.

The same considerations apply to fitting cv'_b by (4-8) as to the other statistics, except that group average values must now lie above 1.0 rather than below.

Not recognizing certain data values is the extreme example of the modification of departures by the log-log transform. The transform departure $y - \hat{y}$, even if finite, becomes large compared to $y - \hat{y}$ of the original variable, if either y or $\hat{y}$ lies near 1.0. The transformed variable y is defined by (IV-3), (IV-6), or (IV-8). Group averaging shifts the relative influence of outliers toward the magnitude of the linear departure of the original variable, and away from the magnitude of their log-log departure. The generally symmetrical scatter of points about final fitted curves on a linear plot of the original variable, e.g., figure 3-1, implies any residual distortion is insignificant.

B. FIRST FIT IN DISTANCE DOMAIN

Steps 2 to 5 are carried out separately for durations of 1, 2, 3, 6, 12, and 24 hr.

Initial value of large duration asymptote M (Step 2)

M is set permanently at 0.5 for $\overline{X}'_m$ and s'_m and at 1.0 for $\overline{X}'_b$, tentatively at $1.0 - y_{min}(\Delta t)$ for cov'_{Ab}, and tentatively at $y_{max}(\Delta t) - 1.0$ for cv'_b. Here $y_{min}(\Delta t)$ and $y_{max}(\Delta t)$ are the smallest and largest group average ordinates, respectively, at any d for a particular Δt.

Transformed group averages (Step 3)

The group average ordinates and distances from step 1 are transformed to Y and Z by (IV-6) for cv'_b and by (IV-3) for the other statistics, using the M assigned in step 2 or 5.

Linear regression fit to group averages (Step 4)

A linear regression fit is made to the transformed group averages from step 3. In solving for coefficients A and B in (IV-4) each group average is weighted by the number of data values it represents. That is, the standard "normal equations" for evaluating the coefficients,

$$nA + B\sum Z - \sum Y = 0 \qquad \text{(V-1)}$$

$$A\sum Z + B\sum Z^2 - \sum YZ = 0 \qquad \text{(V-2)}$$

are used in the form

$$A\sum n_k + B\sum n_k Z_k - \sum n_k Y_k = 0 \qquad \text{(V-3)}$$

$$A\sum n_k Z_k + B\sum n_k Z_k^2 - \sum n_k Y_k Z_k = 0 \ , \qquad \text{(V-4)}$$

where Y_k and Z_k are the group averages for the kth group comprised of n_k points and the summations are over groups. Simultaneous solution gives A and B. The coefficients for the original equation are obtained from $a = e^A$ and $b = B$ [(IV-3) and (IV-6)].

Find M (Step 5)

Omit this step for $\bar{X}'_m$, s'_m, and $\bar{X}'_b$, as they have fixed M values. Otherwise, compute the sum of squares of deviations of the original variable,

$$S = \sum (y - \hat{y})^2 \ , \qquad \text{(V-5)}$$

where y is the group average ordinate, $\hat{y}$ the computed value from (4-8) or (4-13) using group mean d and coefficients a and b from step 4, and the summation is over groups. The group averages are not weighted at this step, discussed later. Save this S for comparison with new values. Change M by a small increment or percentage of itself, and repeat steps 3 and 4 and the first part of this step. Continue until a least S is found. The corresponding $M(\Delta t)$ and its associated $a(\Delta t)$ and $b(\Delta t)$ are the coefficient values sought.

C. FIRST FIT IN DURATION DOMAIN

Steps 6 to 8 are carried out separately for distances of 2.5, 5.0, 7.5, 10, 20, and 30 mi.

Input data for duration fit (Step 6)

Read $y(d,\Delta t)$ values at d = 2.5 mi from the distance first fit profiles at each of the six standard durations. Repeat for other standard distances.

Zero duration intercept, y_o (Step 7)

Set $y_o(d)$ tentatively at 0.001 less than $y_o(d,1\text{-hr})$ if the 1-hr value is the smallest of the $y(d,\Delta t)$ values for the distance being fit, for statistics other than cv_b'. The transform will not recognize $y_o(d) \geq$ any $y(d,\Delta t)$ for these statistics. If the 2-hr value because of scatter is less than the 1-hr y, average the two and fit to the resulting 1-1/2-hr value. For cv_b' set y_o tentatively at 0.001 larger than $y_o(d,1\text{-hr})$. Set M = 1.0. Now transform y's at distance d from step 6 to Y by (IV-8) and Δt to Z. Solve for coefficients A and B by linear regression fit. The points are unweighted. That is, (V-1) and (V-2) are used. Transform A and B back to g and h by (IV-8). Compute sum of squares of deviations of the original variable, S, as in step 5. Increment $y_o(d)$ to a smaller (larger for cv_b') value and repeat. By varying $y_o(d)$ find least S. Adopt corresponding $y_o(d)$ as final (for this fit). This is permissible because $y_o(d)$ is insensitive to M(d), not yet finalized.

Large duration asymptote M (Step 8)

Increment M(d) to a smaller value than 1.0. Transform the y's at distance d from step 6 to Y by (IV-8) and Δt to Z, with this M(d) and $y_o(d)$ held at the value determined in step 7. Repeat the other parts of step 7 to find least S, except now vary M(d) instead of $y_o(d)$. Adopt M(d) corresponding to least S and the associated g(d) and h(d) as final values of the coefficients for this fit. The final value of $y_o(d)$ was determined in step 7.

D. 2ND FIT OF SURFACE

2nd fit in distance domain (Step 9)

Read values of $y(d,\Delta t)$ from each of the first-fit duration profiles at each of the six standard durations, and also at 30-min. Hereafter, treat 30-min as a standard duration.

At each duration, fit a y,d profile as in B (steps 2-5), except that the points are now weighted equally in the log-log transform fit.

2nd fit in duration domain (Step 10)

Repeat C (steps 6-8), except that 30-min is now included as a standard duration.

E. FURTHER ITERATION (Step 11)

The process is repeated until all y values converge to fixed values plus or minus a tolerance. $\bar{X}$ statistics converged to $\Delta y \leq 0.001$ by the 3rd fit in the duration domain and standard deviation statistics converged by the 7th fit.

F. DEFINITION OF BEST FIT

The approximate definition of best fit of a surface is least sum of squares of deviations of observed $y(d,\Delta t)$ from $\hat{y}(d,\Delta t)$ defined by the relevant distance and duration domain equations.

The more exact definition is sequential. The surface is defined only within tolerance ε. (a) First, the surface has the property that it is specified by a combination of possible (defined below) distance domain profiles and possible duration domain profiles such that at each standard distance-duration intersection (e.g., 5-mi, 30-min) the $y(d,\Delta t)$ and $\hat{y}(d,\Delta t)$ from the respective profiles differ by no more than ε. (The coefficients $M(d)$, $M(\Delta t)$, and $y_o(d)$ are chosen to produce this result.) (b) A "possible profile" in the distance domain is one that, for a given value of $M(\Delta t)$, provides a least squares fit of the log-log transformed variable to group averages (defined below). (Coefficients a and b are chosen to produce this result.) Similarly, "possible profile" in the duration domain is one that provides a best fit of the transformed variable for a combination of $y_o(d)$ and $M(d)$ values. (Coefficients g and h are chosen to produce this result.) (c) A "group average" is an arithmetic average as defined in step 2.

The logic of the above is:

(1) Arithmetic averages are used for groups so as to not exaggerate the influence of outliers in scattered data as would be the case with squared deviations.

(2) The least squares fit to transformed data is a mathematical convenience acceptable for points that are close to the curve.

Note that minimizing S in choosing $M(d)$, $M(\Delta t)$, and $y_o(d)$ is an efficient way of requiring the interprofile differences at intersections converge to ε, but does not appear explicitly in the definition of best fit.

G. MODIFIED ROUTINE FOR C_c SURFACE

The fitting routine is modified for the $C_c(\Delta\theta,\Delta t)$ surface, figure 5-10. Changes and their rationale are noted below. Step numbers correspond to the previous ones.

Step 1. For each duration, $\overline{C_c}$ and $\overline{\Delta\theta}$ group averages are calculated from the original data by 10^o $\Delta\theta$ bands. These group averages are the points on the curves in the upper panel of figure 5-10.

Steps 2-5. (IV-9) is fit at each duration by these steps, as before. M is defined by the fit.

Step 5A. To smooth the spacing of the curves from step 5 within the $0° < \Delta\theta < 70°$ range where there are no data, an average common point within this band is assigned by inspection of the curves. This is at $C_c = 0.85$, $\Delta\theta = 10°$. Steps 2-5 are repeated, with all curves forced through this point by treating it as a group mean with a large n.

Step 6. Read $\Delta\theta(C_c, \Delta t)$ from the curves of step 5A at selected fixed C_c. $C_c = 0$ and $C_c = 0.3$ were selected.

Steps 7-8. The fit in the duration domain here is simply a linear regression fit to (IV-10), using (IV-12), to define $g(C_c)$ and $h(C_c)$ at each of the selected C_c levels.

Step 9. Solve for $\Delta\theta(C_c, \Delta t)$ by (IV-10) at the selected C_c levels, at each standard duration including 30 min, using g and h from steps 7-8.

Step 10. Refit the $\Delta\theta$ domain curves defined by (IV-9) through three points, the two from step 9 and the common point from step 5A. The three points suffice to define three constants, M, a, and b, and this is a determinate fit. These curves are the final profiles on the surface, and are depicted in figure 5-10. The constants are listed in appendix VII.

APPENDIX VI. CURVE SPLICING

The profiles of cov'_{Ab} in the distance domain for shorter durations are comprised of two fits of

$$y = 1 - Me^{-[a(d/d_1)^b]^{-1}} \tag{4-13}$$

spliced at a common point (chapter 4), where $y - cov'_{Ab}$. The ordinates and slopes of the inner and outer segments are the same at the splice point, s:

$$(y_{in})_s = (y_{out})_s \ , \tag{VI-1}$$

$$(\partial y_{in})/\partial d)_s = (\partial y_{out}/\partial d)_s . \tag{VI-2}$$

The splicing requirement is to find the constants of the inner segment in (4-13), a_{in} and M_{in}, from given values of the splice distance d_s, and the constants of the outer segment, a_{out}, b_{out}, and M_{out}. Constant b_{in} is set at 1.0. Differentiating (4-13),

$$\partial y/\partial d = -Me^{-[a(d/d_1)^b]^{-1}} a^{-1} b(d/d_1)^{-b-1} . \tag{VI-3}$$

Combining with (4-13),

$$\partial y/\partial d = a^{-1} b(d/d_1)^{-b-1}(y - 1) \ . \tag{VI-4}$$

Combining (VI-4) and (VI-2) at d_s,

$$(a_{in})^{-1}(d_s/d_1)^{-2}(y_s - 1) = (a_{out})^{-1}(d_s/d_1)^{-b_{out}-1}(y_s - 1)b_{out} . \tag{VI-5}$$

Solving for a_{in},

$$a_{in} = a_{out}(b_{out})^{-1}/(d_s/d_1)^{b_{out}-1} \ . \tag{VI-6}$$

To evaluate M_{in} combine (4-13) and (VI-1) at d_s,

$$1 - M_{in}e^{-[a_{in}(d_s/d_1)]^{-1}} = 1 - M_{out}e^{-[a_{out}(d_s/d_1)^{b_{out}}]^{-1}} \tag{VI-7}$$

Solving for M_{in},

$$M_{in} = M_{out} e^{[(a_{in})^{-1}(d_s/d_1)^{-1} - (a_{out})^{-1}(d_s/d_1)^{-b_{out}}]} . \qquad \text{(VI-8)}$$

The constants for the inner segment of the cov'_{Ab} profiles calculated by (VI-6) and (VI-8) are listed in appendix VII.

APPENDIX VII. FITTING CONSTANTS

This appendix lists the final fitting constants for the $\overline{X}'_m$, s'_m, $\overline{X}'_b$, cv'_b, cov'_{Ab}, and C_c surfaces, with cross reference to the figures in which profiles of these variables appear. The surfaces for depth-length and depth-area ratios, as well as s'_b, $\overline{X}'_L$, and s'_L, are derived from other surfaces rather than being fit to data. Thus these variables do not appear here.

All fitting constants are dimensionless.

Table VII-1.--Fitting constants for $\overline{X}'_m$, figure 3-7, upper.

$$\overline{X}'_m(d) = 1 - 0.5e^{-[a(d/d_1)^b]^{-1}} \quad (3\text{-}4)$$

Δt (hr)	a	b
0.5	.28992	.81347
1	.27865	.59401
2	.25546	.48375
3	.24506	.43625
6	.23405	.36746
12	.23077	.30609
24	.23377	.24843

Table VII-2.--Fitting constants for X'_m, figure 3-7, lower.

$$\overline{X}'_m(\Delta t) = y_o + (M-y_o)e^{-[g(\Delta t/\Delta t_1)^h]^{-1}} \quad (3\text{-}5)$$

d (mi)	g	h	M	y_o
2.5	16.97556	.84091	.987	.1426
5.0	10.34209	.77635	.981	-.1851
7.5	9.08752	.70575	.979	-.4511
10	7.37538	.65378	.979	-.4434
20	6.53480	.49570	.993	-.8769
30	2.67187	.47288	1.000	.0063

Table VII-3.--Fitting constants for s'_m, figure 3-8, upper.

$$s'_m(d) = 1 - 0.5e^{-[a(d/d_1)^b]^{-1}} \quad (3\text{-}4)$$

Δt (hr)	a	b
0.5	.17410	.98816
1	.17580	.96458
2	.19301	.80838
3	.20584	.67519
6	.21384	.48085
12	.20672	.34937
24	.19483	.26122

Table VII-4.--Fitting constants for s'_m, figure 3-8, lower.

$$s'_m(\Delta t) = y_o + (M - y_o)e^{-[g(\Delta t/\Delta t_1)^h]^{-1}} \quad (3\text{-}5)$$

d (mi)	g	h	M	y_o
2.5	.28538	.90101	1.000	.9509
5.0	.29919	1.13170	.996	.8448
7.5	.28872	1.14953	.995	.7717
10	.27876	1.14606	.994	.7228
20	.25325	1.06774	.998	.6286
30	.23870	1.02346	1.000	.5903

Table VII-5.--Fitting constants for $\overline{X}'_b$, figure 4-4.

$$\overline{X}'_b(d) = 1 - e^{-[a(d/d_1)^b]^{-1}} \qquad (4\text{-}3)$$

Δt (hr)	a	b
0.5	.39511	1.14322
1	.29274	.88829
2	.25037	.74318
3	.24021	.67101
6	.23766	.55692
12	.24706	.45155
24	.26372	.35499

Table VII-6.--Fitting constants for $\overline{X}'_b$, figure 4-5.

$$\overline{X}'_b(\Delta t) = y_o + (M - y_o)e^{-[g(\Delta t/\Delta t_1)^h]^{-1}} \qquad (3\text{-}5)$$

d (mi)	g	h	M	y_o
2.5	5.84185	1.22502	.939	0.0692
5.0	5.17712	.78623	.914	-1.1055
7.5	4.97438	.61070	.919	-1.7410
10	4.34749	.50012	.944	-1.9135
20	.98439	.44855	.997	-0.2338
30	.61802	.46932	1.000	-0.0557

Table VII-7.--Fitting constants for cv'_b, figure 4-10.

$$cv'_b(d) = 1 + M[1 - e^{-a(d/d_1)^b}] \quad (4\text{-}8)$$

Δt (hr)	a	b	M
0.5	0.06868	0.96499	8.1402
1	.06545	1.01191	4.1772
2	.06756	0.98900	2.3579
3	.07048	.97458	1.7716
6	.07534	.90157	1.3310
12	.07995	.87213	1.1000
24	.07875	.81595	1.1000

Table VII-8.--Fitting constants for cv'_b, figure 4-11.

$$cv'_b(\Delta t) = y_o + (M - y_o)e^{-[g(\Delta t/\Delta t_1)^h]^{-1}} \quad (3\text{-}5)$$

d (mi)	g	h	M	y_o
2.5	8.20673	1.29411	1.160	5.3176
5.0	7.02189	1.23940	1.260	8.2054
7.5	5.77924	1.22966	1.340	9.5512
10	5.26022	1.24945	1.410	10.9259
20	5.05857	1.22429	1.600	15.4316
30	4.37608	1.26389	1.730	15.9568

Table VII-9.--Fitting constants for cov'_{Ab}, figure 4-17.

$$cov'_{Ab}(d) = 1 - Me^{-[a(d/d_1)^b]^{-1}} \quad (4\text{-}13)$$

Δt (hr)	d (mi)	a	b	M
0.5	0-3.45	1.27215	1.0	.70538
	3.45-	.17453	.05323	119.9771
1	0-3.45	.70431	1.0	.74511
	3.45-	.39039	.20782	3.5770
2	0-3.45	.53694	1.0	.61705
	3.45-	.32631	.30256	2.9573
3	0-3.45	.46287	1.0	.51718
	3.45-	.27278	.28963	3.5804
6		.25357	.33936	2.1891
12		.27724	.48932	.6826
24		.24174	.98000	.1906

Table VII-10.--Fitting constants for cov'_{Ab}, figure 4-18.

$$cov'_{Ab}(\Delta t) = y_o + (M - y_o)e^{-[g(\Delta t/\Delta t_1)^h]^{-1}} \quad (3\text{-}5)$$

d (mi)	g	h	M	y_o
2.5*	.64303	1.07877	.984	0.4633
5.0	.39173	1.00743	.983	.3750
10	.24776	1.02419	.993	.2499
20	.15489	1.11208	.994	.1009
30	.10725	1.25330	1.000	-.0121

*Coefficients at d = 2.5 mi apply to durations of 6 hr and more only. Profiles at this distance on fig. 4-18 adjusted by hand at durations of 3 hr and less to agree with fig. 4-17.

Table VII-11.--Fitting constants for C_c, figure 5-10.

$$C_c(\Delta\theta) = 1 - Me^{-[a\Delta\theta^b]^{-1}} \quad \text{(IV-9)}$$

Δt (hr)	a	b	M
0.5	.02957	1.20304	1.2561
1	.04271	1.03766	1.2812
2	.06380	.85057	1.3652
3	.07628	.76619	1.4204
6	.09603	.65423	1.5073
12	.11015	.59083	1.5375
24	.12824	.51336	1.6383

Table VII-12.--Fitting constants for C_c, figure not shown.

$$\Delta\theta(\Delta t) = g(\Delta t/\Delta t_1)^h \quad \text{(IV-10)}$$

C_c	g	h
0	34.622	.2426
0.3	80.343	.3114

APPENDIX VIII.--OUTLINE OF METHOD

Figure VIII-1 is a schematic outline of the material in chapters 3 to 6. Notation is listed at the beginning of the report.

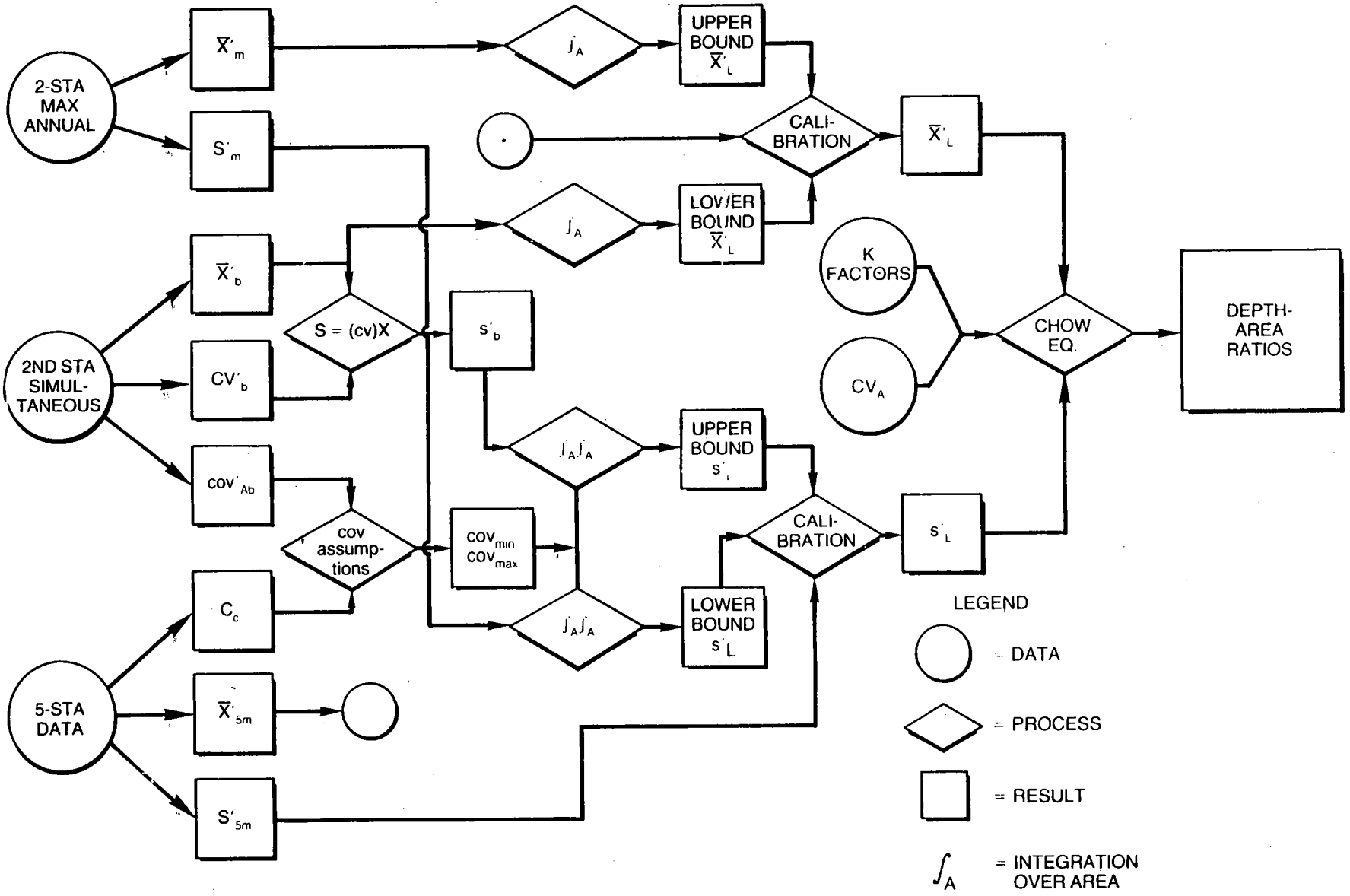

Figure VIII-1.--Schematic diagram of computation of depth-area ratios.

APPENDIX IX. ANNUAL MAXIMUM RAINFALLS

The tables of this appendix list the arrays of April - October season maximum rainfalls at the stations in table 2-1 for the six standard durations of 1, 2, 3, 6, 12, and 24 hours. 18 hours is also included. The period of record is 1948-72, except for years indicated as not used at the bottom of each table. These seasonal maxima are termed "annual maxima" throughout this report (chapter 2).

The date time group 7121557 is read "first hour of the annual maximum precipitation period ends at 1500 CST July 12, 1957."

Similar data are on file, on microfiche, at the office of the authors for the station pairs in table 3-1 and the 5-station sets in table 5-1.

MAXIMUM ANNUAL VALUES AND TIME OF OCCURRENCE (MONTH,DAY, HOUR AND YEAR)

1522 CHICAGO CALUMET TREATMENT WORKS PRECIPITATION IN INCHES

1-HR	DATE	2-HR	DATE	3-HR	DATE	6-HR	DATE	12-HR	DATE	18-HR	DATE	24-HR	DATE
2.42	8221572	3.36	10030854	4.21	10030754	5.57	7121957	6.06	7121557	6.06	7121557	6.88	10091954
2.25	7231855	2.79	8221572	3.44	7211763	5.18	10030654	5.24	10091954	5.92	10091754	6.06	7121557
2.13	7121957	2.53	7211763	3.21	7121957	3.49	7211463	3.49	7211463	3.69	9231361	3.77	5110366
1.88	10030854	2.50	7121957	2.88	8221572	2.96	8291955	3.22	8291855	3.49	7211463	3.71	9230361
1.84	7022360	2.30	7231755	2.71	6252159	2.91	8221472	3.07	9231361	3.22	8291855	3.49	7211463
1.74	8241971	2.23	9260851	2.63	9212051	2.85	9260551	3.00	6250268	3.13	6241868	3.24	5100451
1.56	9212051	2.17	8241971	2.31	7231755	2.72	6252159	2.91	8221472	3.02	5111166	3.24	6241868
1.47	7191359	2.05	4300270	2.22	8241971	2.35	7172464	2.74	7172464	2.91	8221472	3.22	8291855
1.47	7172464	1.96	7022360	2.22	7172464	2.30	6250668	2.72	6252159	2.88	5100251	3.09	10150567
1.46	6231768	1.70	8210364	2.05	4300270	2.30	9132261	2.63	5111466	2.88	6020450	2.91	6020450
1.41	7211863	1.59	6252259	2.03	7022260	2.22	8241971	2.46	8052051	2.75	7172464	2.91	8221472
1.27	5191249	1.51	6231668	1.84	6250868	2.10	4300270	2.22	8241971	2.72	6252159	2.75	7172464
1.13	7211753	1.51	5191249	1.69	9132461	2.07	6020550	2.20	4300270	2.42	4300270	2.72	6252159
1.13	8262465	1.50	8262365	1.68	5191249	2.03	7022260	2.13	6020450	2.35	10150567	2.69	4300270
1.08	10150567	1.46	9132461	1.55	8262365	1.83	5191249	2.03	7022260	2.22	8241971	2.22	8241971
1.06	6170152	1.42	10150567	1.53	6020750	1.74	7270366	1.89	8262365	2.22	7210749	2.22	7210749
1.05	4300370	1.28	7171353	1.47	10150567	1.71	8262365	1.84	10150467	2.03	7022260	2.03	7022260
0.88	9140161	1.25	6020850	1.33	4091753	1.54	5311858	1.79	5311558	1.91	5311658	1.98	5311558
0.82	7161656	1.13	6170152	1.13	5172469	1.51	10150467	1.75	7170353	1.89	8262365	1.89	8262365
0.80	6080558	1.09	7221662	1.13	7221662	1.47	9010852	1.57	7090649	1.79	7170153	1.85	4280856
0.79	7191450	0.91	6080558	1.13	6170152	1.39	5172369	1.56	4281956	1.66	4281956	1.79	7170153
0.72	4201866	0.88	5172469	1.04	6130166	1.33	4091753	1.53	9010852	1.53	9010852	1.53	9010852
0.63	7190469	0.85	6131766	0.94	6080558	1.30	4282356	1.39	5172369	1.44	5172369	1.44	5172369
0.59	7201462	0.84	7161656	0.88	4290156	1.13	7221662	1.34	8052362	1.39	8052162	1.39	8052162

NO DATA PRIOR TO 1948 ON TAPE. ZERO INDICATES YEAR NOT AVAILABLE, 5 INDICATES YEAR WAS USED

48	49	50	51	52	53	54	55	56	57	58	59	60	61	62	63	64	65	66	67	68	69	70	71	72
0	5	5	5	5	5	5	5	5	5	5	5	5	5	5	5	5	5	5	5	5	5	5	5	5

MAXIMUM ANNUAL VALUES AND TIME OF OCCURRENCE (MONTH,DAY, HOUR AND YEAR)

1532 CHICAGO LAKEVIEW PRECIPITATION IN INCHES

1-HR	DATE	2-HR	DATE	3-HR	DATE	6-HR	DATE	12-HR	DATE	18-HR	DATE	24-HR	DATE
2.31	7122257	2.92	7122257	3.40	7122157	4.88	7121857	5.69	7121457	5.77	7121357	6.27	10091854
1.56	6221864	2.01	8041661	2.23	6142149	3.03	7020962	3.77	10091954	4.60	10092354	5.77	7121357
1.48	7162450	1.98	6142249	2.18	7162250	3.00	6141849	3.27	6141849	4.02	6020550	4.06	6140549
1.42	10101654	1.97	7162350	2.02	5241355	2.66	6020550	3.08	7020462	3.59	6140649	4.06	6029450
1.36	8041761	1.89	5241355	2.01	8041661	2.56	9132161	2.80	9121561	3.10	7012262	3.10	7012262
1.30	8292356	1.82	7191756	2.00	7191756	2.45	5241355	2.75	6020450	2.95	8041661	3.06	9120761
1.27	7271858	1.61	6221764	1.74	7021162	2.35	10091954	2.45	5241355	2.45	5241355	2.59	4270259
1.25	5241355	1.60	7021362	1.72	9202164	2.29	7022060	2.29	7022060	2.31	7022060	2.56	4290763
1.13	7021362	1.58	10101654	1.68	10101554	2.26	6252059	2.26	6252059	2.26	6252059	2.45	5241355
1.13	6252459	1.47	6130858	1.65	7022160	2.00	7191756	2.17	6122358	2.17	6122358	2.31	7022060
1.11	4301853	1.26	7022260	1.64	6130758	1.95	9202064	2.10	9201964	2.17	9201264	2.28	4262456
1.10	7022360	1.20	5230159	1.60	5222459	1.64	6130758	2.05	4262356	2.05	4262356	2.19	6121558
1.08	6142249	1.13	4301753	1.14	4301753	1.39	7131263	1.94	4291963	1.97	4291963	2.17	9201264
0.80	7191863	0.88	6120252	1.04	7131363	1.21	5011653	1.60	4301553	1.60	4301553	1.96	4301853
0.53	6162452	0.85	7191863	1.02	6120252	1.15	6120152	1.15	6120152	1.38	4121152	1.58	4120752

NO DATA PRIOR TO 1948 ON TAPE. ZERO INDICATES YEAR NOT AVAILABLE, 5 INDICATES YEAR WAS USED

48	49	50	51	52	53	54	55	56	57	58	59	60	61	62	63	64	65	66	67	68	69	70	71	72
0	5	5	0	5	5	5	5	5	5	5	5	5	5	5	5	5	0	0	0	0	0	0	0	0

MAXIMUM ANNUAL VALUES AND TIME OF OCCURRENCE (MONTH,DAY, HOUR AND YEAR)

1537 CHICAGO LOYOLA UNIVERSITY PRECIPITATION IN INCHES

1-HR	DATE	2-HR	DATE	3-HR	DATE	6-HR	DATE	12-HR	DATE	18-HR	DATE	24-HR	DATE
1.72	7122257	2.68	8122056	2.78	7122057	3.95	7121757	4.79	7121357	4.84	7121357	6.01	10091854
1.68	8122056	2.39	8041661	2.77	8122056	2.80	7020962	3.95	10091954	4.61	10091854	4.88	7121357
1.48	7021362	2.35	7122157	2.39	8041661	2.77	8122056	3.24	8041661	3.48	6140849	3.61	6140449
1.34	8041761	1.74	6051965	2.04	7021162	2.73	6141849	2.98	6141849	3.45	8041661	3.45	8041661
1.26	6051965	1.72	7021362	1.93	6142149	2.56	9132161	2.88	7020862	2.98	6020550	3.17	4290763
1.11	4232358	1.71	6142249	1.74	6051965	2.52	10091954	2.78	8122056	2.96	7080551	3.14	7080551
1.08	6142249	1.40	6020650	1.63	8060251	2.11	10081250	2.65	4291963	2.96	7020962	3.00	7020562
1.05	6011851	1.33	6011851	1.60	6020550	2.06	7022060	2.46	8291755	2.78	8122056	2.98	6020550
0.99	7290354	1.25	7010259	1.58	6130758	1.95	8060151	2.13	10080950	2.78	4291963	2.79	8120556
0.95	7191863	1.24	7290254	1.56	10091954	1.78	8291755	2.10	8051951	2.46	8291755	2.46	8291755
0.94	8061355	1.21	6130758	1.52	7022160	1.78	6051665	2.09	6122358	2.09	6122358	2.11	6121558
0.91	6221864	1.20	7022260	1.29	7010159	1.61	7021658	2.06	7022060	2.07	7022060	2.07	7022060
0.91	6020750	1.02	7191863	1.23	7181552	1.58	4291963	1.78	6051665	1.78	6051665	1.81	4270259
0.89	9182153	1.00	8061255	1.06	7191863	1.47	4271959	1.65	7070664	1.68	4270859	1.78	6051665
0.86	7022360	0.98	6221764	1.03	8061355	1.36	7181452	1.65	9182153	1.67	9182153	1.69	7181352
0.85	5031759	0.95	6120152	0.98	6221764	1.28	9182153	1.56	4271459	1.65	7070664	1.67	9182153
0.79	7181752	0.95	9182153	0.96	9182153	0.98	6221764	1.39	7181352	1.59	7180152	1.65	7070664

NO DATA PRIOR TO 1948 ON TAPE. ZERO INDICATES YEAR NOT AVAILABLE. 5 INDICATES YEAR WAS USED

48	49	50	51	52	53	54	55	56	57	58	59	60	61	62	63	64	65	66	67	68	69	70	71	72
0	5	5	5	5	5	5	5	5	5	5	5	5	5	5	5	5	5	0	0	0	0	0	0	0

MAXIMUM ANNUAL VALUES AND TIME OF OCCURRENCE (MONTH,DAY, HOUR AND YEAR)

1542 CHICAGO MAYFAIR PRECIPITATION IN INCHES

1-HR	DATE	2-HR	DATE	3-HR	DATE	6-HR	DATE	12-HR	DATE	18-HR	DATE	24-HR	DATE
3.72	7211353	3.72	7211353	3.72	7211353	6.47	7121857	7.67	7121357	7.69	7121357	7.69	7121357
2.14	7122257	2.81	7122257	3.69	7122057	3.85	7211353	4.16	7211353	4.58	10092354	6.53	10091854
2.00	4232358	2.15	8162068	2.71	8162068	3.63	7021062	3.77	10091854	4.58	6020550	4.64	6140449
1.69	8162068	2.13	8252172	2.70	7021362	3.38	8161868	3.77	7020762	4.28	6140749	4.61	6020450
1.67	9051769	2.13	6142249	2.52	6142149	3.31	9132161	3.48	9131961	4.16	7211353	4.16	7211353
1.47	8180654	2.03	6020650	2.28	6020550	3.14	6142049	3.38	8161868	3.77	7020762	3.79	7012162
1.43	8241971	2.01	4232358	2.28	9132261	2.85	6020550	3.30	6141649	3.48	9131961	3.58	9130461
1.40	7161855	1.80	8241871	2.27	8252072	2.85	10101969	3.14	10101869	3.38	8161868	3.43	10100469
1.39	6020750	1.80	7021462	2.10	10102169	2.39	9171872	2.91	6020450	3.29	10101069	3.38	8161868
1.32	7210849	1.75	9051669	2.02	4232258	2.34	10030554	2.76	8291655	2.97	5100151	3.16	5091951
1.30	8252272	1.72	8180554	1.92	8180554	2.34	5241255	2.49	9171872	2.85	8060355	2.95	5110366
1.20	7191756	1.63	9132361	1.84	8241871	2.17	7022060	2.25	5100651	2.56	9171872	2.85	8060355
1.16	9222161	1.45	7191756	1.57	7191756	2.06	7042171	2.23	5111566	2.55	5111366	2.57	9171872
1.11	5251751	1.40	7161855	1.45	7022160	2.02	4232258	2.17	7022060	2.32	4231058	2.35	4262456
1.07	6161967	1.26	5251751	1.40	7161855	1.98	6252059	2.15	4231258	2.18	7022060	2.32	4231058
0.97	7132165	1.23	9202164	1.39	5251751	1.91	4262456	2.07	7042171	2.07	7042171	2.18	7022060
0.93	9252470	1.18	7132165	1.38	6252259	1.61	6101567	2.01	4262356	2.01	4262356	2.07	7042171
0.90	7021562	1.18	6161967	1.38	6101867	1.52	9202064	1.98	6252059	1.98	6252059	2.01	4290763
0.90	7022360	1.14	6120252	1.33	9202064	1.49	6120152	1.81	6210170	1.88	9201164	1.98	6252059
0.81	7141152	1.10	7022260	1.33	6120252	1.47	5111866	1.72	9201964	1.85	6210170	1.88	9201164
0.80	9202164	1.00	6252159	1.24	7132165	1.41	6210270	1.71	4291963	1.80	9200867	1.88	6201770
0.80	7191863	0.97	7191863	1.03	7191863	1.39	5251751	1.61	6210867	1.75	4291963	1.85	9200467
0.72	5282159	0.95	9252470	1.00	10142366	1.27	7132165	1.49	6120152	1.61	7180152	1.81	4120752
0.60	4280266	0.85	10142466	0.96	9252370	1.14	7191863	1.27	7132165	1.27	7132165	1.44	8081365

NO DATA PRIOR TO 1948 ON TAPE. ZERO INDICATES YEAR NOT AVAILABLE. 5 INDICATES YEAR WAS USED

48	49	50	51	52	53	54	55	56	57	58	59	60	61	62	63	64	65	66	67	68	69	70	71	72
0	5	5	5	5	5	5	5	5	5	5	5	5	5	5	5	5	5	5	5	5	5	5	5	5

MAXIMUM ANNUAL VALUES AND TIME OF OCCURRENCE (MONTH,DAY, HOUR AND YEAR)

1547 CHICAGO N BRNCH PUMPING STA PRECIPITATION IN INCHES

1-HR	DATE	2-HR	DATE	3-HR	DATE	6-HR	DATE	12-HR	DATE	18-HR	DATE	24-HR	DATE
2.25	7122257	2.99	7122257	3.52	7122157	5.28	7121857	6.19	7121357	6.33	7121357	6.33	7121357
1.57	8162068	2.38	8041761	2.47	8041661	3.38	7020962	3.53	10091854	4.17	10091854	5.38	10091854
1.55	4232358	2.14	6142249	2.40	6142149	3.16	6141849	3.48	7020462	3.92	6140749	4.43	6140449
1.35	8041761	2.09	7021362	2.28	8162068	3.03	9132061	3.41	6141749	3.50	7012262	3.51	7012062
1.19	8060462	1.70	8162068	2.25	7021262	2.73	8161868	3.21	9132061	3.21	9132061	3.34	9130261
1.17	6142249	1.56	4232258	1.69	7220551	2.54	6101567	2.75	8161868	3.13	6020550	3.20	6020450
1.15	6151967	1.50	6101567	1.67	6101667	2.22	10091854	2.56	6101467	2.75	8161868	2.89	5100251
1.15	8292356	1.47	7220651	1.56	4232258	2.01	6020550	2.53	7212151	2.70	5100251	2.89	4290763
1.10	8180654	1.35	6020650	1.54	6020550	1.73	8060151	2.38	4291963	2.56	6101467	2.81	7231168
1.08	7220651	1.31	8180554	1.47	8180554	1.60	4262456	2.14	8291755	2.46	4291963	2.74	5110466
1.07	10081350	1.27	8292256	1.41	7191756	1.56	4232258	2.13	6122358	2.35	5111466	2.56	6101467
1.06	8061355	1.21	6221764	1.22	8061355	1.49	8291755	2.08	5111566	2.17	8060255	2.27	10050355
0.85	7191863	1.09	8061355	1.21	6221764	1.49	4291963	2.06	6020450	2.13	6122358	2.14	6121558
0.83	6221864	1.00	7211353	1.04	7211353	1.31	5111966	1.72	7070564	1.72	7070564	2.04	4270256
0.78	7211353	0.91	6120152	1.03	6120152	1.27	9201964	1.67	4262356	1.70	4121152	1.95	4120852
0.64	7230952	0.89	7191863	0.95	7191863	1.21	6112452	1.32	4120852	1.67	4262356	1.72	7070564
0.64	8011966	0.80	6090566	0.90	5232066	1.18	7211353	1.26	7211353	1.27	7211353	1.27	7211353

NO DATA PRIOR TO 1948 ON TAPE. ZERO INDICATES YEAR NOT AVAILABLE, 5 INDICATES YEAR WAS USED

48	49	50	51	52	53	54	55	56	57	58	59	60	61	62	63	64	65	66	67	68	69	70	71	72
0	5	5	5	5	5	5	5	5	5	5	0	0	5	5	5	5	0	5	5	5	0	0	0	0

MAXIMUM ANNUAL VALUES AND TIME OF OCCURRENCE (MONTH,DAY, HOUR AND YEAR)

1552 CHICAGO ROSELAND PRECIPITATION IN INCHES

1-HR	DATE	2-HR	DATE	3-HR	DATE	6-HR	DATE	12-HR	DATE	18-HR	DATE	24-HR	DATE
2.21	8182070	3.08	10030754	4.18	10030754	5.24	7121857	6.00	7121457	6.03	7121457	6.80	10091954
1.91	7121857	2.52	7121857	3.14	7121857	5.04	10030654	5.10	10091954	5.45	10091954	6.03	7121457
1.74	8180654	2.28	8181970	2.85	6252159	3.23	8162068	3.30	8162068	3.42	8182070	3.74	8181970
1.47	6252359	2.10	9202167	2.51	7211763	2.89	6252159	3.10	7270166	3.34	6020550	3.63	5100451
1.40	4281851	1.91	6252259	2.33	8162068	2.86	7211463	3.06	8291755	3.33	5100351	3.56	5110366
1.23	7161655	1.85	7211763	2.28	8181970	2.86	8291955	2.89	6252159	3.31	8162068	3.52	10150567
1.23	8231872	1.65	8162068	2.21	9202167	2.47	9202167	2.86	7211463	3.23	5111266	3.36	6020450
1.16	8242071	1.58	8221472	2.06	8292055	2.39	9132261	2.85	8182070	3.06	8291755	3.32	8161368
1.15	9202267	1.55	7270766	1.90	7162150	2.34	7270366	2.71	5100651	2.89	6252159	3.17	10051855
1.14	6221069	1.51	4281851	1.83	7270666	2.28	8181970	2.59	9202067	2.86	7211463	3.02	4271159
1.05	7270866	1.51	8242071	1.83	9132361	2.28	7042371	2.53	9121561	2.76	9120861	2.88	9120761
1.01	8090552	1.51	9132461	1.81	8221472	2.16	7090649	2.46	7042071	2.72	9201067	2.86	7211463
1.00	7211763	1.49	8292155	1.74	7050171	2.02	6020550	2.25	7090549	2.46	7042071	2.69	6140449
1.00	7090749	1.40	162150	1.51	4281851	1.90	8221372	2.04	7162150	2.25	7090549	2.46	7042071
1.00	8021653	1.38	7022360	1.38	7022360	1.84	5311958	1.94	6122358	2.07	5311958	2.13	6080558
1.00	8162068	1.27	8262365	1.36	7132265	1.74	5100751	1.90	8221372	1.90	8221372	1.90	8221372
0.97	7191550	1.23	7221662	1.33	7221662	1.63	7132265	1.73	4301453	1.74	4300853	1.74	4301453
0.93	7132265	1.19	6221069	1.31	5311958	1.38	7022360	1.71	8262365	1.71	8262365	1.71	8262365
0.93	7221762	1.13	7090649	1.20	6221069	1.35	6100353	1.64	7172364	1.65	7172364	1.65	7172364
0.86	9101964	1.04	6130758	1.14	7090649	1.34	6191764	1.47	8052362	1.50	8052262	1.65	4280856
0.86	6082058	1.04	8090552	1.11	4301753	1.33	7221662	1.45	6221069	1.47	6221069	1.52	4120752
0.86	6101761	1.03	8021553	1.05	8090452	1.30	9010852	1.38	7022360	1.41	4281956	1.50	6221069
0.75	7222060	0.94	9101864	1.03	7172464	1.20	6221069	1.35	4281956	1.38	7022360	1.50	8052262
0.69	7161656	0.86	8122156	0.89	8122156	1.07	4282456	1.32	9010852	1.33	4120952	1.38	7022360

NO DATA PRIOR TO 1948 ON TAPE. ZERO INDICATES YEAR NOT AVAILABLE, 5 INDICATES YEAR WAS USED

48	49	50	51	52	53	54	55	56	57	58	59	60	61	62	63	64	65	66	67	68	69	70	71	72
0	5	5	5	5	5	5	5	5	5	5	5	5	5	5	5	5	5	5	5	5	5	5	5	5

MAXIMUM ANNUAL VALUES AND TIME OF OCCURRENCE (MONTH,DAY, HOUR AND YEAR)

1557 CHICAGO SAN DISP(CHI RACINE PUMP) PRECIPITATION IN INCHES

1-HR	DATE	2-HR	DATE	3-HR	DATE	6-HR	DATE	12-HR	DATE	18-HR	DATE	24-HR	DATE
3.89	6101467	4.73	6101467	5.18	6101367	5.66	7121857	6.49	7121457	6.54	7121457	6.54	7121457
2.20	7261450	2.57	7121857	2.88	7122157	5.27	6101467	5.98	6101367	5.98	6101367	5.98	6101367
1.55	8031257	2.35	7261450	2.49	7162250	3.50	8161868	3.86	7262266	3.94	7261766	4.67	10092054
1.35	9282172	2.04	7160263	2.35	8162068	2.97	6252059	3.55	8161868	3.55	8161868	3.94	7261766
1.51	8180654	2.04	9282172	2.33	7170369	2.65	9132161	2.97	6252059	3.48	7162250	3.55	8161868
1.50	7170369	1.86	7170369	2.18	7160163	2.57	7162150	2.75	9132061	3.32	10100154	3.54	7162150
1.48	6130170	1.71	6130758	2.16	9282072	2.51	7270266	2.64	7162250	2.97	6252059	3.28	5092351
1.34	10061655	1.69	8180654	2.13	9132361	2.33	7170369	2.46	10091954	2.80	5100551	3.10	7170369
1.28	9031861	1.58	6122470	2.04	8180654	2.28	7160163	2.33	7170369	2.75	9231261	3.07	6140449
1.26	6130758	1.51	8162268	1.97	6130758	2.27	9282072	2.31	5101051	2.44	10052355	2.97	6252059
1.16	8292356	1.48	9132361	1.79	6252059	2.23	8180554	2.28	7160163	2.33	7170369	2.88	10051855
1.13	8041048	1.45	10061655	1.77	7270166	2.00	6130558	2.28	9282072	2.28	7160163	2.75	9231261
1.08	7160363	1.39	7270266	1.71	6122370	1.76	6202370	2.23	6122358	2.28	9282072	2.28	7190163
0.97	7270266	1.33	6142249	1.45	10061655	1.73	8292055	2.16	6141749	2.23	6122358	2.28	9282072
0.95	8090352	1.20	6252059	1.42	6142249	1.73	6141849	2.04	6202170	2.16	6141749	2.25	6121458
0.93	8162268	1.19	8292256	1.22	8040948	1.59	7020962	1.99	8291555	2.06	6201370	2.06	6201370
0.80	7081949	1.19	8040948	1.19	8292256	1.55	8060151	1.63	7020762	1.80	5092156	2.03	5091056
0.76	7021062	1.10	8090352	1.16	7020962	1.26	8040748	1.41	5091056	1.63	7020762	1.63	7020762
0.75	9101864	0.96	7021062	1.15	8060251	1.24	6120152	1.35	8040148	1.39	4120952	1.57	4120752
0.69	6302459	0.90	9260851	1.13	6120152	1.19	8292256	1.24	6120152	1.35	8040148	1.35	8040148
0.67	7212351	0.79	9101864	0.84	9101864	0.88	8202364	1.23	4051464	1.33	4051164	1.33	4051164

NO DATA PRIOR TO 1948 ON TAPE. ZERO INDICATES YEAR NOT AVAILABLE, 5 INDICATES YEAR WAS USED

48	49	50	51	52	53	54	55	56	57	58	59	60	61	62	63	64	65	66	67	68	69	70	71	72
5	5	5	5	5	0	5	5	5	5	5	5	0	5	5	5	5	0	5	5	5	5	5	0	5

MAXIMUM ANNUAL VALUES AND TIME OF OCCURRENCE (MONTH,DAY, HOUR AND YEAR)

1562 CHICAGO SAN DISTRICT OFFICE PRECIPITATION IN INCHES

1-HR	DATE	2-HR	DATE	3-HR	DATE	6-HR	DATE	12-HR	DATE	18-HR	DATE	24-HR	DATE
2.78	8252272	4.64	6101467	4.66	6101367	5.52	7121857	6.39	7121457	6.39	7121457	6.39	7121457
2.58	6101567	3.33	7122157	4.01	7122157	5.32	6101467	5.56	6101467	5.84	6101367	5.84	6101367
2.50	7122257	2.92	8252272	3.00	8252172	4.67	7162150	4.73	7162150	5.29	7162150	5.40	7162150
1.71	8241971	2.72	8311961	2.81	8311861	3.27	7020962	3.50	7020462	3.84	10091854	5.32	10091854
1.65	8180654	2.05	7071264	2.79	7162350	3.02	8252172	3.31	10091954	3.51	7012262	3.51	7012262
1.58	7071264	1.99	8180554	2.18	8180554	2.84	9132161	3.02	8252172	3.30	7261766	3.35	7261666
1.51	7051449	1.86	7162450	2.14	7071264	2.56	6252059	2.98	7262366	3.17	7231468	3.18	7231468
1.42	8312061	1.80	8241971	2.11	7021262	2.48	8180554	2.97	9132061	3.02	8252172	3.06	8252172
1.39	7021462	1.77	7021362	2.11	6252259	2.15	7071264	2.63	7070564	2.97	9132061	2.97	9132061
1.38	7172469	1.76	6252359	1.80	8241971	2.05	8161868	2.56	6252059	2.67	5100451	2.95	6140649
1.25	7191863	1.63	6142249	1.73	6142249	2.01	7042371	2.38	7232068	2.63	7070564	2.83	5100251
1.14	7240268	1.49	7231955	1.68	8162068	2.01	8292055	2.25	4291963	2.59	7020758	2.81	10051955
1.13	6222065	1.48	7172469	1.67	6130758	1.98	6142249	2.21	8291555	2.56	6252059	2.76	4290763
1.06	6212156	1.42	7270166	1.55	7172469	1.91	7270266	2.20	6141749	2.38	4291963	2.75	7170469
0.96	6021950	1.39	6130758	1.54	7270166	1.73	7131163	2.18	7212151	2.35	10052455	2.64	4270259
0.96	6252459	1.32	7191863	1.49	7231955	1.67	6130758	2.10	7041971	2.20	6141749	2.63	7070564
0.96	8090352	1.26	6212056	1.40	7191863	1.55	7172469	2.10	6122358	2.10	7041971	2.63	7020758
0.88	7270266	1.23	6222065	1.35	6122370	1.38	7061865	1.71	6072269	2.06	6072169	2.10	7041971
0.88	6130858	1.21	7240268	1.27	6212056	1.38	6122370	1.61	6202170	1.75	4121052	1.98	4120752
0.84	7232055	1.09	6122470	1.24	6222065	1.29	7212151	1.41	7061865	1.74	10131670	1.74	10131670
0.80	4301853	1.06	8090352	1.06	8090352	1.27	6212056	1.38	4120852	1.41	7061865	1.67	4280756
0.79	6130170	0.92	6281351	1.02	7212351	1.11	6112452	1.27	6212056	1.39	4281056	1.51	6222065
0.68	6281351	0.83	4301753	0.83	4301753	1.06	6100353	1.10	6100253	1.10	6100253	1.25	4301853

NO DATA PRIOR TO 1948 ON TAPE. ZERO INDICATES YEAR NOT AVAILABLE, 5 INDICATES YEAR WAS USED

48	49	50	51	52	53	54	55	56	57	58	59	60	61	62	63	64	65	66	67	68	69	70	71	72
0	5	5	5	5	5	5	5	5	5	5	5	0	5	5	5	5	5	5	5	5	5	5	5	5

MAXIMUM ANNUAL VALUES AND TIME OF OCCURRENCE (MONTH,DAY, HOUR AND YEAR)

1564 CHICAGO S FILTER PLANT PRECIPITATION IN INCHES

1-HR	DATE	2-HR	DATE	3-HR	DATE	6-HR	DATE	12-HR	DATE	18-HR	DATE	24-HR	DATE
2.11	8180654	3.00	8031157	3.07	8031157	3.36	8292055	4.11	10092054	4.47	10091954	6.53	10092054
2.00	8031257	2.65	7021754	2.70	7021754	3.35	7121857	4.09	7121457	4.21	7121457	4.21	7121457
1.80	7231955	1.88	7231955	2.41	8162068	3.30	10030654	3.56	8291855	3.90	7230755	3.93	7230255
1.35	6130758	1.78	6130758	2.15	8292055	3.25	8162068	3.32	8162068	3.32	8162068	3.32	8162068
1.33	6021950	1.76	6021950	2.03	6130758	2.69	9132261	2.94	6101267	3.28	6020550	3.29	6020450
1.24	6130170	1.74	7022360	1.98	9132361	2.43	4272059	2.70	4271959	2.95	6101267	3.20	5110366
1.17	8210164	1.65	7290153	1.94	6021950	2.38	7160163	2.70	9132261	2.90	5100351	3.15	5100351
1.13	7160363	1.65	4300170	1.93	7160263	2.14	7042371	2.51	5111566	2.90	9120761	3.01	9120761
1.13	6131552	1.63	7160263	1.91	9082265	2.11	6101867	2.43	5100651	2.84	5111266	2.95	6101267
1.13	4301953	1.61	7170469	1.90	4272359	2.10	6130558	2.38	7160163	2.70	4271959	2.75	4271159
1.11	7170469	1.60	8162068	1.77	7290153	1.98	6021950	2.32	6122358	2.38	7160163	2.38	7160163
1.10	4281951	1.60	4272359	1.75	7022260	1.97	9082265	2.22	7042271	2.32	6122358	2.32	6122358
1.06	7022360	1.60	9082265	1.65	7170469	1.81	7290153	2.07	6020950	2.22	7042271	2.22	7042271
1.05	6252359	1.55	9132461	1.65	4300170	1.76	7022160	2.04	4301653	2.06	4301653	2.10	4301853
1.00	9082365	1.30	8210164	1.40	7270666	1.72	7270366	2.00	8191760	2.02	8191760	2.09	7170469
0.95	9122461	1.21	8090452	1.33	8090352	1.67	4300170	1.97	9082265	1.97	9082265	2.08	4300170
0.92	8162068	1.20	7270766	1.30	8210164	1.65	7170469	1.76	4300170	1.90	4300170	2.02	8191760
0.86	6182271	1.15	4281951	1.21	7050171	1.53	5100751	1.65	7170469	1.65	7170469	1.97	9082265
0.80	4301462	0.95	6101867	1.15	4281951	1.48	7090649	1.58	7090649	1.59	7090649	1.75	4120852
0.73	7090749	0.92	7090749	1.15	6101867	1.34	8090352	1.35	4282056	1.53	4120952	1.60	6140449
0.70	7270866	0.92	4301462	0.95	4301462	1.30	8210164	1.34	8090352	1.48	4282056	1.59	4281056
0.60	8122156	0.90	7050171	0.95	7090649	1.06	4282456	1.30	8210164	1.30	8210164	1.30	8210364
0.55	6101867	0.67	8122156	0.80	4290156	1.02	8060362	1.20	8060162	1.20	8060162	1.20	8060162

NO DATA PRIOR TO 1948 ON TAPE. ZERO INDICATES YEAR NOT AVAILABLE, 5 INDICATES YEAR WAS USED

48	49	50	51	52	53	54	55	56	57	58	59	60	61	62	63	64	65	66	67	68	69	70	71	72
0	5	5	5	5	5	5	5	5	5	5	5	5	5	5	5	5	5	5	5	5	5	5	5	0

MAXIMUM ANNUAL VALUES AND TIME OF OCCURRENCE (MONTH,DAY, HOUR AND YEAR)

1567 CHICAGO SPRINGFIELD PRECIPITATION IN INCHES

1-HR	DATE	2-HR	DATE	3-HR	DATE	6-HR	DATE	12-HR	DATE	18-HR	DATE	24-HR	DATE
1.95	8241971	2.68	8252172	2.83	8252172	3.60	7020962	3.77	7020462	4.84	6020550	6.18	10091954
1.68	8180654	2.56	8180554	2.72	8180554	3.30	6021850	3.39	6141749	4.57	10092354	4.88	6020450
1.64	8041761	2.56	6142249	2.67	6142249	3.18	9132161	3.31	9132061	4.05	6140649	4.50	6140549
1.63	8252272	2.14	6022150	2.49	6022050	3.06	6142049	3.30	6021850	3.79	7012162	3.79	7012162
1.50	7021362	2.10	8241971	2.29	9132361	3.06	8251872	3.30	10091954	3.31	9132061	3.43	9130461
1.47	6142249	1.92	7021362	2.25	6081765	2.89	8180554	3.06	8251872	3.06	8251872	3.06	8251872
1.24	6130758	1.80	6081865	2.20	7042471	2.52	6081765	2.70	6101367	3.00	7020658	3.01	7020658
1.16	8092260	1.73	7071264	2.04	7021162	2.47	7042171	2.53	8291755	2.71	6101367	2.98	5110366
1.15	7170469	1.70	7191756	1.86	7020658	2.35	6252059	2.52	6081765	2.65	5111366	2.86	7170469
1.13	6022150	1.67	9132361	1.80	7071264	2.26	7022060	2.51	7042171	2.53	8291755	2.72	4290763
1.10	6161967	1.63	7170469	1.79	7191756	2.11	6101867	2.45	5111566	2.52	6081765	2.72	6101367
1.09	9202064	1.59	7020658	1.78	7170469	1.97	8291755	2.35	6252059	2.51	7042171	2.53	8291755
1.05	9252470	1.22	8202352	1.54	4272259	1.90	9201964	2.26	7022060	2.35	6252059	2.52	6081765
0.95	6081865	1.22	4272259	1.36	7022060	1.86	7020658	2.21	7020658	2.26	7022060	2.51	7042171
0.90	7191856	1.22	6161967	1.35	8292155	1.79	7191756	2.20	7070564	2.20	7070564	2.46	4270259
0.88	8292155	1.19	8092260	1.33	8202252	1.79	7170469	2.08	4291963	2.14	4291963	2.26	7022060
0.81	4301853	1.10	8292155	1.27	6161967	1.63	5111966	1.79	7191756	1.88	10101069	2.20	7070564
0.76	8202352	1.07	9252470	1.08	9252370	1.58	4292363	1.79	7170469	1.84	5120670	2.08	5120670
0.75	6252059	0.90	4301853	1.02	4292463	1.36	6120152	1.64	10131870	1.83	7190456	1.83	7190456
0.60	7310963	0.78	4292363	0.93	5232066	1.33	7300170	1.38	4301653	1.66	8200852	1.70	4120752
0.52	8211966	0.72	5232066	0.93	4301653	1.21	6100353	1.36	6120152	1.38	4301653	1.43	4301853

NO DATA PRIOR TO 1948 ON TAPE. ZERO INDICATES YEAR NOT AVAILABLE, 5 INDICATES YEAR WAS USED

48	49	50	51	52	53	54	55	56	57	58	59	60	61	62	63	64	65	66	67	68	69	70	71	72
0	5	5	0	5	5	5	5	5	0	5	5	5	5	5	5	5	5	5	5	0	5	5	5	5

MAXIMUM ANNUAL VALUES AND TIME OF OCCURRENCE (MONTH,DAY, HOUR AND YEAR)

1572 CHICAGO UNIVERSITY PRECIPITATION IN INCHES

1-HR	DATE	2-HR	DATE	3-HR	DATE	6-HR	DATE	12-HR	DATE	18-HR	DATE	24-HR	DATE
1.93	7121957	2.45	7121857	2.69	8162068	4.43	7121857	5.17	7121457	5.28	7121457	6.05	10092054
1.70	10092154	2.25	10092054	2.60	7121957	3.48	8162068	4.13	10092054	4.66	10091754	5.29	7121457
1.68	8051755	2.10	7162250	2.54	10092054	3.07	10092054	3.63	8161868	3.63	8160968	3.71	7162150
1.57	6051553	2.00	8162268	2.41	7162150	2.78	8292055	3.22	7041971	3.57	7162150	3.63	8160968
1.42	6241450	1.94	7022360	2.15	7170369	2.72	7050171	3.10	7262266	3.43	7261766	3.59	5100351
1.31	8162268	1.93	8051655	1.95	7022260	2.61	7162150	3.07	9211851	3.35	5100451	3.50	8051655
1.25	4301462	1.68	7170469	1.94	8292055	2.50	7170369	2.96	8291655	3.25	8051655	3.43	7261766
1.21	7022360	1.66	4272259	1.92	6130758	2.35	4271959	2.63	4271659	3.22	7041971	3.24	7170369
1.21	8241971	1.63	6130758	1.88	6252159	2.33	9132161	2.61	7162150	2.69	4271059	3.22	7041971
1.13	9022263	1.58	6051553	1.85	9202067	2.10	9202067	2.50	7170369	2.52	9120861	2.75	4270959
1.11	7170569	1.43	9202067	1.67	9211851	1.98	7022160	2.40	9132061	2.50	7170369	2.53	6140449
1.05	9211851	1.40	9211851	1.63	9132361	1.98	6130558	2.14	1967	2.15	6122358	2.53	9120761
1.02	6252359	1.32	4301462	1.63	7160163	1.89	7160163	2.14	6122358	2.14	9201967	2.17	9200567
0.89	6030649	1.31	7160263	1.59	6051553	1.80	7270366	2.00	7022160	2.01	7022160	2.17	6121458
0.88	6130758	1.31	8241971	1.55	7270666	1.73	8060151	1.94	6141749	1.98	6141249	2.11	4290763
0.85	7061865	1.23	9132461	1.38	7050171	1.61	6051553	1.91	7160163	1.91	7160163	2.01	7022160
0.82	9202167	1.13	7270766	1.35	4301462	1.55	6141949	1.79	6050453	1.88	6042353	1.91	6042353
0.79	9122161	1.03	9082365	1.23	9082365	1.38	7020962	1.59	6201765	1.61	6201765	1.76	4280956
0.75	6131852	1.02	6142249	1.13	6142249	1.30	9082365	1.40	7020462	1.58	4120952	1.72	4120752
0.75	5232066	0.88	6120152	1.04	6120152	1.20	6112452	1.36	4281956	1.43	4281956	1.61	6201765
0.65	5122264	0.70	5122264	0.83	8210164	1.06	4282356	1.31	4051464	1.40	7020462	1.43	4301462
0.58	8122156	0.67	8122156	0.75	4290156	1.02	8202364	1.20	6112452	1.40	4051164	1.40	4051164

NO DATA PRIOR TO 1948 ON TAPE. ZERO INDICATES YEAR NOT AVAILABLE, 5 INDICATES YEAR WAS USED

48	49	50	51	52	53	54	55	56	57	58	59	60	61	62	63	64	65	66	67	68	69	70	71	72
0	5	5	5	5	5	5	5	5	5	5	5	5	5	5	5	5	5	5	5	5	5	0	5	0

MAXIMUM ANNUAL VALUES AND TIME OF OCCURRENCE (MONTH,DAY, HOUR AND YEAR)

1577 CHICAGO WBAP PRECIPITATION IN INCHES

1-HR	DATE	2-HR	DATE	3-HR	DATE	6-HR	DATE	12-HR	DATE	18-HR	DATE	24-HR	DATE
2.32	9282172	3.73	6252259	4.41	6252159	5.23	7121857	6.20	7121457	6.24	7121457	6.24	7121457
2.08	7121957	2.93	9282072	3.45	9282072	4.58	6252159	4.90	7262166	5.39	7261766	5.55	10091954
2.06	6252359	2.52	7170369	3.13	10030654	3.93	10030654	4.58	6252159	4.58	6252159	5.39	7261766
1.83	7022360	2.48	7121857	2.91	8162068	3.73	8161968	3.94	10030654	3.94	10030654	4.58	6252159
1.78	7270266	2.13	10030654	2.65	7170369	3.65	9282072	3.83	8161868	3.83	8161868	3.83	8161868
1.75	6130170	2.10	6101367	2.63	7122157	3.24	7270266	3.68	9282072	3.68	9282072	3.68	9282072
1.69	6241350	2.06	7162250	2.41	7162250	2.84	7170369	2.94	6101367	3.41	7162250	3.51	7162150
1.61	8162068	2.02	7270166	2.39	7270666	2.54	6101367	2.92	6202070	2.95	6101367	3.29	7170369
1.55	6101467	2.00	6122470	2.35	6122370	2.52	9132161	2.84	7170369	2.94	6201470	3.09	8051655
1.55	7170469	1.97	8162068	2.32	6101367	2.50	7162150	2.63	9132061	2.84	7170369	2.97	6201270
1.53	7221662	1.97	7022260	2.05	7022260	2.48	6202270	2.61	7162250	2.83	8051655	2.95	6101367
1.50	4281851	1.86	6100353	1.99	9132361	2.42	6100353	2.42	6100353	2.68	5100451	2.92	5100451
1.41	10030654	1.71	7221662	1.97	6130758	2.19	7160163	2.38	8052051	2.63	9132061	2.73	6140449
1.38	9031861	1.64	9031761	1.95	6100353	2.15	8060151	2.19	7160163	2.42	6100353	2.63	9132061
1.19	8090352	1.64	6130758	1.81	7221662	2.05	7022260	2.18	6122358	2.21	4291963	2.57	4290763
1.16	7080671	1.60	4281851	1.74	9260751	2.03	6130558	2.11	8291555	2.19	6140749	2.42	6100353
1.13	10061655	1.59	9051471	1.73	7160163	1.84	7231471	2.06	7022260	2.18	6122358	2.25	6080558
1.07	8122156	1.59	8090352	1.63	9051371	1.82	7221562	2.05	7172364	2.09	7172364	2.09	7172364
1.04	6082058	1.44	10061655	1.60	8090352	1.69	8060255	1.99	6141749	2.06	7022260	2.06	7022260
1.02	6100353	1.43	8292256	1.44	10061655	1.64	7132165	1.89	9051371	1.91	9051371	1.91	9051371
0.91	9022263	1.18	6142249	1.43	8292256	1.60	8090352	1.82	7221562	1.82	7221562	1.82	7221562
0.86	6222065	1.13	7160263	1.34	7172464	1.58	6142049	1.80	7132165	1.80	7132165	1.80	7132165
0.79	5191249	1.03	7180164	1.32	7132165	1.56	7172464	1.60	8090352	1.60	8090352	1.60	8090352
0.65	7180164	1.00	9082365	1.27	6142249	1.43	8292256	1.43	8292256	1.57	8290856	1.57	8290856

NO DATA PRIOR TO 1948 ON TAPE. ZERO INDICATES YEAR NOT AVAILABLE, 5 INDICATES YEAR WAS USED

48	49	50	51	52	53	54	55	56	57	58	59	60	61	62	63	64	65	66	67	68	69	70	71	72
0	5	5	5	5	5	5	5	5	5	5	5	5	5	5	5	5	5	5	5	5	5	5	5	5

MAXIMUM ANNUAL VALUES AND TIME OF OCCURRENCE (MONTH,DAY, HOUR AND YEAR)

1582 CHICAGO WB CITY — PRECIPITATION IN INCHES

1-HR	DATE	2-HR	DATE	3-HR	DATE	6-HR	DATE	12-HR	DATE	18-HR	DATE	24-HR	DATE
2.10	7122257	2.75	7122257	3.39	7122157	4.94	7121857	5.96	7121457	6.00	7121357	6.00	7121357
1.60	8180654	2.43	8311961	2.76	8311861	3.13	7020962	3.54	10091954	4.09	10091854	5.67	10091954
1.59	8312061	2.10	7162350	2.58	7162250	2.96	9132161	3.24	7020462	4.08	6020550	4.09	6020450
1.57	7162350	1.91	8180554	2.13	8180554	2.71	7162150	3.01	9132061	3.24	7020462	3.64	6140449
1.55	7071264	1.79	6142249	2.10	6252259	2.50	4271959	2.74	7162250	3.01	9132061	3.24	7020462
1.47	7051449	1.73	7021362	1.94	6142249	2.38	6142049	2.72	6141749	3.00	5100451	3.23	5100351
1.39	7191863	1.68	7231955	1.86	7021262	2.35	8180554	2.57	4271659	2.84	7020658	3.04	7190163
1.30	7022360	1.66	7071264	1.73	7071264	2.26	7231655	2.36	5100751	2.81	7190263	3.01	9132061
1.25	8292356	1.60	6252359	1.71	6130758	1.77	7071164	2.30	7230955	2.75	6141649	2.86	4270259
1.20	6130858	1.60	6130858	1.68	7231955	1.76	6130160	2.26	7020758	2.71	4270959	2.86	7020658
0.99	7090855	1.49	7191863	1.61	7191863	1.73	6130758	2.13	7070564	2.58	10052455	2.84	10051955
0.95	6252359	1.46	7022260	1.51	7022260	1.70	7191863	2.10	4291963	2.13	7070564	2.13	7070564
0.88	7021462	1.27	8292356	1.29	8292256	1.48	8060151	1.85	6122460	1.85	6122460	1.88	6130160
0.84	8090352	0.93	8090352	1.07	8060251	1.29	8292256	1.33	6100253	1.63	4121052	1.81	4120752
0.77	4301853	0.84	4301753	0.96	8090352	1.28	6100353	1.29	8292256	1.41	8290856	1.63	4280756
0.64	7081251	0.78	6281351	0.84	4301753	1.13	6112452	1.25	4120852	1.33	6100253	1.33	6100253

NO DATA PRIOR TO 1948 ON TAPE. ZERO INDICATES YEAR NOT AVAILABLE, 5 INDICATES YEAR WAS USED

48	49	50	51	52	53	54	55	56	57	58	59	60	61	62	63	64	65	66	67	68	69	70	71	72
0	5	5	5	5	5	5	5	5	5	5	5	5	5	5	5	5	0	0	0	0	0	0	0	0

MAXIMUM ANNUAL VALUES AND TIME OF OCCURRENCE (MONTH,DAY, HOUR AND YEAR)

2011 CRETE — PRECIPITATION IN INCHES

1-HR	DATE	2-HR	DATE	3-HR	DATE	6-HR	DATE	12-HR	DATE	18-HR	DATE	24-HR	DATE
1.74	5191149	2.80	5201959	3.14	10100154	4.45	10100154	4.96	10092354	6.08	10100154	7.45	10092254
1.54	8062072	2.00	10100254	3.03	5201859	3.29	5201759	3.33	5201559	3.33	5201559	3.53	9221861
1.40	5202059	1.86	5191149	1.98	6100353	2.57	8291855	3.28	8291755	3.28	8291755	3.50	4262259
1.38	7211261	1.85	8061972	1.97	5191149	2.47	6020650	2.67	9221861	2.73	5092351	3.28	8291755
1.25	6100453	1.65	6100453	1.93	7211061	2.38	8262465	2.53	6020650	2.68	9221861	3.02	6020650
1.23	10100354	1.52	8292255	1.91	8061972	2.20	5191049	2.40	7081351	2.63	6121072	2.95	5092151
1.15	8262465	1.48	7211261	1.89	8292255	2.06	7081951	2.38	8262465	2.61	6020650	2.90	6080658
1.10	7022360	1.31	8262465	1.50	8262465	2.05	7210961	2.28	5191049	2.60	6080658	2.63	6121072
1.04	5122270	1.24	7022360	1.40	6020850	2.05	6100353	2.26	5122270	2.38	8262465	2.38	8262465
1.03	8292355	1.21	5122270	1.38	7022260	1.93	8061872	2.25	6121372	2.29	5191049	2.29	5191049
1.00	4281851	1.14	6020950	1.28	6120352	1.84	5122270	2.09	6100253	2.26	5122270	2.26	5122270
0.95	6131852	1.13	6120352	1.25	7082051	1.45	7022260	1.70	6081958	2.09	6100253	2.09	6100253
0.79	8021863	1.10	7081951	1.22	5122270	1.40	6120352	1.65	7130563	1.69	7130563	1.88	7190263
0.74	9210750	0.91	6082058	1.18	6081958	1.39	6081958	1.55	4010667	1.57	4010467	1.76	10150467
0.65	4160867	0.90	6211467	1.07	7190363	1.38	7131063	1.45	6131052	1.50	6131052	1.50	6131052
0.57	7271758	0.79	8021863	1.05	6211367	1.36	4010767	1.45	7022260	1.45	7022260	1.45	7022260

NO DATA PRIOR TO 1948 ON TAPE. ZERO INDICATES YEAR NOT AVAILABLE, 5 INDICATES YEAR WAS USED

48	49	50	51	52	53	54	55	56	57	58	59	60	61	62	63	64	65	66	67	68	69	70	71	72
0	5	5	5	5	5	5	5	0	0	5	5	5	5	0	5	0	5	0	5	0	0	5	0	5

MAXIMUM ANNUAL VALUES AND TIME OF OCCURRENCE (MONTH,DAY, HOUR AND YEAR)

7990 SKOKIE T WORKS — PRECIPITATION IN INCHES

1-HR	DATE	2-HR	DATE	3-HR	DATE	6-HR	DATE	12-HR	DATE	18-HR	DATE	24-HR	DATE
2.15	7122257	2.88	8122056	3.27	7122057	4.63	7121857	5.36	7121357	5.54	7121357	6.34	10091854
1.85	8122056	2.71	7122157	2.94	8122056	2.96	9132161	4.05	10091854	4.66	10091854	5.60	7121357
1.52	8271849	1.77	8252172	2.06	9132261	2.94	8122056	3.13	9132061	3.13	9132061	3.49	6140449
1.27	10081350	1.68	7021362	2.03	6142149	2.66	7020962	2.94	8122056	2.94	6140649	3.35	9130261
1.27	7191863	1.54	8241871	1.90	7021262	2.61	10091854	2.78	7020862	2.94	8122056	3.06	5100151
1.20	6042169	1.54	8041661	1.88	8252072	2.43	10102069	2.70	10101969	2.88	5100251	2.94	8122056
1.19	10101654	1.53	8271849	1.78	10102269	2.40	6142149	2.66	6141649	2.80	7020562	2.93	10100569
1.14	8041661	1.48	10081250	1.73	10091954	2.30	4242250	2.47	4241750	2.79	10101169	2.84	7012262
1.09	9151958	1.46	10102369	1.63	10081250	2.19	8161868	2.27	5100851	2.65	6020550	2.70	5110366
1.02	6182071	1.36	10101554	1.55	8241871	2.02	7022060	2.20	8161868	2.33	5111366	2.37	6020550
0.99	7271251	1.35	7191863	1.55	8162068	2.01	8251872	2.13	4291963	2.20	8161868	2.37	10030355
0.95	8252272	1.35	6130758	1.51	6130758	1.77	6101667	2.13	5111566	2.16	4291963	2.53	4290763
0.92	6081962	1.33	7022260	1.40	6101867	1.61	7021658	2.02	7022060	2.03	6141572	2.20	8161868
0.88	8041453	1.30	8161968	1.38	7022160	1.56	8060151	2.02	6141572	2.02	7022060	2.03	6141572
0.88	8162068	1.23	6241267	1.38	7191863	1.55	8241871	1.95	6122358	1.95	6122358	2.02	7022060
0.88	5080364	1.13	8250365	1.29	8060251	1.44	7191863	1.86	8291755	1.92	10052355	1.97	6121958
0.86	7181752	1.06	9222464	1.16	7132065	1.43	10052355	1.77	6101667	1.84	9051471	1.84	9051471
0.83	6241367	1.03	8060251	1.13	10052455	1.41	5111866	1.55	8241871	1.77	6101667	1.77	6101667
0.81	7090855	0.98	7181652	1.10	9222364	1.21	7181452	1.42	9261559	1.45	4120952	1.68	5120670
0.80	8310166	0.88	4280266	1.09	7181552	1.20	7132065	1.36	8202264	1.42	9261559	1.65	4120852
0.77	9041365	0.88	8041453	1.03	7262466	1.11	9261559	1.31	6130952	1.39	8202264	1.50	6211964
0.75	7022360	0.81	7090855	0.90	5222459	1.10	9222364	1.21	6202070	1.30	5120670	1.42	9261559
0.68	9252470	0.78	5230159	0.89	6122370	1.07	9061070	1.20	7132065	1.20	7132065	1.32	4301853
0.56	8151559	0.78	9061270	0.88	8041453	1.04	8041453	1.11	4301553	1.13	4300953	1.26	8081365

NO DATA PRIOR TO 1948 ON TAPE. ZERO INDICATES YEAR NOT AVAILABLE, 5 INDICATES YEAR WAS USED

48	49	50	51	52	53	54	55	56	57	58	59	60	61	62	63	64	65	66	67	68	69	70	71	72
0	5	5	5	5	5	5	5	5	5	5	5	5	5	5	5	5	5	5	5	5	5	5	5	5

MAXIMUM ANNUAL VALUES AND TIME OF OCCURRENCE (MONTH,DAY, HOUR AND YEAR)

8278 STICKNEY W SIDE T WORKS — PRECIPITATION IN INCHES

1-HR	DATE	2-HR	DATE	3-HR	DATE	6-HR	DATE	12-HR	DATE	18-HR	DATE	24-HR	DATE
2.09	7121957	2.85	7121857	3.23	7170369	5.32	7121857	6.18	7121457	6.38	7121457	6.38	7121457
1.96	8090352	2.81	7170369	2.98	7121857	3.84	6252059	4.53	7262266	4.63	7262066	5.40	10092054
1.83	7270266	2.57	9282072	2.90	8162068	3.38	7270166	3.84	6252059	3.88	10100154	4.78	7170369
1.70	9282172	2.32	7270166	2.79	9282072	3.25	7170369	3.34	8161868	3.84	6252059	4.63	7262066
1.69	8160170	2.18	6130758	2.53	7270166	3.24	8162068	3.25	7170369	3.34	8161868	3.84	6252059
1.63	8162068	2.16	8090352	2.51	10030654	2.94	10030654	2.97	9282072	3.25	7170369	3.56	6140549
1.56	10101654	2.09	10030654	2.36	6130758	2.94	9282072	2.94	10030654	2.97	9282072	3.34	8161868
1.50	7170469	1.89	9051471	2.31	6252259	2.72	9132161	2.85	9132061	2.91	9120861	3.06	9120761
1.48	6241450	1.88	8152470	2.16	8090352	2.48	7042371	2.63	6122358	2.79	7080651	2.97	9282072
1.46	6130758	1.85	8162068	2.15	7042471	2.44	6130558	2.60	6141749	2.76	6140549	2.83	7080651
1.43	9051471	1.66	6142249	2.11	9132361	2.38	7160163	2.54	7042171	2.69	6020550	2.72	6020450
1.40	9122161	1.66	7160263	2.07	7160163	2.19	6142049	2.38	7160163	2.63	6122358	2.64	6121458
1.15	10061655	1.59	8041761	1.90	8152370	2.16	8090352	2.16	8090352	2.54	7042171	2.54	7042171
1.08	6142249	1.54	6252359	1.78	6142249	1.97	6091362	2.01	6202070	2.38	7160163	2.45	6081962
1.06	9022263	1.48	6241450	1.56	7162250	1.96	8152270	2.00	8052051	2.24	6091362	2.44	4290763
1.03	6091862	1.38	8292256	1.55	9260751	1.77	8060151	1.98	6090862	2.16	8090352	2.42	10051855
1.01	7212351	1.35	9260851	1.38	8292256	1.70	7132165	1.95	8291555	2.04	6201370	2.16	8090352
0.89	8292356	1.33	5221455	1.33	5221455	1.69	6101367	1.76	6101367	2.00	8060255	2.06	6201270
0.86	7300159	1.14	7061765	1.30	7132165	1.64	8291955	1.76	7132165	1.84	6101367	1.84	6101367
0.77	5082164	1.09	7020962	1.28	7020962	1.61	7162150	1.72	7162250	1.76	7132165	1.76	7132165
0.68	6161367	0.88	6101467	1.05	6101367	1.38	8292256	1.66	7172364	1.68	7172364	1.68	7172364
0.64	7132165	0.82	7180164	0.96	7172364	1.24	7172364	1.38	8292256	1.52	8290856	1.54	5091036

NO DATA PRIOR TO 1948 ON TAPE. ZERO INDICATES YEAR NOT AVAILABLE, 5 INDICATES YEAR WAS USED

48	49	50	51	52	53	54	55	56	57	58	59	60	61	62	63	64	65	66	67	68	69	70	71	72
0	5	5	5	5	0	5	5	5	5	5	5	0	5	5	5	5	5	5	5	5	5	5	5	5

MAXIMUM ANNUAL VALUES AND TIME OF OCCURRENCE (MONTH,DAY, HOUR AND YEAR)

2888 EVANSTON PUMP STATION PRECIPITATION IN INCHES

1-HR	DATE	2-HR	DATE	3-HR	DATE	6-HR	DATE	12-HR	DATE	18-HR	DATE	24-HR	DATE
1.96	6151256	2.74	7122157	3.33	7122057	4.56	7121857	5.21	7 57	5.34	7121357	6.98	10091854
1.85	7122257	2.64	8122056	2.71	8122056	3.17	10091854	4.53	10091854	5.14	10091854	5.34	7121357
1.45	8171750	1.63	7021658	2.14	6142149	2.79	9132161	2.97	9132061	3.14	6140749	3.64	6140549
1.33	10101654	1.63	6142149	1.90	7021658	2.72	8122056	2.85	6141649	2.97	9132061	3.08	9130261
1.13	7070564	1.59	8171650	1.88	9132361	2.49	6142049	2.72	8122056	2.73	8120656	3.08	4290763
1.06	8041661	1.54	10101554	1.82	10091954	2.44	7021658	2.55	4291963	2.68	7080551	2.88	10050355
1.06	8191560	1.38	8191560	1.69	8171550	2.22	7020962	2.45	7021658	2.64	4291863	2.88	7080551
1.05	9151958	1.38	9132361	1.50	10052455	2.08	4242250	2.26	7020762	2.63	7020658	2.77	5110466
1.04	7181752	1.23	6120152	1.43	8191460	1.89	7022060	2.24	4241750	2.45	5111466	2.73	8120656
1.04	8271849	1.17	7070564	1.40	7021162	1.68	10052355	2.19	5111566	2.34	4241750	2.64	7020658
1.03	9190666	1.11	9190566	1.38	6112452	1.63	8060251	1.96	8291755	2.29	7012262	2.45	7162150
0.94	9041365	1.09	10052455	1.31	8060251	1.58	6112452	1.89	7022060	2.28	10052455	2.30	7012262
0.90	7191863	1.03	7132065	1.24	7262466	1.51	4291963	1.78	5100651	1.89	7022060	1.89	7022060
0.90	5031759	0.98	7191863	1.17	7070564	1.44	5111966	1.67	7070564	1.71	10210865	1.88	10210865
0.86	7212151	0.94	7021262	1.14	4230465	1.36	8202364	1.58	6112452	1.67	7070564	1.34	4120852
0.85	10052455	0.93	5031759	1.02	4291963	1.23	4230265	1.35	9261559	1.64	4121152	1.67	7070564
0.70	7021362	0.91	6212051	0.99	5222459	1.20	5222259	1.28	10211565	1.35	9261559	1.50	5220559
0.68	6271653	0.69	6271653	0.69	6271653	0.99	6042353	1.05	8020453	1.14	6042353	1.32	4301853

NO DATA PRIOR TO 1948 ON TAPE. ZERO INDICATES YEAR NOT AVAILABLE, 5 INDICATES YEAR WAS USED

48	49	50	51	52	53	54	55	56	57	58	59	60	61	62	63	64	65	66	67	68	69	70	71	72
0	5	5	5	5	5	5	5	5	5	5	5	5	5	5	5	5	5	5	0	0	0	0	0	0

MAXIMUM ANNUAL VALUES AND TIME OF OCCURRENCE (MONTH,DAY, HOUR AND YEAR)

5136 LOCKPORT POWER HOUSE PRECIPITATION IN INCHES

1-HR	DATE	2-HR	DATE	3-HR	DATE	6-HR	DATE	12-HR	DATE	18-HR	DATE	24-HR	DATE
2.38	7122457	3.75	7122457	4.28	7122457	5.25	7122457	5.57	7121657	6.45	7121457	6.45	7121457
1.86	7172464	2.11	8252072	2.33	7021858	2.96	8162068	3.09	7172464	3.59	7080651	3.67	7162150
1.76	6211856	1.91	9082465	2.20	8162268	2.54	7270266	3.03	8162068	3.58	7162150	3.61	7080651
1.71	8252072	1.90	7021958	2.16	9082465	2.43	6202170	3.00	6201970	3.17	7172364	3.40	5110366
1.65	7271858	1.88	7172364	2.13	8251972	2.39	7021858	2.88	7262166	3.03	7261966	3.40	10150467
1.50	5191249	1.77	6211856	2.07	7162150	2.38	8251672	2.64	7081251	3.03	8162068	3.17	7172364
1.47	9260751	1.75	9202067	2.04	7270566	2.31	8052355	2.56	10150467	3.02	6201370	3.04	8160868
1.45	8050268	1.74	8052355	2.00	7172464	2.22	7172364	2.45	8262365	2.93	10150467	3.02	6201370
1.38	4231661	1.71	7162250	1.91	8052355	2.19	5191049	2.41	7021858	2.76	8051455	3.00	9221961
1.33	6131652	1.66	5191249	1.88	6211856	2.18	9132061	2.40	8251572	2.53	9230161	2.99	10050555
1.29	8052455	1.61	6131652	1.88	10150467	2.17	7162150	2.36	8051855	2.45	8262365	2.74	6080458
1.23	7061765	1.60	8162268	1.84	5191049	2.16	9082465	2.31	7162150	2.43	7021858	2.45	8262365
1.20	9202167	1.57	9260651	1.68	9260551	2.13	9202067	2.30	9131961	2.40	8251572	2.40	8251572
1.19	7171450	1.55	7270566	1.66	6131652	2.10	7081751	2.27	5191049	2.27	5191049	2.30	6140349
0.95	7270666	1.49	4231661	1.52	6202170	1.94	6211856	1.94	6211856	2.01	6211856	2.01	6211856
0.92	4301462	1.34	7172469	1.52	9132261	1.70	6131652	1.79	6130852	1.81	6130852	1.93	7221559
0.91	7172469	1.23	6202270	1.42	7172469	1.61	7172469	1.63	7172469	1.63	7172469	1.81	6130852
0.89	8031660	0.97	7022360	1.23	8031660	1.42	7042371	1.57	7042271	1.61	7221559	1.63	7172469
0.82	8152270	0.97	4301462	1.16	6302459	1.33	4271859	1.45	4271859	1.57	7042271	1.57	7042271
0.79	9051471	0.89	8241971	1.00	7042371	1.24	9022460	1.42	8031660	1.42	8031660	1.42	8031660
0.72	10081659	0.84	10081659	1.00	9092362	1.17	9092362	1.18	9092362	1.18	9092362	1.18	9092362

NO DATA PRIOR TO 1948 ON TAPE. ZERO INDICATES YEAR NOT AVAILABLE, 5 INDICATES YEAR WAS USED

48	49	50	51	52	53	54	55	56	57	58	59	60	61	62	63	64	65	66	67	68	69	70	71	72
0	5	5	5	5	0	0	5	5	5	5	5	5	5	5	0	5	5	5	5	5	5	5	5	5

(Continued from inside front cover)

NWS 16 Storm Tide Frequencies on the South Carolina Coast. Vance A. Myers, June 1975, 79 p. (COM-75-11335)

NWS 17 Estimation of Hurricane Storm Surge in Apalachicola Bay, Florida. James E. Overland, June 1975. 66 p. (COM-75-11332)

NWS 18 Joint Probability Method of Tide Frequency Analysis Applied to Apalachicola Bay and St. George Sound, Florida. Francis P. Ho and Vance A. Myers, November 1975, 43 p. (PB-251123)

NWS 19 A Point Energy and Mass Balance Model of a Snow Cover. Eric A. Anderson, February 1976, 150 p. (PB-254653)

NWS 20 Precipitable Water Over the United States, Volume 1: Monthly Means. George A. Lott, November 1976, 173 p. (PB-264219)

NWS 20 Precipitable Water Over the United States, Volume II: Semimonthly Maxima. Francis P. Ho and John T. Riedel, July 1979, 359 p. (PB-300870)

NWS 21 Interduration Precipitation Relations for Storms - Southeast States. Ralph H. Frederick, March 1979, 66 p. (PB-297192)

NWS 22 The Nested Grid Model. Norman A. Phillips, April 1979, 89 p. (PB-299046)

NWS 23 Meteorological Criteria for Standard Project Hurricane and Probable Maximum Hurricane and Probable Maximum Hurricane Windfields, Gulf and East Coasts of the United States. Richard W. Schwerdt, Francis P. Ho, and Roger R. Watkins, September 1979, 348 p. (PB-80 117997)

NOAA SCIENTIFIC AND TECHNICAL PUBLICATIONS

The National Oceanic and Atmospheric Administration was established as part of the Department of Commerce on October 3, 1970. The mission responsibilities of NOAA are to assess the socioeconomic impact of natural and technological changes in the environment and to monitor and predict the state of the solid Earth, the oceans and their living resources, the atmosphere, and the space environment of the Earth.

The major components of NOAA regularly produce various types of scientific and technical information in the following kinds of publications:

PROFESSIONAL PAPERS — Important definitive research results, major techniques, and special investigations.

CONTRACT AND GRANT REPORTS — Reports prepared by contractors or grantees under NOAA sponsorship

ATLAS — Presentation of analyzed data generally in the form of maps showing distribution of rainfall, chemical and physical conditions of oceans and atmosphere, distribution of fishes and marine mammals, ionospheric conditions, etc.

TECHNICAL SERVICE PUBLICATIONS — Reports containing data, observations, instructions, etc. A partial listing includes data serials; prediction and outlook periodicals; technical manuals, training papers, planning reports, and information serials; and miscellaneous technical publications.

TECHNICAL REPORTS — Journal quality with extensive details, mathematical developments, or data listings.

TECHNICAL MEMORANDUMS — Reports of preliminary, partial, or negative research or technology results, interim instructions, and the like.

Information on availability of NOAA publications can be obtained from:

ENVIRONMENTAL SCIENCE INFORMATION CENTER (D822)
ENVIRONMENTAL DATA AND INFORMATION SERVICE
NATIONAL OCEANIC AND ATMOSPHERIC ADMINISTRATION
U.S. DEPARTMENT OF COMMERCE

6009 Executive Boulevard
Rockville, MD 20852

NOAA--S/T 79-334